This document was produced by scanning the original publication.

Ce document est le produit d'une numérisation par balayage de la publication originale.

Geological Survey of Canada
Commission géologique du Canada

MEMOIR 409

RECONNAISSANCE GEOLOGY OF THE PRECAMBRIAN SHIELD OF ELLESMERE, DEVON AND COBURG ISLANDS, CANADIAN ARCTIC ARCHIPELAGO

THOMAS FRISCH

Canada

1988

GEOLOGICAL SURVEY OF CANADA
MEMOIR 409

RECONNAISSANCE GEOLOGY OF THE PRECAMBRIAN SHIELD OF ELLESMERE, DEVON AND COBURG ISLANDS, CANADIAN ARCTIC ARCHIPELAGO

THOMAS FRISCH

1988

Energy, Mines and Resources Canada
Énergie, Mines et Ressources Canada

© Minister of Supply and Services Canada 1988

Available in Canada through

authorized bookstore agents
and other bookstores

or by mail from

Canadian Government Publishing Centre
Supply and Services Canada
Ottawa, Canada K1A 0S9

and from

Geological Survey of Canada offices:

601 Booth Street
Ottawa, Canada K1A 0E8

3303-33rd Street N.W.,
Calgary, Alberta T2L 2A7

A deposit copy of this publication is also available
for reference in public libraries across Canada

Cat. No. M46-409E Canada: $25.00
ISBN 0-660-12864-0 Other countries: $30.00

Price subject to change without notice

Cover

Typical Precambrian Shield terrain in Makinson Inlet, Ellesmere Island, late June, 1977. The summit of Bowman Island, in the middle distance, is 570 m high.

Critical reader
R.F. Emslie

Original manuscript submitted: 1986-06
Approved for publication: 1987-05

CONTENTS

1 Abstract/Résumé
2 Summary/Sommaire
5 Introduction
5 Location
5 Access
6 Physiography
6 Climate and wildlife
7 Previous geographic and geological exploration
7 Present work
7 Field
8 Office and laboratory
8 Acknowledgments
8 Field
8 Office and laboratory
8 Rock and mineral nomenclature
9 General geology
10 Metamorphic rocks
10 Cordierite gneiss
10 Orthopyroxene-free cordierite gneiss
15 Mineral chemistry
15 Metamorphic conditions
19 Rock chemistry and origin
20 Orthopyroxene-bearing cordierite gneiss
23 Mineral chemistry
23 Metamorphic conditions
25 Pyroxene-bearing quartzofeldspathic gneiss
27 Orthopyroxene tonalite gneiss
28 Mineral chemistry
30 Rock chemistry and origin
36 Orthopyroxene granodiorite and granite gneiss
37 Mineral chemistry
38 Rock chemistry and origin
38 Tectonic setting of the orthopyroxene-bearing quartzofeldspathic gneiss
39 Metamorphic conditions
42 Age
43 Marble and calc-silicate rocks
46 Mineral chemistry
47 Metamorphic conditions
47 Origin
47 Quartzite
47 Pyribolite and amphibolite
49 Mineral chemistry
50 Metamorphic conditions
51 Rock chemistry
52 Tectonic setting
55 Ultramafite
57 Orthopyroxene tonalite-granodiorite-granite
57 Orthopyroxene tonalite
58 Mineral chemistry
58 Orthopyroxene granite
60 Mineral chemistry
60 Retograded orthopyroxene granite
62 Rock chemistry
62 Origin

69 Age
70 Anatectic biotite granite
72 Rock chemistry
72 Origin
74 Age
75 Amphibolite facies acid to intermediate rocks
76 Metamorphosed acid and intermediate dykes
77 Rock chemistry and origin
77 Structural geology
78 Review of metamorphic conditions
80 Origin and tectonic development of the Ellesmere-Devon crystalline terrane
81 Unmetamorphosed rocks
81 Neohelikian rocks
81 Thule Group
81 Strathcona Sound Formation
82 Diabase dykes
82 Chemistry and origin
83 Age
84 Phanerozoic rocks
84 Economic geology
85 References

93 **Appendix** — Mineral and rock analyses

Tables

9 Table of formations
12 1. Mineral assemblages of cordierite gneiss
17 2. Temperatures and pressures, orthopyroxene-free cordierite gneiss
20 3. Pressures at 750°C, garnet-plagioclase-sillimanite-quartz assemblages
25 4. Mineral assemblages of pyroxene-bearing quartzofeldspathic gneiss
41 5. Temperatures, garnet-pyroxene gneiss
42 6. Pressures obtained from garnet-pyroxene-plagioclase-quartz geobarometry
45 7. Mineral assemblages of marble and calc-silicate rocks

Illustrations

in pocket Map 1572A Geology, Prince of Wales Mountains, District of Franklin, Northwest Territories
in pocket Map 1573A Geology, Makinson Inlet, District of Franlin, Northwest Territories
in pocket Map 1574A Geology, Devon Ice Cap, District of Franklin, Northwest Territories

Figures

5 1. Location of the map area.
6 2. Areas covered by the geological maps.
10 3. General aspects of gneisses, Devon Island and vicinity.
11 4. Garnet-sillimanite-cordierite gneiss.
12 5. Illustrations of the reaction garnet + sillimanite = cordierite + spinel in cordierite gneiss.
13 6. Replacement of garnet by cordierite + K-feldspar in cordierite gneiss.
13 7. Pinitization of cordierite in cordierite gneiss.
13 8. Cordierite dusted with inclusions and mantling garnet in cordierite gneiss.
14 9. Sillimanite in perthite mantled by plagioclase.
14 10. Complex perthite in cordierite gneiss.

16 11. Composition of garnet in cordierite gneiss and quartzofeldspathic gneiss.
16 12. Cordierite, garnet and biotite of orthopyroxene-free cordierite gneiss in the metamorphic AFM diagram.
18 13. Cordierites of "7-phase" migmatitic cordierite gneisses.
18 14. Pressure and temperature of formation of orthopyroxene-free cordierite gneiss.
21 15. Orthopyroxene-free cordierite gneisses in La Roche's (1965) diagram.
21 16. Orthopyroxene-free cordierite gneisses in Maccarrone et al.'s (1983) diagram.
21 17. Orthopyroxene-free cordierite gneisses in Gray's (1977) diagram.
21 18. Harker plots of orthopyroxene-free cordierite gneisses.
22 19. Symplectite of orthopyroxene and cordierite surrounding garnet in cordierite gneiss.
22 20. Sapphirine mantled by cordierite and spinel against orthopyroxene in Mg + Al-rich gneiss.
24 21. Sapphirine-free orthopyroxene-cordierite gneisses in the metamorphic AFM diagram.
24 22. Composition of sapphirine of orthopyroxene-cordierite gneiss in Higgins et al.'s (1979) diagram.
26 23. Modal classification of quartzofeldspathic granulite facies rocks.
26 24. Quartzofeldspathic gneisses in the IUGS classification.
28 25. Composition of pyroxenes and amphibole of garnet-free quartzofeldspathic gneiss.
29 26. Fe-Mg distribution between coexisting mafic silicates of garnet-free tonalitic gneiss.
30 27. Composition of pyroxenes and amphibole of garnetiferous quartzofeldspathic gneiss.
31 28. Quartzofeldspathic gneisses in the O'Connor (1965) diagram.
32 29. Quartzofeldspathic gneisses and metabasalts in the igneous AFM diagram.
32 30. Quartzofeldspathic gneisses and metabasalts in the Ca-Na-K diagram.
33 31. Quartzofeldspathic gneisses in La Roche's (1965) diagram.
33 32. K vs. Rb in quartzofeldspathic gneisses.
34 33. Quartzofeldspathic gneisses in Gray's (1977) diagram.
34 34. TiO_2-SiO_2 distribution in quartzofeldspathic gneiss.
35 35. Harker plots of quartzofeldspathic gneisses and metabasalts.
36 36. Mesoperthite and perthite in orthopyroxene granite gneiss.
37 37. Two generations of garnet in mesoperthite-rich orthopyroxene granite gneiss.
39 38. Quartzofeldspathic gneisses in the Q-Ab-Or diagram.
43 39. Paleopressures of garnetiferous quartzofeldspathic gneiss.
44 40. U-Pb concordia diagrams of zircon from orthopyroxene tonalite gneiss and granite gneiss, Devon Island.
45 41. Marble north of Makinson Inlet.
46 42. Replacement of diopside by tremolite in marble.
46 43. Evidence of retrogression in marble.
48 44. Replacement of sillimanite by muscovite in quartzite.
48 45. Granoblastic texture of pyribolite.
49 46. Composition of pyroxenes and amphibole of pyribolite.
50 47. Mineral intergrowth at hornblende-plagioclase contacts in pyribolite.
51 48. Fe-Mg distribution between coexisting mafic silicates of pyribolite.
52 49. Metabasaltic rocks in Berthelsen's (1960) modal classification.
53 50. Metabasalts in the diagrams of Leake (1964).
54 51. Discriminant diagrams of alkalic and tholeiitic metabasalts.
54 52. Metabasalts in the igneous AFM diagram.
55 53. Ti-Zr covariation in metabasalt compared to modern volcanic rock.
55 54. Metabasalts in the Zr/Y vs. Zr diagram of Pearce and Norry (1979).
55 55. Metabasalts in the Ti-Cr diagram of Pearce (1975).
56 56. Chemical variation diagrams for metabasalts.

56	57. Metabasalts in the Ti-Zr-Y diagram of Pearce (1975).
56	58. Metabasalts in the diagram of Mullen (1983).
56	59. Nickel contents of metabasalts compared to those of Archean and modern tholeiites.
58	60. Clouded plagioclase and late biotite in orthopyroxene tonalite.
58	61. Composition of pyroxenes and amphibole of meta-igneous tonalite and granite.
59	62. Orthopyroxene granite, southern Ellesmere Island.
59	63. Meta-igneous granitoid rocks in the IUGS classification.
60	64. Mafic xenoliths in orthopyroxene-bearing granitoid rock.
61	65. Fluorite-bearing, coarse-grained granite west of Cory Glacier.
62	66. Garnetiferous, retrograded orthopyroxene granite with layers and lenses of orthopyroxene tonalite.
63	67. Rocks of the orthopyroxene tonalite-granodiorite-granite suite in the O'Connor (1965) diagram.
63	68. Rocks of the orthopyroxene tonalite-granodiorite-granite suite in the igneous AFM diagram.
64	69. Rocks of the orthopyroxene tonalite-granodiorite-granite suite in the Ca-Na-K diagram.
64	70. Rocks of the orthopyroxene tonalite-granodiorite-granite suite in La Roche's (1965) diagram.
65	71. K vs. Rb in the orthopyroxene tonalite-granodiorite-granite suite.
65	72. Rocks of the orthopyroxene tonalite-granodiorite-granite suite in Gray's (1977) diagram.
66	73. Harker plots of the orthopyroxene tonalite-granodiorite-granite suite.
67	74. Rocks of the orthopyroxene tonalite-granodiorite-granite suite in the Q-Ab-Or diagram.
70	75. U-Pb concordia diagram of zircon from orthopyroxene granite, Grise Fiord.
71	76. U-Pb concordia diagram of zircon from garnetiferous orthopyroxene granite and included orthopyroxene tonalite.
72	77. Mafic schlieren and lenses in anatectic granite.
73	78. Anatectic biotite granites in Debon and Le Fort's (1983) classification.
75	79. U-Pb concordia diagram of zircon from anatexite.
76	80. Replacement of pyroxene by cummingtonite in amphibolite facies retrograde pyroxene tonalite gneiss.
76	81. Contact of retrograde orthopyroxene granite dyke and cordierite gneiss.
77	82. Late open fold in gneisses, Devon Island.
78	83. Extreme flattening in orthopyroxene tonalite gneiss, Devon Island.
78	84. Downfaulted Paleozoic strata, Ellesmere Island.
79	85. Summary diagram of pressure and temperature data.
82	86. Sketch map of geology along southern shore of Bache Peninsula.
83	87. Chemical variation diagrams of diabase dykes.
in pocket	88. Locations of chemically (including isotopically) analyzed samples.

Preface

In 1977, twenty-five years after helicopter-supported systematic geological mapping of the northern Canadian Shield was initiated by the Geological Survey of Canada, the crystalline terranes north of Lancaster Sound in the High Arctic remained as the last large area of the shield to be mapped.

This report presents the results of mapping on Ellesmere and Coburg islands, completed in 1977, and on Devon Island, completed in 1982.

The Precambrian Shield of the region consists of highly deformed granulite facies rocks belonging to the Churchill Structural Province. They include abundant late Archean or early Proterozoic supracrustal rocks intruded by late Aphebian, high grade metagranitoid bodies, and are magnificently exposed in rugged, highly glaciated terrain. Differences in structural trends, lithology and metamorphic history indicate that the shield areas of Ellesmere and Coburg islands and of Devon Island may constitute two distinct tectonic blocks.

Although no commercially significant mineral deposits have as yet been found, the abundant signs of mineralization, particularly in metasediments, suggest that the economic potential of the region is limited only by the harsh climate and remoteness.

R.A. Price
Assistant Deputy Minister
Geological Survey of Canada

Préface

En 1977, soit vingt-cinq ans après le début de la cartographie géologique systématique aérienne par hélicoptère du nord du Bouclier canadien par la Commission géologique du Canada, les terrains cristallins, au nord du détroit de Lancaster, dans le Grand Nord, demeuraient la dernière grande surface du Bouclier à cartographier.

Cette étude expose les résultats de la cartographie des îles Ellesmere et Coburg, terminée en 1977, et celle de l'île de Devon, terminée en 1982.

Le Bouclier précambrien de la région consiste en roches du faciès granulite hautement déformées, appartenant à la province structurale de Churchill. Elles comprennent d'abondantes roches supracrustales datant de l'Archéen supérieur ou du Protérozoïque inférieur pénétrées par des masses granitoïdes hautement métamorphisées, de l'Alphébien supérieur, et sont magnifiquement exposées dans un terrain accidenté à modelé glaciaire très marqué. Des différences dans les tendances structurales, la lithologie et l'histoire métamorphique indiquent que les régions du bouclier des îles Ellesmere et Coburg et de l'île de Devon peuvent constituer deux entités tectoniques distinctes.

Bien qu'aucun dépôt de minéraux présentant un intérêt commercial n'ait encore été découvert, les nombreux signes de minéralisation, surtout dans les sédiments métamorphisés, laissent supposer que le potentiel économique de la région n'est limité que par la rudesse du climat et l'éloignement.

R.A. Price, sous-ministre adjoint,
Commission géologique du Canada

Frontispiece. View eastward down Tanquary Glacier and Baird Inlet, east coast of Ellesmere Island, showing typical topography and exposures of the northernmost Canadian Shield. Inglefield Land, northwest Greenland, is visible on the horizon. (NAPL T405R-57.)

RECONNAISSANCE GEOLOGY OF THE PRECAMBRIAN SHIELD OF ELLESMERE, DEVON AND COBURG ISLANDS, CANADIAN ARCTIC ARCHIPELAGO

Abstract

The extensively ice- and snow-covered highland areas of southeastern Ellesmere Island, eastern Devon Island and Coburg Island are underlain by highly deformed granulite facies rocks of the northernmost Canadian Shield. The bulk of the terrane comprises a late Archean or early Proterozoic continental margin sequence now made up of garnet-sillimanite-cordierite gneiss, marble, quartzite, quartzofeldspathic gneiss of calc-alkaline composition, and metabasalt chemically of oceanic affinity, in interleaved belts trending northerly on Ellesmere and Coburg islands, easterly on Devon Island.

These rocks were intruded by a granitoid suite under granulite facies conditions between 1.9 and 2.0 Ga. Orthopyroxene-bearing tonalitic to granitic rocks, retrograded to varying degree, form especially extensive terranes in the southern and northern parts of the shield on Ellesmere Island. Xenolith-rich peraluminous granite with garnet, cordierite and/or sillimanite is abundant on Ellesmere Island. Most, if not all, of the intrusions are thought to have originated by crustal anatexis related to the granulite facies metamorphism and are moderately to strongly deformed.

Pressures and temperatures of metamorphism range from 7 to 3 x 10^5 kPa and about 750 to 500°C, largely reflecting decompression and cooling during uplift. Pressures recorded in Devon Island rocks are generally higher than elsewhere in the map area.

The interleaving of belts of diverse lithologies, the high metamorphic grade, and significant partial melting are probably due to crustal thickening by thrust stacking, possibly resulting from continental collision.

The crystalline rocks are overlain on the east coast of Ellesmere Island by unmetamorphosed sediments and basalts of the Neohelikian Thule Group and are bordered on the west and north by lower Paleozoic strata of the Arctic Platform.

Résumé

Les régions des hautes-terres presque complètement recouvertes de glace et de neige du sud-est de l'île Ellesmere, de l'est de l'île de Devon et de l'île Coburg reposent sur des roches à faciès des granulites hautement déformées de la partie la plus septentrionale du Bouclier canadien. La plus grande partie du terrain comprend une suite de marge continentale datant de l'Archéen supérieur ou du Protézoïque inférieur actuellement constituée de gneiss à grenat-sillimanite-cordiérite, de marbre, de quartzite, de gneiss de composition calco-alcaline riche en quartz et en feldspath et de basalte métamorphisé dont la composition chimique suggère une origine océanique, dans des ceintures intercalées se dirigeant vers le nord sur les îles Ellesmere et Coburg et vers l'est sur l'île de Devon.

Une suite granitoïde a pénétré ces roches dans des conditions qui s'apparentent à celles associées au faciès granulite entre 1,9 et 2,0 Ga. Des roches contenant de l'orthopyroxène, allant des tonalites aux granites, rétrogradées à des degrés différents, forment des régions particulièrement importantes dans les parties sud et nord du bouclier sur l'île Ellesmere. Du granite hyperalumineux riche en xénolithe et contenant du grenat, de la cordiérite et/ou de la sillimanite abonde sur l'île Ellesmere. On pense que la plupart des intrusions, sinon toutes, se sont formées par anatexie crustale liée au métamorphisme du faciès granulite et ont subi une déformation allant de modérée à intense.

Les pressions et températures de métamorphisme varient entre 7 et 3 x 10^5 KPa et environ 750 et 500 °C, ce qui reflète largement la décompression et le refroidissement lors du soulèvement. Les pressions relevées dans les roches de l'île Devon sont en général plus élevées que dans le reste de la région figurant sur la carte.

L'intercalation de zones de lithologies diverses, le haut degré de métamorphisme et la fusion partielle relativement importante ont probablement été causés par l'épaississement crustal dû à l'imbrication de nappes chevauchantes, résultant peut-être de collision continentale.

Les roches cristallines, sur la côte est de l'île Ellesmere, reposent sous des sédiments et des basaltes non métamorphisés du groupe néohélikien de Thule et sont bordés à l'ouest et au nord par des strates du Paléozoïque inférieur de la plate-forme arctique.

SUMMARY

Highly deformed and metamorphosed rocks of the Canadian Shield underlie southeastern Ellesmere Island, eastern Devon Island and all of Coburg Island. The shield terranes of these islands are essentially the highland areas that are largely covered by ice and snow, totalling about 60 000 km^2 in area.

The crystalline rocks include late Archean or early Proterozoic infracrustal and supracrustal gneisses and 1.9-2.0 Ga meta-intrusive granitoid rocks, all in the medium- pressure granulite facies. The Precambrian Shield is overlain, locally, by unmetamorphosed Neohelikian rocks and, to the west and north, by lower Paleozoic strata of the Arctic Platform.

Lithological layering and foliations are generally steep. They trend northerly on Ellesmere and Coburg islands, easterly on Devon Island.

Major units of the crystalline terrane are orthopyroxene-bearing quartzofeldspathic gneiss and migmatitic garnet-sillimanite-cordierite gneiss. Metasedimentary belts consisting of the latter accompanied by marble, quartzite and pyribolite are especially prominent in eastern Ellesmere Island and Coburg Island. On Devon Island, metasediments are also abundant but they are commonly interlayered with quartzofeldspathic gneiss and rarely include marble or quartzite. Although much of the quartzofeldspathic gneiss is of infracrustal aspect, a basement-cover relationship has not been recognized anywhere in the shield terrane.

The garnet-sillimanite-cordierite gneisses, hereinafter referred to simply as cordierite gneisses, are characterized by retrograde development of cordierite as a result of reaction between garnet and sillimanite. Almost invariably, cordierite occurs mantling and partly replacing pyrope-almandine garnet. Sillimanite and K-feldspar commonly coexist in, and primary muscovite is absent from, the cordierite gneisses. In a related, but volumetrically unimportant, sillimanite-free variety of gneiss, garnet is replaced by orthopyroxene+cordierite.

Chemical evidence suggests that the protolith of the cordierite gneisses was mainly shale with subordinate psammitic sediment. There is no indication from their chemistry that the cordierite gneisses are residua of partial melting of pelitic rocks.

SOMMAIRE

Le sud-est de l'île Ellesmere, l'est de l'île Devon et toute l'île Coburg reposent sur des roches du Bouclier canadien fortement déformées et métamorphisées. Les terrains du Bouclier de ces îles sont essentiellement les régions de hautes-terres qui sont largement recouvertes par de la glace et de la neige, et représentent une région d'environ 60 000 km^2.

Les roches cristallines comprennent des gneiss infracrustaux et supracrustaux de l'Archéen supérieur ou du Protérozoïque inférieur et des roches méta-intrusives granitoïdes, appartenant toutes à la catégorie du faciès des granulites formées sous pression moyenne. Le Bouclier précambrien est recouvert, à certains endroits, par des roches néohélikiennes non métamorphisées et, à l'ouest et au nord, par les strates du Paléozoïque inférieur de la plate-forme arctique.

Les couches lithologiques et les foliations sont généralement très inclinées. Elles sont orientées vers le nord sur les îles Ellesmere et Coburg, et vers l'est sur l'île Devon.

Les masses les plus importantes du terrain cristallin sont constituées de gneiss riches en quartz et en feldspath contenant de l'orthopyroxène et de gneiss migmatitiques à grenat-sillimanite-cordiérite. Les zones métasédimentaires comprenant des gneiss des types décrits ci-dessus accompagnés de marbre, de quartzite et de pyribole occupent une place particulièrement importante dans l'est de l'île Ellesmere et dans l'île Coburg. Sur l'île Devon, les métasédiments abondent aussi, mais ils sont en général intercalés dans du gneiss quartzofeldspathique, et contiennent rarement du marbre ou de la quartzite. Même si beaucoup de gneiss quartzofeldspathique présente un aspect infracrustal, une relation socle/couverture n'a été reconnue nulle part dans le terrain du Bouclier.

Les gneiss à grenat-sillimanite-cordiérite, mentionnés ci-après simplement sous le nom de gneiss à cordiérite, sont caractérisés par le développement régressif de la cordiérite résultant de la réaction entre le grenat et la sillimanite. Presque invariablement, la cordiérite se trouve à recouvrir et remplacer partiellement le grenat pyrope-almandin. La sillimanite et le feldspath potassique coexistent habituellement dans les gneiss à cordiérite, mais la muscovite primaire en est absente. Dans une quantité mineure de gneiss sans sillimanite ayant des liens avec les précédents, le grenat est remplacé par de l'orthopyroxène et de la cordiérite.

Des données chimiques laissent à penser que le protolithe des gneiss à cordiérite était principalement un schiste argileux accompagné de sédiment psammitique associé. D'après leur composition chimique on ne peut pas conclure que les gneiss à cordiérite sont des résidus de la fusion partielle des roches pélitiques.

Marble is calcitic and contains diopside, olivine, clinohumite, and spinel as the most common mafic minerals. Wollastonite occurs locally in marble and calc-silicate rock. Quartzite has sillimanite as an important constituent. The thinness and persistence of the marble and quartzite layers suggest they represent shelf-type sediments.

Pyribolite, which occurs chiefly in concordant sheets, typically contains ortho- and clinopyroxene, olive or brown, Ti- and Al-rich amphibole, and plagioclase. Chemically, these rocks are metabasalts of oceanic affinity.

The bulk of the quartzofeldspathic gneisses carry orthopyroxene and biotite; garnet and hornblende are less common and clinopyroxene is comparatively rare. Compositionally, the gneisses range from quartz norite to granite but tonalite, chemically equivalent to K-poor dacite, predominates. Generally normal crustal K/Rb ratios signify little Rb depletion in the gneisses. The origin of the gneisses is uncertain but very probably they are meta-igneous rocks. Some may be metamorphosed supracrustal volcanogenic rocks (e.g. tuff) or sediments (e.g. immature greywacke), others may originally have been intrusive. The gneisses and pyribolites together form an association chemically similar to the classical Archean bimodal amphibolite-"grey gneiss" suite.

Interlayered orthopyroxene tonalite gneiss and granite gneiss from southern Devon Island yield U-Pb zircon concordia ages of 2518 +56/−33 and 2428 +36/−31 Ma, respectively.

The metasedimentary and meta-igneous gneisses and related rocks are interpreted as a continental margin sequence laid down in late Archean or early Proterozoic time and metamorphosed in the granulite facies in the latter part of the Aphebian era. Temperature and pressure estimates of metamorphism, derived from mineral thermometry and barometry, fall into two groupings: one with T over 700°C (probably about 750°C) and P between 5 and 7 $\times$ 10^5 kPa, the other with 500-700°C and 3-5 $\times$ 10^5 kPa. Pressures appear to have been slightly higher on Devon than on Ellesmere Island. The higher temperatures and pressures correspond to conditions of the transitional granulite facies; the lower values reflect the retrograde conditions of cooling and decompression during uplift, under which cordierite grew and local retrogression to the amphibolite facies occurred.

Granitoid rocks of meta-intrusive aspect form major bodies on Ellesmere Island in particular. Most are tonalitic or granitic, are moderately to strongly gneissic, and have gradational or indefinite contacts with their host rocks. However, crosscutting relations and inclusions of country rock, locally present, confirm the intrusive origin of the granitoids.

Tonalitic-quartz noritic intrusions exhibit features of I-type granitoids. Their mineral assemblage is

Le marbre est calcitique et les principaux minéraux mafiques communs qu'il contient sont le diopside, l'olivine, la clinohumite et le spinelle. Dans certains endroits, le marbre et les roches calcosilicates contiennent de la wollastonite. La sillimanite est un constituant important de la quartzite. La minceur et la persistance des couches de marbres et de quartzite permettent de croire qu'elles représentent des sédiments du type plateau continental.

La pyribole localisée surtout dans des couches concordantes contient essentiellement de l'orthopyroxène et du clinopyroxène, de couleur olive ou brune, de l'amphibole riche en Ti et en Al, et des plagioclases. Chimiquement, ces roches sont des basaltes métamorphisés d'origine océanique.

Les gneiss quartzofeldspathiques contiennent en grande partie de l'orthopyroxène et de la biotite; le grenat et la hornblende sont moins courants et, par comparaison, le clinopyroxène est plutôt rare. Du point de vue de leur composition, les gneiss vont de la norite quartzique au granite, mais la tonalite, équivalant chimiquement à la dacite pauvre en K, prédomine. En général, des rapports crustaux normaux K/Rb, signifient un faible appauvrissement du gneiss en Rb. L'origine des gneiss est incertaine; mais ce sont très probablement des roches ignées métamorphisées. Certaines peuvent être des roches métamorphisées supracrustales d'origine volcanique (p. ex. du tuf) ou des sédiments (p. ex. de la grauwacke non évoluée), d'autres peuvent, à l'origine, avoir été des roches intrusives. Les gneiss et les pyriboles forment ensemble une association chimiquement similaire à la suite archéenne classique bimodale "amphibolite - gneiss gris".

La datation U-Pb appliquée au zircon des gneiss à orthopyroxène et à tonalite interstratifiés avec du granito-gneiss du sud de l'île Devon a permis de fixer leur âge à respectivement 2518 +56/−33 Ma et 2428 +36/−31 Ma.

Les roches sédimentaires métamorphisés, les gneiss métaignés et les roches associées sont considérés comme une suite de marge continentale déposée pendant l'Archéen supérieur ou le Protérozoïque inférieur et métamorphisée au faciès granulite au cours de la dernière partie de l'Aphébien. Les estimations des températures et pressions de métamorphisme, tirées de la thermométrie et de la barométrie des minéraux, sont classés dans deux groupes dont l'un a une température supérieure à 700°C (probablement 750°C environ) et une pression située entre 5 et 7 $\times$ 10^5 kPa, et dont l'autre a une température de 500-700°C et une pression de 3-5 $\times$ 10^5 kPa. Les pressions semblent avoir été légèrement plus élevées sur l'île Devon que sur l'île Ellesmere. Les températures et les pressions plus élevées correspondent à des conditions de faciès granulite de transition; les valeurs inférieures reflètent les conditions régressives de refroidissement et de décompression pendant le soulèvement, au cours duquel la cordiérite se développe et un métamorphisme rétrograde au faciès des amphibolites se produisit à certains endroits.

Les roches granitoïdes d'aspect méta-intrusif forment les masses principales, plus particulièrement sur l'île Ellesmère. La plupart sont tonalitiques ou granitiques, modérement à fortement gneissiques, et elles ont des contacts graduels ou indéfinis avec les roches hôtes. Toutefois les relations de pénétration et les inclusions de roches encaissantes, présentes à certains endroits, confirment l'origine intrusive des granitoïdes.

orthopyroxene(+clinopyroxene)+green-brown hornblende+Ti-rich biotite+quartz+andesine. They are metaluminous (molecular $Al_2O_3/(CaO + Na_2O + K_2O) \leq 1$) and diopside normative. Rb is low and Na/K and K/Rb are high. Rb/Sr and K/Ba are low, as in lower (depleted) crustal rocks. The tonalitic rocks may have formed from partial melting of the lower crust by mantle-generated magmas.

Granites of S-type considerably outweigh in abundance the tonalitic bodies and are of two main types. One type carries orthopyroxene (or biotite pseudomorphs thereof), brown biotite (hornblende is absent), abundant perthite, and quartz; variants of this granite contain almandine garnet and/or green spinel. Orthopyroxene granite has normative corundum, low Na/K, high Rb, and upper crustal K/Rb and K/Ba ratios.

The other granite type is very felsic and associated with migmatitic cordierite gneiss. It forms bodies ranging from stringers and thin layers in gneiss to plutons several kilometres long and locally rich in xenolithic mafic material.

Typically, the mafic minerals of the granite are biotite and two of the aluminous minerals, almandine, cordierite, sillimanite and green spinel. Average abundances and ratios of the alkali metals are similar to those in the orthopyroxene granite but normative corundum is higher, generally exceeding 2%.

Both varieties of granite are believed to have formed by anatexis of overthickened sialic crust (aluminous gneiss in the case of the felsic granite) under deep level, high temperature, relatively anhydrous conditions.

U-Pb ages of zircons from the meta-intrusive granitoid rocks indicate emplacement between 1.9 and 2.0 Ga, which is thought to approximate the time of granulite facies metamorphism.

The anomalously thick crust implied by the widespread granulite facies metamorphism and anatectic magmatism may have resulted from some form of continental collision. Large-scale thrusting would explain the interleaving of different lithologies and the abundant evidence of flattening and ductile shear in the Precambrian Shield terrane. However, low-angle structures, such as nappes and shallow-dipping foliation, have not been recognized on a regional scale.

Locally on Ellesmere and Devon islands, the basement is overlain by unmetamorphosed, little deformed rocks of Neohelikian age (1.1-1.2 Ga): basalt sills and lavas and shallow-water clastic sediments of the Thule Group on eastern Ellesmere Island, and siltstone-sandstone of the Strathcona Sound Formation on southern Devon Island.

The youngest Precambrian rocks in the area are tholeiitic diabase dykes. On Ellesmere Island they do not appear to favour any particular orientation but on

Les intrusions tonalitiques/quartz noritiques ont des caractéristiques des granitoïdes de type I. Leur assemblage est constitué d'orthopyroxène (+ du clinopyroxène) + de la hornblende verte-brune + de la biotite riche en Ti + du quartz + de l'andésine. Elles sont méta-alumineuses ($Al_2O_3/(CaO + Na_2O + K_2O) \leq 1$) et normatives en diopside. La teneur en Rb est faible, mais les rapports Na/K et K/Rb sont élevés. Les teneurs en Rb/Sr et en K/Ba sont faibles, comme dans les roches crustales inférieures (appauvries). Les roches tonalitiques peuvent s'être formées à partir de la fusion partielle de la croûte inférieure par des magmas générés dans le manteau.

Les granites de type S dépassent de beaucoup en abondance les masses tonalitiques et il en existe deux principaux types. L'un contient de l'orthopyroxène (ou des pseudomorphes de biotite qui en proviennent), de la biotite brune (la hornblende est absente), de la perthite en abondance, et du quartz; des variantes de ce granite contiennent du grenat almandin et/ou du spinelle vert. Le granite à orthopyroxène a du corindon normatif, un faible rapport Na/K, une teneur élevée en Rb, et des rapports K/Rb et K/Ba correspondant à la croûte supérieure.

L'autre type de granite est felsique et est associé à du gneiss migmatique à cordiérite. Il forme des masses qui vont des petits filons et des fines couches dans le gneiss jusqu'aux plutons de plusieurs kilomètres de longueur et dont certains endroits sont riches en matériau mafique xénolithique. Essentiellement, les minéraux mafiques du granite sont la biotite et deux des minéraux alumineux, almandine, cordiérite, sillimanite et spinelle vert. Les abondances moyennes et les rapports des métaux alcalins sont identiques à ceux dans le granite à orthopyroxène, mais la teneur en corindon normatif est plus élevée et dépasse généralement 2%.

Les deux variétés de granite ont été probablement formées par anatéxie de la croûte sialique sur-épaissie (du gneiss alumineux dans le cas du granite felsique), réalisée à de grandes profondeurs, à haute température et dans des conditions relativement anhydres.

Les âges U-Pb des zircons provenant des roches granitoïdes intrusives métamorphisées indiquent une époque de mise en place située entre 1,9 et 2,0 Ga, ce qu'on pense être l'époque approximative du métamorphisme du faciès granulite.

La croûte terrestre irrégulièrement épaisse que suppose le métamorphisme très répandu du faciès des granulites et le magmatisme anatectique peuvent être le résultat d'une certaine forme de collision continentale. Des chevauchements à grande échelle expliquerait l'intercalation de différentes lithologies et les nombreuses preuves d'aplatissement et de cisaillement ductile dans le terrain du Bouclier précambrien. Toutefois, des structures faiblement inclinées, telles que nappes de charriage et foliations à plongement peu profond, n'ont pas été identifiées à l'échelle régionale.

Dans certains endroits sur les îles Ellesmere et Devon, le socle est recouvert par des roches non métamorphisées et peu déformées du Néohélikien (1,1 à 1,2 Ga): filons-couches et laves de basalte et sédiments clastiques d'eau peu profonde du groupe de Thule dans l'est de l'île Ellesmere, et de l'aleuronite-grès de la formation de Strathcona Sound dans le sud de l'île Devon.

Les roches précambriennes les plus jeunes de la région sont des dykes de diabase tholéiitique. Sur l'île Ellesmere, ils ne semblent pas suivre une orientation préférentielle; mais sur l'île Devon

Devon Island easterly trending dykes predominate and locally form swarms. According to whole-rock K-Ar age determinations, most of the dykes are Hadrynian.

The Precambrian Shield is bordered on the west and north by sedimentary rocks of the Arctic Platform, chiefly Cambrian and Ordovician shelf carbonates. Paleozoic outliers, many of which occur as downdropped fault blocks, in the interior of the crystalline terrane indicate that the Paleozoic seas once covered most, if not all, of the Precambrian Shield.

Metallic mineral showings are principally Cu and Fe sulphides (pyrrhotite, pyrite and subordinate chalcopyrite) forming lenses and layers in pelitic and semipelitic gneiss. They appear to be most abundant in the northern part of the area but no mineral deposit of commercial significance has been discovered as yet.

les dykes orientés vers l'est prédominent et par endroit forment des essaims. Si on se base sur les déterminations de l'âge K-Ar sur la roche totale, la plupart des dykes sont d'âge hadrynien.

Le Bouclier précambrien est bordé à l'ouest et au nord par des roches sédimentaires de la plate-forme arctique, surtout des carbonates du plateau continental principalement du Cambrien et de l'Ordovicien. Les avant-buttes paléozoïques, dont beaucoup se trouvent sous forme de blocs faillés à l'intérieur du terrain cristallin indiquent qu'au Paléozoïque les mers ont recouvert complètement ou presque le Bouclier précambrien.

Les traces de minéraux métalliques sont principalement les sulfures de Cu et de Fe (la pyrrhotite, la pyrite et, en quantité moindre, la chalcopyrite) qui forment des lentilles dans les gneiss pélitiques et semi-pélitiques. Ces traces semblent être plus abondantes dans la partie nord de la région, mais aucun dépôt d'intérêt commercial n'a encore été découvert.

INTRODUCTION

The northernmost part of the Canadian Shield, which forms a rugged fringe to the eastern High Arctic, was the last large area of the Shield to be mapped at a reconnaissance scale by the Geological Survey of Canada. This report presents the result of that work.

Location

The study area (Fig. 1) includes the areas of Precambrian Shield in (1) southeastern Ellesmere Island, south of 79° 15′N and east of 82°W and the south coast east of 86°W; (2) Devon Island east of 87°W; and (3) all of Coburg Island.

In this report, the map area is frequently referred to simply as the Ellesmere- Devon terrane.

The geological map (in pocket) is divided into three sheets with divisions at 78°N and 76°N (Fig. 2): a northern sheet, Map 1572A Prince of Wales Mountains, a central sheet, Map 1573A Makinson Inlet, and a southern sheet, Map 1574A Devon Ice Cap.

Access

The map area is accessible by air and, for part of the year, by sea. The only human settlement is the hamlet of Grise Fiord (population 106) on the south shore of Ellesmere Island. It is serviced regularly by aircraft from Resolute Bay on Cornwallis Island, 300 km to the southwest, which has airline connections with the south. Thule Air Base in Green-

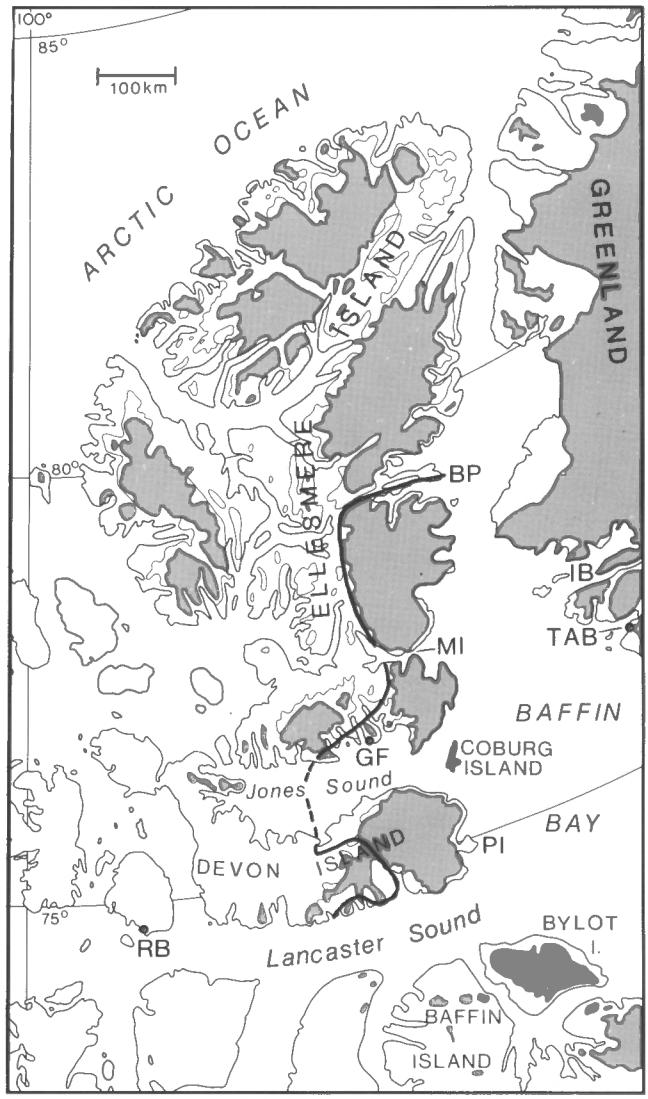

Figure 1. Location of the map area, which lies east of the heavy line. BP = Bache Peninsula; MI = Makinson Inlet; GF = Grise Fiord settlement; RB = Resolute Bay; PI = Philpots Island; IB = Inglefield Bredning; TAB = Thule Air Base. ►

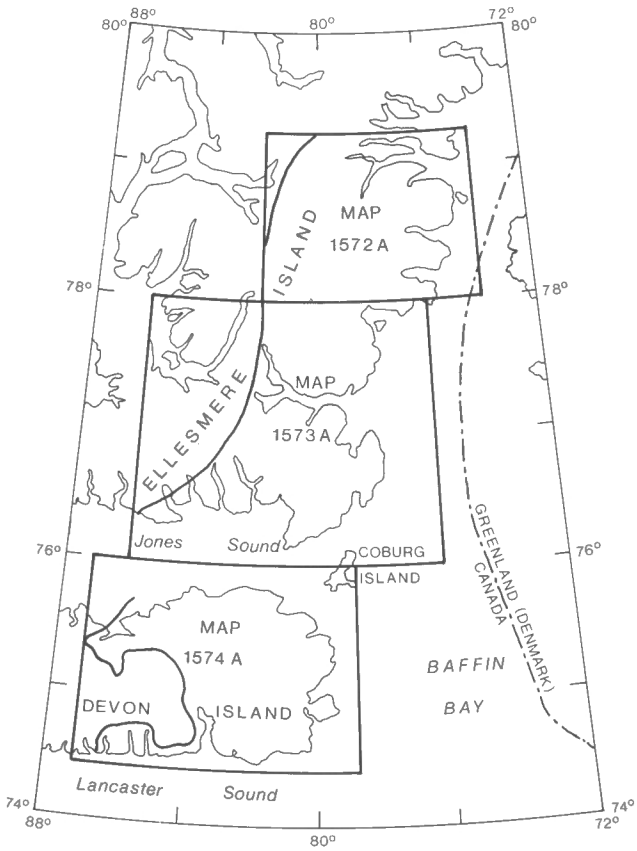

Figure 2. The areas covered by the three geological maps (in pocket) lie to the east of the heavy line.

land lies 360 km east of Grise Fiord. STOL aircraft equipped with strengthened undercarriages, big wheels and low pressure tires can operate from a number of locations such as marine terraces and river deltas. Airstrips of this type that are used more or less regularly during summer exist at the unoccupied RCMP post on Alexandra Fiord, Ellesmere Island (Map 1572A); at the head of Piliravijuk Bay, off Makinson Inlet, Ellesmere Island (where operations by DC-3 aircraft are possible); and at the Arctic Institute of North America field station near Truelove Inlet, northern Devon Island. Fixed wing aircraft are available for charter at Resolute Bay.

During August and September much of the area may be reached by ship although drifting pack ice may be heavy and icebreakers are necessary. Grise Fiord is supplied annually by icebreaker. Commonly navigable fiords on Ellesmere Island are Alexandra Fiord, Makinson Inlet and those on the south coast; on eastern Devon Island the north and south coasts are generally accessible by icebreaker in the shipping season.

Physiography

Much of the area underlain by the Precambrian Shield on Ellesmere, Devon and Coburg islands is a rugged highland largely covered by permanent ice and snow. It forms the northern end of the Davis Highlands, which stretch southward across Bylot Island and along the east coast of Baffin Island (Bostock, 1970).

Ice-free bedrock occurs mainly as cliffs along the numerous fiords and bays that indent the coast and as nunataks lining glaciers (Frontispiece). The tops of coastal cliffs are commonly at 500 m and many nunataks reach heights of 1500 m above sea level. The highest ground lies west of Jokel Fiord, Ellesmere Island (Map 1572A), where the relief exceeds 2300 m and nunataks occur at elevations of nearly 2000 m. Nunataks are not as common on the Devon Ice Cap and the higher part of it rises unbroken to an elevation of nearly 1900 m.

Extensive ice-free areas of Precambrian Shield are found only locally, particularly in southern Ellesmere Island and on Devon Island, in regions where the crystalline rocks form a basement to Paleozoic strata. Philpots Island, near the southeast corner of Devon Island, and the coastal region of northern Devon Island between Bear Bay and Brae Bay are among the few low areas of exposed Precambrian Shield.

Climate and wildlife

The macroclimate of the Canadian High Arctic is that of a high latitude continental land mass, i.e. low precipitation and low mean annual temperature. The map area, however, ranging as it does from inland areas near sea level to mountain peaks more than 2000 m high, can be divided into many different microclimatic zones. Inland areas such as the western margins of the ice caps on Ellesmere and Devon islands and Sverdrup Pass (northern margin of Map 1572A) are certainly warmer and drier than the eastern coast. Experience over three summers on Devon Island suggest that weather is particularly changeable, and often poor, over the Devon Ice Cap east of 82° 30′W.

At the head of Piliravijuk Bay, 70 km west of the mouth of Makinson Inlet, temperatures in 1977 averaged 4°C for the last three weeks of June, 10° in July, and 7° for the first three weeks of August. On Truelove Lowland, north of Truelove Inlet, northern Devon Island, mean summer (June-August) temperatures in 1971, 1972 and 1973 were 5, 3 and nearly 10°C, respectively (Courtin and Labine, 1977). On Coburg Island, mean monthly temperatures in June, July and August for the period 1972-76 were 0.6, 3.7 and 2.9°C, respectively (Müller, 1977).

What precipitation there is in summer falls mainly as rain or sleet so that low lying land stays snow free from about mid-June through August. Exceptionally warm weather in 1977 rendered the permanent snow on the ice cap in Ellesmere Island so mushy in places that the skids on the helicopter had to be replaced with floats in order for landings to be effected.

Sea ice breakup generally begins in July and fiords such as Makinson Inlet may be largely free of ice in August. However, some fiords, such as Cadogan Inlet (Map 1572A) remain choked with ice throughout the summer.

Larger forms of wildlife seen in the area include polar bear, muskox, Peary caribou, walrus, beluga whale, narwhal and seal. Polar bears are especially common in Smith Bay (Map 1573A) and on the east and south coasts of Devon Island. Muskoxen inhabit, on Ellesmere Island, areas north and west of the ice cap and the heads of the southern fiords. On Devon Island they are most abundant in the lowlands between Truelove Inlet and Sverdrup Glacier. Caribou are rare: two animals were seen in Cadogan Inlet in 1977. Marine life is particularly abundant in the polynyas of northern Baffin Bay and Buchanan Bay (northern part of Map 1572A).

Previous geographical and geological exploration

The large expanse of the "North Water" in northern Baffin Bay — open or only thinly ice covered even in winter — encouraged the exploration of the seaway between Ellesmere Island and Greenland as a possible access route to the North Pole. Exploration was particularly intense in the 19th century and included the expeditions of, among others, Kane, Hayes, Nares, Greely and Peary. The geographical and geological results of this activity are well summarized by Taylor (1955) and Dawes and Christie (1982), respectively. Christie (1962a,b) has plotted the locations of exploration-related historic sites on his geological maps. Perhaps the most famous of these sites is Camp Clay on Pim Island (Map 1572A), where most of Greely's party starved to death in 1884. (Note that this site is actually about 1 km northwest of the location shown on Christie's map).

Of the early geological observations in the Precambrian Shield, those made by Per Schei and Albert P. Low were the most significant. Schei was geologist to the Second Norwegian Arctic Expedition, led by Capt. Otto Sverdrup in the "Fram", which spent the period 1898-1902 in the Queen Elizabeth Islands, wintering in Fram Haven behind Pim Island and in Harbour Fiord (Map 1573A). The results of Schei's work were published by Bugge (1910) after Schei's death three years after returning from the Arctic. Low was leader of the Canadian Government expedition of 1903-04, which reached as far north as Cape Herschel (Map 1572A). Credit must go to Schei for finding evidence of granulite facies metamorphism and to Low (1906) for recognizing the presence of marble cut by granitic rock at Cape Isabella (Map 1572A). Dawes and Christie (1982) give a fuller account of these and other important findings by these two pioneers.

In the latter part of the 1930s, Robert Bentham (Dawes and Christie, 1982) carried out geological studies in Ellesmere Island and Greenland. Thin sections of Bentham's samples from Ellesmere Island are housed in the Department of Earth Sciences, Cambridge University, and were examined by the writer.

During the Geological Survey of Canada's reconnaissance of the Arctic Islands, Operation Franklin, in 1955, E.F. Roots (1963a, b) examined outcrops of the Precambrian Shield in southern Ellesmere and northern Devon islands. He described the gneisses west of South Cape (Map 1573A) — the westernmost exposures of basement in Ellesmere Island — in some detail and identified them as belonging to the granulite facies but gave no supporting evidence (Roots, 1963a). Roots (1963b) also described the crystalline rocks near Cape Sparbo, Devon Island, interpreting the bulk of them as high grade metasediments to a large extent recrystallized to leucocratic granite.

It was not until 1961 that an areally extensive survey of the Precambrian Shield on Ellesmere Island was undertaken. In that year and in 1962, R.L. Christie traversed the coastal regions using dog sledges and published the results mainly in the form of two maps (scale 1:253 440) with marginal notes (Christie, 1962a, b). He made a similar reconnaissance of eastern Devon Island in 1968 and 1969 (Christie, 1978). Christie's work provided the first overall picture of the Ellesmere-Devon crystalline terrane, including recognition of the contrasting structural trends in Ellesmere and Devon islands, but the inland regions remained largely unknown.

Samples of cordierite-bearing gneisses collected by Christie in Ellesmere Island were studied petrographically by P.W. Hay, who presented textural and optical data on cordierite and associated minerals in an unpublished doctoral dissertation (Hay, 1965).

In 1971, J. Krupička examined the crystalline rocks of the Truelove Lowland, northern Devon Island. His careful petrographic studies focussed on the mineralogical and textural changes in orthopyroxene-bearing quartzofeldspathic gneiss during retrogression (Krupička, 1973).

Discovery of massive sulphide occurrences and gossans on Ellesmere Island, by Christie (1962a) and in 1977 during this project, encouraged geological mapping and prospecting by Petro-Canada Ltd. in 1982 and 1983 (Gibbins, 1985). No deposits of economic value were found, however, and the prospecting permits were relinquished in late 1983.

Present work

Field

The fieldwork which forms the basis of this report was conducted over the course of several seasons, beginning in 1977 and ending in 1984.

Supplies for the 1977 field season were shipped to Ellesmere Island by icebreaker in 1976 and offloaded at the proposed base camp site on Piliravijuk Bay and at the Alexandra Fiord RCMP post.

In 1977, the Precambrian Shield on Ellesmere and Coburg islands was mapped by ground and aerial traversing using a Hughes 500C helicopter. Operations were based at a camp on the north shore of Piliravijuk Bay near its head and occupied from June 10 to August 25.

The shield terrane of Devon Island was mapped during parts of three field seasons: three weeks of foot and helicopter traversing in July 1978; one week of helicopter

reconnaissance in July 1980; and three days of helicopter work in late August 1982, during which time the nunataks (in previous years inaccessible due to low cloud) were reconnoitred. While all the geological mapping on this project was essentially of a reconnaissance nature, coverage of Devon Island is even less detailed than the rest of the map area.

In late August 1984, Cape Isabella and Makinson Inlet on Ellesmere Island were revisited for several days mainly to collect further samples for dating.

Office and laboratory

Optical determination of plagioclase composition was made on the flat stage, using the charts of Burri et al. (1967). Modal compositions reported are based on at least 1000 points per thin section.

Mineral analyses were made by the author on a MAC 400 electron microprobe fitted with an energy-dispersive system interfaced with automated data correction and reduction to produce simultaneous analyses for up to 10 elements. Most analyses are averages of at least 5 closely agreeing spot analyses.

Bulk rock chemical analyses have been made only on samples from Ellesmere and Coburg islands. The analyses were performed by staff of the Analytical Chemistry Section of the Geological Survey using "everyday" methods as described by Abbey (1979).

Isotopic age determinations were made by the Geochronology Laboratory of the Geological Survey, under the direction of, first, R.K. Wanless and, later, O. van Breemen. All U-Pb ages reported here were calculated using the decay constants, $1.55125 \times 10^{-10}/a$ for ^{238}U and $9.8485 \times 10^{-10}/a$ for ^{235}U.

The locations of samples chemically analyzed (bulk rock, microprobe and isotopic) are plotted in Figure 88 (in pocket).

Acknowledgments

Field

In 1977, W.C. Morgan shared the mapping duties with the author on Ellesmere Island and is alone responsible for the mapping of Coburg Island. The author is grateful to him for his enthusiasm, expertise and good companionship in the field. Important additional fieldwork was done by our senior assistant, G.R. Dunning, and all three of us were ably assisted by D.I. Brisbin and E.T. Lisle. W.F. Christensen served efficiently and cheerfully as camp manager-radio operator and D.A. MacDonald was an excellent cook.

Field operations in 1977 were also greatly facilitated by: the efficient caching of materiel in the field by the crew of CCGS **Louis St. Laurent** in 1976; expediting by E. Zwick in Resolute Bay; the support and co-operation of W. Blake, Jr.; the many courtesies and hospitality extended by Cpl. J.E. Grant, RCMP, and Mrs. Grant at Grise Fiord; help from M. Vaydick, DINA settlement manager at Grise Fiord; and permission from the Royal Canadian Mounted Police to use their buildings at Alexandra Fiord.

L.M. MacLaren was a capable field assistant on Devon Island in 1978. For other help on Devon Island the author thanks: R. Thorsteinsson, who freely provided base camp facilities and flying time in 1978; the Arctic Institute of North America, which graciously allowed use of their Truelove Inlet camp during all three field seasons; and D.R. Pattie, for his co-operation at Truelove.

In 1984, R.K. Herd accompanied the author to Ellesmere Island, providing valuable mineralogical and petrological expertise.

The demands of helicopter operations in difficult terrain were easily met by the skills of the helicopter crews: in 1977, J. Carlton, G. Curtis and M. Holzscheiter (pilots) and G. Arton (engineer) of Liftair International; in 1978, J. Sutherland (pilot) and E. Godleski (engineer), Liftair International; in 1980, T. Stauffer, Okanagan Helicopters; in 1982, C. Dynes (pilot) and C. Arnott (engineer), Quasar Helicopters; and in 1984, G. Webb, Quasar Helicopters.

None of the fieldwork would have been possible without the support of the Polar Continental Shelf Project. Over the years, PCSP provided fixed wing and helicopter flying time, accommodation at Resolute Bay, and much other assistance. Special thanks are extended to F. Alt, G.D. Hobson, B. Hough, and F.P. Hunt and their staff at Resolute Bay and to the Twin Otter crews of Bradley Air Services for their skill and hard work.

Office and laboratory

The author is greatly indebted to M. Bonardi for his patient instruction in, and subsequent help with, the techniques of energy-dispersive microprobe analysis and related data reduction. J.H. Maley was very helpful in data processing and adapted a number of computer programmes for geothermobarometry to the available facilities. J.A. Percival and M.R. St-Onge also helped in this regard and provided petrological expertise. S. Navratil conscientiously measured a large number of modes. P. Hunt contributed much to the isotope geochronology. S.O. Agrell of Cambridge University kindly arranged for the loan of thin sections of R. Bentham's samples from the Harker Collection.

Most of the figures in this report were drawn by K. Bencik.

Critical reading by R.F. Emslie resulted in substantial improvements to the first draft of this report but any errors that remain are the author's.

Rock and mineral nomenclature

The terminology of the quartzofeldspathic, i.e. granitoid, rocks used in this report is that proposed by the IUGS Subcommission on the Systematics of Igneous Rocks (Streckeisen, 1976). The pyroxene-bearing varieties are classified according to the IUGS system for "charnockitic"

TABLE OF FORMATIONS

Eon	(Sub)Era	Period	Unit	Formation	Lithology
Phanerozoic	Cenozoic	Quaternary	Qu		Stream, deltaic, glacial and marine beach sediments
		Unconformity			
		Tertiary	P-C	Eureka Sound	Sandstone, shale and coal
		Unconformity			
	Paleozoic	Cambrian-Ordovician	P-C		Dolomite, limestone and sandstone
Proterozoic	Neohelikian-Hadrynian	Unconformity			
			Hd, Hda		Diabase dykes
		Intrusive contact			
	Neohelikian		Nss NT	Strathcona Sound Thule Group	Shale, siltstone and sandstone Sandstone, shale, siltstone, dolomite, conglomerate and basalt
		Unconformity			
Archean and Proterozoic	Aphebian		ag hg, hgn ogd ot, og, gt		Anatectic biotite granite Hornblende granite and gneiss Metamorphosed acid to intermediate dykes Orthopyroxene tonalite-granodiorite-granite
		Intrusive contact			
	Archean and(?) Aphebian		um am qz mb tg, gn ms		Ultramafite Pyribolite and amphibolite Quartzite Marble and calc-silicate rock Orthopyroxene-bearing quartzofeldspathic gneiss Garnet-sillimanite-cordierite gneiss and related metasediments
Stratigraphic order of Archean and Aphebian units is uncertain.					

rocks, slightly modified by the substitution of "hypersthene" by "orthopyroxene" (Fig. 23). To avoid confusion and controversy, names such as charnockite, enderbite and granulite are not used to designate rock types.

Gneisses with garnet, sillimanite, cordierite and biotite are the most abundant metasedimentary rocks. For brevity, these rocks are called cordierite gneisses. This term includes the volumetrically minor garnet-orthopyroxene-cordierite gneiss.

A metamafic rock with colour index greater than 50 and consisting essentially of pyroxene, hornblende and plagioclase is called pyribolite. This term was coined and defined by Berthelsen (1960, p.20) but is used more loosely in this report (*see* Fig. 49). Amphibolite is reserved for rocks in which amphibole greatly predominates over pyroxene.

Gneisses with colour index less than 50 but greater than 20 are called mafic gneisses.

While rock textures (microstructures) are not described in great detail, the terminology used stems from Collerson's (1974), except that "texture" is used in place of "microstructure" and grain sizes are less than 1 mm for fine, between 1 and 5 mm for medium and greater than 5 mm for coarse.

Mineral abbreviations used in tables and figures are listed in the Appendix.

General geology

The largely ice-covered highlands of southeastern Ellesmere Island, eastern Devon Island and Coburg Island are underlain by highly metamorphosed and deformed Archean and Proterozoic rocks, which constitute the Alexandra Subprovince of the Churchill Structural Province of the Canadian Shield (Stockwell, 1982). Infracrustal and supracrustal (Fig. 3) rocks include quartzofeldspathic gneisses, metabasalts, metapelites-psammites, quartzite and marble; the latter is, however, scarce on Devon Island. The rocks probably are of late Archean age and were metamorphosed in the medium pressure granulite facies in the late Aphebian, then rapidly uplifted. Orthopyroxene-bearing intrusive bodies of tonalitic to granitic composition are considered to have formed by crustal melting during the granulite facies metamorphism. Abundant peraluminous granite originated by anatexis of aluminous metasediments.

Structural trends are northerly on Ellesmere and Coburg islands, easterly on Devon Island. Foliation generally parallels lithological boundaries and dips steeply to moderately.

The crystalline rocks are unconformably overlain by little-deformed, unmetamorphosed Neohelikian sedimentary and volcanic rocks on the east coast of Ellesmere Island and the south coast of Devon Island.

Unmetamorphosed diabase dykes, particularly abundant in parts of Devon Island, cut all Precambrian rocks.

The western edge of the shield is overlain by a gently westward-dipping homoclinal succession of Lower Paleozoic strata of the Arctic Platform. The Precambrian-Paleozoic contact follows the edge of the ice cap on Ellesmere Island very closely. Small grabens in the Paleozoic terrane near the Precambrian contact are filled by Tertiary sediments.

The present high elevations in the map area are the result of Miocene uplift.

METAMORPHIC ROCKS

This section deals with all aspects of the metamorphic rocks of the Precambrian Shield terrane. The rocks are considered, for the most part, in the order in which they appear in the legend to the geological map. Since the relative (and absolute) ages of many of the map units are not known with certainty, the order is not necessarily chronological. For example, cordierite-bearing metasedimentary gneisses are described before the quartzofeldspathic gneisses although at least some of the latter may be older (basement to the metasediments?).

Following the description of supracrustal and gneissic rocks, rocks of intrusive aspect are considered. An account of the structural geology completes the descriptive part of the section.

The section concludes with reviews of the metamorphic and tectonic history of the shield terrane.

Cordierite gneiss (ms)

Orthopyroxene-free cordierite gneiss

Cordierite-bearing gneisses with garnet, sillimanite and biotite, constitute one of the major units in the map area. Rocks with this mineral assemblage range widely in lithology, structure, and composition. They include varieties such as white, relatively fine grained, well layered

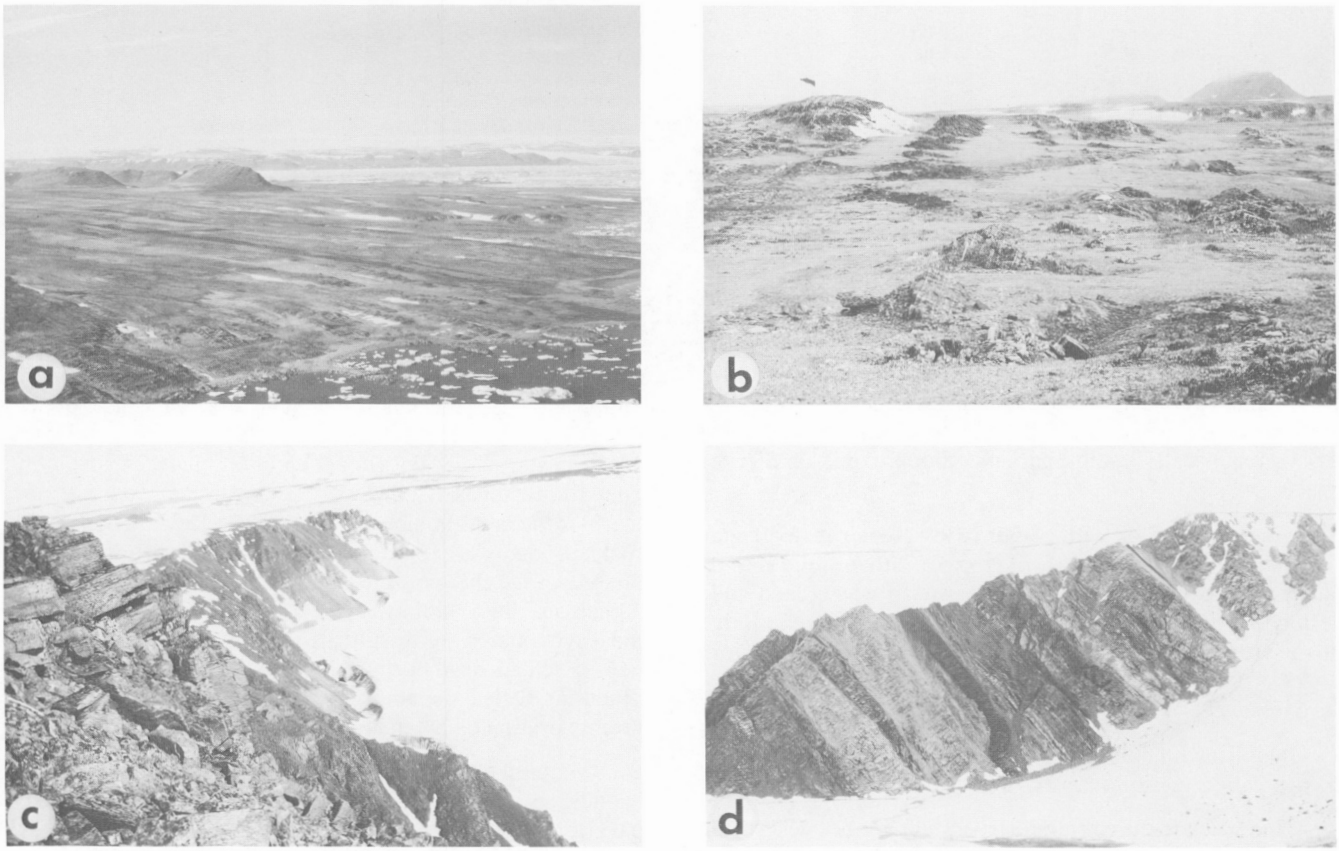

Figure 3. General aspects of gneisses, Devon Island and vicinity.

a) View northwestward across northern Philpots Island (Devon Island in background), showing east-trending supracrustal rocks (ribbed pattern) in sharp contact with orthopyroxene tonalite gneiss (left foreground).

b) Close-up of supracrustal terrane shown in Figure 3a. The chief rock type is garnet-sillimanite-cordierite gneiss.

c) Typical appearance of orthopyroxene tonalite gneiss, probably meta-igneous, in southern Devon Island. Note homogeneous, dark colour, contrasting with the metasedimentary gneisses (Fig. 3b, d). (The break between dark and light rock in the distance is the firn line and does not mark a change in lithology.)

d) Typical supracrustal sequence of cordierite gneiss, pyribolite and quartzitic gneiss, cut by diabase dykes, at head of Sverdrup Glacier, northern Devon Island.

gneiss; reddish porphyroblastic gneiss with irregularly spaced leucocratic granitic layers, lenses and pods; and highly migmatitic gneiss (Fig. 4), which locally grades into thick, poorly foliated granite studded with garnets. Most common is a migmatitic (stromatic (Mehnert, 1968)) gneiss composed of relatively mafic, reddish weathering, foliated rock rich in pink garnet and bluish cordierite porphyroblasts and biotite, and more leucocratic, pink to white layers and lenses of garnetiferous granite that are generally concordant but locally discordant to the gneissic foliation in the melanosome. Contacts between melanosome and leucosome tend to be gradational and may be marked by concentrations of mafic minerals such as biotite and garnet. Porphyroblasts are characteristically of medium to coarse grain size; garnet and cordierite crystals 2 cm in diameter are not uncommon.

Cordierite gneisses typically form major portions of heterogeneous supracrustal assemblages in which they are associated, or even interlayered, with pyroxene gneiss, quartzite, marble and the like. They may also be associated with large bodies of pink garnetiferous granite (units ag, agl) mineralogically similar to that forming layers and lenses in migmatitic cordierite gneiss. Such granite bodies commonly contain lenses and schlieren of cordierite gneiss. A third common associate is pegmatite, locally garnetiferous, which cuts highly to slightly discordantly across the typical outcrop of cordierite gneiss.

Despite great differences in lithology, the mineralogy of the cordierite gneisses is remarkably constant. Mafic components of the gneisses typically consist of garnet, cordierite, sillimanite, biotite, green spinel, plagioclase, perthite, and quartz. The proportions of these minerals vary widely and one or more of them (except cordierite) may be absent from a particular thin section (a result most probably of the heterogeneity and coarseness of the rock sectioned). Felsic portions of the gneisses are composed largely of perthite, plagioclase and quartz, with scattered flakes of biotite and irregularly distributed, minor garnet and sillimanite. Table 1 lists the main mineral assemblages.

The appearance of the cordierite gneisses in thin section is characterized by disequilibrium textures among the minerals. In none of the more than 70 thin sections of garnet-bearing varieties examined could garnet be deemed a stable mineral. Crystals are invariably anhedral and embayed, in some instances to such a degree that only skeletal remnants or small granules remain. Inclusions are

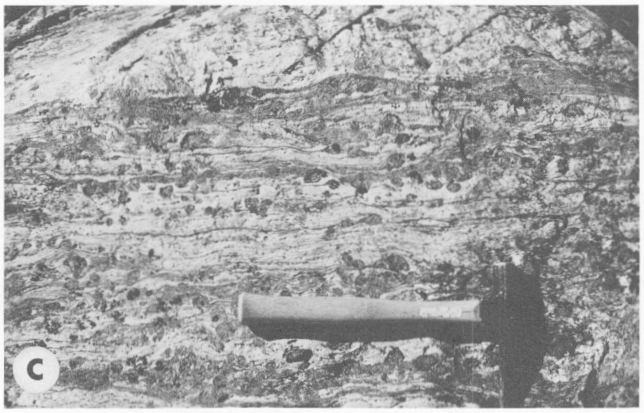

Figure 4. Garnet-sillimanite-cordierite gneiss.

a) Migmatitic cordierite gneiss, Leffert Glacier, Ellesmere Island.

b) Well layered cordierite gneiss (of similar mineralogy to that of the rock in Fig. 4a) in an east-trending ductile shear zone, east coast of Devon Island.

c) Characteristic appearance of cordierite gneiss. Note coarsely porphyroblastic garnet. Philpots Island.

common: tiny needles of sillimanite (slightly coarser than fibrolite) are most abundant, followed by biotite, quartz, spinel and Fe-Ti oxide. The sillimanite inclusion trails follow the foliation and layering of the rock, as do the elongate garnet crystals themselves.

Table 1. Mineral assemblages of the cordierite-bearing gneisses.

Quartz + perthite + plagioclase + biotite + garnet + sillimanite + cordierite + spinel (+ graphite)
Quartz + perthite + garnet + sillimanite + cordierite (+ plagioclase + spinel)
Quartz + perthite + biotite + garnet + cordierite (+ plagioclase + spinel)
Quartz + plagioclase + perthite + biotite + garnet + cordierite + orthopyroxene + spinel (+ sillimanite)
Plagioclase + perthite + biotite + cordierite + orthopyroxene + sapphirine
All assemblages contain Fe-Ti oxide (chiefly ilmenite).

The chief mineral replacing garnet is cordierite and indeed most, if not all, the cordierite in the map area originated in this manner. Cordierite is commonly concentrated in layers parallel to foliation, in which lie garnet, sillimanite and spinel. It also occurs forming rims of varying width around garnet adjacent to sillimanite and spinel (Fig. 5), implying the reaction

$$\text{garnet} + 2\ \text{sillimanite} = \text{cordierite} + \text{spinel}$$

Cordierite replacing garnet in many rocks forms symplectitic intergrowths with K- feldspar (Fig. 6), suggestive of the reaction

$$\text{biotite} + \text{garnet} + 5\ \text{sillimanite} + 7\ \text{quartz} = 3\ \text{cordierite} + \text{K-feldspar} + H_2O$$

Less commonly, cordierite is intergrown with vermicular quartz, probably derived from a reaction involving plagioclase rather than K-feldspar. In a very few rocks, cordierite occurs as discrete grains without any apparent direct association with, or relationship to, garnet. Significantly, such rocks contain only a few scattered, small grains of garnet.

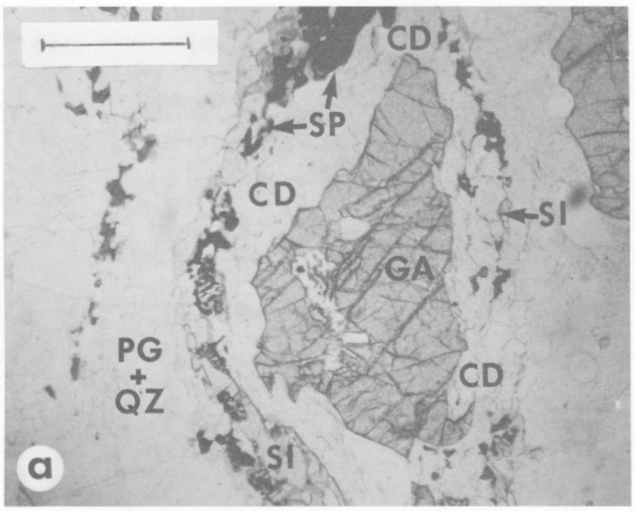

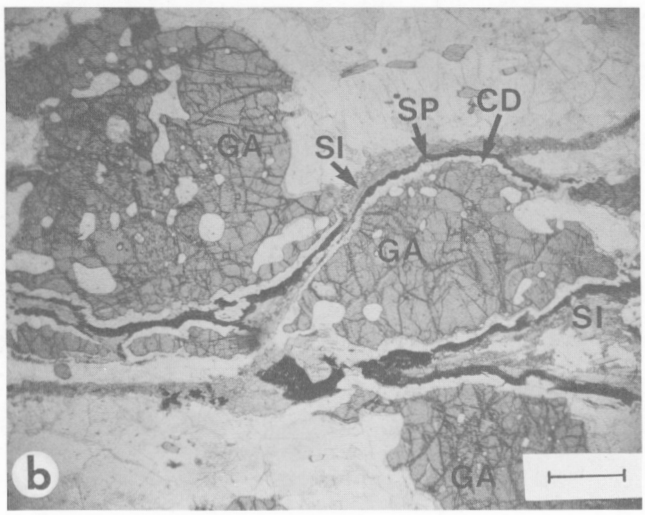

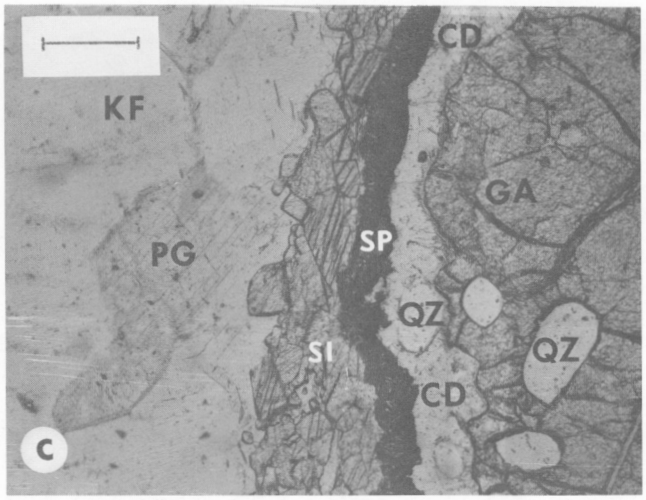

Figure 5. Illustrations of the reaction garnet + 2 sillimanite = cordierite + spinel in cordierite gneiss. Plane light. Bar scales: a) and b) 1.0 mm; c) 0.5 mm.

The coarser varieties of cordierite commonly exhibit well developed polysynthetic twinning, the lamellae characteristically extending only part way across the grains; rarely, crystals are sector twinned. Some form of alteration is virtually ubiquitous but generally has not progressed beyond pale greenish yellow pinitization along cracks (Fig. 7). In more altered rocks, pinitization and/or replacement by fine grained muscovite has extended over entire crystals of cordierite. Another earmark of cordierite that helps to identify it is abundant minute inclusions that give it a dusty appearance (Fig. 8). Larger inclusions, of zircon for example, typically are surrounded by yellow pleochroic haloes.

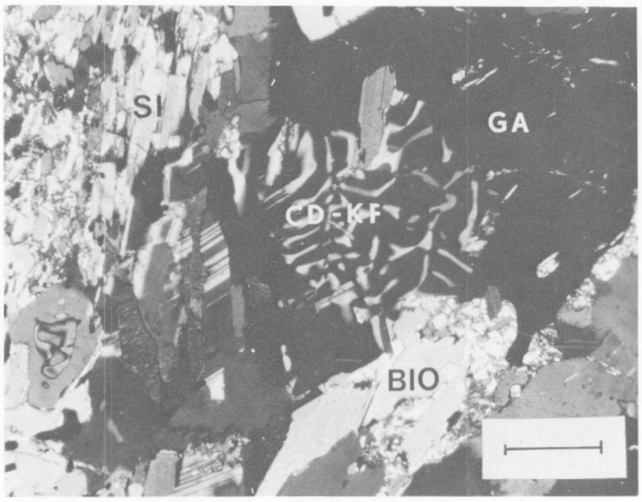

Figure 6. Replacement of garnet by cordierite (largely in extinction) + K-feldspar symplectite in cordierite gneiss. Crossed nicols. Bar scale 0.5 mm.

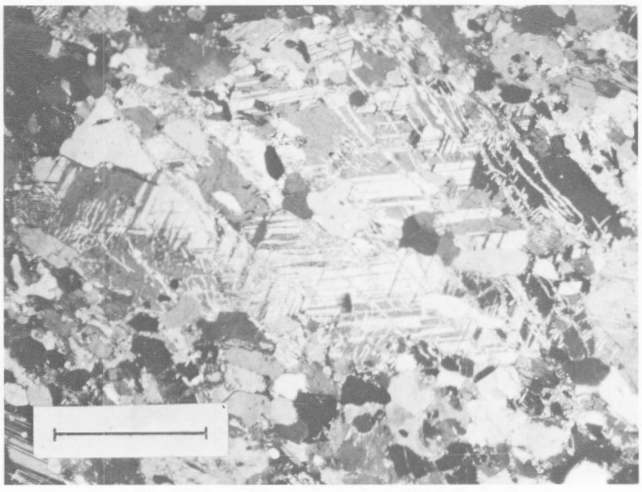

Figure 7. Pinitization of twinned cordierite along cracks, in cordierite gneiss. Crossed nicols. Bar scale 1.0 mm.

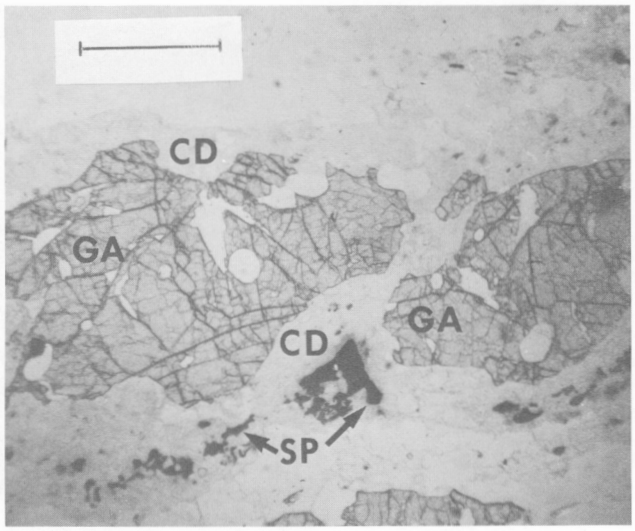

Figure 8. Cordierite characteristically dusted with inclusions and mantling garnet in cordierite gneiss. Plane light. Bar scale 1.0 mm.

Sillimanite is rarely absent from the cordierite gneisses and outside garnet occurs in well crystallized prisms, commonly up to 2 mm, exceptionally 4 mm, in diameter. Sillimanite grains included in garnet are generally finer needles than those outside but are certainly coarser than fibrolite. Sillimanite is generally confined to cordierite- and spinel-rich layers and segregations and is concentrated in trains of prisms and needles. Trains of fine needles commonly pass through garnet porphyroblasts, indicating garnet growth postdated crystallization of early sillimanite. The coarser sillimanite is probably a later recrystallization product. A third variety of sillimanite was noted in very small amounts in a few rocks: tiny vermicules extending more or less radially from the ends of coarser prisms of sillimanite. These vermicules must represent a late, higher-temperature overgrowth.

Sillimanite and K-feldspar are generally in textural equilibrium but their association became unstable with advanced retrogression. In FSM-77-273-4 (Appendix, Table 1A), in which cordierite has been totally replaced, sillimanite prisms included in perthite are mantled by twinned plagioclase (An_{34}) (Fig. 9).

Hercynite spinel — green to opaque in transmitted light — is an ubiquitous, if not a major, constituent of the cordierite gneisses, particularly in the garnet+cordierite-rich melanosomes. Grain size ranges from relatively coarse (2 mm) to fine but all grains are anhedral — evidence that the spinel is not a primary mineral but the product of a secondary reaction. Coarser grains may show lamellae of iron oxide, presumably magnetite, that has exsolved during a fall in temperature (Turnock and Eugster, 1962).

The close spatial association of spinel with sillimanite and cordierite signifies a reaction relationship, as specified above. No doubt spinel was produced not only by garnet

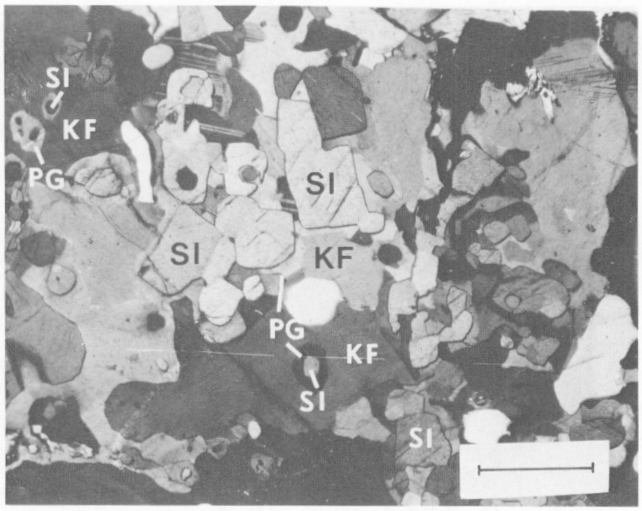

Figure 9. Sillimanite grains in K-feldspar (perthite) are mantled by twinned plagioclase (An_{34}), in cordierite gneiss FSM-77-273-4. Instability of sillimanite + Kfeldspar, which are normally in equilibrium in these rocks, is probably the result of a pressure and temperature drop. Bar scale 0.5 mm.

reacting with coarse sillimanite (Fig. 5c) but also by reaction between garnet and its fine grained included sillimanite. Although the production of spinel is favoured by a silica-deficient environment, the quartz-rich nature of the cordierite gneisses certainly has not inhibited its crystallization. Indeed, spinel completely surrounded by quartz has been noted in a cordierite gneiss from Devon Island and is consistent with an Fe-rich spinel composition. In the extremely silica-deficient environment locally attained in melanosomes of some rocks, vermicular corundum, intergrown with cordierite, has developed between spinel and sillimanite. This exemplifies the reaction

2 spinel + 5 sillimanite = cordierite + 5 corundum

Biotite is rarely absent from the cordierite gneisses and, like sillimanite, is an early formed mineral which has participated in major reactions. Its characteristic pleochroic formula is X = pale yellow, Z = reddish brown but Z shades of chestnut brown are also found and these differences appear to be related chiefly to TiO_2 content. Biotite is concentrated in, or along, the melanosomes of the gneisses, where it is particularly associated with garnet (in which it is also commonly found as inclusions). Frayed edges and partial replacement of flakes adjoining garnet, cordierite and sillimanite are common evidence of the participation of biotite in cordierite-forming reactions.

Secondary, pale green biotite occurs in association with altered cordierite in FSM-77-216, which also contains primary, reddish brown biotite (Appendix, Table IA).

The major felsic minerals of the cordierite gneisses comprise plagioclase, K- feldspar and quartz. All but ultramafic (garnet-cordierite-biotite-spinel-Fe-Ti oxide melanosome) portions of cordierite gneiss contain abundant quartz; virtually all varieties of gneiss contain K-feldspar and more than 90 % have at least minor plagioclase. Quartz is invariably strained and commonly displays trails of abundant fluid inclusions.

K-feldspar in discrete grains exhibits a bewildering variety of perthite textures. In many rocks the K-feldspar would be termed hair perthite (Fig. 10), considered by Eskola (1952) to characterize rocks of the granulite facies. The "hairs" range widely in shape and density, apparently grading into mesoperthite (Smith, 1974, p. 403) or into patches of widely spaced plagioclase blebs separated by clear areas. Mesoperthite grains have a distinctive opalescent bluish hue in plane light, a feature also observed by Eskola (1952) in the Finnish Lapland granulite complex. The most common perthite in the Ellesmere-Devon cordierite gneisses is one wherein a very fine, dense microperthite is traversed by coarser blebs or rods in a more open arrangement (Fig. 10). By analogy with optically identical feldspars in garnet + sillimanite + biotite-bearing rocks of the Lapland granulite complex (Yund et al., 1980), this perthite variety is probably a three-feldspar type consisting of an albite-rich phase in a cryptoperthite-microperthite matrix that originated as a ternary feldspar solid solution. Yund et al. (1980) believed the coarse blebs exsolved out at a higher temperature than did the matrix.

Some of the K-feldspar in the cordierite gneisses of Ellesmere and Coburg islands shows diffuse patches of microcline grid twinning indicating incipient microclinization. Extensively microclinized K-feldspar is widespread in the cordierite gneisses of Devon Island. There, the rocks commonly appear to be more strained and the development of microcline is likely to be a related phenomenon, as noted

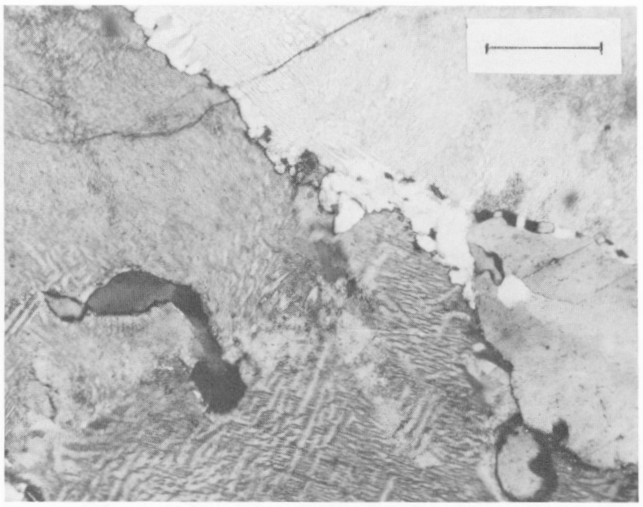

Figure 10. Complex three-feldspar perthite in cordierite gneiss. Crossed nicols. Bar scale 0.5 mm.

previously by Krupička (1973). Eskola (1952) detailed the evidence for shearing stress in promoting microclinization of orthoclase in the Lapland granulite complex and Smith (1974) has reviewed many other examples.

The bulk of the plagioclase in the cordierite gneisses is albite-twinned and variably antiperthitic. Composition ranges from An_{21} to An_{31} with compositions around An_{26-27} being the most common; zoning is insignificant. Although common, antiperthite is irregularly developed both within individual grains of a particular rock and from one rock to another. The K-feldspar component typically occurs in blocky form.

Accessory minerals in the cordierite gneisses include, in addition to the Fe-Ti oxide and corundum already mentioned, zircon and graphite. Graphite in thin, feathery laths is widely disseminated in some rocks and appears to be more common on Devon than on Ellesmere Island.

Mineral chemistry

Microprobe analyses of mineral assemblages from orthopyroxene-free cordierite gneisses are presented in Table 1A of the Appendix.

The garnets of the cordierite gneisses are mixtures essentially of almandine and pyrope; mole per cent of spessartine is typically around unity and never exceeds 2; and mole per cent grossular + andradite reaches a maximum of 8 (Fig. 11). Garnets are, with few exceptions, markedly zoned: relative to cores, rims are enriched in Fe, Mn and Ca and depleted in Mg. Detailed traverses across grains have not been made during microprobe analysis but spot checks indicate that the iron-rich rim of a typical garnet is characteristically narrow. Figures 11 and 12 show that core and rim compositions are relatively restricted but emphasize the significant gap between them.

Biotite is more inhomogeneous than garnet, exhibiting irregular compositional differences both within and between grains. Compositional heterogeneity is so severe that meaningful average compositions commonly are not determinable with certainty. Where compositions range especially widely, the extreme values of FeO, MgO and TiO_2 are given in the tabulated analyses. Fe/Fe+Mg commonly falls between 0.30 and 0.50, and TiO_2 between 3 and 5%. Biotite occurring as inclusions in garnet is consistently more magnesian than biotite outside garnet. The included biotite may be a relict high temperature phase or may equally well have re-equilibrated with garnet by Fe-Mg exchange during cooling (Indares and Martignole, 1985). The AFM diagram of Figure 12 illustrates well the compositional variability of biotite in cordierite gneiss.

Secondary, pale green biotite, which was involved in the alteration of cordierite in FS-77-216, is Ti poor (0.56% TiO_2) and is less siliceous and more aluminous than the coexisting primary reddish brown biotite.

Of the three major mafic minerals in the cordierite gneisses, cordierite is the most homogeneous and restricted in composition. The majority of cordierites analyzed have Fe/Fe+Mg between 0.26 and 0.34; extreme values are 0.21 and 0.36. No measurable zoning was detected within any grain and no difference in composition of rim cordierite and discrete cordierite was observed in any thin section.

Spinel in most of the cordierite gneisses is a hercynite-spinel solid solution with minor (calculated) ferric iron; Fe/Fe+Mg ranges from 0.74 to 0.88. Zinc is present in some of the spinels but has not been analyzed; ferric iron calculated on the basis of stoichiometry would be exaggerated if the spinel contained appreciable Zn. Only in one sample (FS-80-55 from Devon Island) is Zn a significant constituent (possibly 2.5% ZnO).

Metamorphic conditions

The complete absence of primary muscovite and the widespread coexistence of sillimanite and K-feldspar, which are commonly in contact, in the orthopyroxene-free cordierite gneisses indicate conditions well beyond those of the "second sillimanite" (sillimanite-orthoclase) isograd (Turner, 1981). Sillimanite is the only aluminosilicate mineral found in the map area and is consistently coarsely crystallized. The migmatitic nature of the cordierite gneisses attests to in situ partial melting. Reference to the generally accepted equilibrium curves for relevant reactions (Fig. 85) shows that temperatures and pressures must have exceeded at least 600°C and 4×10^5 kPa.

The mineralogy and texture of the cordierite gneisses make it evident that "secondary" thermobarometric events have pervasively affected the rocks. The main manifestation of such events is, of course, the all but ubiquitous occurrence of cordierite as a breakdown product of garnet. Thus pressure-temperature estimates will necessarily be strongly influenced by the conditions of this breakdown reaction.

Both theoretical and experimental studies have shown that the cordierite-garnet- sillimanite-quartz association is a potential indicator of pressure and temperature. The reaction

$$2\ (Fe,Mg)\text{garnet} + 4\ \text{sillimanite} + 5\ \text{quartz} = 3\ (Fe,Mg)\text{cordierite}$$

is pressure dependent — cordierite being the low pressure phase — and Fe-Mg exchange between garnet and cordierite is temperature sensitive. Thus P-T estimates should be obtainable from the intersections of isopleths of Fe/Fe+Mg of coexisting cordierite and garnet (*see*, for example, Lonker, 1981).

Unfortunately, application of the cordierite-garnet geothermobarometer is beset with difficulties, largely due to (a) disagreement between theory and experiment as to the slopes and positions of the equilibria in P-T space and (b) the hydrous nature of cordierite (for a recent review, *see* Thompson (1984)). For example, some workers have postulated a negative slope for the Fe-cordierite-forming reaction, others a positive slope; H_2O and CO_2 stabilize cordierite to higher pressures at a given temperature (Martignole and Sisi, 1981).

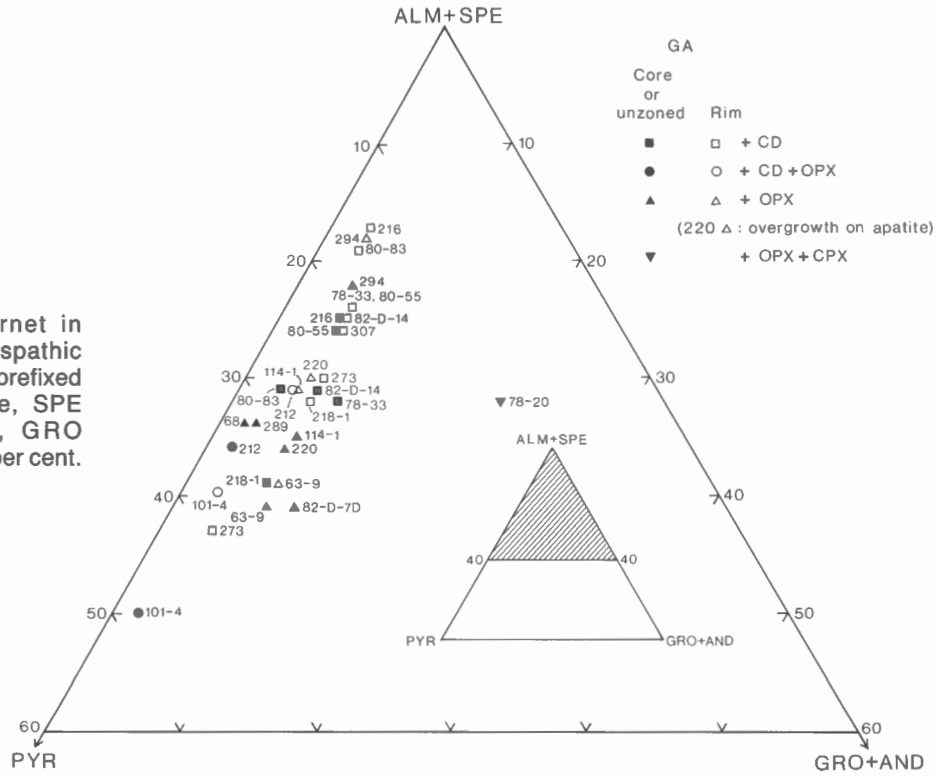

Figure 11. Composition of garnet in cordierite gneiss and quartzofeldspathic gneiss. Numbers refer to samples (prefixed by FS or FSM). ALM = almandine, SPE = spessartine, PYR = pyrope, GRO = grossular, AND = andradite. Mole per cent.

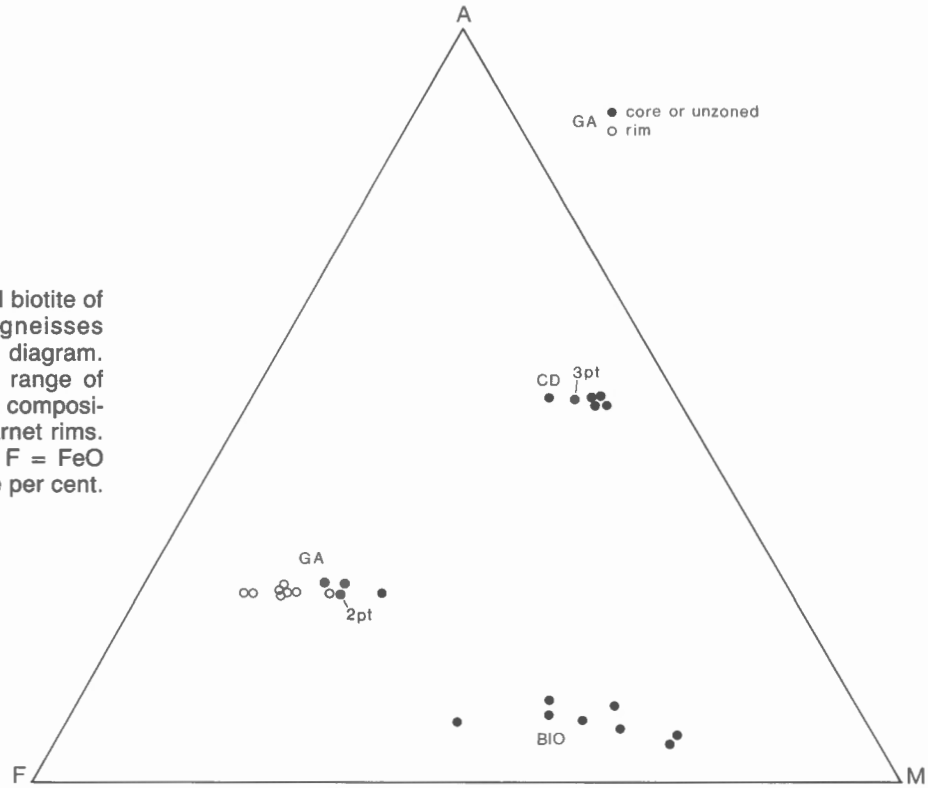

Figure 12. Cordierite, garnet and biotite of orthopyroxene-free cordierite gneisses plotted in the metamorphic AFM diagram. Note the restricted compositional range of cordierite, the variability of biotite composition and the iron enrichment of garnet rims. A = Al_2O_3 – (K_2O + Na_2O + CaO), F = FeO – Fe_2O_3 – TiO_2, M = MgO. Mole per cent.

The reaction between garnet and sillimanite to produce cordierite clearly occurred on a regional scale in the Ellesmere-Devon terrane. Textural relations furthermore indicate that the reaction was a relatively late-stage phenomenon, apparently due to a pressure drop (formation of cordierite). Zoning of garnet associated with cordierite from a Mg-rich core to a Fe-rich rim reflects a temperature decrease, as well (Thompson, 1976). Also, the cordierite-forming reaction took place at reduced P_{H_2O}, as suggested by the common occurrence of graphite and of the assemblage cordierite+garnet+K-feldspar, which is stable only at low P_{H_2O} (Lee and Holdaway, 1977). The coexistence of cordierite, garnet and K-feldspar with biotite, sillimanite and quartz implies the equilibrium

$$2 \text{ garnet} + 3 \text{ cordierite} + 4 \text{ K-feldspar} + 4\ H_2O = 4 \text{ biotite} + 8 \text{ sillimanite} + 13 \text{ quartz}$$

which is highly dependent on P_{H_2O} (Lee and Holdaway, 1977).

In the migmatitic Ellesmere-Devon cordierite gneisses, the six-phase assemblage is commonly accompanied by plagioclase and by a granitic leucosome, signifying the former presence of a melt phase. For such a combination, knowledge of the Fe/Fe+Mg of any of the mafic phases uniquely fixes temperature T, pressure P_{tot} and the ratio of water pressure to total pressure X_{H_2O} (Lee and Holdaway, 1977). In the case of the Ellesmere-Devon rocks, the composition of the most homogeneous phase, cordierite, is used.

Application of Lee and Holdaway's (1977, Fig. 4) P-T-X_{H_2O} diagram to migmatitic "seven phase" cordierite gneisses from Ellesmere and Devon islands yields T = 705-710°C, P_{tot} = 5.1-5.3 × 10^5 kPa and X_{H_2O} = 0.3-0.4 (Table 2, Fig. 13). According to M.J. Holdaway (pers. comm., 1984), these results are probably accurate to about ±50°C, ±0.75 × 10^5 kPa and ±0.2 X_{H_2O} and are thus rough indicators of physical conditions during the cordierite-forming event.

Temperature and pressure estimates derived from cordierite-garnet equilibria must be made with caution since they involve textural relations between cordierite with unknown volatile content and strongly zoned garnet, and are based on conflicting theoretical and experimental data. The latest formulation of cordierite-garnet-sillimanite-quartz equilibrium is by Aranovich and Podlesskii (1983), which is supported by experimental as well as theoretical work. Aranovich and Podlesskii's calibration is based on the Fe-cordierite-almandine-sillimanite reaction having a positive slope, which fits evidence from both theory and nature (Martignole and Sisi, 1981). A major uncertainty in this calibration is the effect of the volatile (H_2O, CO_2 and other species) content of cordierite. Aranovich and Podlesskii

Table 2. Temperature and pressure estimates of various mineral assemblages in orthopyroxene-free cordierite gneisses.

	Temperature (°C)						Pressure (kPa × 10^5)						
	L&H	A&P	M&S	L	V	P&L	L&H	A&P	M&S	L	V	N&H 600°	N&H 700°
A.													
Ellesmere Is.													
FS-77-216	710	475	400	390	480	479	5.3	3.3	2.5	7.9	8.1	2.7[a](1.0)[a]	4.1[b](2.1)[b]
FSM-77-218-1	710	650	620	640	773	628	5.3	5.7	4.7	6.8	6.6	3.7(2.7)	4.9(3.8)
307	705	680	680	635	788	634	5.1	5.4	4.7	6.2	6.0	3.0(1.5)	4.2(2.6)
Devon Island													
FS-78-33	705	630	580	590		570	5.2	5.0	4.0	6.6		3.4(1.9)	4.7(3.0)
80-55	705	630	600	590	621	581	5.2	5.0	4.2	6.6	7.3	4.2(2.8)	5.6(4.0)
82-D-14	710	675	550	590		569	5.2	6.0	3.8	6.6		3.7(2.1)	5.0(3.3)
B.													
Ellesmere Is.													
FSM-77-247-3		700	670	675		661		5.5	4.5	4.8			
C.													
Devon Island													
FS-80-83		620	560	600	507	584		4.3	3.4		7.4		
D.													
Ellesmere Is.													
FS-77-191					686						6.5		

[a]at 500° [b]at 600°

Calibrations: Garnet-cordierite: L&H (Lee and Holdaway, 1977) A&P (Aranovich and Podlesskii, 1983; P = P_{H_2O})
M&S (Martignole and Sisi, 1981; 0.5 mole H_2O in cordierite) L (Lonker, 1981; activity of H_2O = 0.5)
P&L (Perchuk and Lavrent'eva, 1983)
Cordierite-spinel: V (Vielzeuf, 1983)
Garnet-plagioclase-Al_2SiO_5: N&H (Newton and Haselton, 1981; value in brackets calculated using garnet activities of Ganguly and Saxena, 1984)

Assemblages: **A.** GA + CD + SI + BIO + PG + KF + QZ (+SP) **B.** GA + CD + SI + KF + QZ
C. GA + CD + SI + BIO + KF + QZ + SP **D.** GA + CD + BIO + PG + KF + QZ + SP

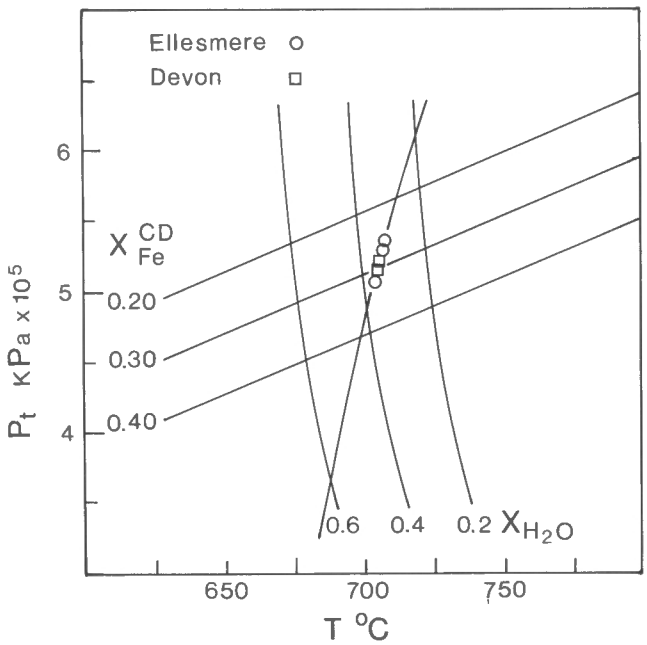

Figure 13. Cordierites of "7-phase" migmatitic cordierite gneisses (garnet-cordierite-sillimanite-biotite-Kfeldspar-plagioclase-quartz plus granite melt) plotted in Lee and Holdaway's (1977) diagram relating mole per cent Fe in cordierite to temperature, total pressure and water pressure (X_{H2O} = P_{H2O}/P_t).

(1983, Fig. 10) assume $P_{tot} = P_{H_2O}$ and that all volatiles in cordierite behave like water and therefore derived pressures are likely to be maximum values, up to 3 × 10^5 kPa greater than for $P_{H_2O} = 0$. It seems unlikely that the Ellesmere-Devon cordierites are completely anhydrous, for the following reasons.

In many rocks, cordierite is moderately altered and in some severely to completely so; the alteration product, pinite, consists of hydrous sheet silicates. Retrograde hydrous minerals such as muscovite and green biotite are present in some cordierite gneisses, implying hydration. Oxide sums of the cordierite analyses cluster around 98 %, suggesting a volatile content of about 2 %. (The optically positive nature and 2Vs greater than 90° of the cordierites indicate that a significant proportion of the volatiles is CO_2 (Armbruster and Bloss, 1982).)

Garnet compositions used are those of crystal rims rather than cores, as cordierite development was clearly a late process in the evolution of the Ellesmere-Devon rocks. It is recognized that this choice entails the risk that garnet compositions may be the result of retrograde re-equilibration by diffusion of Fe and Mg long after the garnet-to-cordierite reaction. Nevertheless, use of garnet core compositions appears to be illogical.

For the cordierites and garnets of the "seven phase" assemblage, temperatures and pressures read off Aranovich and Podlesskii's (1983, Fig. 10) diagram range, with one exception, from 630 to 680°C and 5.0 to 6.0 × 10^5 kPa (Table 2). The exception is sample FS-77-216, for which 475°C and 3.3 × 10^5 kPa are obtained. These are conditions of the andalusite-kyanite boundary, well outside the sillimanite field, according to Holdaway (1971), yet coarse sillimanite is abundant in the rock. Much of the cordierite is altered to green biotite (Appendix, Table IA) and some of the primary biotite is relatively pale brown with a hint of green. There seems little doubt that this rock has been strongly affected by retrogression, during which extensive re- equilibration between cordierite and garnet resulted in a garnet rim anomalously rich in iron (Fe/Fe+Mg = 0.83). In this instance, data from the cordierite-garnet-sillimanite system probably have no validity.

Application of Martignole and Sisi's (1981) calibration, assuming cordierite has 0.5 moles H_2O per formula unit, gives temperatures and pressures somewhat lower than those from Aranovich and Podlesskii's (1983) diagram — about 550 to 680°C and 3.8 to 4.7 × 10^5 kPa (Table 2) — but still falling in the sillimanite stability field. Conditions for FS-77-216 are correspondingly even lower, being those of the andalusite-kyanite boundary (Table 2, Fig. 14).

Comparable values of temperature and pressure, with similarly systematic differences, are obtained from the two calibrations for cordierite-garnet-sillimanite assemblages of less than seven phases, e.g. plagioclase absent (Table 2).

Martignole and Sisi's (1981) calibration also includes a somewhat rough indication of water fugacity of the fluid in equilibrium with garnet + sillimanite + cordierite. It

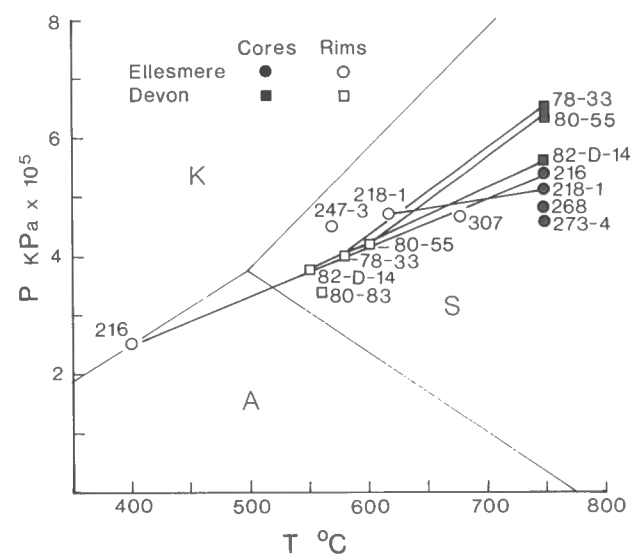

Figure 14. Pressure and temperature of formation of orthopyroxene-free cordierite gneisses. Pressures of garnet cores according to Newton and Haselton's (1981) garnet-Al_2SiO_5-quartz geobarometer, at an assumed temperature of 750°C. Garnet rim pressures and temperatures from Martignole and Sisi's (1981) garnet-cordierite calibration, assuming 0.5 mole H_2O in cordierite.

amounts to about 1×10^5 kPa or less (assuming 0.5 mole H_2O in cordierite), i.e. about one quarter of the total pressure, in essential agreement with the results of Lee and Holdaway's (1977) formulation. In any migmatite system, H_2O is strongly partitioned into the melt phase and the residual garnet-sillimanite-cordierite assemblage will be water-poor.

Newton (1983, Fig. 3) has presented P-T diagrams of Mg-isopleths of cordierite according to the theoretical constructions of several investigators. Disregarding those with negatively-sloped isopleths and using Mg/Mg+Fe = 0.7 and T = 650°C, we obtain with the Hutcheon et al. (1974) construction for $P_{H_2O} = P_{tot}$, 5.1×10^5 kPa; with Newton and Wood's (1979) diagram for $P_{H_2O} = 0$, we obtain 4.4×10^5 kPa.

It may be noted that pressures yielded by Lonker's (1981) calibration are considerably higher, exceeding 6×10^5 kPa and, in the case of FS-77-216, nearly 8×10^5 kPa. At these relatively low temperatures, the negatively sloped Mg-Fe isopleths of Lonker give pressures that seem geologically unreasonable.

Vielzeuf (1983) has proposed a geothermometer and a geobarometer based on thermodynamic calculations on the reaction

$$2 \text{ spinel} + 5 \text{ quartz} = \text{cordierite}$$

and has applied them with reasonable results to metasedimentary xenoliths that equilibrated at high temperature with enclosing basalt. The coexistence of spinel and quartz in the presence of cordierite is a common feature of the Ellesmere-Devon cordierite gneisses. Temperatures and pressures obtained for them (Table 2) range widely from 480°C (for FS-77-216) to 788°C and from 6.0×10^5 kPa to 8.1×10^5 kPa (for FS-77-216). Considering that both spinel as well as cordierite are late minerals, these values for the most part seem excessive. The apparent inapplicability of Vielzeuf's calibrations can probably be attributed to (a) temperatures being lower than those for which Vielzeuf's measured distribution coefficients give a reasonable correlation with temperature and (b) uncertainty as to the composition of spinel (e.g. unknown zinc content).

The latest version of the cordierite-garnet geothermometer has been formulated by Perchuk and Lavrent'eva (1983). Derived temperatures, given in Table 2, are virtually identical to those in Thompson's (1976) calibration and with those of Martignole and Sisi (1981); correspondence with Aranovich and Podlesskii's (1983) temperatures is good to moderate.

Independent estimates of pressure may be made with the use of the garnet-plagioclase-aluminosilicate-quartz geobarometer, which derives from pressure dependency of Ca partitioning between garnet and plagioclase coexisting with aluminosilicate and quartz (Newton, 1983). Several versions of the geobarometer have been proposed (Brown and Earle, 1983); the one used here is by Newton and Haselton (1981), corrected as in Ganguly and Saxena (1984, p. 93, footnote). The geobarometer is critically dependent on the correctness of activity coefficients of grossular in garnet, which is typically Ca poor in the assemblages of interest, and of anorthite in plagioclase. Uncertainties inherent in the activity models, not to mention errors in analyses of minor elements, lead to errors of perhaps as much as 2×10^5 kPa. Furthermore, application of the geobarometer requires a temperature estimate be made.

Pressures obtained for coexisting plagioclase and garnet rims in the seven-phase cordierite gneisses from the Ellesmere-Devon terrane are presented in Table 2 for 600 and 700°C (500 and 600°C in the case of FS-77-216). Where anorthite determinations differ in any rock (never by more than 2 mole per cent), an average An content is used.

One data set uses the activity models of Newton and Haselton (1981), the other incorporates the garnet activity model of Ganguly and Saxena (1984). The former set comprises pressures ranging from 3.0 to 4.2×10^5 kPa at 600°C and 4.2 to 5.6×10^5 kPa at 700°C, values in reasonable agreement with those derived from cordierite-garnet equilibria. Pressures obtained using the Ganguly-Saxena activity model are systematically lower by 1 to 2×10^5 kPa and seem unreasonably low. It appears that combination of the "Al-avoidance" model of anorthite activity (Newton and Haselton, 1981) with the garnet activity model of Ganguly and Saxena (1984) leads to significant underestimates of pressure in rocks of the type found in the Ellesmere-Devon terrane.

On the assumption that core compositions have remained unaltered from an earlier stage in the metamorphic evolution of the cordierite gneisses, application of the garnet-plagioclase geobarometer to garnet cores should give insight into pressures prevailing nearer the peak of metamorphism. Assuming a temperature of 750°C, which seems reasonable (*see* also the section on metamorphic conditions of the quartzo-feldspathic gneisses, below), we obtain pressures ranging from 4.8 to 6.4×10^5 kPa, using Newton and Haselton's (1981) thermodynamic base (Table 3). Whereas pressures in Ellesmere and Coburg islands do not exceed 5.4×10^5 kPa, those in Devon Island range from 5.6 to 6.4×10^5 kPa. As will become apparent later in this report, paleopressures do indeed seem to have been generally higher in Devon Island than in the rest of the map area.

Pressure and temperature data from garnet-cordierite-sillimanite relations are graphically summarized in Figure 14.

Rock chemistry and origin

Twenty-one samples of cordierite gneisses from Ellesmere and Coburg islands have been chemically analyzed (Appendix, Table I). All contain the assemblage garnet-cordierite-sillimanite(-biotite)-feldspar(plagioclase and/or K-feldspar)-quartz. Coarse grained, strongly migmatitic rocks were excluded from analysis. A popular hypothesis for the origin of garnet-cordierite gneisses is that they are the residue of partial melting of pelitic rocks (Dostal, 1975; Harris, 1976; Lee and Holdaway, 1977; Sighinolfi et al., 1979), a process which would significantly modify the major and minor element chemistry.

Table 3. Pressures (kPa x 10^5) at 750°C of garnet-plagioclase-sillimanite-quartz assemblages, obtained from the geobarometer of Newton and Haselton (1981). Values in brackets are calculated using garnet activities of Ganguly and Saxena (1984). All pressures were calculated from garnet core compositions and average compositions of zoned plagioclase.

Ellesmere Island		Devon Island	
FS-77-216	5.4 (3.5)	FS-78-33	6.3 (5.0)
268	4.8 (3.8)	80-55	6.4 (5.4)
FSM-77-218-1	5.1 (4.8)	82-D-14	5.6 (4.4)
273-4	4.8 (5.0)		

The wide compositional range of the rocks analyzed is not unexpected considering their diverse textures and structures. Comparable scatter is evident in most compilations of chemical compositions of sedimentary rocks, e.g. Archean and Aphebian shales listed in Table I of the Appendix, and meaningful averages are difficult to calculate.

The cordierite gneisses show considerable scatter in the MgO-Na_2O-K_2O diagram (La Roche, 1965) but most lie in or near the field of shales and between the shale and arkose fields (Fig. 15). A similar affinity with shales and more siliceous compositions is also apparent in the CaO/MgO-SiO_2 diagram (Maccarrone et al., 1983) (Fig. 16). This diagram can also be used to assess the degree to which partial melting has been involved in the origin of the rocks: residua of partial melting should plot in the field of low CaO/MgO (due to enrichment of MgO relative to CaO) and SiO_2. Few samples plot in this region outside the field of unmetamorphosed shale and thus, by this criterion, the bulk of the cordierite gneisses are not residua of partial melting.

Neither do trace element abundances support a residual origin for the cordierite gneisses. Granitic melting should result in Rb entering the melt and Sr and Ba remaining in the residuum (McCarthy, 1976). Low Rb, Rb/Sr and K/Ba and high Sr, Ba and K/Rb are recorded from a number of granulite terranes (Clough and Field, 1980). The Ellesmere-Coburg cordierite gneisses, however, have K/Rb ratios closely comparable to those in unmetamorphosed crustal rocks (Fig. 17). Rb/Sr generally far exceeds the value of 0.12 for the continental crust as a whole, a value which itself is greater than that for the (presumably depleted) lower crust, 0.02 (Taylor and McLennan, 1985). K/Ba is also high, as in undepleted (K/Ba 51) and bulk crust (36) (Taylor and McLennan, 1985).

It is of interest to note that, although depletion of the large-ion lithophile elements (LILE: K, Rb, Sr, Ba, Zr, Th and the light rare earths) is widely held to be characteristic of granulite facies rocks (Clough and Field, 1980 and references therein), garnet-sillimanite(-cordierite) gneisses in granulite terranes generally do not show any significant such depletion. Migmatitic as well as non-migmatitic aluminous gneisses from Finnish Lapland (Barbey and Cuney, 1982), Calabria, southern Italy (Maccarrone et al., 1983) and Namaqualand, South Africa (Moore, 1983) have K/Rb, Rb/Sr and K/Ba ratios very like those of the continental crust as a whole. So do sillimanite(-garnet-cordierite) gneisses from Bahia, Brazil, which are specifically assigned a residual origin by Sighinolfi et al. (1979). The minimal change in these element ratios during high grade metamorphism is probably attributable mainly to the stability of K, Rb and Ba-retaining minerals in the rocks. Both K-feldspar and biotite are major constituents of both restite and melt fractions in high grade anatexis. The stability of these low K/Rb (biotite) and K/Ba (K-feldspar) phases promotes low K/Rb and K/Ba in the restite. Assumptions as to degree of partial melting based on these trace elements must, therefore, be made with caution.

The foregoing data suggest that the protolith of the cordierite gneisses was sedimentary and was not significantly modified by anatexis or dehydration. Further evidence of a sedimentary protolith is provided by the negative correlation of silica with other major elements, such as aluminium, iron and magnesium (Fig. 18), as is observed in detrital sediments (Hirst and Kaye, 1971; Barbey et al., 1982). Furthermore, the gneisses show K_2O exceeding Na_2O while MgO exceeds CaO, which is diagnostic of illite- and montmorillonite-rich argillaceous rocks (cf. Blackburn, 1974).

In summary, the chemical evidence points to shale as the main protolith of the cordierite gneisses. A number of gneisses are relatively silica-rich, suggesting that some of the argillaceous sediments were significantly psammitic. The apparently mature, fine grained and well sorted nature of the shaly sediments indicates a deep water environment of deposition. This environment contrasts with that envisaged for the quartzite and marble, viz. a shallower shelf(?) zone. The interleaving of rocks of the two environments could be interpreted as resulting from tectonic juxtaposition, possibly in a collision zone.

Orthopyroxene-bearing cordierite gneiss

Gneisses containing both cordierite and orthopyroxene have been found in only four, widely scattered places in the map area. All four occurrences are in migmatitic supracrustal sequences that include garnetiferous gneiss, pyribolite, marble and/or quartzite. Cordierite-orthopyroxene gneisses are mafic rocks with granitic layers and lenses, superficially similar to many of the garnet-sillimanite-cordierite gneisses with which they may be associated.

The two garnetiferous varieties found both show the breakdown of garnet to orthopyroxene and cordierite. In one rock (FSM-77-101-4), from southern Coburg Island (Map 1574A), rounded porphyroblasts of garnet, 0.5 to 1.5 cm in diameter, are rimmed by radiating vermicules of orthopyroxene in a matrix of coarse, partly pinitized cordierite (Fig. 19). Slightly pleochroic orthopyroxene also occurs in coarser grains, which are probably coalesced vermicules. Green spinel occurs symplectitically intergrown with some of the coarser orthopyroxene and as discrete grains irregularly distributed throughout cordierite.

Also present in this very coarse grained and mafic rock are reddish brown biotite, a little oligoclase (An_{27}) and minor, strained quartz.

The other garnetiferous sample (FSM-77-212), from 10 km west of the head of Jokel Fiord (Map 1572A), exhibits complex textures. The dark minerals — garnet, orthopyroxene, biotite and green spinel — occur in cordierite-bearing aggregates dispersed in a matrix of perthite, quartz, cordierite and minor plagioclase (An_{28}). The dark minerals are intergrown with cordierite: vermicular orthopyroxene in cordierite rims garnet and spinel is generally enclosed in cordierite. Some of the orthopyroxene is altered along crystal margins to greenish brown biotite. The occurrence and paragenesis of the dark minerals suggest that they have replaced an earlier mineral or mineral aggregate, such as sapphirine and sillimanite.

The leucocratic portion of this rock includes cordierite + quartz + spinel symplectites up to 5 mm long. These could represent breakdown of the high temperature and pressure assemblage, orthopyroxene + sillimanite.

The production of cordierite from garnet in these rocks is thought to have resulted from the reaction

2 garnet + 3 quartz = cordierite + 4 orthopyroxene

which contrasts with that in sillimanite-rich rocks,

garnet + 2 sillimanite = cordierite + spinel.

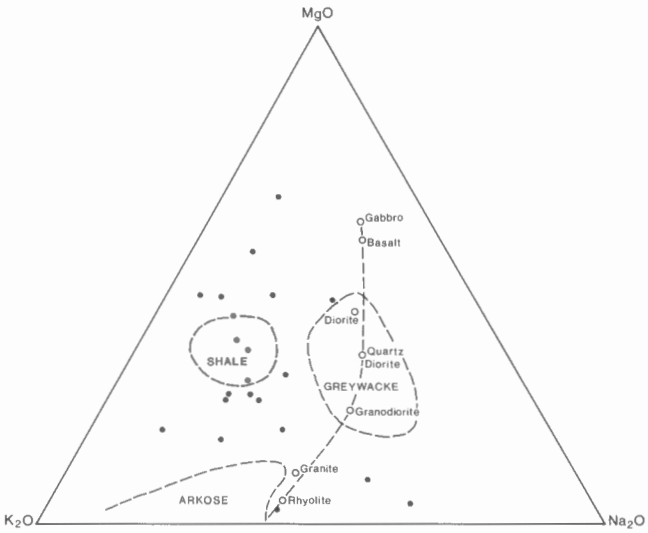

Figure 15. Orthopyroxene-free cordierite gneisses in La Roche's (1965) diagram, showing compositions of common crustal rocks in terms of MgO, Na_2O and K_2O. Weight per cent.

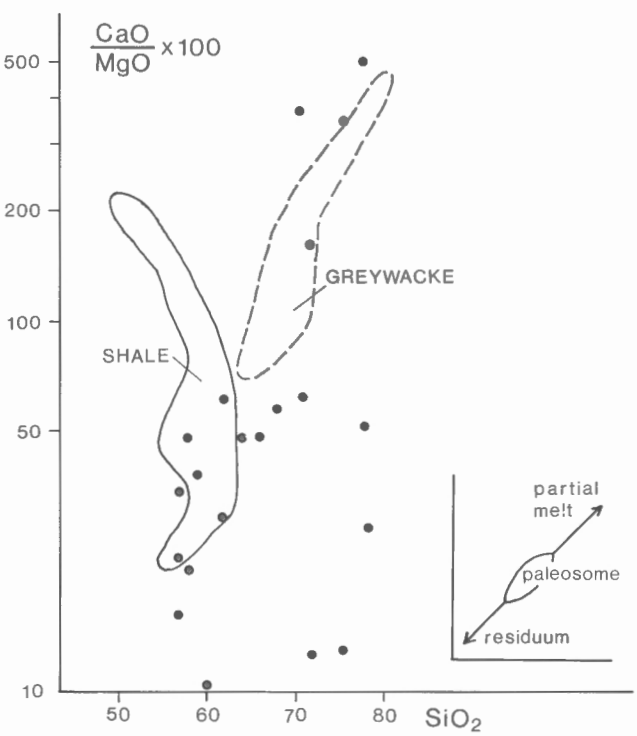

Figure 16. Orthopyroxene-free cordierite gneisses in Maccarrone et al.'s (1983) diagram, suggesting their compositional similarity to shale more than greywacke and only minor tendency toward a "residual" composition. Weight per cent.

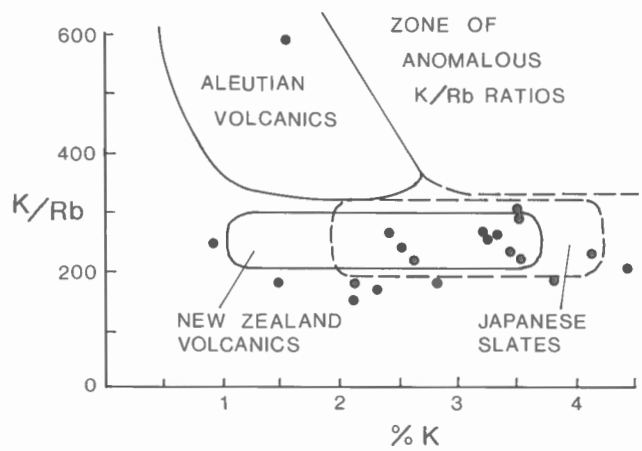

Figure 17. Orthopyroxene-free cordierite gneisses plot in the fields of common crustal rocks in Gray's (1977) diagram.

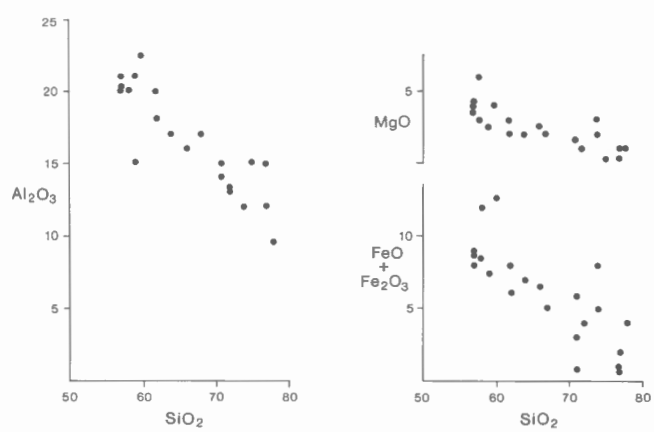

Figure 18. Harker plots of orthopyroxene-free cordierite gneisses. Note the strongly negative correlations. Weight per cent.

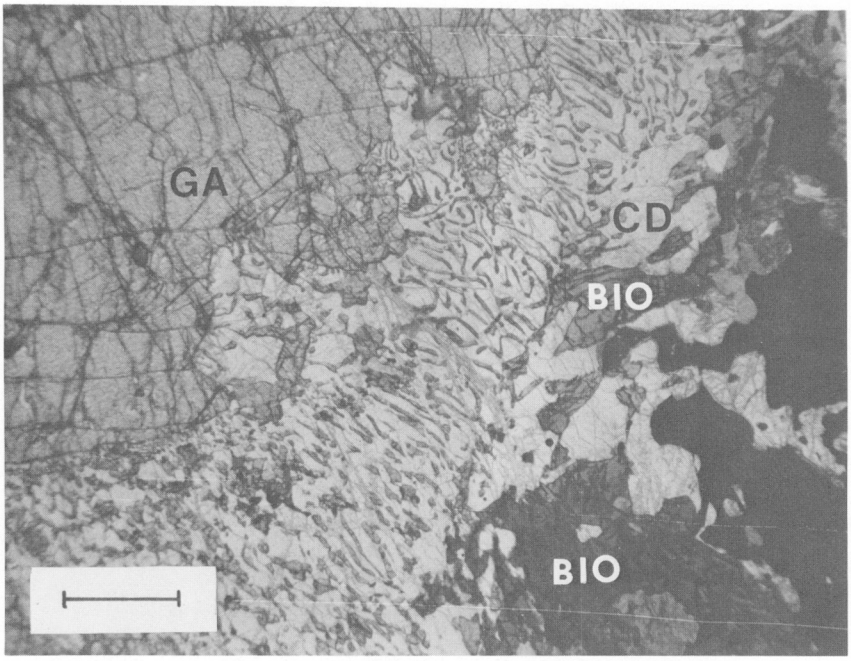

Figure 19. Symplectite of vermicular orthopyroxene and cordierite surrounding garnet, probably formed by the decompression reaction, 2 garnet + 3 quartz = cordierite + 4 orthopyroxene, in cordierite gneiss FSM-77-101-4. Plane light. Bar scale 0.5 mm.

The close association of rocks showing these reactions indicates that separation of quartz-saturated and sillimanite-saturated rocks can occur on a quite local scale. Clearly, in the Ellesmere-Devon terrane, alumina-rich sediments predominated over quartz-rich ones.

The other two gneisses with cordierite and orthopyroxene are garnet free but are interbedded with garnet-cordierite-sillimanite gneisses. Cordierite and orthopyroxene in these rocks appear to have grown in equilibrium: both minerals are abundant and coarse grained (1-4 mm).

One of the rocks, from northwest of the Devon Ice Cap, contains sericitized plagioclase and perthite, quartz and pale brown (magnesian?) biotite. The orthopyroxene is fresh but the cordierite is highly altered to sericite and fine grained muscovite.

The other rock (FS-80-84), from the east coast of Devon Island 13 km west of Cape Caledon, consists largely of abundant perthite, fresh cordierite, weakly pleochroic orthopyroxene and magnesian biotite; plagioclase is very minor, zircon is a common accessory and quartz is absent. One thin layer in the hand sample taken contains sapphirine, which has not been found elsewhere in the map area. The mineral forms elongate grains, 2-3 mm long, parallel to the foliation; a single tiny grain was seen under the microscope enclosed in a large cordierite crystal outside the sapphirine-bearing layer in the same thin section. The sapphirine is almost black in hand specimen and pleochroic in thin section, X = pale yellow, Z = blue. Every grain is rimmed by cordierite and some grains have an intervening, very thin, discontinuous rim of green spinel (Fig. 20). Textural relations (Fig. 20) suggest mantling of sapphirine by orthopyroxene, which subsequently reacted as follows:

sapphirine (7:9:3) + orthopyroxene =
cordierite + 7 spinel

Despite the abundance of aluminous rocks and the high metamorphic grade in the map area, the distribution of sapphirine appears to be severely restricted, due most likely to a scarcity of suitable parent rock compositions.

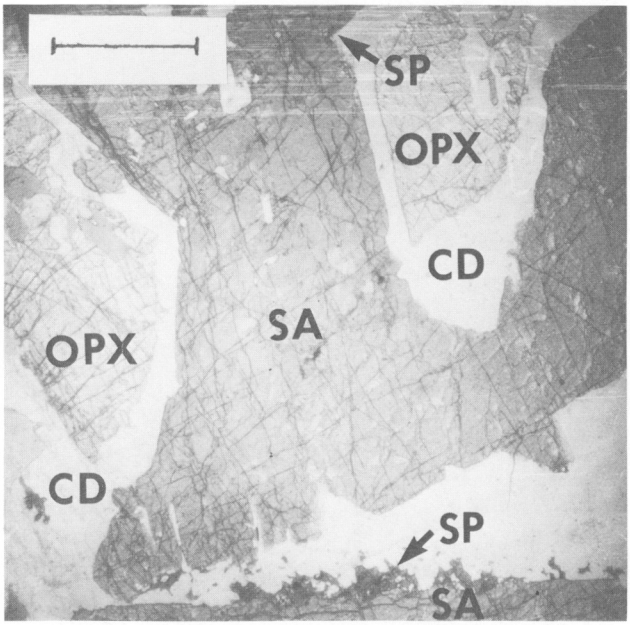

Figure 20. Sapphirine mantled by cordierite and minor spinel against orthopyroxene in Mg + Al-rich gneiss FS-80-84, east coast of Devon Island. The formation of cordierite from the reaction of orthopyroxene and sapphirine is another manifestation of decompression. Plane light. Bar scale 1.0 mm.

Mineral chemistry

Analyses of the minerals of the two garnetiferous and the sapphirine-bearing gneisses are given in Table 1B of the Appendix.

Garnetiferous gneiss. The garnets are pyrope-almandine (-spessartine) mixtures more magnesian than the typical garnets of the cordierite gneisses (Fig. 11). Zoning is pronounced in sample FSM-77-101-4, with Fe, Mn and Ca increasing from core to rim, as in the cordierite gneisses (Fig. 11, 21).

Orthopyroxene is aluminous hypersthene with 7% Al_2O_3. No compositional difference was detected between the vermicules intergrown with cordierite and the coarser discrete grains, which supports the interpretation that the coarse orthopyroxene formed by coalescing of vermicules.

Only in the sapphirine-bearing gneiss is cordierite as magnesian as that found in sample 101-4: Fe/Fe+Mg = 0.14. Cordierite in FSM-77-212 has Fe/Fe+Mg = 0.22, at the Mg end of the compositional range found in the cordierite gneisses.

The biotites have at least 18% MgO and those included in garnet of 101-4 contain up to 20%. TiO_2 ranges from 3 to 5%, the higher values being found in matrix biotite.

Spinel is a hercynite-spinel solid solution and shows compositional variation whose significance is uncertain. In 101-4 spinel of orthopyroxene-spinel symplectites is less magnesian than spinel in cordierite, possibly a result of late diffusion following symplectite growth. The opposite is true for 212, where spinel intergrown with orthopyroxene is more magnesian than spinel associated with cordierite. The more magnesian spinel may be a relic from the breakdown of a higher pressure-temperature phase such as sapphirine.

Sapphirine-bearing gneiss. Cordierite, biotite and plagioclase are comparable to their counterparts in the garnetiferous gneisses. However, orthopyroxene is iron-rich bronzite with 4% Al_2O_3 and spinel is also more magnesian (Fe/Fe+Mg = 0.55) than in the garnetiferous gneisses.

The sapphirine analysis was recalculated according to the method of Higgins et al. (1979). The sapphirine is iron-rich and, like the majority of sapphirines from granulite facies rocks (Higgins et al., 1979, Ackermand et al., 1982), falls between the compositions $2MgO.2Al_2O_3.SiO_2$ (2:2:1) and $7MgO.9Al_2O_3.3SiO_2$ (7:9:3) (Fig. 22).

Metamorphic conditions

Garnetiferous gneiss. Orthopyroxene+cordierite coronas around garnet have been described from a number of localities and are generally recognized as indicating relatively low pressures of formation (Berg, 1977; Schreyer and Abraham, 1978; Lonker, 1980; Van Reenen, 1983). Hensen and Green (1973) have studied the reaction

2 garnet + 3 quartz = cordierite + 4 orthopyroxene

experimentally at P-T conditions relevant to the granulite facies. They presented a P-T diagram of Mg-isopleths for garnet and cordierite in the presence of orthopyroxene. It should be noted that the diagram involves considerable extrapolation of experimental data across a wide range of pressure and temperature and is based on a negative slope for the breakdown reaction of cordierite to garnet + sillimanite + quartz.

Assuming that the rims of garnets were in equilibrium with cordierite and hypersthene, we obtain 580 and 620°C and 8.1 and 6.0 × 10^5 kPa for samples FSM-77-101-4 and 212, respectively. The conditions obtained for 101-4 are suspect, due to intersection of the isopleths well beyond the low temperature limit of Hensen and Green's (1973) diagram.

Application of Vielzeuf's (1983) model based on spinel-cordierite equilibrium yields 608°C and 8.8 × 10^5 kPa for 101-4 and 705°C and 7.5 × 10^5 kPa for 212 (in each instance, the composition of the spinel directly associated with cordierite was used). The low temperatures indicated for these rocks renders successful application of Vielzeuf's model unlikely because his calibration is based on considerably higher temperatures.

Temperatures indicated by Thompson's (1976) calibration of garnet-cordierite equilibria essentially agree with Hensen and Green's and, in the case of 101-4, Vielzeuf's temperatures: 610°C for 101-4 and 615°C for 212.

Expressions derived solely from thermochemical data relating compositions of mafic phases to pressure of the reaction

garnet + quartz = cordierite + orthopyroxene

have been formulated by Harris and Holland (1984). One expression relates to the Mg end-member reaction (equilibrium 3 of Harris and Holland, 1984, Table 3), the other takes Fe into account (p. 1043). Using the activity models of Newton (1983) and assuming T = 650°C, we obtain 3.6 and 3.7 × 10^5 kPa for 101-4. In the case of 212, results diverge: 2.0 × 10^5 kPa for the Mg reaction and 3.2 × 10^5 kPa for the Fe-Mg equilibrium.

These low pressures, at relatively high temperatures, signify decompression conditions in the same way that the garnet + sillimanite = cordierite + spinel reaction does in the less magnesian pelitic gneisses.

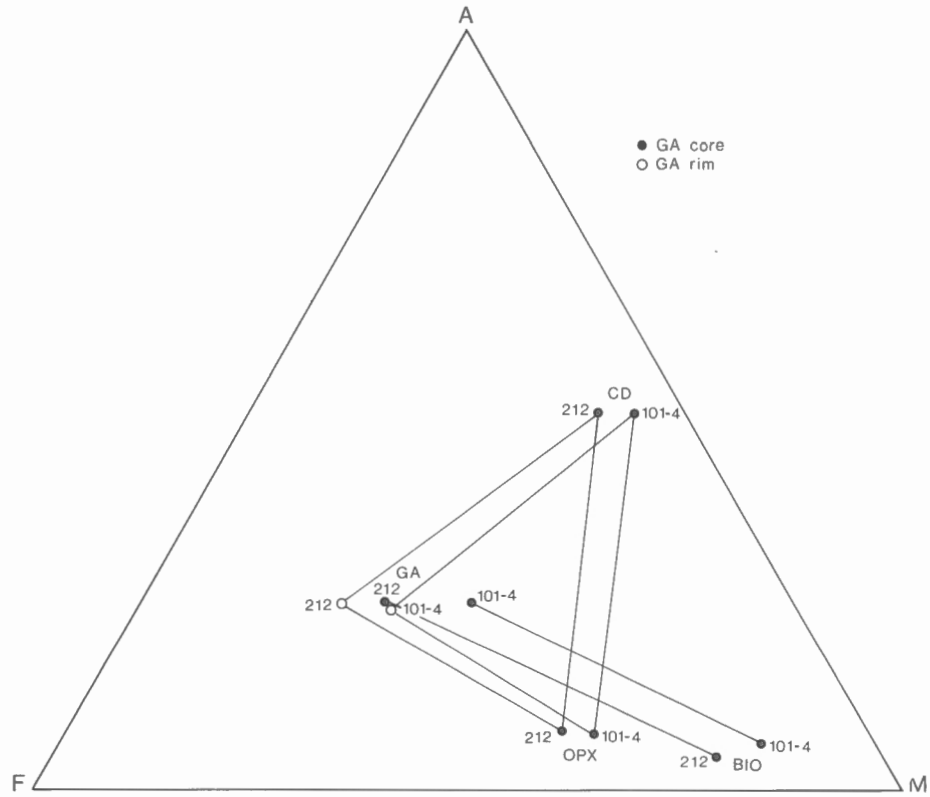

Figure 21. Sapphirine-free orthopyroxene-cordierite gneisses (FSM-77-101-4 and 212) in the metamorphic AFM diagram. Orthopyroxene and cordierite have formed by garnet reacting with quartz. Mole per cent.

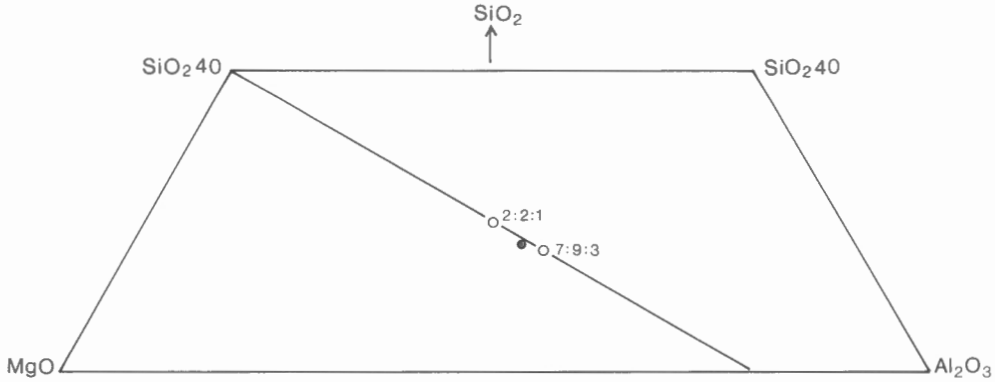

Figure 22. The composition of sapphirine (black dot) of orthopyroxene-cordierite gneiss FS-80-84 in Higgins et al.'s (1979) diagram is intermediate between the $2MgO.2Al_2O_3.SiO_2$ and $7MgO.9Al_2O_3.3SiO_2$ compositions. Mole per cent.

Sapphirine-bearing gneiss. Experimental work in the MgO-Al_2O_3-SiO_2 system (Seifert, 1974) has shown that the assemblage sapphirine+enstatite, stable at high pressure, breaks down to cordierite+spinel at low pressure (less than 4×10^5 kPa). Although the effect of Fe on mineral stabilities is difficult to quantify, petrographic and theoretical studies all confirm that this breakdown is favoured by a pressure drop, commonly during retrograde metamorphism (Hermans et al., 1976; Ellis et al., 1980; Ackermand et al., 1982; Droop and Bucher-Nurminen, 1984).

Hermans et al. (1976) described a sapphirine-bearing rock from southwestern Norway with a mineralogy very similar to the sample from Devon Island; the similarity extends even to the mineral chemistry (except that the Norwegian orthopyroxene has 9 % Al_2O_3). The Norwegian rock also comes from a granulite facies migmatite terrane with abundant garnet-cordierite-sillimanite gneisses and orthopyroxene-bearing quartzofeldspathic rocks. Hermans et al. concluded that sapphirine+orthopyroxene is a relic of an earlier stage of metamorphism under a pressure of 3 to 6×10^5 kPa at a temperature of 900°C and that the cordierite + spinel replacement formed at lower pressure and temperature.

In discussing Fe-poor sapphirine-bearing rocks from the Limpopo Belt of southern Africa, Ackermand et al. (1982) suggested pressures of 3 to 4×10^5 kPa for the breakdown of orthopyroxene + sapphirine to cordierite+spinel.

Droop and Bucher-Nurminen (1984) have made a detailed study of sapphirine-bearing rocks from the Gruf Complex of migmatitic gneisses in Italy (including garnet-cordierite-sillimanite gneiss). Petrographic evidence and thermodynamic calculations led them to conclude that cordierite-producing breakdown reactions of Fe-bearing sapphirine occurred during a nearly isothermal decompression that reached $5 \pm 1 \times 10^5$ kPa at 750 ± 100°C.

A temperature of 700°C and a pressure of 4.5×10^5 kPa would appear to be a reasonable estimate of the retrograde conditions under which the orthopyroxene-sapphirine-cordierite gneiss from Devon Island formed.

Pyroxene-bearing quartzofeldspathic gneiss

Of all the rock groups in the map area, the pyroxene-bearing quartzofeldspathic rocks are the most difficult to subdivide into map units. They tend to have the dark, weakly gneissic, rather homogeneous appearance so characteristic of granulite facies quartzofeldspathic rocks. Their colours are brown or red on weathered surfaces and greasy green or, less commonly, grey on fresh surfaces. A complete gradation exists between strongly gneissic and completely massive rocks, with the majority falling between the two extremes. As grain size tends towards the coarse and platy minerals are generally scarce, foliation is commonly not readily apparent from a distance. Quartzofeldspathic rocks termed gneisses in this report are those with a moderate to well defined gneissic structure that was recognized in the field. Such structure is most commonly expressed by quartz-rich layers and elongate lenses or by aligned quartz ribbons (*Plättung* quartz). In more mafic gneisses, hornblende- and biotite-rich layers define the gneissosity. Because of the difficulties just outlined and the fact that all later intrusive granitoid rocks are pre- or syntectonic and therefore commonly crudely gneissic, quartzofeldspathic gneisses shown on the map undoubtedly include in part rocks that properly belong to the intrusive orthopyroxene tonalite-granodiorite- granite suite.

The modal composition of the gneisses ranges from orthopyroxene quartz norite to orthopyroxene granite (following the classification scheme in Fig. 23). Tonalite compositions predominate and monzonitic to syenitic rocks are comparatively rare. The chief mineral assemblages are listed in Table 4 and modal compositions in terms of feldspar and quartz are plotted in Figure 24.

The gneisses doubtless include both infra- and supracrustal varieties but field criteria for distinguishing them are virtually absent. As most of the gneisses are associated with metasediments, it may be inferred that they are largely of supracrustal origin. Quartzofeldspathic gneisses that are actually interlayered with metasediments or have partly metapelitic mineralogy (abundant garnet, K-feldspar and biotite) are very likely to be supracrustal (e.g. tuffs or feldspar-rich sandstones). Locally on Devon Island, metasediments and gneisses are so closely associated that they have been mapped as a single unit, mg. The predominance of tonalitic gneiss containing little or no K-feldspar suggests that most of the gneisses are meta-igneous but whether originally extrusive or intrusive is uncertain.

Few outcrops of quartzofeldspathic gneiss are free of granitic or pegmatitic veining. These pink or white veins commonly contain orthopyroxene and locally may be garnetiferous. Although clearly late, their mineralogy indicates that they formed during granulite facies metamorphism. In contrast to the metasedimentary aluminous

Table 4. Mineral assemblages of the pyroxene-bearing quartzofeldspathic gneisses.

Quartz + plagioclase + biotite + orthopyroxene (+ hornblende)
Quartz + plagioclase + biotite + orthopyroxene + clinopyroxene (+ hornblende)
Quartz + plagioclase + biotite + orthopyroxene + garnet (+ hornblende)
Quartz + plagioclase + orthopyroxene + clinopyroxene + garnet (+ biotite + hornblende)
Quartz + perthite + biotite + orthopyroxene + garnet (+ plagioclase)
Quartz + perthite + orthopyroxene + clinopyroxene + hornblende (+ biotite)
All assemblages contain Fe-Ti oxide (chiefly ilmenite).

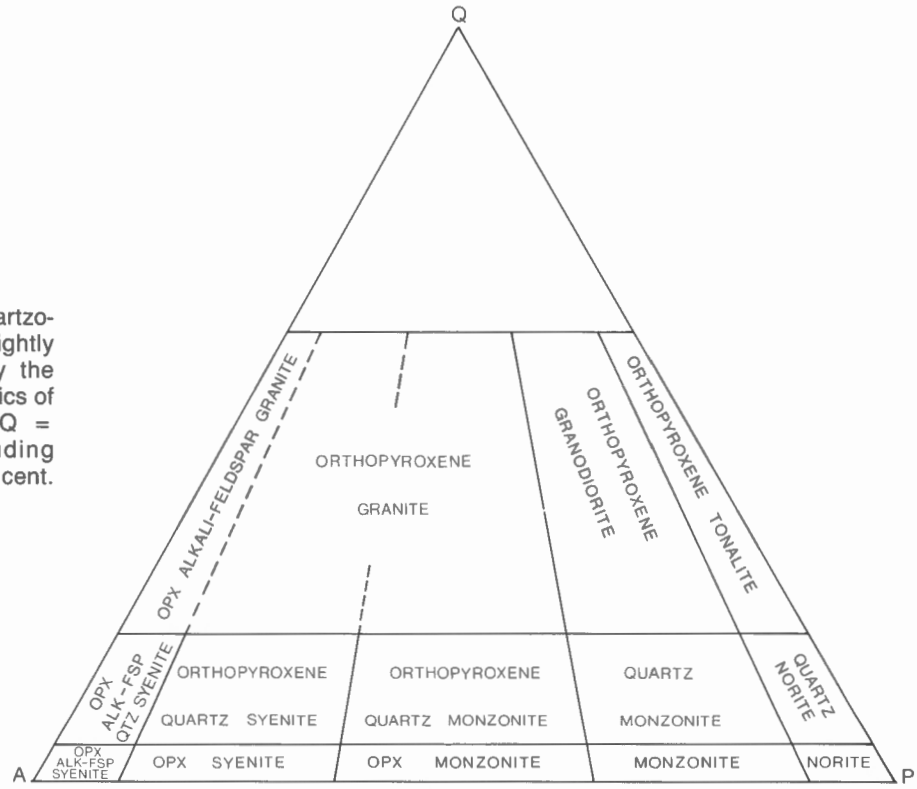

Figure 23. Modal classification of quartzofeldspathic granulite facies rocks, slightly modified from that recommended by the IUGS Subcommission on the Systematics of Igneous Rocks (Streckeisen, 1976). Q = quartz, A = alkali feldspar (including perthite), P = plagioclase. Volume per cent.

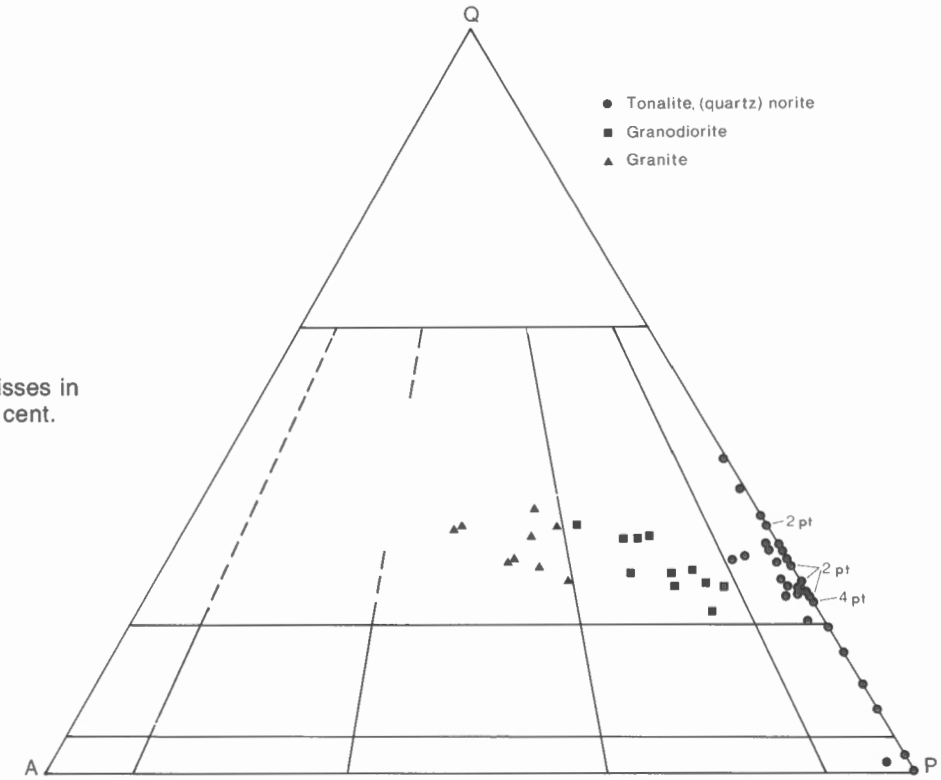

Figure 24. Quartzofeldspathic gneisses in the IUGS classification. Volume per cent.

gneisses, migmatite is not developed to any significant extent in the quartzofeldspathic gneisses except in some strongly retrograded rocks. Outcrops showing abundant veining were mapped as unit gnv.

Retrogression of the quartzofeldspathic gneisses is marked mainly by the replacement of orthopyroxene by secondary minerals and the microclinization of K-feldspar. Orthopyroxene is replaced by a fine grained aggregate of green biotite and chlorite (locally also carbonate), the replacement starting along cracks and then spreading through the rest of the grain. Changes in K-feldspar begin with the appearance of diffuse grid twinning indicative of incipient microclinization, which becomes progressively better developed with increasing retrogression. Granitic veining appears to have accompanied retrogression in many places.

Krupička (1973) made a detailed petrographic study of the retrogression of orthopyroxene tonalite gneiss in Truelove Lowland, northern Devon Island. He traced the transformation of fresh gneiss into a pink amphibolite facies granitic rock containing no hypersthene, plagioclase of reduced anorthite content, and significant growth of discrete microcline.

What are termed retrograded orthopyroxene-bearing gneisses (unit gnr) in this report are rocks which show incomplete replacement of orthopyroxene and incipiently microclinized feldspar and which retain the greenish to dull pinkish weathering colour that characterizes granulite and retrograded granulite facies rocks.

Orthopyroxene tonalite gneiss (tg, gn, gnv, gnr)

Orthopyroxene tonalite gneisses fall into two major groups: relatively felsic rocks (colour index less than 20) with orthopyroxene and biotite (and, rarely, garnet) as the only mafic silicates and more mafic rocks (colour index 20-50) in which hornblende and clinopyroxene may also be present and which grade through quartz norite into orthopyroxene diorite composition.

Rocks of the felsic group are typically characterized by the simple mineral assemblage, orthopyroxene-biotite-quartz-plagioclase-Fe-Ti oxide. The rare garnetiferous gneisses are described separately below. Grain size, texture and intensity of gneissic layering may differ but the differences are generally ascribable to variations in the degree of deformation. The majority of the rocks have an equigranular granoblastic texture in which the grains have gently curved or embayed boundaries; grain size is 1 to 2 mm. The remainder are fine grained rocks showing inequigranular granoblastic texture and embayed and serrated grain boundaries; grain size is 0.6 to 1 mm.

Orthopyroxene in the felsic gneisses is characteristically strongly pleochroic with X = deep pink and Z = green with a blue tinge. It is generally fresh but in some rocks is altered along cracks and margins to a yellowish mixture of biotite and chlorite. Reddish or chestnut-brown biotite tends to be associated with orthopyroxene but there is no obvious genetic relationship between them. Plagioclase composition ranges from An_{27} to An_{50} with values of $An_{33\pm2}$ being most common. Plagioclase is unzoned but generally shows irregularly developed bead or string antiperthite. Potassium feldspar, if present, forms poorly perthitic grains interstitial to plagioclase and quartz; shadowy microcline twinning is locally seen. Quartz is commonly a subordinate mineral, irregularly distributed and locally forming ribbons. Accessory minerals include apatite and Fe-Ti oxide.

Mafic orthopyroxene tonalite gneisses in thin section show well developed equigranular granoblastic texture in which medium sized grains have gently curved boundaries meeting at 120° angles. Orthopyroxene, pleochroic in pink and green but less intensely than in the felsic gneisses, is the only essential mafic silicate but is generally accompanied by red-brown biotite. Two other mafic silicates are also commonly present: olive-green or brownish green (Z colour) hornblende and pale green clinopyroxene. Garnet is found in some clinopyroxene-free gneisses on Devon Island. Although the mafic silicates may be aggregated, they show little evidence of being genetically related through replacement or alteration. In a few rocks, minor partial replacement of clinopyroxene by olive or brownish green hornblende appears to have occurred. Plagioclase is well twinned with broad lamellae and in some rocks is zoned. Compositions lie in the range from An_{40} to An_{56}. Quartz is a very subordinate mineral rarely exceeding 5 % by volume, so that most of these rocks are properly termed orthopyroxene diorite gneiss. Apatite and Fe-Ti oxide are the main accessory minerals.

Some quartz-poor, two-pyroxene, mafic gneisses in southern Devon Island contain appreciable scapolite as an accessory mineral. The scapolite occurs interstitially to plagioclase and appears to be a primary mineral.

Although garnet is abundant in the associated metasediments, it is uncommon in the orthopyroxene tonalite gneisses. However, because of their potential for providing information on pressure and temperature of metamorphism, garnetiferous pyroxene gneisses are accorded particular attention.

Two felsic garnet-bearing gneisses have been examined in detail. The first (FSM-77-114-1), from the east coast of Coburg Island, is an inequigranular gneiss with abundant fresh, weakly pleochroic orthopyroxene, chestnut biotite and garnet in highly embayed and spongy, but otherwise fresh, crystals rich in quartz and biotite inclusions. The garnet crystals are up to 6 mm in diameter, much coarser than the orthopyroxene and biotite. Plagioclase is well twinned, normally zoned, An_{49-46}, and free of antiperthite. A modal analysis of this rock is given in Appendix, Table II.

The second garnet gneiss (FSM-77-63-9) comes from an assemblage of metasedimentary and metaigneous rocks 15 km north of the mouth of Makinson Inlet. The assemblage includes quartzite, marble, garnet-sillimanite gneiss, pyribolite and ultramafite sheets, orthopyroxene tonalite gneiss, garnetiferous granite, and pegmatite. The garnet gneiss consists of strongly and irregularly zoned andesine-labradorite, garnet, orthopyroxene, red-brown biotite,

quartz, green spinel, and Fe-Ti oxide. Garnet and orthopyroxene, which is moderately pleochroic, are medium grained (3-4 mm) and fresh. Rounded grains of green spinel are abundant is some garnet crystals. A few garnets contain nests of tiny sillimanite needles. Although an equilibrium association cannot be demonstrated, the coexistence of early-formed sillimanite and coarse, primary orthopyroxene suggests high temperature and pressure (Newton, 1978).

An example of a mafic garnet-orthopyroxene tonalite gneiss belongs to a sequence of tonalitic gneisses and pyribolite near Cape Sherard, southeastern Devon Island. The rock (FS-82-D-7D) is made up of well-twinned calcic plagioclase, quartz (some of it in ribbon form), garnet, orthopyroxene, red-brown biotite and Fe-Ti oxide. All the minerals are fresh and intergrown in a well developed inequigranular granoblastic texture. Garnet (0.5-2 mm) is almost colourless and orthopyroxene (0.02 - 0.05 mm) is very weakly pleochroic.

Mineral chemistry

Garnet-free gneiss. Minerals of nine orthopyroxene tonalite gneisses (including four mafic varieties) free of garnet have been analyzed; analyses are tabulated in Appendix, Table 2A.

Orthopyroxene. Zoning was not detected in orthopyroxene.

All but one of the orthopyroxenes of the five felsic gneisses analyzed are hypersthenes ranging from $Fe_{53}Mg_{47}$ to $Ca_1Fe_{34}Mg_{65}$; the fifth is bronzite $Fe_{29}Mg_{71}$ (Fig. 25). They generally are distinguished from orthopyroxenes of the mafic gneisses by higher Al_2O_3 content, 2.7 to 6.5 %, and more marked pleochroism, the intensity of which correlates positively with alumina content. One of the felsic gneisses contains clinopyroxene and the coexisting orthopyroxene has only 0.8 % Al_2O_3.

Orthopyroxene in the mafic gneisses is hypersthene $Ca_1Fe_{48}Mg_{51}$ to $Ca_1Fe_{34}Mg_{65}$ and ferrohypersthene $Ca_1Fe_{63}Mg_{36}$ with 0.8 to 1.3 % Al_2O_3 and weak pleochroism. The low-alumina orthopyroxenes have insufficient aluminium to fill, along with silicon, the tetrahedral site and all the orthopyroxenes have high cation totals, 4.04 to 4.05 (based on 6 oxygen atoms and assuming all Fe to be Fe^{2+}). Both features imply appreciable Fe^{3+} (Robinson, 1980) and, indeed, recalculation of the analyses on the basis of 4 cations results in 0.106-0.148 Fe^{3+} per formula unit. The bulk analysis of only one of the nine tonalite gneisses is available — the two-pyroxene felsic gneiss FSM-77-104 — and this rock contains significant ferric iron, Fe_2O_3/FeO being 0.5 (Appendix, Table II).

Clinopyroxene. Clinopyroxene occurs mainly in the mafic gneisses. It is compositionally more restricted than orthopyroxene and in four samples (including one felsic gneiss) ranges from $Ca_{44}Fe_{14}Mg_{42}$ to $Ca_{44}Fe_{19}Mg_{37}$ (Fig. 25) with less than 0.4 % Na_2O. The clinopyroxene in the felsic gneiss is slightly and irregularly zoned but the clinopyroxene of the other rocks appears homogeneous.

Clinopyroxenes and coexisting orthopyroxenes show sympathetic regular chemical variations and a plot of Fe/Fe +Mg ratios (Fig. 26A) suggests equilibrium between the two minerals, supporting the evidence from textural relations. The distribution coefficient

$$K_D = (Fe/Fe+Mg)_{opx}/(Fe/Fe+Mg)_{cpx}$$

where Fe = total Fe as Fe^{2+}, is 1.3 ± 0.1. K_D's calculated using Fe = Fe^{2+} only range from 1.16 to 1.54 for igneous rocks and 1.54 to 1.96 for metamorphic rocks (Deer et al., 1978, p. 64). Recent analyses of coexisting pyroxenes of similar composition and from rocks comparable to those of the Ellesmere-Devon granulite terrane yield K_D values corrected for Fe^{3+}, that, for the most part, fall between 1.4 and 2.4 (Coolen, 1980; Raith et al., 1983; Stephenson, 1984). Coolen (1980) has clearly shown how critically the absolute value of the Fe-Mg distribution coefficient depends on the ferric/ferrous ratio: K_D's calculated from total Fe data from a large number of pyroxene pairs from the Furua Granulite Complex of Tanzania range from 1.20 to 1.56 but

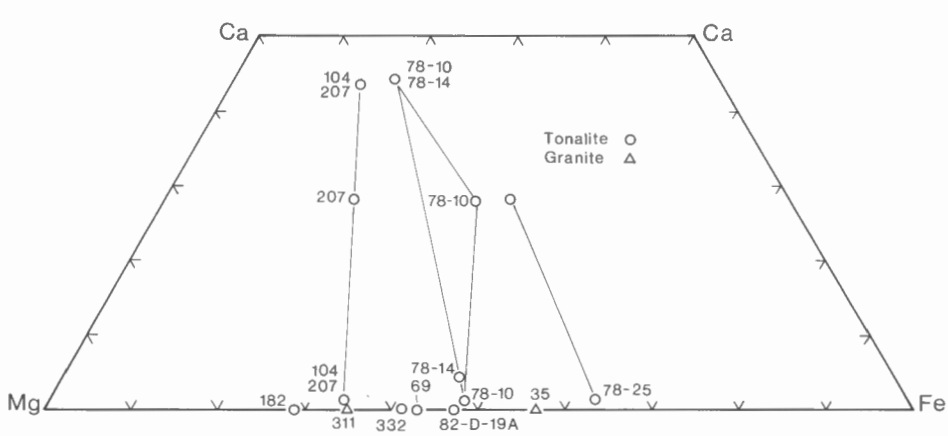

Figure 25. Composition of pyroxenes and amphibole (central part of diagram) of garnet-free quartzofeldspathic gneisses in terms of Ca, Mg and Fe. Atom per cent.

when corrected for Fe^{3+} the range becomes 1.40 to over 2.50 (the very high values are thought by Coolen to be due to overcorrections). Similar marked changes in K_D are apparent in Raith et al.'s and Stephenson's data. These results provide further indirect evidence of significant Fe^{3+} in the Ellesmere-Devon pyroxenes.

Amphibole. Amphibole tends to occur only in the mafic orthopyroxene tonalite gneisses and has been analyzed in three such rocks. The analyzed amphiboles are calcic hornblendes relatively rich in magnesium. When their analyses are recalculated and classified according to Rock and Leake (1984) (Appendix, Table 7), two of the hornblendes, which are broadly similar in composition, are termed ferrian magnesio- hornblende and potassium ferrian tschermakitic hornblende; the third, which coexists with ferrohypersthene, is potassian magnesian hastingsite plotting very close to the hornblende field. Calculated ferric iron contents expressed as 100 $Fe^{3+}/Fe^{3+}+Fe^{2+}$ are 56, 40 and 32. These are relatively high values for granulite facies hornblendes, which generally are lower than 20 (Coolen, 1980; Jan and Howie, 1982).

On the evidence of regular Fe-Mg distribution between hornblende and orthopyroxene (Fig. 26B), two of the three mineral pairs analyzed crystallized in equilibrium.

Biotite. Biotite in both felsic and mafic gneisses is markedly titaniferous, TiO_2 ranging from 4.7 to 6.5 %. Fe/Fe+Mg of biotite is generally about 0.3 in the felsic, and 0.4 to 0.5 in the mafic gneisses, correlating with pyroxene composition. Fe/Fe+Mg distribution between biotite and pyroxene (Fig. 26C) shows considerable scatter. Although the scatter might be due to analytical uncertainties, such as significant Fe^{3+} in the minerals, it is noteworthy that similarly irregular distribution of Fe and Mg in orthopyroxene-biotite pairs is found in granulite facies rocks from several localities worldwide (Leelanandam, 1970). Fe-Mg partitioning between biotite and hornblende seems more regular but only three mineral pairs have been analyzed (Fig. 26D).

Plagioclase. The composition of plagioclase ranges widely in these rocks, from An_{29} to An_{49}. There is no systematic difference in An content between plagioclase of felsic and mafic gneisses. Zoning, if present at all, is not pronounced.

Garnetiferous gneiss

Mineral analyses are listed in Appendix, Table 2B. A bulk chemical analysis of FSM-77-114-1 is included in Appendix, Table II.

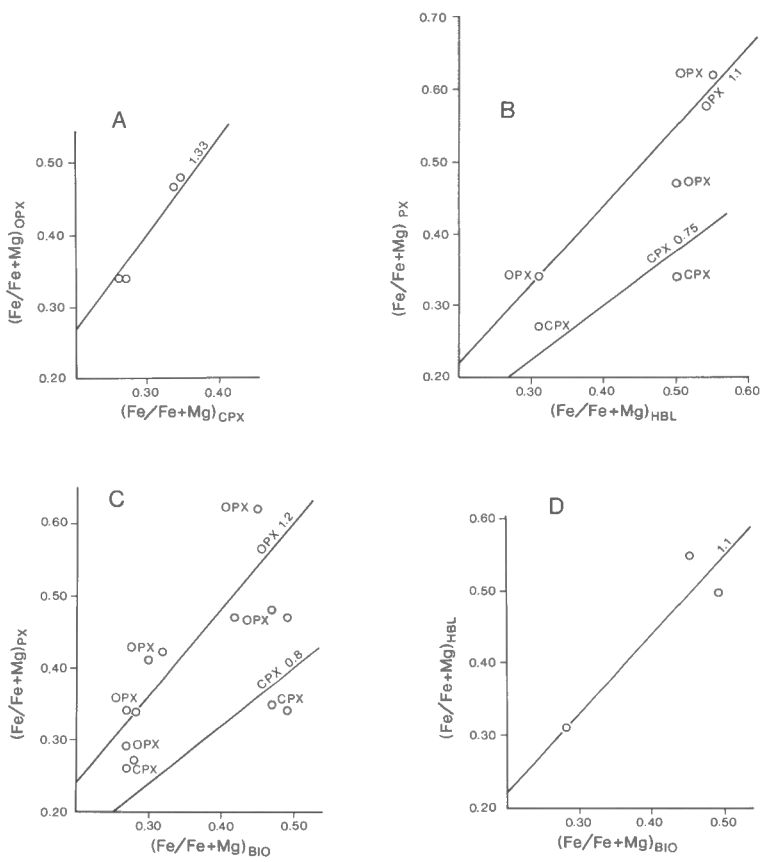

Figure 26. Fe-Mg (atomic) distribution between coexisting mafic silicates of garnet-free tonalitic gneisses. Lines are drawn for various distribution coefficients as marked.

Garnet in the three gneisses analyzed is essentially a pyrope-almandine mixture (about 60 to 70 mole per cent almandine+spessartine), more magnesian than garnet in the majority of cordierite gneisses (Fig. 11). In zoned grains, rims are slightly Fe-richer and Ca-poorer than cores (Fig. 11). Manganese content is negligible (less than 1.4% MnO).

Orthopyroxene is hypersthene $Fe_{37-44}Mg_{63-56}$ (Fig. 27) with Al_2O_3 ranging from 2.4 to 4.9% (in sillimanite-bearing gneiss). Zoning was not detected.

Biotite shows a range of composition and is markedly heterogeneous (inter-grain variability) in FSM-77-114-1. Fe/Fe+Mg ratios of biotite outside garnet fall between 0.3 and 0.4 but biotite included in garnet is more magnesian (Fe/Fe+Mg = 0.2). TiO_2 exceeds 4% and the red-brown biotite in the mafic gneiss from Devon Island has nearly 7% TiO_2.

Generally, plagioclase is relatively calcic in these rocks, ranging from calcic andesine to bytownite and is virtually free of orthoclase component. Slight normal zoning, from An_{49} to An_{46}, was measured in FSM-77-114-1. Plagioclase in the sillimanite-bearing gneiss shows extreme and irregular zoning within and between grains: 35 to 51 mole per cent An and about 2 mole per cent Or. Compositions as K-rich as 15% Or were measured. Compositions could not be related to cores and rims so the direction of zoning is unknown.

Rock chemistry and origin

Chemical analyses of 18 "felsic" (colour index less than 20) and 3 "mafic" (C.I. 20-50) orthopyroxene tonalite-quartz norite gneisses are listed in Table II of the Appendix.

The felsic varieties, with few exceptions, have SiO_2 greater than 65, Al_2O_3 greater than 15, CaO and Na_2O greater than 4, and K_2O less than 1.5 weight per cent. Most of them plot in the tonalite field of O'Connor's (1965) ternary classification scheme as modified by Barker (1979) (Fig. 28). They follow Barker and Arth's (1976) trondhjemitic trend in the AFM diagram (Fig. 29) and Na-enrichment paths in the Ca-Na-K (Fig. 30) and K_2O-MgO-Na_2O (Fig. 31) triangles. Although the average of the 21 gneisses is chemically comparable to calcic trondhjemite as defined by Barker (1979), it does have significantly more iron and magnesium. The average gneiss is more siliceous and less ferromagnesian, calcic and potassic than the average tonalite of Le Maitre (1976). Except for low K_2O, the average is not dissimilar in major element abundances to Le Maitre's (1976) average dacite (Appendix, Table II). Lastly, the gneisses are chemically not unlike greywackes of island arcs, which, compared to sandstones of other tectonic settings, have relatively low SiO_2 and K_2O and high Al_2O_3 and (Fe_2O_3t+MgO) (Bhatia, 1983); an appropriate example of such a sediment is listed in Appendix, Table II. Again, however, low K_2O sets the gneisses apart from sandstones of similar SiO_2 content tabulated by Bhatia (1983).

As might be expected from their K-poor nature, Rb in the gneisses is low; in only one rock does Rb exceed 80 ppm and in most rocks is much less. A plot of K vs. Rb (Fig. 32) shows the flat trend characteristic of low-K granulite facies rocks (Rudnick et al., 1985). Although the majority of the rocks have K/Rb greater than the upper crustal average of about 250, only seven have K/Rb greater than 500 (maximum 854); average K/Rb is 253.

Average Rb/Sr, 0.07, and K/Ba, 18, are lower than the average bulk (upper and lower) crustal values, 0.12 and 36, respectively, given in Taylor and McLennan (1985, Table 3.5). In fact, these two ratios are closer to values for the lower (presumably depleted) crust, as estimated by Taylor and McLennan (1985, Table 4.4): Rb/Sr 0.02 and K/Ba 19. Average Rb/Sr and K/Ba in K- and Rb-poor granulite facies acid rocks assumed to be of lower crustal origin are: Scourian Complex, Scotland, 0.03 and 12 (Weaver and Tarney, 1983); Enderby Land (Napier Complex), East Antarctica,

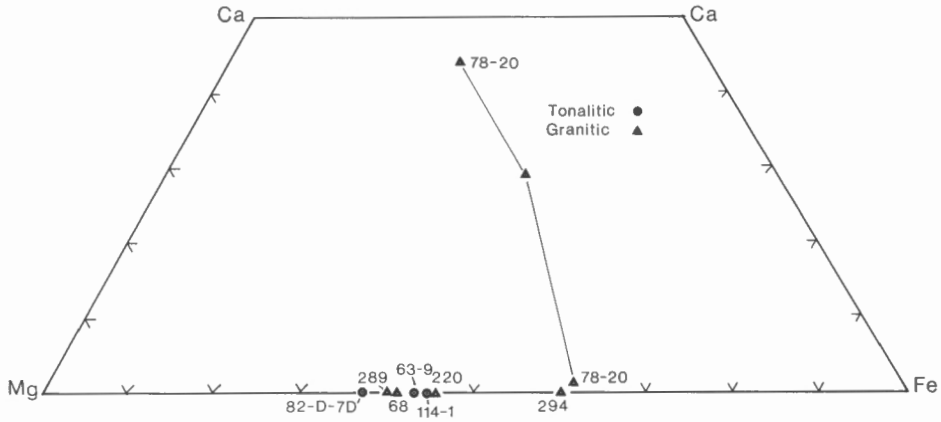

Figure 27. Composition of pyroxenes and amphibole of garnetiferous quartzofeldspathic gneisses. Atom per cent.

0.039 and 13 (Sheraton and Black, 1983); Qianxi Group, China, 0.016 and 21 (Jahn and Zhang, 1984).

A variety of unmetamorphosed intermediate to acid rocks, in particular calc-alkaline volcanics, exhibit K/Rb well above the crustal average (Rudnick et al., 1985). For example, low-K dacites of island arcs have high K/Rb (500 to 800+) and low Rb/Sr (about 0.05) (Ewart, 1979). None of the Ellesmere-Coburg tonalitic gneisses plots in Gray's (1977) "zone of anomalous K/Rb ratios" (Fig. 33). Nevertheless, there does exist (Fig. 32), for gneisses with K/Rb greater than 200, a trend of decreasing Rb with decreasing K and the commonly very low levels of K do suggest some depletion of Rb, widely regarded as characteristic of granulite facies rocks (Rudnick et al., 1985). However, the degree of depletion is far less than for low-K acid rocks in the granulite terranes of the Scourian complex (Weaver and Tarney, 1983), Enderby Land (Sheraton and Black, 1983) and Qianxi Group (Jahn and Zhang, 1984), in which K/Rb ratios exceeding 1000 are common. It is interesting to note that the average K/Rb of the Ellesmere-Coburg gneisses (253) is comparable to that of pyroxene gneisses from Bahia, Brazil, 237 (Sighinolfi et al., 1979), and from the Lapland Granulite belt, Finland, 271 for rocks of dacitic composition (Barbey and Cuney, 1982). In all these instances, the gneisses are associated with sillimanite (-garnet-cordierite) gneisses showing little or no LILE depletion (*see* the section on cordierite gneisses above).

In summary, the low levels of K and Rb in the Ellesmere-Coburg orthopyroxene tonalitic gneisses could signify limited depletion of these elements after protolith emplacement, presumably during high grade metamorphism. Comparisons with unmetamorphosed and metamorphosed rocks from other areas, however, show that depletion is not required to account for the elemental abundances and if it did occur, was not severe.

As is implied above, the gneisses could be of either igneous or sedimentary origin. Shaw (1972) developed a discriminant function DF = 10.44 − 0.21SiO_2 − 0.32 (total Fe as Fe_2O_3) − 0.98 MgO + 0.55 CaO + 1.46 Na_2O + 0.54 K_2O for distinguishing between igneous and sedimentary protoliths of an amphibolite facies biotite-feldspar- quartz gneiss. Positive DF indicates an igneous, negative a sedimentary, origin. Six of the Ellesmere-Coburg gneisses have negative DF. Two of these are mafic gneisses with more than 5 % MgO and unlikely to qualify as suitable candidates for Shaw's discriminant test. They are probably of igneous origin but if they were sediments, they would most likely have been highly immature greywackes derived from basic igneous rocks, such as greywackes from oceanic island arcs (*see* Bhatia, 1983, Table 5). Most of the other gneisses have strongly positive DF.

Tarney (1976) has proposed a distinction between igneous and sedimentary origins of Archean gneisses based on TiO_2-SiO_2 abundance levels. Figure 34 shows that the Ellesmere-Coburg gneisses all plot in the field of calc-alkaline igneous rocks.

In the AFM diagram as well, the gneisses for the most part plot along a calc-alkaline trend (Fig. 29). The felsic biotite-orthopyroxene gneisses in particular follow the

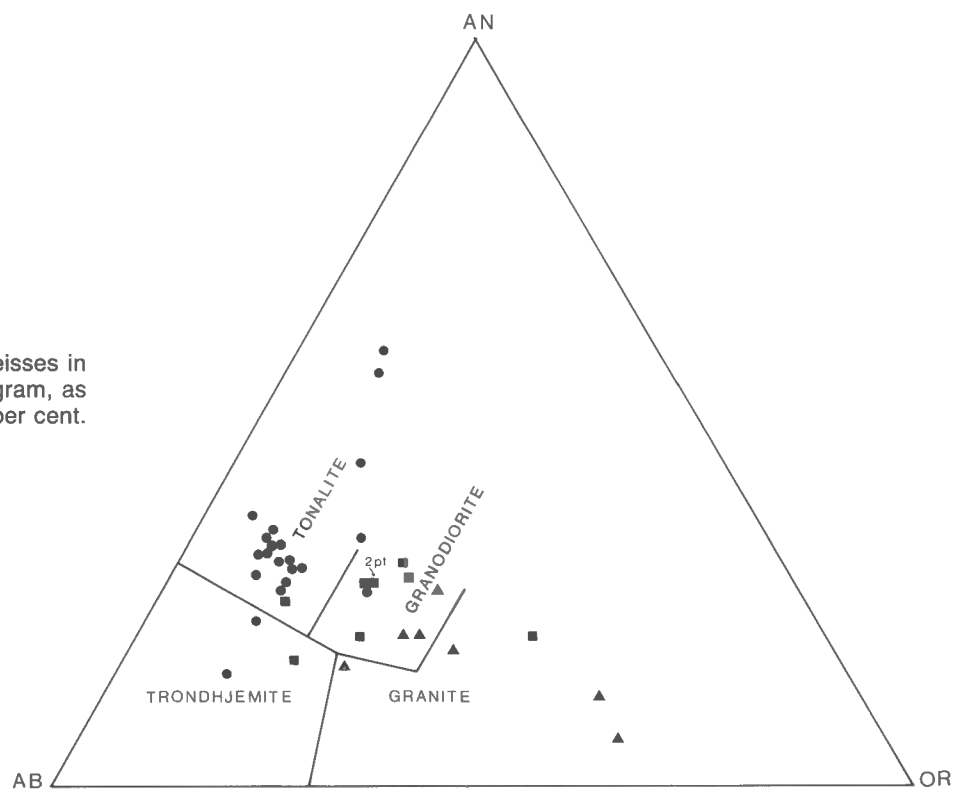

Figure 28. Quartzofeldspathic gneisses in the normative O'Connor (1965) diagram, as modified by Barker (1979). Weight per cent. Symbols as in Figure 24.

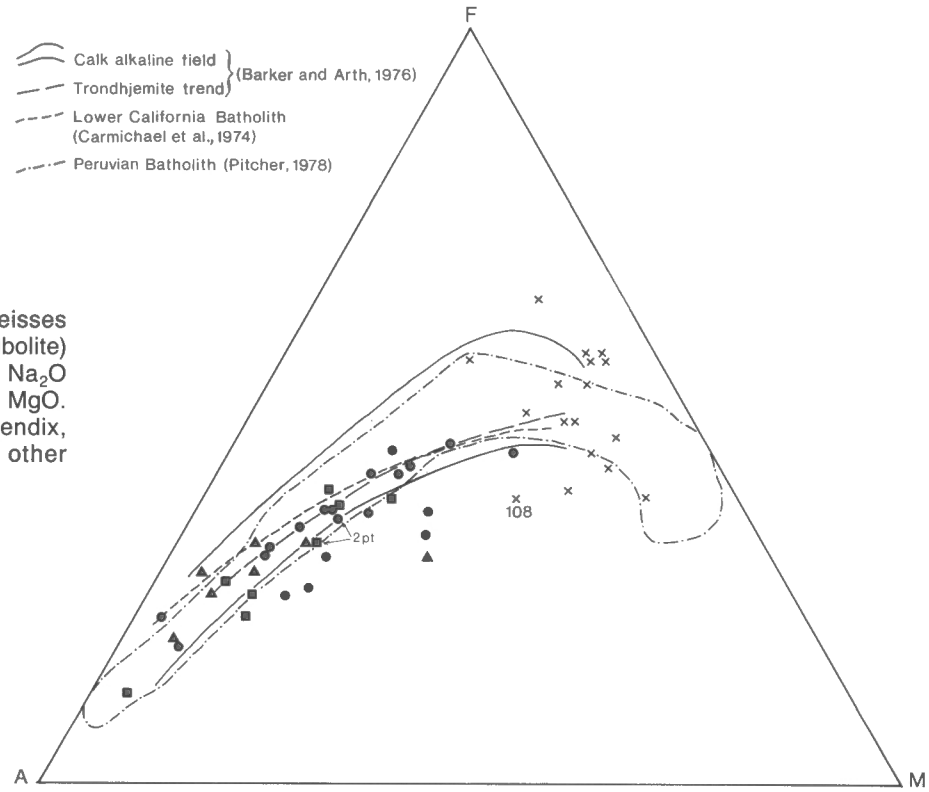

Figure 29. Quartzofeldspathic gneisses and metabasalts (pyribolite and amphibolite) in the igneous AFM diagram. A = $Na_2O + K_2O$, F = total Fe as FeO, M = MgO. Weight per cent. Metabasalts (Appendix, Table IV) designated by crosses, other symbols as in Figure 24.

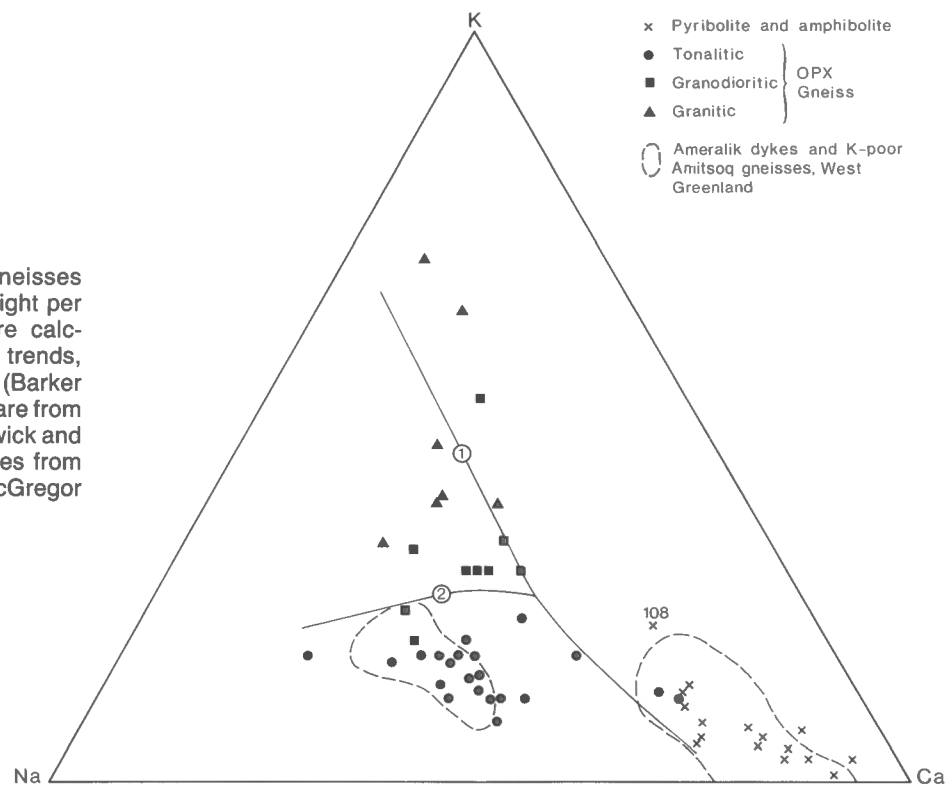

Figure 30. Quartzofeldspathic gneisses and metabasalts in the Ca-Na-K (weight per cent) diagram. Curves 1 and 2 are calc-alkaline granitic and trondhjemitic trends, respectively, of continental margins (Barker et al., 1981). Data on Ameralik dykes are from Gill and Bridgwater (1979) and Chadwick and Coe (1983), data on Amitsoq gneisses from Lambert and Holland (1976) and McGregor (1979). Symbols as in Figure 24.

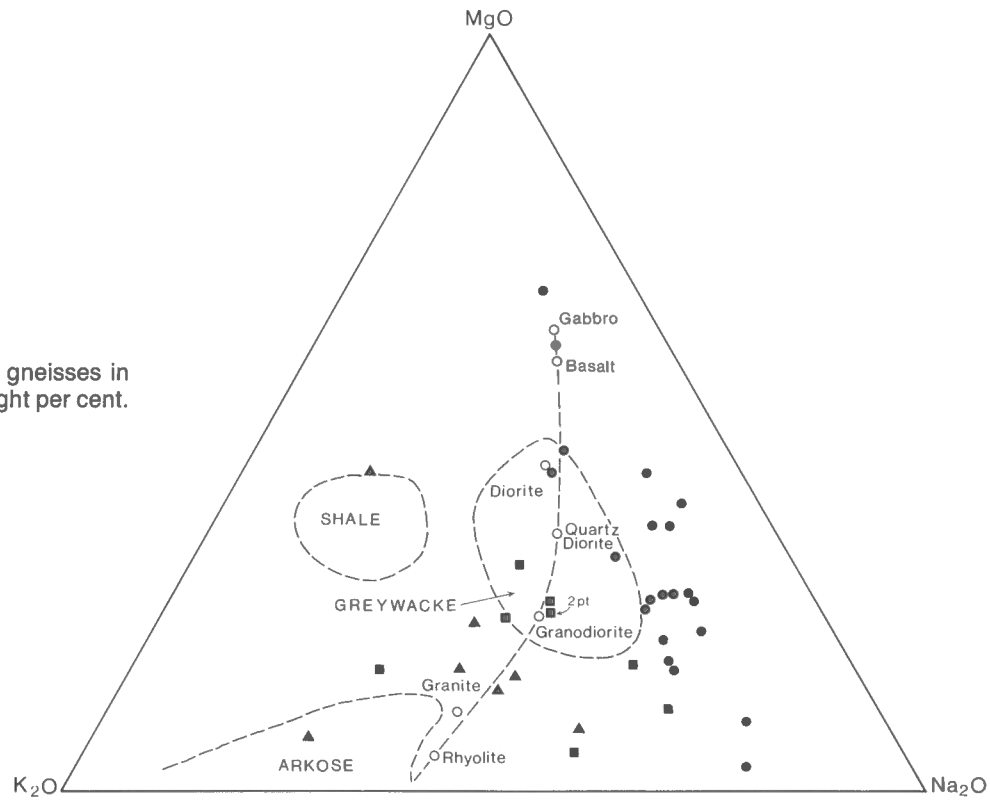

Figure 31. Quartzofeldspathic gneisses in La Roche's (1965) diagram. Weight per cent. Symbols as in Figure 24.

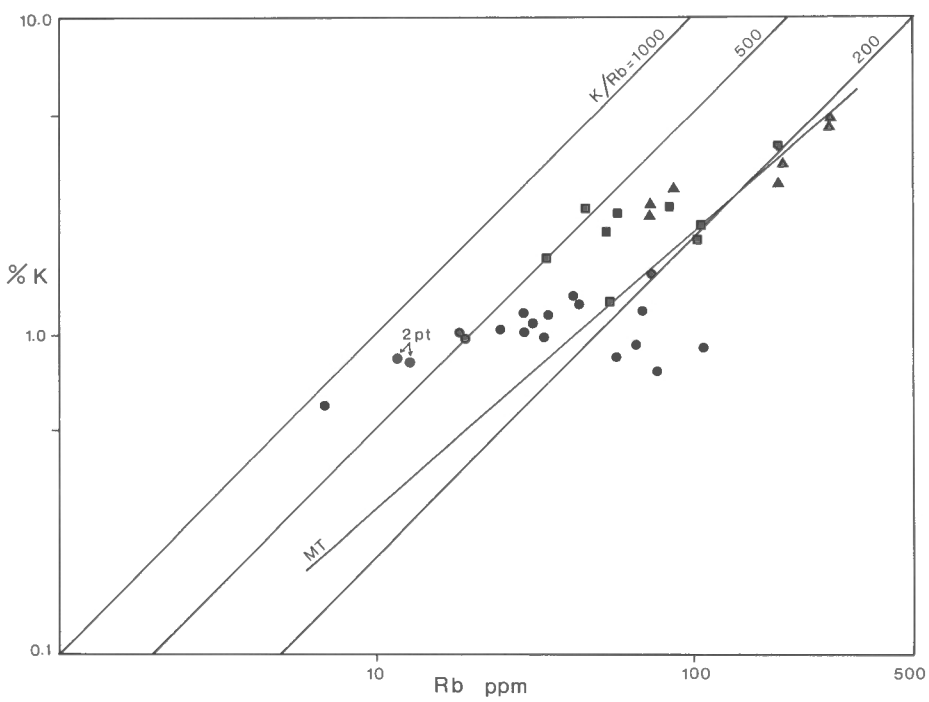

Figure 32. K vs. Rb in the quartzofeldspathic gneisses. MT is the "main trend" of Shaw (1968). Symbols as in Figure 24.

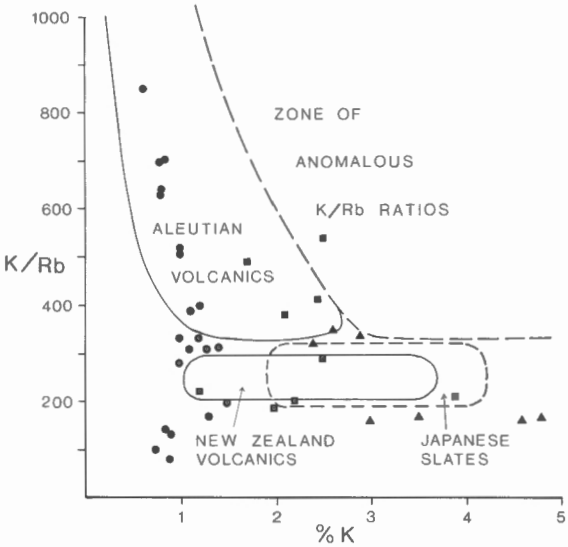

Figure 33. Quartzofeldspathic gneisses in Gray's (1977) diagram. Symbols as in Figure 24.

trondhjemitic trend of Barker and Arth (1976). Robinson and Leake (1975), however, have demonstrated how an entirely sedimentary series of greywackes can define a trend indistinguishable from that of an igneous calc-alkaline suite. At this point it may be noted that the Ellesmere-Coburg gneisses are, with few exceptions, slightly corundum-normative. Although high (greater than 5 %) normative corundum is considered to indicate sedimentary parentage (Blackburn, 1974), calc-alkaline suites typically change from diopside- to corundum-normative at SiO_2 values in the middle to high 60s (Barker, 1979).

In both the Ca-Na-K (Fig. 30) and K_2O-MgO-Na_2O (Fig. 31) diagrams, the tonalitic gneisses follow a sodic trend. In the K_2O-MgO-Na_2O triangle they neither plot in any of the sedimentary rock fields nor do they follow a normal igneous trend.

Both the AFM and Ca-Na-K diagrams show a distinct gap existing between the metamafites (pyribolites and mafic gneisses) and the tonalitic gneisses of the Ellesmere-Coburg terrane. Harker plots (Fig. 35) show that only two tonalitic gneisses fall in the range 53 to 62 % SiO_2, i.e. andesitic compositions appear to be rare in the map area.

Bimodality of chemical composition of mafic and felsic gneisses is characteristic of Archean high grade (amphibolite and granulite facies) terranes (Barker et al., 1981; Windley, 1984). A prime example is the early Archean amphibolite facies metabasalts and tonalitic-granodioritic Amitsoq gneisses of West Greenland (McGregor, 1979). There is a close similarity in major element chemistry between the average Amitsoq felsic gneiss and Ellesmere-Coburg tonalitic gneiss (Appendix, Table II). Potassium and rubidium are lower (K only slightly so) and K/Rb is higher in the Ellesmere-Coburg rocks but the general correspondence between the two rock groups of different metamorphic grade bears out Glikson's (1979) conclusion that tonalite-trondhjemite suites of different tectonic settings and ages (Archean and post-Archean) are geochemically similar.

Largely on geochemical grounds (including REE distribution), an igneous origin for the felsic gneisses of the Archean bimodal association is favoured by the majority of workers (Barker, 1979; Glikson, 1979; Windley, 1984). Indeed, quartzofeldspathic gneisses of intermediate to acid composition from granulite facies terranes all over the world have been interpreted almost exclusively as orthogneisses (Windley, 1984). The generally favoured theory for the formation of tonalitic-trondhjemitic liquids involves their derivation from basaltic material by processes of partial melting and differentiation (Barker, 1979). High-alumina (Al_2O_3 greater than 15 %) melts which would crystallize to felsic rocks of the Archean bimodal suite are thought to have formed by partial melting of amphibolite, itself formed by metamorphism of an earlier accumulation of basalt. Emplacement of the felsic rocks as either intrusions or extrusions was accompanied by basaltic volcanism (Barker, 1979).

As outlined above, the evidence — largely chemical — preponderantly supports an igneous origin for the Ellesmere-Coburg orthopyroxene-bearing tonalitic gneisses. Prior to granulite facies metamorphism they may have been dacitic tuffs and/or chemically equivalent intrusive rocks. Their chemical composition and that of the associated metamafites suggest parallels with the typical

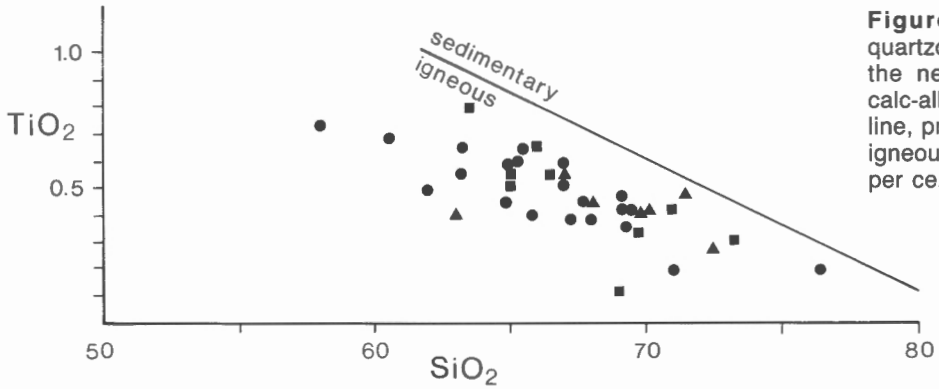

Figure 34. TiO_2-SiO_2 distribution in quartzofeldspathic gneisses. The rocks show the negative correlation characteristic of calc-alkaline igneous rocks and fall below a line, proposed by Tarney (1976), separating igneous and metasedimentary rocks. Weight per cent. Symbols as in Figure 24.

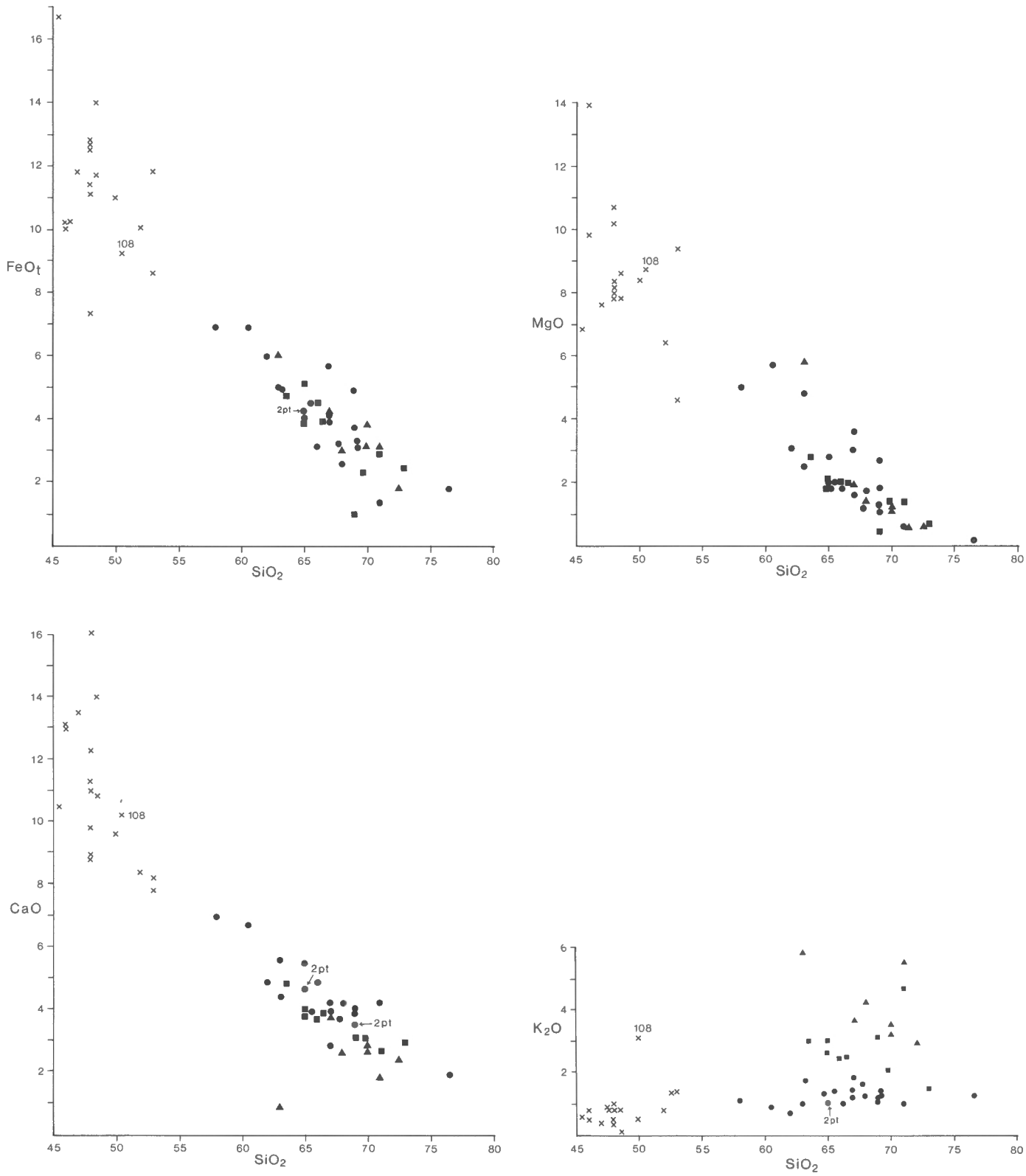

Figure 35. Harker plots of quartzofeldspathic gneisses and metabasalts (Appendix, Table IV). Weight per cent. Note the compositional gap between the two rock groups approximately in the andesite range.

Archean bimodal suite. Possible tectonic settings for this association are discussed below, following a description of the related more potassic gneisses.

Orthopyroxene granodiorite and granite gneiss
(gn, gnv, gnr)

Orthopyroxene-bearing quartzofeldspathic gneisses rich in potassium feldspar are very subordinate to tonalitic varieties on both Ellesmere and Devon islands; granodioritic types are somewhat more abundant but still subordinate to tonalitic ones. Potassium feldspar-rich gneisses occur locally in metasedimentary sequences and in areas underlain mainly by massive to poorly foliated granitoid rock of plutonic aspect. The latter occurrences are thought to be deformed intrusive igneous rocks and are discussed under that heading.

Aside from the presence of potassium feldspar, the orthopyroxene granodiorite-granite gneisses differ little from their tonalitic counterparts. However, whereas mafic varieties of tonalite gneiss are common, mafic orthopyroxene granite gneiss is rare. Modification of granoblastic texture by deformation appears to be particularly common in orthopyroxene granite gneiss interlayered with metasediments. In his study of the Truelove Inlet area of northern Devon Island, Krupička (1973) correlated increasing K-feldspar content with increasing degree of cataclastic deformation. Some of the K-feldspar in the granitic gneisses described here may well have originated by expulsion of the potassic component from plagioclase and its precipitation as discrete grains during and after tectonism. However, the larger, discrete grains of perthite are undoubtedly of primary origin.

Orthopyroxene in the granitic gneisses is characteristically strongly pleochroic (X = pink, Z = bluish green) and is invariably accompanied by brown to reddish brown biotite. Potassium feldspar is either dense hair perthite grading into mesoperthite or, less commonly, intergrown graphically with plagioclase (Fig. 36). Shadowy grid twinning is seen in the K-feldspar of some rocks. Plagioclase, which is rarely absent, ranges from An_{24} to An_{35} but is little zoned; antiperthite is ubiquitous.

As in the tonalitic gneisses, garnet is uncommon. Five garnetiferous gneisses have been studied in detail. Two of them — one felsic, the other mafic — contain appreciable discrete plagioclase, the others have perthite as virtually the only feldspar.

The felsic plagioclase-bearing gneiss (FS-77-68) is a leucocratic rock of granitic composition from near the southern side of Jakeman Glacier, east of Fram Fiord (Map 1573A). Its texture has been modified by deformation: medium- to coarse-grained portions are separated by fine grained lenses that are recyrstallized crush zones. The felsic minerals are hair perthite, subordinate, well twinned plagioclase (An_{26}) with blocky antiperthite, and strongly strained quartz. Rounded garnet crystals, 2-4 mm across, are fresh but embayed and rich in inclusions of biotite, feldspar and quartz. Orthopyroxene, typically in little altered, anhedral grains 2 mm long, is strongly pleochroic in pink and pale green.

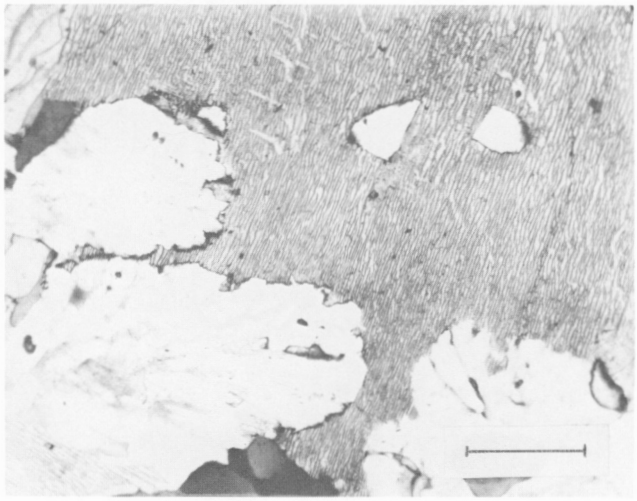

Figure 36. Fine mesoperthite and coarse perthite in orthopyroxene granite gneiss. Crossed nicols. Bar scale 0.5 mm.

A garnetiferous gneiss (FS-77-289) from a sequence of orthopyroxene-bearing quartzofeldspathic gneiss and cordierite gneiss on the north side of Stygge Glacier (Map 1572A) contains both orthopyroxene and sillimanite. The bulk of the rock consists of quartz and variably perthitic K-feldspar: mesoperthite, hair perthite and irregularly developed spindles and blebs of Na-feldspar. Mafic minerals include anhedral to skeletal garnet (0.5-1 mm) with inclusions of green spinel, strongly pleochroic orthopyroxene (1-2 mm), discrete green spinel (up to 0.5 mm), and minor chestnut biotite. The orthopyroxene is altered along cracks to mica and chlorite. The green spinel is to a large extent intergrown with orthopyroxene but invariably separated from it by a "moat" of oligoclase (An_{21}) (not sillimanite as reported by Frisch (1983, p. 5)). Some spinel is in direct contact with quartz. Common aggregates of orthopyroxene, garnet and spinel suggest a genetic relationship between these minerals, possibly the result of the breakdown of a high pressure Mg-rich garnet to less magnesian garnet and orthopyroxene, spinel and plagioclase (O'Hara and Yarwood, 1978, Barnicoat, 1983). Tiny prisms of sillimanite (up to 0.2 mm but generally 0.1 mm long) are enclosed in perthite and quartz. The immediate area around sillimanite in K-feldspar is free of perthite texture indicating that sillimanite is an early mineral incorporated prior to feldspar exsolution. Although sillimanite and orthopyroxene are not in contact, they lie within 1 mm of each other, were apparently both formed early and may well have once been in equilibrium, providing further evidence of an earlier high pressure stage in the history of this rock.

Second-generation garnet is also evident in mesoperthite-rich orthopyroxene gneiss (FSM-77-220) from 8 km east of Jokel Fiord on Thorvald Peninsula (Map

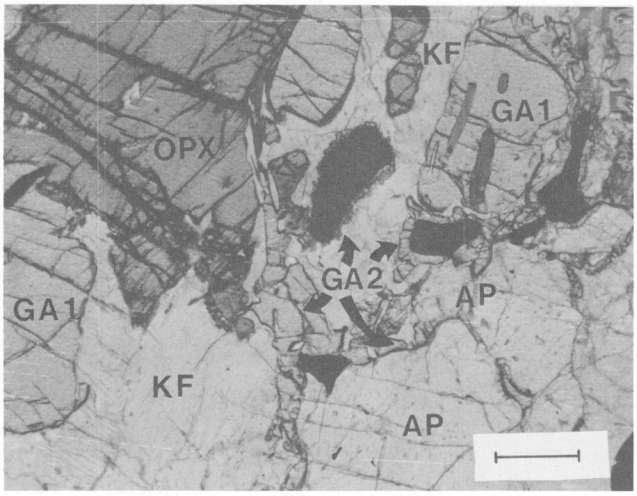

Figure 37. Two generations of garnet in mesoperthite-rich orthopyroxene granite gneiss FSM-77-220. The finely granular, late garnet (GA 2) rimming Fe-Ti oxide and apatite is richer in iron than the coarse, early garnet (GA 1). Plane light. Bar scale 0.5 mm.

1572A). This rock is characterized by extremely pleochroic orthopyroxene (X = deep pink, Z = bluish green) and coarse apatite, which forms elongate aggregates, up to 4 mm long, of millimetre size grains containing abundant, aligned fluid inclusions. Some of the orthopyroxene is replaced by well crystallized brown biotite.

Two generations of garnet occur in this rock: (1) grains up to 2 mm in diameter with inclusions of biotite and (2) fine granules rimming Fe-Ti oxide, apatite and biotite (Fig. 37). The finely granular garnet in most cases is associated with biotite that replaces orthopyroxene and may be a product of the retrograde hydration of orthopyroxene

orthopyroxene + Ca + K + Ti + H_2O = garnet + biotite

with Ca being derived from apatite and/or mesoperthite, K from mesoperthite and Ti from Fe-Ti oxide. This is the type of reaction that produces amphibolite facies assemblages from granulite facies ones.

The coarse early garnet also shows signs of instability, being separated from perthite by a narrow rim of sodic plagioclase.

The remaining garnet+orthopyroxene-bearing granitic gneiss of interest is a mafic rock from gneisses of supracrustal aspect outcropping at Inglefield Hill, Dundas Harbour, southern Devon Island. The rock consists of andesine, subordinate weakly perthitic K-feldspar, quartz, two pyroxenes, garnet and hornblende. Its texture is inequigranular granoblastic with some of the quartz in ribbons 3 mm long. Garnet is abundant in pink subhedral grains generally 0.5 to 1 mm but up to 2 mm across. Distinctly pleochroic pale green clinopyroxene, orthopyroxene and hornblende (X = brownish green, Z = olive) are intergrown, with clinopyroxene the most abundant of the three minerals. The abundance of calciferous minerals and significant quartz content suggest a calc-silicate affinity.

Mineral chemistry

Minerals of two garnet-free and five garnet-bearing orthopyroxene granite gneisses have been analyzed (Appendix, Table 2B).

Garnet-free gneiss. As in the tonalitic gneisses, orthopyroxene is significantly aluminous: Fe_{57} Mg_{43}, Al_2O_3 2.37 % and Fe_{35} Mg_{65}, Al_2O_3 5.04 %. Biotite is markedly titaniferous (more than 4 % TiO_2) and may be chemically inhomogeneous. Plagioclase is oligoclase or sodic andesine low in K, presumably due to exsolution of nearly pure K-feldspar. Perthitic intergrowth makes analysis of the K-feldspar difficult and the compositions of discrete K-feldspar obtained in the two samples suggest that this mineral ranges widely in composition in these rocks.

Garnetiferous gneiss. Compositions of garnet in this rock group tend to resemble those in the tonalitic gneisses (Fig. 11) but are slightly higher in iron, mole per cent (almandine +spessartine) ranging generally from 64 to 70. Rims of zoned grains and second generation garnet are richer in Fe and Mn and poorer in Ca than earlier formed garnet but MnO does not exceed 3 % (and is generally less than 2 %) and, except in the mafic gneiss FS-78-20, CaO is at most slightly over 1 %. Garnet in the perthite-rich, plagioclase-free gneiss FS-77-294 is exceptionally almandine-rich with compositions of cores approaching those of rims of garnets in cordierite gneisses. Garnet of the mafic gneiss FS-78-20 is quite distinct from all other garnets analyzed in non-calcareous rocks in being grossular rich (7.16 % CaO) and pyrope poor (3.09 % MgO).

Orthopyroxene is unzoned hypersthene $Fe_{40\text{-}45}Mg_{60\text{-}55}$ in three of the gneisses, ferrohypersthene $Fe_{60}Mg_{40}$ in the almandine-rich aluminous gneiss and $Ca_1Fe_{60}Mg_{39}$ in the mafic, calciferous gneiss (Fig. 27). The hypersthenes are all highly aluminous, Al_2O_3 contents ranging from 6.96 to 8.33 % in the sillimanite-bearing gneiss FS-77-289. Alumina is moderate (3.58 %) in the ferrohypersthene of FS-77-294 and low (1.11 %) in the orthopyroxene of the mafic gneiss. The latter also contains unzoned, Ca- and Fe-rich augite $Ca_{27}Fe_{30}Mg_{43}$ with 1.91 % Al_2O_3, and calciferous hornblende with appreciable TiO_2 (1.77 %), which, when classified in the scheme of Rock and Leake (1984), is termed potassian magnesian hastingsite.

Biotite in the garnetiferous granitic gneisses has Fe/Fe +Mg = 0.3 to 0.4 and, compared to biotite in most of the other rocks in the map area, is no more than moderately titaniferous (3-4 % TiO_2). Compositional variability is common and biotite included in garnet is Mg- and Ti-richer than discrete biotite in the rock matrix.

All plagioclase present in these gneisses is sodic, andesine (An_{37}) in the mafic gneiss from Devon Island being

the most calcic feldspar analyzed. In the other gneisses, plagioclase is oligoclase: discrete plagioclase in the two-feldspar gneiss FS-77-68 is An_{26} and secondary plagioclase separating spinel or garnet from orthopyroxene in the aluminous gneisses is An_{20-21}. Perthite in the two-feldspar gneiss has the composition $An_4Ab_{21}Or_{75}$. Perthite in the other rocks was too coarsely or irregularly exsolved to be analyzed by microprobe.

Spinel in the two-feldspar gneiss and sillimanite-bearing gneiss FS-77-289 is hercynite with Fe/Fe+Mg between 0.65 and 0.72, slightly more magnesian than the hercynite of the garnet-cordierite-sillimanite gneisses.

Rock chemistry and origin

Sixteen granodioritic and granitic orthopyroxene gneisses, all of them garnet-free, were analyzed (Appendix, Table III). Most of them plot in the granodiorite and granite fields of the Ab-An-Or diagram but the correspondence between modal and chemical classifications is poor (Fig. 28). They are distinguished from the tonalitic gneisses mainly by higher K_2O and plot toward the K apex of the Ca-Na-K (Fig. 30) and K_2O-MgO-Na_2O triangles (Fig. 31), diverging markedly from the tonalitic rocks. As well, Ba is higher and Rb lower in the granodioritic-granitic gneisses.

TiO_2 vs. SiO_2 (Fig. 34) and Shaw's (1972) discriminant function indicate that the granodioritic-granitic gneisses are of igneous derivation. A number of the rocks approximately follow the normal igneous trend in the K_2O-MgO-Na_2O diagram (Fig. 31) and nearly all of them follow the calc-alkaline trend in the AFM diagram (Fig. 29).

The average granodioritic gneiss corresponds very closely in major elements with Le Maitre's (1976) average granodiorite (Appendix, Table III). The average granitic gneiss is slightly more magnesian and calcic and a little less sodic than Le Maitre's average granite. The lack of significant depletion of K relative to fresh, unmetamorphosed rocks suggests that this element has not been lost during high grade metamorphism. If anything, it may have been added. For example, the magnesian (MgO 5.80 %) granitic gneiss FS-77-140 has 5.81 % K_2O and plots anomalously in the Q-Ab-Or triangle (Fig. 38). In general, however, there is little evidence for movement — in or out — of potassium during the granulite facies metamorphism and the compositions of the rocks are considered (perhaps too optimistically?) to be near pristine.

The only sediments chemically similar to some of the granodioritic-granitic gneisses are immature greywackes of continental margin or island arc environments, e.g. analyses 13 and 22 in Bhatia (1983); the latter is included in Table III of the Appendix.

Silica variation diagrams (Fig. 35) show the granodioritic-granitic gneisses largely overlap the tonalitic varieties in SiO_2, FeO_t and MgO. This and the divergent trends noted above essentially preclude a genetic relation between the two groups of gneisses. In this regard, it may be noted that K-rich members of the Amitsoq gneisses — the Amitsoq augen gneisses, which chemically are broadly similar to the Ellesmere-Coburg K-rich gneisses — are unrelated chemically to the tonalitic suite (McGregor, 1979). The sodic and potassic granulite facies gneisses in Enderby Land are also regarded by Sheraton and Black (1983) as having separate origins: sodic gneisses were derived from mafic sources, potassic gneisses from felsic crustal rocks.

In the K vs. Rb diagram (Fig. 32) the granodioritic and granitic gneisses plot along a trend separate from, but parallel to that of the tonalitic rocks with K/Rb greater than 200, i.e. decreasing K/Rb with increasing K. Only one rock (granodioritic) has K/Rb exceeding 500 and plots in Gray's (1977) anomalous K/Rb zone (Fig. 33). Rb/Sr is much higher than (depleted) lower continental crust. The relatively low K/Ba (22 to 26) is more like a lower crustal ratio and results from the high average Ba (greater than 1000) in these gneisses. High Ba is common in Archean high grade gneiss terranes, especially in the more K-rich rocks (Glikson, 1979).

K-rich meta-intrusive rocks younger than the tonalitic-trondhjemitic gneisses seem to be virtually ubiquitous in Archean high grade terranes (Barker, 1979, p. 7). Together, these granitoid rocks commonly define a continuous calc-alkaline trend in the AFM diagram (Fig. 29); the Ellesmere-Coburg rocks are no exception.

On the evidence from the map area and from similar rocks in other areas, it is concluded that the bulk of the orthopyroxene-bearing granodioritic-granitic gneisses are igneous rocks metamorphosed in the granulite facies.

The highly aluminous garnet-bearing gneisses are of semipelitic composition and probably sedimentary parentage.

Tectonic setting of the orthopyroxene-bearing quartzofeldspathic gneiss

The quartzofeldspathic gneisses of the Ellesmere-Coburg terrane are interpreted to be of igneous derivation and follow two evolutionary trends, best seen in the Ca-Na-K triangle (Fig. 30). Most of the tonalitic rocks lie on a trondhjemitic trend, separated from the metamafic rocks, with which they may be genetically related. The distribution of points resembles that of typical Archean bimodal grey gneiss- amphibolite suites.

In the Ca-Na-K diagram, a few tonalitic rocks bridge the gap between the metamafites and the more potassic granitic rocks along a calc-alkaline trend as found in modern continental margins (Barker et al., 1981). No clear distinction between calc-alkaline trondhjemitic trends is evident but the granitic trend is the better defined of the two. Plots of the calc-alkaline Peruvian Batholith and Lower Californian Batholith are shown in the AFM diagram of Figure 29 for comparison with the Ellesmere-Coburg rocks. It may be noted that plutonic rocks equivalent to andesites, i.e. diorites, are absent from the Lower California Batholith (Larsen, 1948).

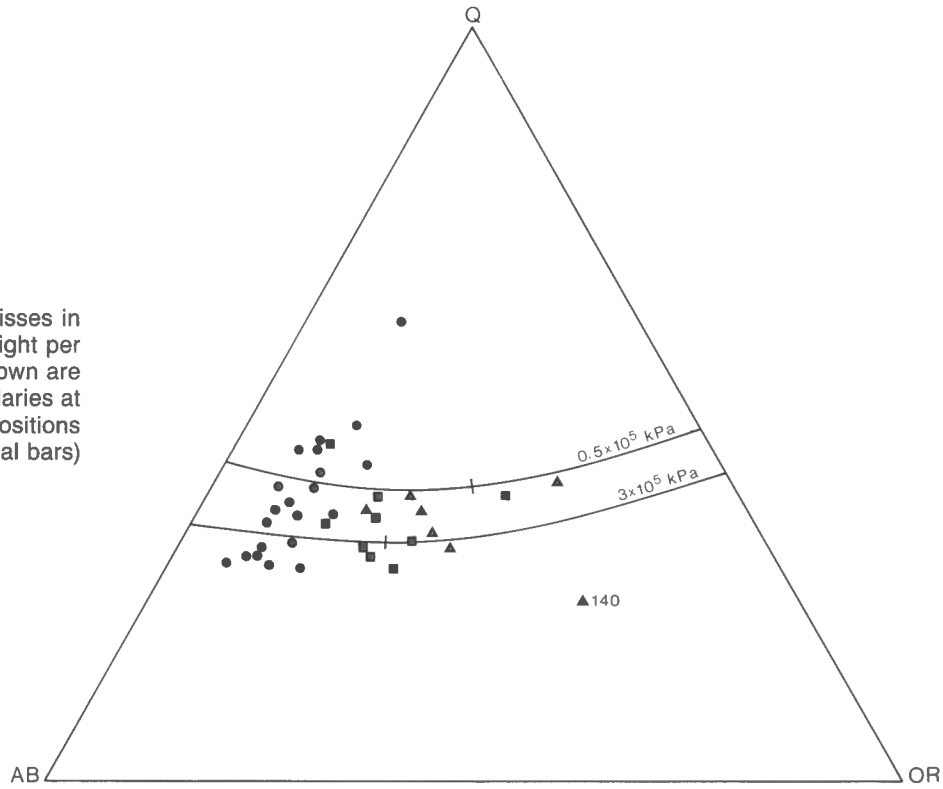

Figure 38. Quartzofeldspathic gneisses in the normative Q-Ab-Or diagram. Weight per cent. Symbols as in Fig. 24. Also shown are projected quartz-feldspar field boundaries at 0.5 x 10^5 and 3 x 10^5 kPa P_{H2O} and positions of quaternary isobaric minima (vertical bars) (after Tuttle and Bowen, 1958).

A favoured interpretation of the orthogneisses of ancient high grade gneiss terranes is that they represent metamorphosed granitoid intrusions emplaced at an active continental margin (Windley, 1984). Modern analogues suggested by Windley are the continental margins of southern Chile and British Columbia, where deep erosion reveals gneissic, predominantly tonalitic, plutons with mafic inclusions and intercalated arkosic, pelitic and calcareous metasediments. This model accounts for both the derivation of the mafic and tonalitic rocks from a basaltic source (oceanic crust or subcontinental mantle) and the presence of continental margin-type sediments, as apparently required for the lithological associations found in the Ellesmere-Devon terrane.

This purely accetionary model has been criticized by Kröner (1985) on the grounds that high grade gneiss terranes do not show evidence of such subduction- related features as tectonic melanges and commonly do not form the expected linear belts. Kröner (1985) and Newton and Hansen (1983) appeal to continental collision with resultant thrust stacking and subsequent tilting as a more plausible mechanism for the origin and present exposure of high grade gneiss-metasediment complexes. Whichever model is favoured, continental margin is involved and, as outlined above, several lines of evidence, from both meta-igneous and metasedimentary rocks, indicate this environment.

An active continental margin is the tectonic setting proposed for granulite grade orthogneisses of Sri Lanka (Munasinghe and Dissanayake, 1980), the Lapland Granulite belt (Barbey et al., 1984) and the Rio de Janeiro region of Brazil (Leonardos and Fyfe, 1974), all areas with rock types and associations similar to those of the map area.

Metamorphic conditions

The widespread occurrence of orthopyroxene in mafic and felsic quartzofeldspathic gneisses unequivocally signifies granulite facies metamorphism. The ubiquitous presence of biotite and common occurrence of hornblende suggest relatively moderate conditions of pressure and temperature. If Turner's (1981) contention that, in the granulite facies, garnet-free mafic rocks are lower grade than garnet-bearing ones is correct, conditions in Ellesmere and Coburg islands were more moderate than in Devon Island.

For useful thermobarometric information on the pyroxene-bearing quartzofeldspathic gneisses, recourse must be made to the garnet-bearing varieties.

Equilibria between garnet, pyroxenes and quartz are pressure dependent and geobarometric expressions have been derived from the reactions:

3 anorthite + 6 enstatite = 2 pyrope + grossular + 3 quartz,
3 anorthite + 3 diopside = pyrope + 2 grossular + 3 quartz.

The geobarometers are based largely on thermochemical data, some of which are not known with certainty, e.g. values of the free energy of solid solution of garnets (Newton, 1983). Resulting pressure uncertainties are estimated by Newton and Perkins (1982) to be $\pm$ 1.5 to 1.7 $\times$ 10^5 kPa. Pressures yielded by various formulations of these geobarometers (Wells, 1979; Newton, 1983; Bohlen

et al., 1983; Perkins and Chipera, 1985) are relatively consistent in many cases and appear to be plausible. Furthermore, the temperature dependence of the geobarometers is only about 0.4 to 0.6 x 10^5 kPa per 100°C (Newton, 1983).

The geobarometers of Wells (1979) and Newton (1983) relate to Mg end-member garnet and pyroxene in the above reaction. Bohlen et al. (1983) calibrated their geobarometer from experimental work on reactions involving Fe end-members in related systems. Perkins and Chipera (1985) have attempted a refinement of these two approaches by incorporating Ganguly and Saxena's (1984) garnet activity model and obtaining, for a given garnet-orthopyroxene-plagioclase assemblage, two values of pressure: one for the Mg reaction, the other for the Fe reaction (P_{Mg} and P_{Fe} in Table 6). Ideally, the two values should agree but in practice discrepancies appear, particularly in more iron-rich samples (those with $(Fe/Fe+Mg)_{opx}$ greater than 0.5); for these, the P_{Fe} value is considered the more reliable (Perkins and Chipera, 1985).

In general, differences in pressures obtained from these various expressions may be ascribed largely to differing thermochemical values employed and possible errors in activity models.

Reviewing applications of the garnet-clinopyroxene-plagioclase geobarometer to two-pyroxene rocks, Newton and Perkins (1982) found that pressures obtained were consistently lower than those from the orthopyroxene geobarometer, commonly by about 2 × 10^5 kPa — most probably due to an error in the standard Gibbs energy of the diopside reaction. Newton (1983) suggested an empirical correction be made to bring the two pressure values into line: 0.5 × 10^5 kPa to be subtracted from the orthopyroxene pressure and 1.5 × 10^5 kPa added to the clinopyroxene pressure.

Harley and Green (1982) developed a geobarometer based on the solubility of alumina in orthopyroxene coexisting with garnet. Although experimentally calibrated, the geobarometer is largely an empirical one, involving considerable simplification of complex processes, such as site distribution of aluminium in orthopyroxene. Another drawback of this geobarometer is its greater dependence on temperature than the geobarometers discussed above. Harley (1984a) presented a modification of the geobarometer, which he considered to be an improvement for Mg-rich pyroxene and garnet formed at high pressures.

Entirely separate from the sources of error mentioned are, of course, problems caused by compositional inhomogeneity of, and disequilibrium between, minerals. Only three out of the five samples with the appropriate garnet-pyroxene-plagioclase assemblage from the Ellesmere-Devon terrane show no obvious sign of mineral zoning or disequilibrium.

Although knowledge of temperature is not critical for the majority of the garnet-pyroxene-plagioclase geobarometers, its estimation is of some interest as an independent check against values obtained from other mineral assemblages in spatially related rocks, such as the cordierite gneisses. Geothermometers used here are based on Fe-Mg exchange between garnet and orthopyroxene (Powell, 1978; Harley, 1984b; Sen and Bhattacharya, 1984); garnet and clinopyroxene (Ellis and Green, 1979); and orthopyroxene and clinopyroxene (Powell, 1978; Lindsley, 1983; Bertrand and Mercier, 1985/86). Also employed were the two geothermometers of Kretz (1982), involving Fe-Mg exchange and transfer of Ca between ortho- and clinopyroxene and the resulting two temperatures averaged. Temperature uncertainties for any of these geothermometers are probably 50 to 60°.

All calculations were made assuming that all iron is divalent and thus temperatures derived are minimum values, considerably so in instances where Fe^{3+} is high (Harley, 1984b).

Temperatures obtained for the garnetiferous gneisses show a considerable range (Table 5). Powell's (1978) garnet-orthopyroxene geothermometer yields 542 to 638°C, which seems too low. As well, temperatures calculated using rim compositions of garnet are higher than those given by cores, which appears unreasonable. Temperatures from Harley's (1984b) and Sen and Bhattacharya's (1984) formulations fall mainly between 700 and 900°, with temperatures of cores exceeding those of rims. Sen and Bhattacharya's temperatures show a smaller spread, largely in the 700-800° range. Their (garnet-orthopyroxene) temperature of 710° for the garnet — two-pyroxene gneiss FS-78-20 esentially agrees with temperatures of 724° from Ellis and Green's (1979) garnet-clinopyroxene geothermometer, and 700° from Lindsley's (1983) and 733° from Bertrand and Mercier's (1985/86) two-pyroxene geothermometers. Ellis and Green's geothermometer is widely regarded to be the most reliable for granulite facies rocks (Newton, 1985).

Two-pyroxene geothermometry was also applied to garnet-free gneisses (samples FSM-77-104, FS-77-207, 78-10 and 78-14). For all but FS-78-14, the temperatures from different formulations of the geothermometer range from 815 to 855° (Powell, 1978), 781 to 973° (Kretz, 1982) and 662 to 844° (Bertrand and Mercier, 1985/86). FS-78-14 contains exceptionally Ca-rich orthopyroxene (1.99% CaO) and gives aberrant temperatures of 1150° (Powell) and 256° (Bertrand and Mercier); the average Kretz temperature is 763°. Temperatures read off Lindsley's (1983, Fig. 9b) diagram for coexisting pyroxenes at 5 × 10^5 kPa are markedly discrepant. They range from 600 to 700° for orthopyroxene and from 900 to 1100° for clinopyroxene; orthopyroxene and clinopyroxene temperatures for FS-78-14 are about 1100 and 650°, respectively. The discrepancy in any one sample is generally in the order of 300°. As well as being so different, the temperatures are probably too low in the case of orthopyroxene and too high in the case of clinopyroxene. Lindsley (1983, p. 489) himself has acknowledged the severe problems attending the application of his geothermometer to granulite facies rocks, which have cooled and re-equilibrated slowly. The two pyroxenes in the garnetiferous mafic gneiss FS-78-20, however, are in excellent agreement at 700° (see above).

In summary, results of geothermometry on the quartzofeldspathic gneisses are equivocal. Temperatures in the 700 to 800°C range appear to be the most reasonable, particularly for the regime in which mineral cores were formed. The temperatures obtained from the pyroxene gneisses generally exceed those from the cordierite gneisses. This is expectable, as the temperatures for the latter are determined from garnet-cordierite assemblages, which were formed in a retrograde stage of the metamorphic evolution.

For consistency and ease of comparison with other terranes, temperatures of 750 and 700° are chosen for cores and rims, respectively, in garnet-pyroxene-plagioclase geobarometry on the quartzofeldspathic gneisses, as follows.

Application of the Newton (1983), Wells (1979) and Bohlen et al. (1983) geobarometers to pyroxene gneisses of the Ellesmere-Devon terrane yields generally consistent results (Table 6). Pressures indicated by cores of, or unzoned, minerals in rocks from Ellesmere and Coburg islands cluster around 4 to 5 $\times$ 10^5 kPa (at 750°C). Garnet cores combined with the most sodic plagioclase (An_{35}) of the highly zoned feldspar in the aluminous gneiss FSM-77-63-9 yield a pressure of 6.6 or 6.3 $\times$ 10^5 kPa according to the Newton (1983) or Wells (1979) geobarometer, respectively. Application of the garnet-plagioclase-Al_2SiO_5 geobarometer (Newton and Haselton, 1981) to the same data results in a pressure of 6.8 $\times$ 10^5 kPa, which is in satisfactory agreement with the Newton and Wells pressures. The relatively high pressures are consistent with the presence of sillimanite (as inclusions in garnet) in this orthopyroxene-bearing gneiss. Rim compositions give lower pressures of 3.1 to 4.3 $\times$ 10^5 kPa (at 700°C); the value for FSM-77-63-9 is a minimum, derived from garnet rims combined with the most calcic plagioclase. The lower pressures presumably reflect decompression during uplift. Pressures obtained from the two Devon Island gneisses are between 6 and 7 $\times$ 10^5 kPa. These high values support the evidence from garnet- plagioclase-sillimanite assemblages in pelites that pressures in Devon Island were, in general, higher than in Ellesmere and Coburg islands.

Pressures given by Newton's (1983) calibration are shown graphically in Figure 39. Note that even the highest pressures are below the stability limit of cordierite in pelitic rocks defined by Newton (1983). The pressure values compare well with those from garnet-plagioclase-sillimanite-quartz assemblages in the cordierite gneisses and together they establish the Ellesmere-Devon terrane as one of medium pressure granulite facies. Continued uplift resulted in pressure decrease and transition to low pressure.

Pressures from Perkins and Chipera's (1985) geobarometer show considerable scatter and, despite Fe/Fe+Mg of orthopyroxenes being less than 0.5, P_{Fe} and P_{Mg} differ by as much as 3.5 $\times$ 10^5 kPa (Table 6). The two-pyroxene rock from Devon Island with its Ca-rich garnet and Fe-rich pyroxene gives considerably higher pressures than the other rocks, no doubt reflecting use of the Ganguly and Saxena (1984) activity model for garnet.

Harley's (1984a) geobarometer yields even more scattered results, with pressures ranging from 1.5 to 10.7 $\times$ 10^5 kPa and little agreement with the other formulations.

The least satisfactory geobarometer appears to be that of Harley and Green (1982), which gives pressures that seem too low for the Ellesmere-Coburg rocks and too high for the Devon Island rocks.

The latter two geobarometers were applied to the perthite-rich aluminous gneisses (FS-77-289 and 294, FSM-77-220), which lack plagioclase in equilibrium with garnet, orthopyroxene, and quartz. Pressures given by Harley and Green's (1982) calibration are less than 1 $\times$ 10^5 kPa or negative for all three rocks. Pressure according to Harley (1984a) for the garnet core + orthopyroxene association in FS-77-294 is 2.9 $\times$ 10^5 kPa (garnet rim pressure is negative); garnet-orthopyroxene temperatures at this pressure are 682°C (Harley, 1984b) or 757°C (Sen and Bhattacharya, 1984). A similar pressure, 3.0 $\times$ 10^5 kPa, is obtained for early garnet + orthopyroxene in FSM-77-220, with a temperature of 745°C (Harley) or 833°C (Sen and Bhattacharya). Harley's (1984a) geobarometer gives a negative result for the sillimanite-bearing gneiss FS-77-289. In view of the generally unsatisfactory results obtained with this geobarometer, no significance is attached to the pressures calculated for the perthite-rich aluminous gneisses.

To summarize: pressures recorded by pyroxene-bearing quartzofeldspathic gneisses from Ellesmere and Coburg islands range mainly from 4 to 6 $\times$ 10^5 kPa. Higher values of up to nearly 7 $\times$ 10^5 kPa are obtained from mineral

Table 5. Temperatures (°C) of garnet-pyroxene gneisses listed in Table 6, obtained from various geothermometers.

	Pressure[a] ($\times 10^5$ kPa)	Powell (1978)	Harley (1984b)	Sen and Bhattacharya (1984)
FS-77-68	4.5	542	684	740
FSM-77-114-1	5.2	588	718	795
	3.8	605	657	708
FS-82-D-7D	6.1	611	674	728
FSM-77-63-9	6.6	628	825	951
	4.3	638	755	847
FS-78-20 OPX	6.2	599[b]	641	710
		813[c]		
		Kretz (1982)	Ellis and Green (1979)	Bertrand and Mercier (1985/86)
FS-78-20 CPX	6.6	803[d]	724	733
		Lindsley (1983)		
		700[e]		

[a] after Newton's (1983) calibration
[b] garnet-orthopyroxene temperature
[c] two-pyroxene temperature
[d] average of calcium transfer and Fe-Mg exchange reactions
[e] assuming a pressure of 5 x 10^5 kPa

Table 6. Pressures obtained from garnet-pyroxene-plagioclase-quartz geobarometry.

	X_{An}	OPX X_{Fe}	OPX X_{Al}	T	N	W	B	P&C Mg	P&C Fe	H	H&G
GA + OPX + PG + BIO + QZ											
Coburg Island FSM-77-114-1											
GA & PG cores	.49	.424	0.092	750	5.2	4.9	4.8	4.7	5.9	6.2	3.0
GA & PG rims	.46	.424	0.092	700	3.8	3.5	4.3	3.3	4.5	4.4	3.2
Devon Island FS-82-D-7D	.76	.348	0.052	750	6.1	5.8	6.0	5.4	7.7	10.7	8.6
GA + OPX + PG + BIO + SP + QZ											
Ellesmere Is. FSM-77-63-9											
GA core	.35	.412	0.110	750	6.6	6.3	5.5	5.4	6.3	8.3	2.1
Ga rim	.51	.412	0.110	700	4.3	4.0	3.1	3.0	4.1	6.8	0.4
Ga + OPX + PG + KF + BIO + SP + QZ											
Ellesmere Is. FS-77-68	.26	.354	0.154	750	4.5	4.2	4.8	3.1	6.6	1.5	1.0
GA + OPX + CPX + PG + KF + HBL + QZ											
Devon Island FS-78-20	.37	.592	0.026	750	6.2[a]	6.4	7.2	9.6	8.2	6.4	9.1
CPX	.37			750	6.6[b]						

X_{An} = mole fraction anorthite in PG; X_{Fe} = Fe/(Fe+Mg) (all Fe as Fe^{+2}); X_{Al} = Al/2 in 6-oxygen unit.
T = temperature in °C; pressure in kPa × 10^5.
Geobarometers; N (Newton, 1983) W (Wells, 1979) B (Bohlen et al., 1983) P&C (Perkins and Chipera, 1985) H (Harley, 1984a) H&G (Harley and Green, 1982).
[a] includes empirical correction -0.5×10^5 kPa (Newton, 1983).
[b] includes empirical correction of $+1.5 \times 10^5$ kPa (Newton, 1983).
Complete analyses listed in Appendix, Table 2B.

cores; lower values of 3 to 4 × 10^5 kPa, generally from rim compositions, probably indicate decompression conditions. Pressures in Devon Island appear to have been consistently slightly higher, viz. 6 to 7 × 10^5 kPa.

Age

Interlayered mafic orthopyroxene tonalite gneiss and felsic granite gneiss, outcropping 16 km east of Croker Bay in southern Devon Island, were chosen for U-Pb dating of zircon.

The tonalite gneiss (FS-78-25; Appendix, Table 2A) is a highly flattened, thinly layered, fine grained rock consisting of slightly altered ferrohypersthene, abundant brownish green hornblende, minor brown biotite, plagioclase (An_{32}), and quartz; rare, very small crystals of garnet were noted in outcrop. Grain size is 0.1 to 0.2 mm, equilibrium triple junctions dominate the texture and most of the quartz occurs as ribbons 2-4 mm long. Interlayered on the scale of a metre or so with the tonalite gneiss is fine grained, pink biotite granite gneiss (FS-78-26) made up of hematite-dusted feldspar (chiefly K-feldspar), ribbon quartz and minor altered reddish brown biotite. No intrusive contacts were seen but the lithology and structure of the outcrop suggest that the granitic rock originally intruded the tonalite rock and both were deformed at the same time to the same degree.

The first attempt at dating the two gneisses involved U-Pb analysis of three fractions of zircon from each rock. The resulting six data points could be fitted to a single discordia line intersecting the concordia curve at 2426 Ma (Frisch, 1983, p. 9). Subsequent work, using improved analytical apparatus and techniques, has refined the age determinations, as follows.

The zircon crystals of the mafic tonalite gneiss FS-78-25 are prismatic with length/width ratios of 3:1 to 4:1, well developed euhedral zoning and somewhat rounded, weakly to non-zoned overgrowths. Core/overgrowth ratio is greater than 4:1 in a typical crystal. The cores show a number of inclusions and cracks. The shape and zoning of the cores suggest growth from a melt (Speer, 1980).

Four fractions of zircon, three of which were abraded, from the tonalite gneiss were analyzed. The zircons are markedly discordant and a best-fit line to the four fractions intercepts the upper part of concordia curve at 2518 + 56/−33 Ma (Fig. 40). The lower intercept age of 1723 Ma is discussed below. The late Archean-earliest Proterozoic age is interpreted as the crystallization age of the protolith of the tonalite gneiss. The age is derived largely from abraded zircons and its interpretation assumes that cores were relatively unaffected by any subsequent event. As documented later in this report, intrusive activity under granulite facies conditions took place in Ellesmere Island

between 1.9 and 2.0 Ga, according to zircon U-Pb geochronology. Any effects of this event in Devon Island are assumed to have been largely confined to overgrowths on the zircons.

If the tonalite gneiss is part of the inferred continental margin sequence in the Ellesmere-Devon terrane, a latest Archean-earliest Proterozoic age is indicated for that sequence. Alternatively, the gneiss belongs to a basement of that age, on which the supracrustal rocks presumably were deposited in early Proterozoic time (as they are intruded by ca. 1.9 Ga rocks).

Zircon crystals of the granite gneiss FS-78-26 consist of well zoned, generally blunted, partly resorbed cores mantled by well rounded, more or less homogeneous overgrowths; length/width ratios are 2:1. Cracks occur throughout the grains but are more pronounced in the cores, which also contain inclusions. Core/overgrowth ratios are generally greater than 4:1 but exceptionally may be as low as 3:2.

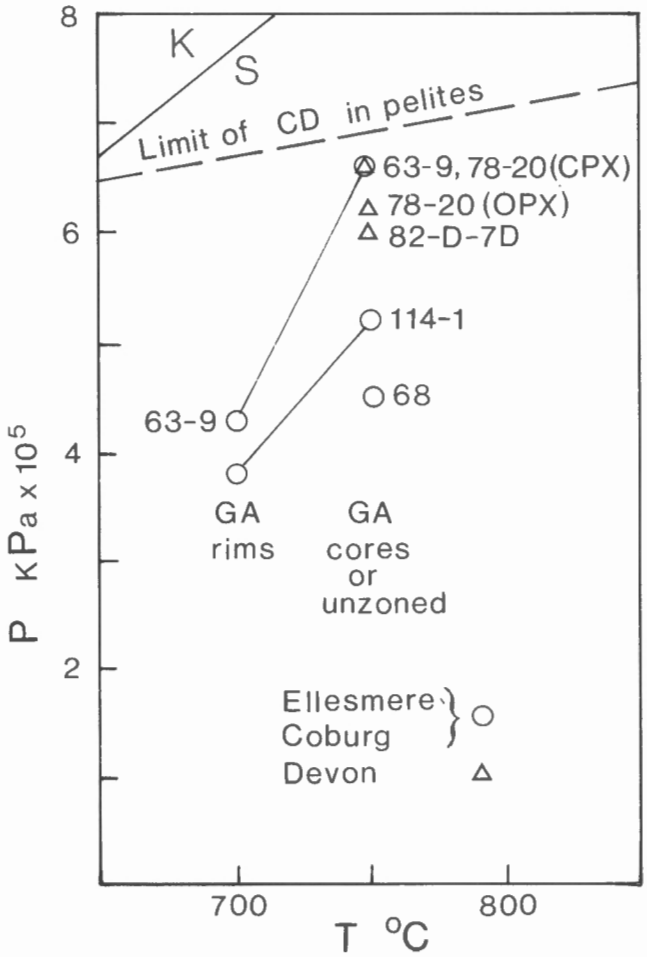

Figure 39. Pressures recorded by garnetiferous quartzofeldspathic gneisses according to Newton's (1983) garnet-pyroxene-plagioclase-quartz geobarometer. K = kyanite S = sillimanite.

Six fractions were analyzed and regression of the data gives an upper intercept age of 2428 +36/−31 Ma (Fig. 40). The lower intercept age is 470 Ma, which can not be related to any known thermal event. The slightly younger age of the granitic rock is consistent with the inference made in the field that it intruded the tonalitic one. The age, taken at face value, indicates a period of granitic intrusion in early Proterozoic time but disturbance of the U-Pb system by later events, which gave rise to the prominent overgrowths on the zircons, is a distinct possibility. The less discordant abraded fractions, particularly C in Figure 40, suggest the presence of an older component. If zircon populations of two distinct ages exist in the sample, the upper intercept age obained may be a mixture of the two. No other ages from the map area indicate an early Proterozoic thermal event. Hence no particular significance is attached to this single Proterozoic date.

K-Ar and U-Pb data provide some indication of the time of uplift of the Ellesmere-Devon crystalline terrane following the late Aphebian granulite facies event. K-Ar ages from metamorphic rocks generally reflect uplift and cooling after the metamorphic peak. Hornblende from the tonalite gneiss and biotite from the granite gneiss give ^{40}K-^{40}Ar ages of 1740 ± 47 Ma and 1769 ± 24 Ma, respectively. The ages agree with an earlier determination of 1760 Ma on biotite from gneiss in southeast Ellesmere Island (Christie, 1962b). Similar (1.7 ± 0.1 Ga) mica and hornblende K-Ar ages have been obtained from basement rocks in northwest Greenland (Larsen and Dawes, 1974), indicating that early Helikian cooling of the crystalline rocks was an event of wide regional significance.

Results of the U-Pb analysis of the tonalitic gneiss zircons can be interpreted as further evidence of ca. 1.7 Ga uplift. The discordia line has its lower intercept with the concordia curve at 1723 Ma. According to the "dilatancy model" for interpreting discordant U-Pb age patterns (Gebauer and Grünenfelder, 1979), the suggested 1.7 Ga lead loss could be ascribed to uplift and erosion, when water carrying radiogenic lead in solution escapes from microchannels in metamict zircon during pressure release.

Marble and calc-silicate rocks (mb)

Bright white marble is a hallmark of the metasedimentary sequences on Ellesmere and Coburg islands (Fig. 41). Belts of marble, up to several hundred metres thick, run from north of Ekblaw Glacier (Map 1572A) to Makinson Inlet (Map 1573A), a distance of some 140 km, highlighting the northerly structural grain of the Ellesmere-Coburg terrane. Marble belts are also abundant south of Smith Bay (Map 1573A) and their extensions are found on Coburg Island (e.g. Princess Charlotte's Monument; Map 1574A). Other major outcrops occur on Thorvald Peninsula and at Cape Isabella (Map 1572A). Marble does not occur to any significant extent west of 79° 30′W on Ellesmere Island. On Devon Island, only a few minor occurrences have been found along the Sverdrup and Belcher glaciers by geologists of Petro-Canada Ltd. (J.C. Harrison, pers. comm., 1983).

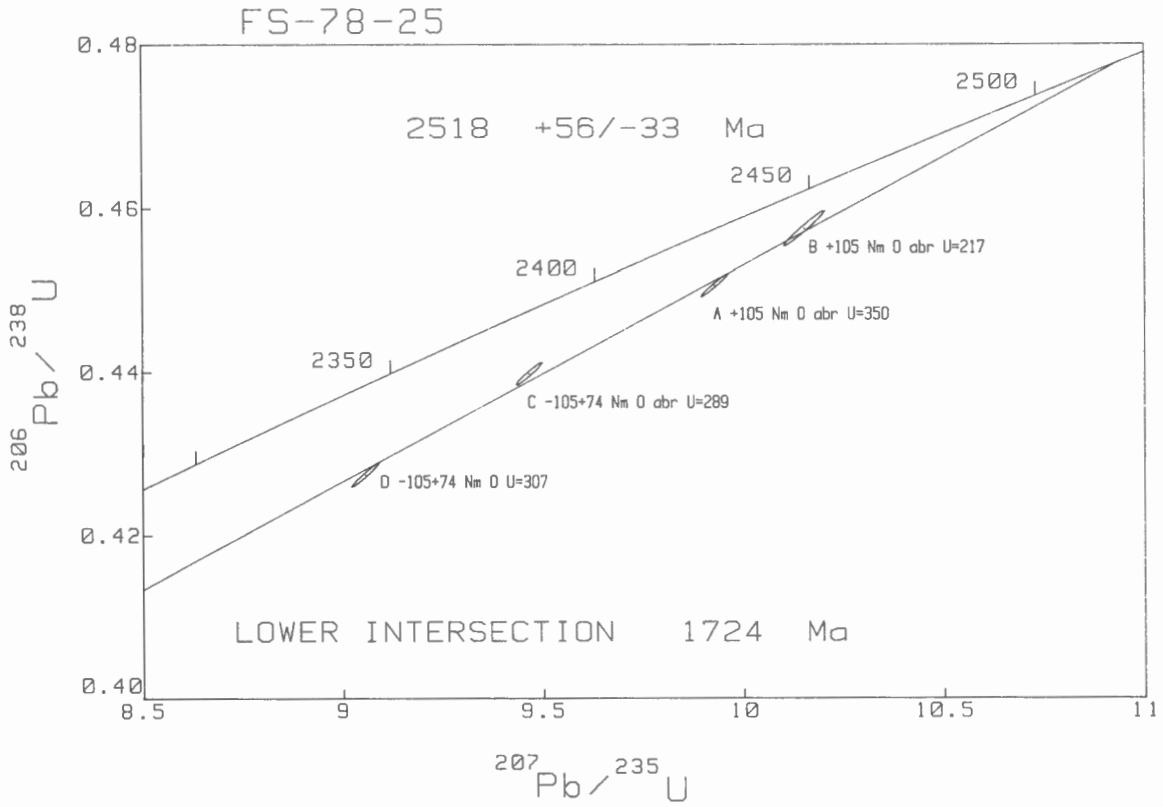

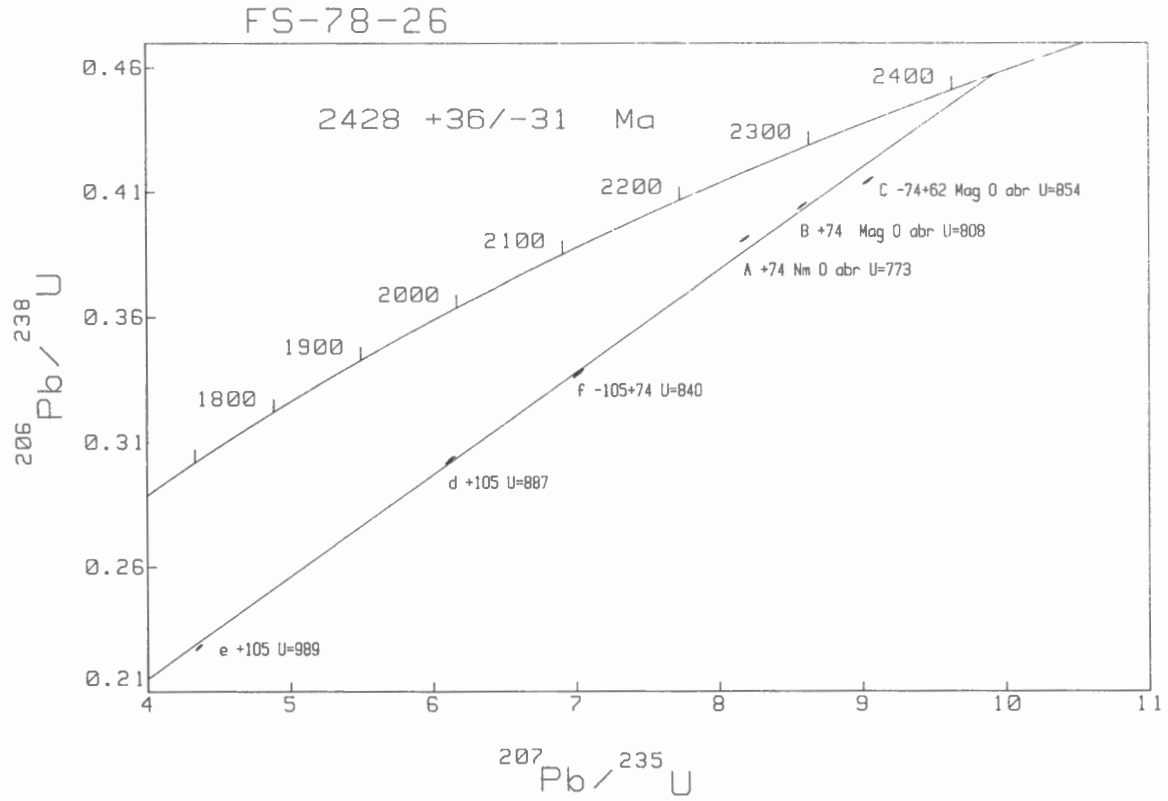

Figure 40. Concordia diagrams showing results of U-Pb analyses of zircon from interlayered orthopyroxene tonalite gneiss FS-78-25 and granite gneiss FS-78-26, southern Devon Island. U contents in ppm. Nm = non-magnetic, abr = abraded.

Figure 41. White marble layers in a supracrustal sequence north of lower Makinson Inlet, Ellesmere Island.

Calc-silicate gneisses are found closely associated with marble and in isolated occurrences among non-calcareous rocks throughout the Ellesmere-Coburg terrane but are scarce on Devon Island.

Marble and calc-silicate rocks are associated most commonly with cordierite gneiss, quartzite and pyribolite. On the western shore of Smith Bay, marble beds alternate with orthopyroxene-bearing quartzofeldspathic gneisses, suggesting that the latter are of supracrustal origin. Fragments of adjacent rocks have commonly been caught up in marble during its deformation by flow. At Cape Isabella, amphibole-rich metasomatic rock has developed at the contact between marble and intrusive granitoid rock.

Marble, typically, is white on fresh and weathered surfaces, medium- to coarse-grained, calcitic and impure to variable degree. As a result of the alteration of accessory minerals such as sulphides, some marble layers weather yellow, orange or pale green. The most common minerals, other than calcite, are diopside, olivine, clinohumite, scapolite, and spinel.

Petro-Canada geologists (Gibbins, 1985) found nearly pure dolomite marble outcropping on several nunataks north of Talbot Inlet, 15 km northwest of Cape Faraday (Map 1573A). The marble consists of talc and serpentine in a dolomite matrix and is interlayered with a variety of calc-silicate rocks and calcitic marble. These occurrences of dolomitic rocks appear to be exceptional.

Calc-silicate rocks not associated with marble are generally characterized by abundant clinopyroxene and green hornblende and minor sphene. Calc-silicate gneiss interlayered with orthopyroxene tonalite gneiss on the north shore of Makinson Inlet contains diopside, bright green hornblende, brown garnet (andradite?), scapolite, plagioclase, perthite, a little quartz, and carbonate.

The metamorphism of calcareous rocks involves an unusually large number of variables: in addition to load pressure, temperature and bulk composition, the concentrations of H_2O, CO_2 and F in the vapour phase and the susceptibility of the rocks to metasomatism play an important role. These factors can lead to complex, high variance parageneses requiring extensive sampling and detailed study to characterize them. In the present work, only a limited number of samples have been collected and examined in detail and the results should be regarded as no more than a rough guide to the more common assemblages in the map area, which are listed in Table 7. The list of assemblages replaces that given in Frisch (1983, p. 9), which contains misidentifications corrected by subsequent microprobe analyses.

Calcite is the predominant mineral and any dolomite present tends to occur as exsolved blebs in calcite. Polysynthetic twinning and triple junctions between grains are characteristic features of most samples.

Although olivine and diopside were identified as coexisting in the field, they have not been found in the same thin section. Diopside appears to be the more common of the two, occurring as a major mineral in both marble and calc-silicate rocks. Olivine is invariably fresh and accompanied by pleochroic yellow clinohumite.

In FSM-77-190-2 the clinohumite has overgrown olivine and is clearly late. In the other olivine-bearing rock examined (FSM-77-107-1), clinohumite and olivine are closely associated and appear to have formed at about the same

Table 7. Mineral assemblages in marble and related calc-silicate rocks.

1.	Calcite + diopside (+ forsterite)
2.	Calcite + forsterite + clinohumite + spinel (+ graphite)
3.	Calcite + diopside + clinohumite + spinel
4.	Calcite + diopside + scapolite + grossular + plagioclase + quartz + corundum + sphene
5.	Calcite + diopside + grossular + apatite + sphene (+ scapolite)
6.	Mg-salite + wollastonite + scapolite (+ calcite + quartz)
7.	Calcite + diopside + phlogopite + edenitic hornblende + tremolite + graphite
8.	Diopside + phlogopite + zoisite + scapolite + tremolite + plagioclase + calcite

Calcite may be accompanied by subordinate dolomite in any of the calcareous rocks.

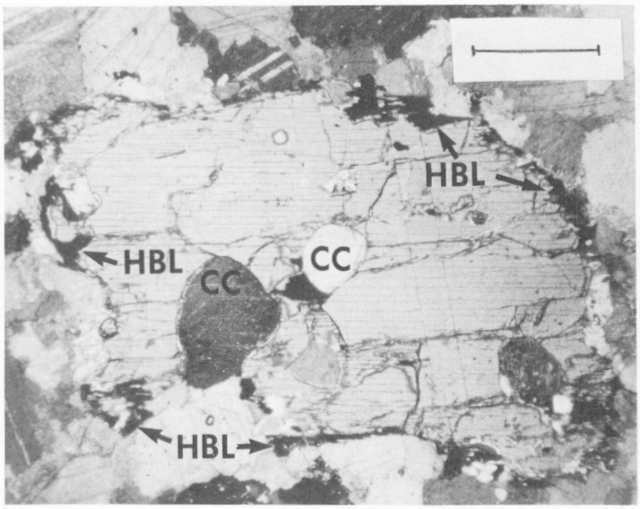

Figure 42. Partial replacement of diopside by tremolite (HBL) in calcite marble. Crossed nicols. Bar scale 1.0 mm.

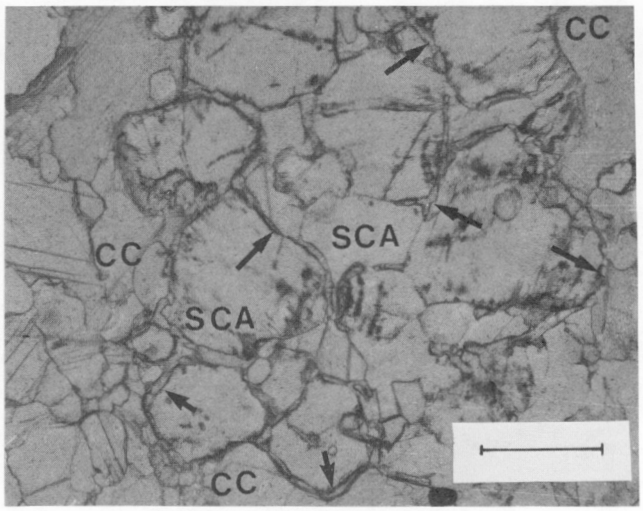

Figure 43. Evidence of retrogression in calcite marble: probably in response to falling temperature and P_{CO_2}, scapolite has reacted with calcite (and quartz) to form grossular rims (arrowed). Plane light. Bar scale 0.5 mm.

time. A third clinohumite-bearing rock (FS-77-223) contains colourless diopside, which is in part overgrown by very weakly pleochroic clinohumite. Pale green or brownish spinel, in euhedral grains up to 0.5 mm across, occurs in all three rocks.

Clinopyroxene occurs as a major constituent of all the other mineral assemblages studied. It is colourless, commonly shows lamellar twinning and may be sector zoned. Although generally fresh, clinopyroxene in amphibole- and phlogopite-bearing marbles may be partly replaced at the margins by tremolite (Fig. 42).

Scapolite appears to have formed early and subsequently become unstable. In one marble (FSM-77-62; assemblage 4, Table 7), it occurs as inclusions in diopside as well as in the carbonate matrix, where it has reacted with calcite (and quartz) to form narrow selvages of grossular (Fig. 43). Grossular in the marbles, generally, has formed by the replacement of scapolite. In FSM-77-62, plagioclase grains are separated from calcite by a narrow desilication rim of corundum.

Wollastonite is a common constituent of skarn-type assemblages and marble, as at Cape Isabella (Map 1572A), where it forms blades several centimetres long intergrown with clinopyroxene, partly altered scapolite and minor calcite and quartz.

Phlogopite and hornblende occur together, along with diopside, in graphite-bearing marble (FS-77-20B). Both minerals are colourless, coarsely crystallized and fresh, in contrast to diopside, which is partly replaced by tremolite. Some of the phlogopite and pargasite discontinuously overgrow diopside, attesting to their relatively late formation.

A rock from the south shore of Hayes Fiord (Map 1572A; FSM-77-198) is an example of a hydrated, retrograded calc-silicate. It consists of diopside, inhomogeneous calcic plagioclase, scapolite, phlogopite, tremolite, zoisite and subordinate calcite. Phlogopite, as well as tremolite, appears to have replaced some of the diopside and much of the plagioclase is replaced by bladed to granular zoisite.

Accessory minerals in the carbonate rocks include spinel, sphene, graphite and rare apatite, Fe-Ti oxide and sulphide. Spinel has been found only in clinohumite-bearing rocks and is commonly pale green but may be zoned, with green cores and brownish green rims. Brown sphene, in rounded grains up to 0.4 mm across, occurs in grossular-bearing rocks.

Mineral chemistry

Chemical analyses of minerals in marble and calc-silicate rocks are listed in Appendix, Table 3.

All but one of the clinopyroxenes analyzed are diopside; the exception is magnesian salite $Ca_{49}Fe_{13}Mg_{38}$, which coexists with scapolite and wollastonite in calc-silicate rock (FSD-77-148-1). In only one sample (FSM-77-62) is clinopyroxene markedly inhomogeneous, showing intergrain differences in Fe content of as much as 5 atom per cent. Intra-grain variations in chemistry were not detected even in optically sector-zoned crystals.

The two analyzed olivines (FSM-77-107-1 and 190-2) coexist with clinohumite. One is forsterite Fe_3Mg_{97}, overgrown and partly replaced by magnesian clinohumite. The other is chrysolite $Fe_{15}Mg_{85}$ and coexists with relatively iron-rich clinohumite and magnesian spinel that has green cores enriched in iron relative to brownish green rims (FSM-77-107-1). Both olivines are virtually calcium-free.

Analyses of clinohumite are only partial as fluorine was not determined. The fluorine content of the clinohumites may be significant, since fluorite was noted in skarn assemblages at two localities near Cape Isabella. The intensity of yellow coloration in clinohumite varies within and between grains but, in agreement with Bourne's (1974) finding, no relation between colour and chemical composition was detected. The microprobe was indispensable in distinguishing between olivine and colourless clinohumite, which optically appear identical but differ consistently in Si and Ti.

Other minerals analyzed — edenitic hornblende, meionitic scapolite, grossular, phlogopite, wollastonite and zoisite — have compositions close to ideal or end-members and, except for Si, Ti and Al in hornblende (FS-77-20B), are homogeneous.

Metamorphic conditions

With the limited data available, the mineral assemblages of the calcareous and calc-silicate rocks of the map area can provide no more than approximate estimates of pressure and temperature of metamorphism. The great predominance of calcite over dolomite implies the complete decarbonation of what presumably were siliceous dolomitic rocks, a process possible only under the highest grade of metamorphism. The widespread development of clinohumite appears to be limited to at least the upper amphibolite facies (Bourne, 1974). The common occurrence of wollastonite and of forsterite indicates moderate to low pressure and high temperature (Winkler, 1979).

A considerable body of experimental data is available for the siliceous impure carbonate system at 5×10^5 kPa pressure (Winkler, 1979, Fig. 9-5; Sauter, 1983, p. 94), around that suggested by many of the metasediments and gneisses associated with the metacarbonates. At this pressure, if the mole fraction of CO_2 was high, the temperature of formation of forsterite would have been close to 700°C. Similar temperatures are required by the coexistence of forsterite and diopside.

The occurrence of wollastonite in several localities is yet another example of this mineral in regionally metamorphosed terranes. Miyashiro (1973) listed several examples of regionally developed wollastonite - all from low-pressure terranes - and Hapuarachchi (1968) emphasized the close association of wollastonite-bearing rocks with cordierite-bearing metasediments in lower granulite facies rocks of Sri Lanka.

Like the gneisses, the calcareous rocks display evidence of retrogression. Tremolite and zoisite occur only as secondary minerals, indicating a late drop in temperature along with a possible influx of water. Similarly, according to Sauter (1983, p. 109), the replacement of forsterite by clinohumite is promoted by low temperature and low P_{CO_2} (probably related to high P_{H_2O}). Most of the grossular in the samples examined occurs as narrow selvages between scapolite and calcite. The breakdown of scapolite to grossular by means of the reaction

$$\text{scapolite} + 5\ \text{calcite} + 3\ \text{quartz} = 3\ \text{grossular} + 6\ CO_2$$

is favoured by decrease in temperature and P_{CO_2} (Mukherjee and Rege, 1972; Schenk, 1984). The presence of minor calcite and quartz in diopside-wollastonite-scapolite rock at Cape Isabella suggests local breakdown of wollastonite to calcite+quartz, a consequence of falling temperature (Winkler, 1979).

It should be noted, however, that retrogression did not reach the stage in which such low-temperature and hydrous processes as serpentinization of olivine and chloritization of phlogopite occurred. This shows that the calcareous rocks were not any more susceptible to retrogression than were the gneisses.

Origin

The thinness and comparative scarcity of calcareous units in the map area leave little doubt that the marble and calc-silicate rocks represent shallow-water deposits such as those which characterize near-shore parts of continental shelves. The quartzites that are locally associated with the marbles are further evidence of this environment.

Quartzite (qz)

Quartzite layers are common, if generally minor, components of metasedimentary sequences in the map area. Quartzite has its most extensive development on southern Coburg Island (Map 1574A) and on Ellesmere Island northeast of Cape Norton Shaw (Map 1573A) in a major, north-trending belt of metasediments. There, rock sequences consisting almost entirely of quartzite range up to several hundreds of metres in thickness. Elsewhere, quartzite beds are rarely more than a few tens of metres thick. Associated rocks are mainly cordierite or pyroxene gneisses and marble.

Quartzite is white, less commonly pale grey, fine grained and contains at least 80 % quartz. Typical impurities include sillimanite, garnet, feldspar (generally K- feldspar), biotite and muscovite. The latter mineral is common in strongly deformed quartzite, where it appears to have formed by the alteration of sillimanite and feldspar (Fig. 44). Highly strained quartz grains and extensive recrystallization (Fig. 44) are typical features. Primary sedimentary structures have not been recognized.

The quartzite originally was probably a mature sediment derived from continental crust and laid down in a shallow-water platform/shelf environment. It seems likely that closely associated rocks, such as cordierite and pyroxene gneisses and marble, were deposited in the same environment. Supracrustal assemblages of quartzite, pelitic schist and marble are characteristic of high grade gneiss belts (Windley, 1984; Kröner, 1985).

Pyribolite and amphibolite (am)

Metamorphosed mafic rocks occur widely throughout the map area but are, with few exceptions, confined to concor-

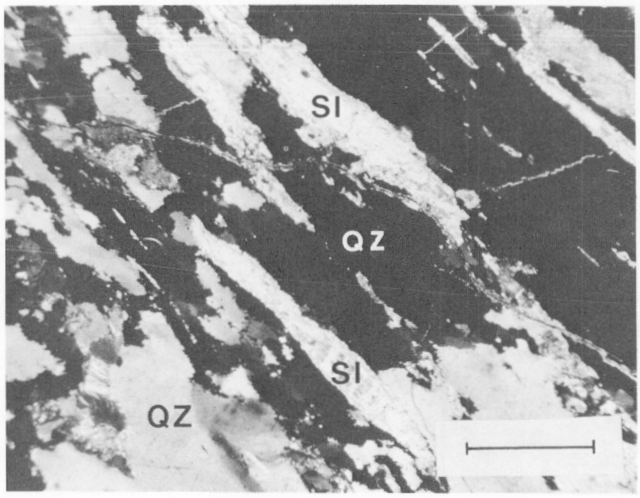

Figure 44. Near total replacement of sillimanite by muscovite in highly strained, retrograded quartzite from Coburg Island. Crossed nicols. Bar scale 1.0 mm.

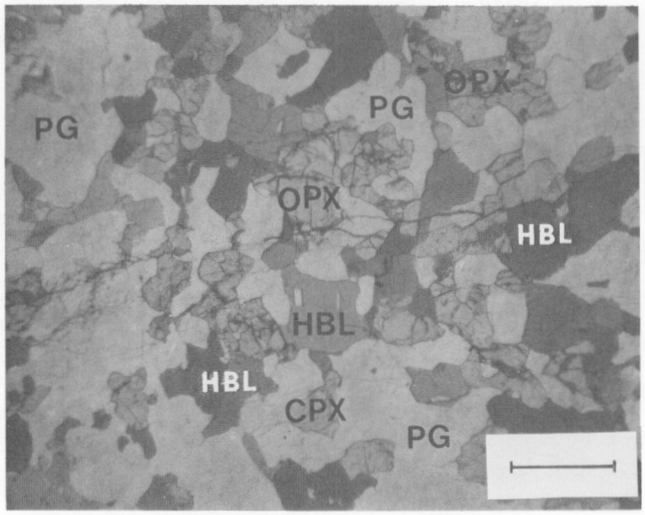

Figure 45. Typical granoblastic texture of pyribolite. Note apparently stable coexistence of hornblende and pyroxene. Plane light. Bar scale 1.0 mm.

dant layers and lenses of relatively small thickness. They are most common in supracrustal sequences, where they are associated with cordierite gneiss, quartzite and marble. Pyribolite is also locally abundant as schlieren in orthopyroxene-bearing gneisses.

A number of mafic bodies are slightly but clearly discordant — rarely, even relict apophyses are present — and these are very probably metadykes.

Pyribolite and amphibolite are dark green to black, predominantly medium grained rocks that generally show pronounced gneissic structure and, commonly, mafic/felsic layering. Constituent minerals typically comprise plagioclase, orthopyroxene, clinopyroxene, hornblende, biotite, Fe-Ti oxide, and sulphide; biotite and the opaque minerals are generally present only in minor amount. (The statement by Frisch (1983, p. 4) that sphene is an important accessory mineral is incorrect; sphene is found only in retrograded metamafites.) Granoblastic texture in which straight-sided polygonal grains meet at triple points is common in the pyribolites (Fig. 45).

In amphibolites, pyroxene and biotite are minor or absent, pyroxene commonly having been replaced by pale green amphibole. A second amphibole of primary aspect and invariably greenish is generally present. A modified granoblastic texture may be preserved as a relic of the granulite facies but many amphibolites are strongly inequigranular.

In most pyribolites, both orthopyroxene and clinopyroxene, whose proportions range widely, are little altered and appear stable. Orthopyroxene typically is weakly pleochroic but is neutral in some rocks and strongly pleochroic in others. Clinopyroxene is very pale green or neutral and may show exsolution lamellae. Both pyroxenes may be fringed by pale green or blue-green amphibole in partly retrograded rocks.

Amphibole is rarely absent from these rocks. In granulite facies (orthopyroxene-bearing) rocks, discrete amphibole is a green to brown hornblende, typically with X = yellowish green, Y = Z = brownish green or greenish brown. This variety of hornblende shows every sign of being a primary, stable metamorphic mineral (Fig. 45). It is well crystallized, relatively coarse, commonly abundant, and may even be rimmed by pyroxene. Only exceptionally does green-brown hornblende appear to have replaced pyroxene. Secondary amphibole forms narrow, fine grained, pale green to bluish green fringes around pyroxene in partially retrograded rocks. In pyroxene-free amphibolites, the replacement of (ortho?)pyroxene by pale green amphibole has gone to completion but the original outlines of the pyroxene crystals remain. An illustrative example of such a rock is a metadyke, 6-10 m wide, outcropping among fresh granulite facies gneisses northwest of Cape Rutherford (Map 1572A); the mode (and a chemical analysis) of this rock, FS-77-279, is given in Appendix, Table IV). In this rock, the pale green amphibole pseudomorphs after pyroxene are accompanied by a coarser, brownish green hornblende, which looks "primary".

Plagioclase tends to be complexly twinned and normally zoned, with compositions commonly in the andesine-labradorite range (An_{40-55}). Drop-like inclusions of quartz are present in the plagioclase of some rocks. Antiperthite is notably absent.

Deep brown or red-brown biotite is commonly present but generally does not exceed a few per cent by volume of the rock. Like the green-brown hornblende, it generally is well crystallized and fresh and forms discrete laths unrelated to any particular mineral. In most rocks, it clearly is the latest mafic silicate to have formed, long flakes lying athwart the foliation or cutting across pyroxene or amphibole crystals.

Whereas garnet has not been found in mafic rocks on Ellesmere and Coburg islands, it does occur in equivalent rocks on Devon Island. Garnet forms pale pink, highly sieved porphyroblasts, up to 1 cm in diameter, but is always subordinate in amount to pyroxene and amphibole.

Mafic rocks of amphibolite facies occur sporadically in the map area and are generally localized in layers or zones within granulite grade rocks. In many instances they can be related to shear and cataclasis, which undoubtedly promoted retrogression. They are relatively abundant in the westernmost exposures of the Precambrian Shield on both Ellesmere and Devon islands, i.e. adjacent to the margin of the Paleozoic Arctic Platform, where they occur amongst clearly retrograded rocks described elsewhere in this report. Amphibolite facies amphibolites lack orthopyroxene and brownish amphibole but may contain clinopyroxene and sphene. The amphibole is green or bluish green, biotite is brown to greenish brown and plagioclase is altered to sericite and/or epidote.

Mineral chemistry

Chemical analyses of minerals of pyribolite are presented in Appendix, Table 4. Zoning was not detected in any of the mafic silicates.

The generally weak pink to green pleochroism of the orthopyroxene appears to be related to alumina content, the more aluminous orthopyroxenes (with up to 1.6 % Al_2O_3) being the most intensely coloured. Of the seven orthopyroxenes analyzed, all but one are hypersthenes, ranging in composition from $Ca_1Fe_{31}Mg_{68}$ to $Ca_2Fe_{46}Mg_{52}$; the exception is ferrohypersthene $Ca_1Fe_{52}Mg_{47}$ (Fig. 46).

In all the orthopyroxenes analyzed, Si and Al (calculated on the basis of 6 oxygens) are insufficient to fill the Z site and cation totals exceed the ideal 4.00 by 0.03 to 0.04. The excess in the WXY site probably reflects the presence of ferric iron.

Clinopyroxene is of more restricted composition than orthopyroxene (Fig. 46). All nine clinopyroxenes analyzed are calcium-rich augites, $Ca_{44}Fe_{15}Mg_{41}$ to $Ca_{44}Fe_{21}Mg_{35}$. Sodium content is low, commonly less than 0.2 % Na_2O, with the notable exception of the clinopyroxene in FSM-77-108, which has 0.74 % Na_2O. The latter coexists with biotite and sodic oligoclase (An_{14}) in a rock forming a layer in marble on Coburg Island. The sodic nature of the clinopyroxene and plagioclase can probably be ascribed to an unusual rock composition, such as a metasomatic mafic calc-silicate rock.

The hornblendes show the olive and brown colours characteristic of Ca- amphiboles of high grade metamorphic rocks (Miyashiro, 1973, p. 254). A correlation between Ti content and brown colour (Miyashiro, 1973, p. 255) is clearly demonstrated by the hornblende in sample FS-77-157, which has a chestnut brown Z colour and 3 % TiO_2. The microprobe analyses of hornblendes have been recalculated on the basis of 23 oxygens and named according to the computerized nomenclature scheme of the International Mineralogical Association, bringing the total S2 cations to 13 by redistribution of total iron between ferrous and ferric iron (Rock and Leake, 1984). This scheme commonly leads to a large number of names even when compositional differences are slight. The six Ca-amphiboles analyzed vary but little in major element chemistry (Appendix, Table 7) and are hastingsitic or tschermakitic in the IMA classification. Calculated Fe^{3+} tends to be high, and Al^{vi} low, resulting in several hornblendes being termed hastingsitic rather than pargasitic or tschermakitic, as is commonly the case for amphiboles from mafic rocks in the granulite facies (e.g. Mengel, 1983b and references therein; Coolen, 1980; Jan and Howie, 1982). Recalculation of microprobe analyses of these published "pargasitic" and "tschermakitic" amphiboles according to the IMA scheme yields a plethora of names similar to that of the present work. Clearly, the IMA name assigned to an amphibole is critically dependent on compositional nuances whose significance and even validity (in the case of partial microprobe analyses) are questionable. The IMA scheme

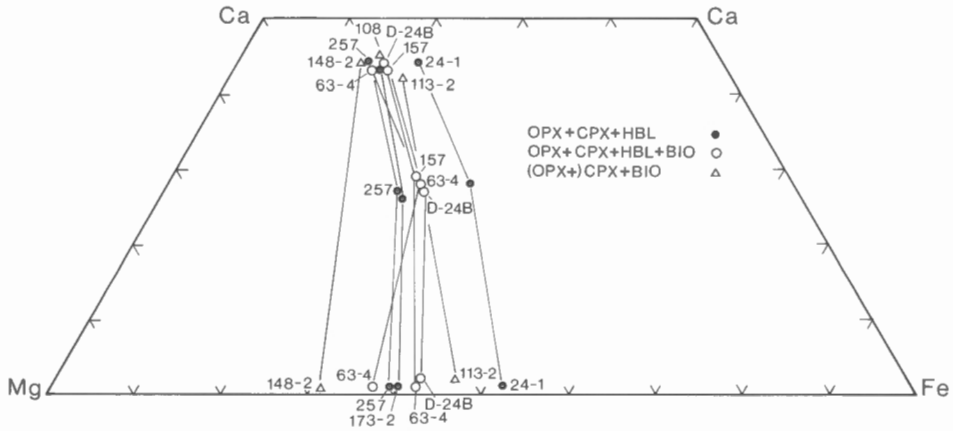

Figure 46. Composition of pyroxenes and amphibole (central part of diagram) of pyribolites in terms of Ca, Mg and Fe. Atom per cent.

does, however, provide as reasonable a method of calculating ferric iron in a microprobe amphibole analysis as possible, allowing comparisons of analytical data to be made on a uniform basis.

The amphiboles from the Ellesmere-Devon terrane all have the high titanium, aluminium and alkali contents that typify amphiboles of the granulite facies (Binns, 1969). TiO_2 exceeds 1 % and typically is close to 2 %, Al_2O_3 exceeds 10 % and total alkalis are greater than 3 %. Al^{vi} is uniformly low (less than 0.2 cations per 23 oxygens).

In sample FSM-77-24-1, from the western shore of Starnes Fiord (Map 1573A), hornblende in contact with plagioclase (An_{79}) is fringed by a fine grained intergrowth of clinopyroxene, plagioclase and minor Fe-Ti oxide (Fig. 47). Clinopyroxene and plagioclase vermicules, which lie perpendicular to the hornblende crystal margin, alternate regularly, and the oxide grains tend to be distributed along the interface between the intergrowth and plagioclase. Except for an increase in titanium (from 0.16 to 0.46 % TiO_2), there was essentially no change in composition from primary to secondary clinopyroxene. (The secondary plagioclase has not been analyzed.)

Analogous intergrowths along hornblende-plagioclase contacts have been noted in granulite facies rocks by Woodford and Wilson (1976), Coolen (1980) and Schenk (1984) but in each of these instances, the secondary pyroxene is either clinopyroxene and orthopyroxene or orthopyroxene alone. All these workers attribute the intergrowth to a second metamorphic event. The Ellesmere Island sample comes from the vicinity of a metadiabase dyke, which may have supplied the heat to cause a dehydration reaction involving hornblende and plagioclase.

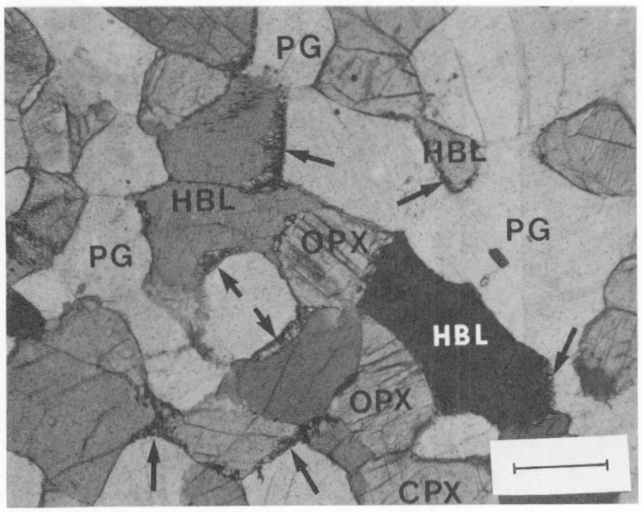

Figure 47. Hornblende in contact with calcic plagioclase in pyribolite FSM-77-24-1 is bordered by finely intergrown clinopyroxene, plagioclase and minor Fe-Ti oxide (arrowed). The compositions of the two generations of clinopyroxene are virtually identical. Plane light. Bar scale 0.5 mm.

Biotite, present in five of the eight metamafic rocks analyzed, is titaniferous and magnesian: TiO_2 ranges from 4.7 to 5.9 % and Fe/Fe+Mg is typically 0.4 (similar to that of coexisting amphibole). In the structural formula calculated on the basis of 22 oxygens and considering all iron to be divalent, there is insufficient Al to fill the tetrahedral site. High Ti and Mg and low Al^{vi} are characteristic features of granulite facies biotite (Guidotti, 1984).

Regular distribution of elements between coexisting minerals is a measure of the degree of equilibrium attained during crystallization. Fe/Fe+Mg of coexisting pyroxenes and amphibole in the metamafites is plotted in Figure 48. Distribution coefficients (K_D's) are relatively constant — particularly in the case of orthopyroxene-clinopyroxene and orthopyroxene-amphibole — suggesting largely equilibrium crystallization. Furthermore, the K_D's are similar to those from other rocks of similar composition and metamorphic grade (see Mengel, 1983b).

As far as can be seen from a relatively small sample population, Fe-Mg distribution between biotite and the other mafic silicates is less regular (Fig. 48). The scatter may be a reflection of the generally late formation of biotite in the rocks. The larger (up to 4 mm) laths of the magnesian biotite in FSM-77-148-2, which plots anomalously in Figure 48, lie discordant to the gneissic layering and clearly formed late.

Plagioclase ranges widely in composition, from oligoclase to bytownite and is strongly zoned in some samples, e.g. 54 to 79 % An in FS-82-D-24B. The more calcic plagioclases are not suitable for anorthite determination on the flat stage. Such methods result in underestimation of An content, as shown by the statement by Frisch (1983, p. 4) that plagioclase in the pyribolites is commonly andesine-oligoclase. Labradorite-bytownite appears to be the typical composition and zoning is of normal type. The remarkably sodic plagioclase $An_{14}Ab_{84}Or_2$ in FSM-77-108 probably formed by metamorphism of an unusually sodic (metasomatic?) calc-silicate rock (see above).

Metamorphic conditions

The absence of garnet from the metamafic rocks analyzed greatly restricts their potential as indicators of physical conditions during their metamorphism. No reliable estimates of pressure can be obtained from the mineral assemblages but estimation of temperature can be attempted by means of two-pyroxene geothermometry.

Temperatures given by Powell's (1978), Kretz's (1982) and Bertrand and Mercier's (1985/86) geothermometers range largely from 800 to 900°C. Excluding anomalously high and low values, average temperatures obtained by these three methods fall between 800 and 850°C. Judged from the more reliable estimates derived from garnetiferous quartzofeldspathic gneisses, these temperatures are probably 50 to 100° too high.

Lindsley's (1983) graphical two-pyroxene geothermometer yields rather scattered results and major discrepancies

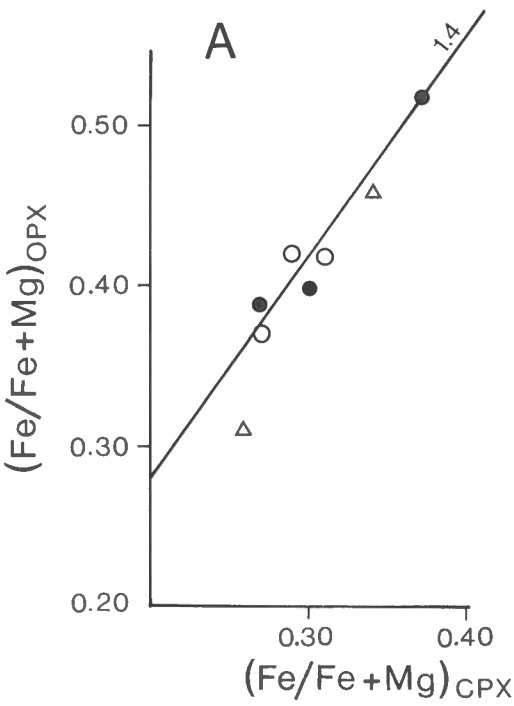

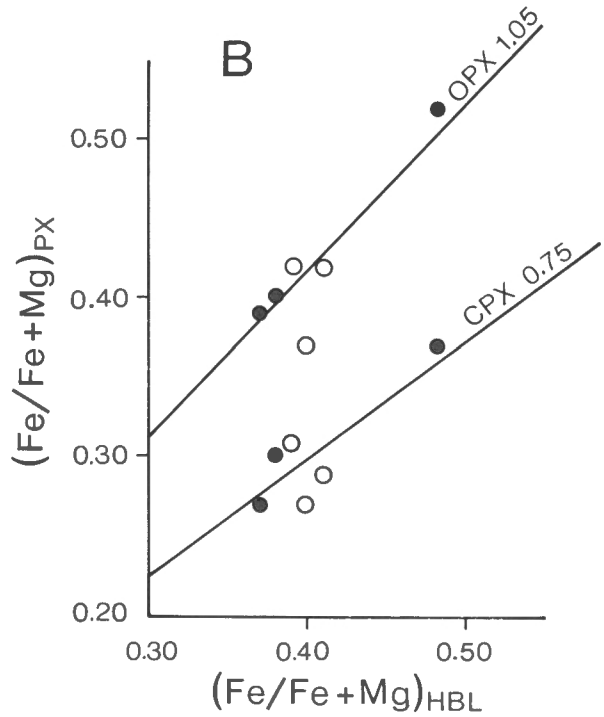

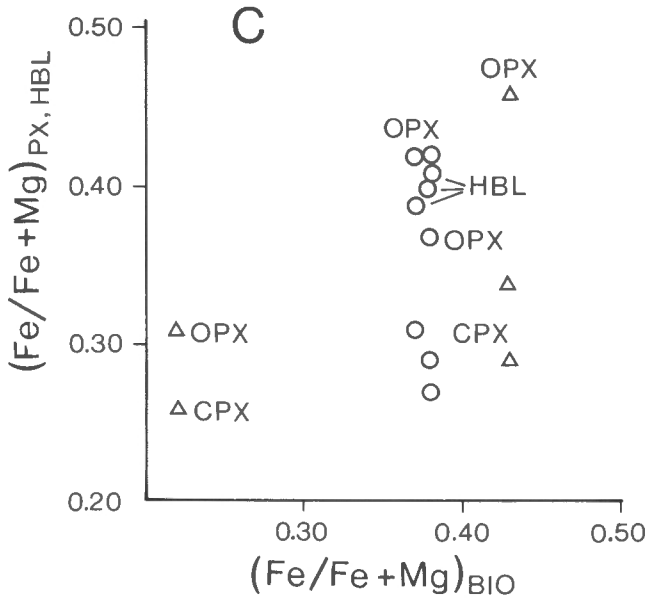

Figure 48. Fe-Mg (atomic) distribution betwen coexisting mafic silicates of pyribolites. Lines are drawn for various distribution coefficients as marked. Symbols as in Figure 46.

between clinopyroxene and orthopyroxene temperatures. The diagram of relations at 5 x 10^5 kPa (Lindsley, 1983, Fig. 9b) was used. Orthopyroxene temperatures range from 650 to 800°C, clinopyroxene temperatures from 750 to 1150°C; average temperatures are 730 and 980°C, respectively. Results from pyroxenes with calculated ferrous and ferric iron are little different. The commonly encountered problems of geothermometry on high grade metamorphic pyroxenes analyzed by microprobe — and consequent compositional uncertainties — alluded to by Lindsley (1983) are once again apparent.

Rock chemistry

Seventeen samples of metamafic rocks — hereafter referred to collectively as pyribolite but see Figure 49 — have been chemically analyzed with a view to determining their protoliths and paleotectonic environment. Analyses are presented in Table IV of the Appendix.

A necessary first step is to attempt to establish whether or not the pyribolites are all meta-igneous. Field relations, described above, clearly indicate an igneous origin for some of the pyribolite bodies. Other bodies, however, particu-

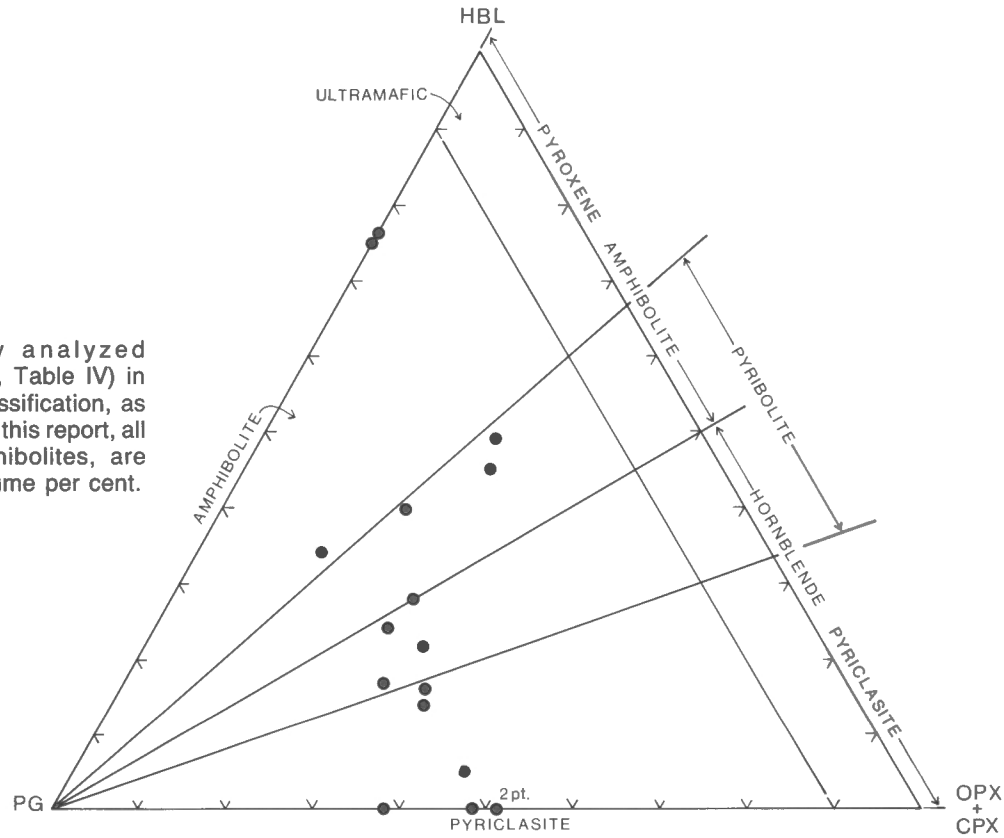

Figure 49. Chemically analyzed metabasaltic rocks (Appendix, Table IV) in Berthelsen's (1960) modal classification, as depicted by Mengel (1983a). In this report, all rocks, except the two amphibolites, are referred to as pyribolites. Volume per cent.

larly those associated with calcareous metasediments, may have formed by the metamorphism of appropriate mixtures of shale and carbonate rock or by metasomatism.

Leake (1964) has devised several discriminant diagrams based on chemical trends of rock suites to aid in distinguishing between igneous and sedimentary origins of metamafites. Cr and Ni (Fig. 50a) in the Ellesmere-Coburg pyribolites show the strong positive correlation with Niggli mg that characterizes differentiated igneous suites. Igneous trends, although perhaps less well developed, are also evident in plots involving Niggli mg, c, al, and alk (Fig. 50b). The displacement of the rocks to the c-100mg side of the Karroo trend in the 100mg-c-(al−alk) triangle appears to be common in metamafites of igneous origin (e.g. Leake, 1964; Kalsbeek and Leake, 1970; Sills and Tarney, 1984). One sample lying off the general trend in two diagrams is FSM-77-108, the pyribolite that forms a layer in marble and contains anomalously sodic plagioclase and clinopyroxene. This rock may well have been affected by metasomatism or indeed may be of entirely non-igneous origin. Nevertheless, the pyribolites as a group can best be interpreted as meta-igneous rocks.

Accepting their igneous origin, we next face the problem of the composition of the magma(s) from which the rocks crystallized. For rocks as highly metamorphosed and thoroughly recrystallized as these, any inference drawn from present chemistry as to original composition must be treated with caution and as many disparate lines of chemical evidence as practical must be used to determine magma type.

The seventeen samples analyzed are of basaltic composition according to the definition proposed by the Basaltic Volcanism Study Project (1981), with the single exception of FS-77-346, which, with 13.9% MgO, exceeds the suggested limit of 12%. All but four are tholeiitic according to the CIPW normative composition. The only rocks with significant normative nepheline are FSM-77-108 (the marble-hosted pyribolite) and the magnesian 346. Only these two and one other sample fall in the alkalic basalt field of the alkali-silica diagram (Fig. 51a). In the discriminant plot of "immobile" trace elements suggested by Floyd and Winchester (1975) (Fig. 51b), all but one of the samples plot in the tholeiitic field. Except for 108 and two other samples, the pyribolites belong to the tholeiitic series in Irvine and Baragar's (1971) AFM diagram (Fig. 52).

Tectonic setting

Discrimination of igneous rock suites of different tectonic environments by chemical criteria has been intensively pursued in recent years. Trends and associations particularly of trace elements that appear to be resistant to the effects of alteration and metamorphism seem to be of some use in characterizing modern volcanic suites and their tectonic settings. Application of these methods to ancient rocks is fraught with pitfalls. No chemical signature is infallible even in the case of completely fresh, modern rocks. Chemical trends and elemental abundances in modern igneous rocks are presumably a result of processes involving the modern upper mantle from which the rocks

were derived. There is no assurance, and indeed some evidence to the contrary, that chemical composition of the upper mantle or heat flow, which influences depth and degree of melting, have remained unchanged since Precambrian time. Nevertheless, it is of interest to at least compare the highly metamorphosed Precambrian metabasaltic rocks of the Ellesmere-Coburg terrane with modern basalts. The fields in the discriminant diagrams considered in the following discussion are defined by modern rocks and should be regarded primarily as providing a framework of reference.

Ti, Zr, Y, Nb and P vary systematically in fresh lavas and are among the least mobile elements in chemical processes of weathering and metasomatism (Floyd and Winchester, 1975). In a plot of Ti vs. Zr, Pearce (1982, Fig. 13) has distinguished not only two suites of modern

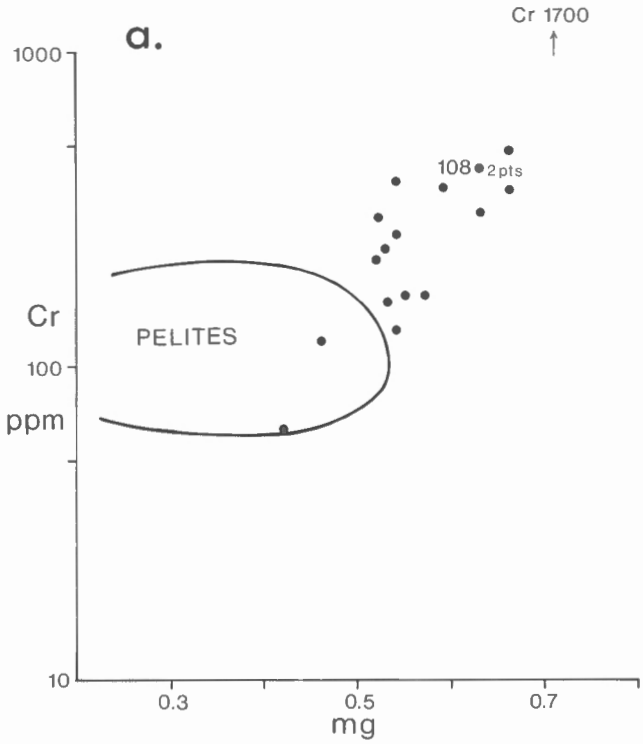

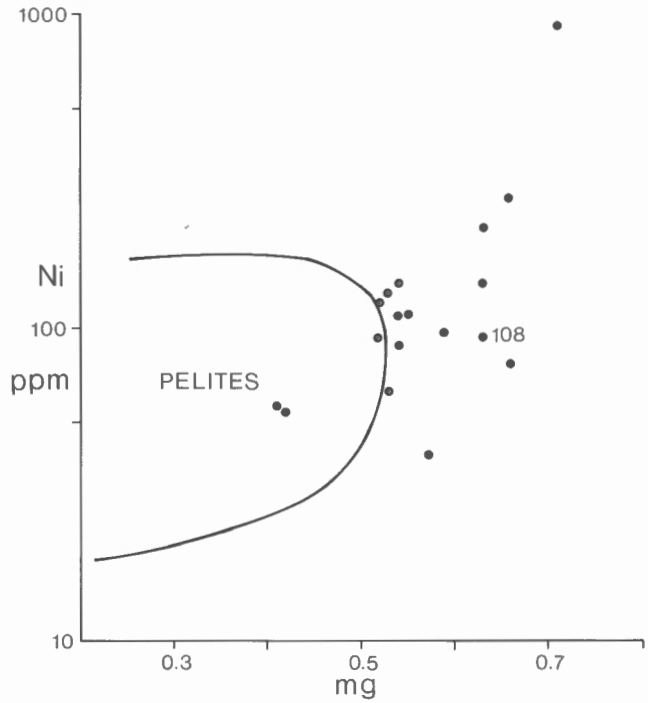

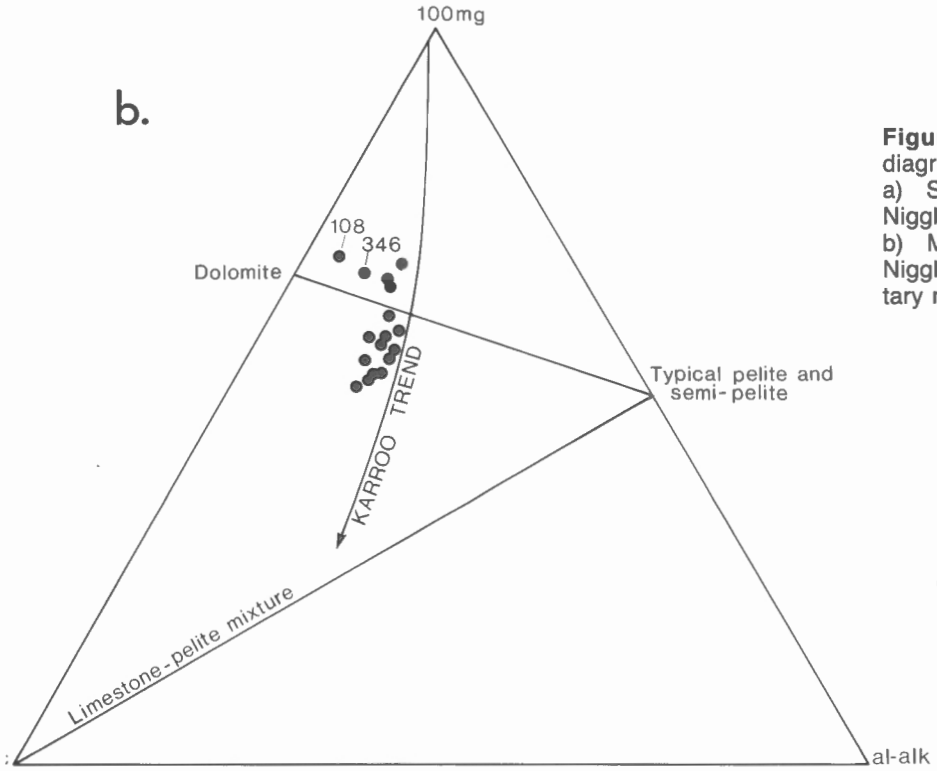

Figure 50. Metabasalts in the discriminant diagrams of Leake (1964).
a) Strong positive correlation of Cr and Ni with Niggli mg, as in igneous suites.
b) Most of the rocks follow igneous trends in Niggli diagrams comparing igneous and sedimentary rocks.

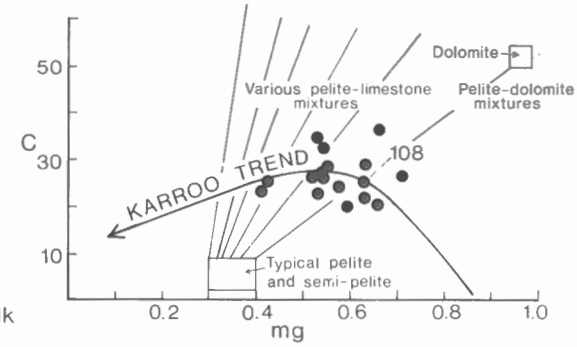

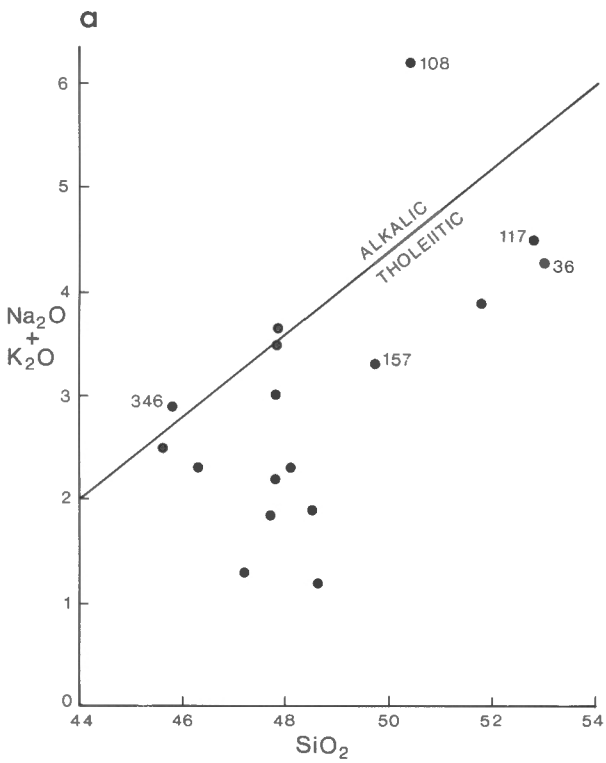

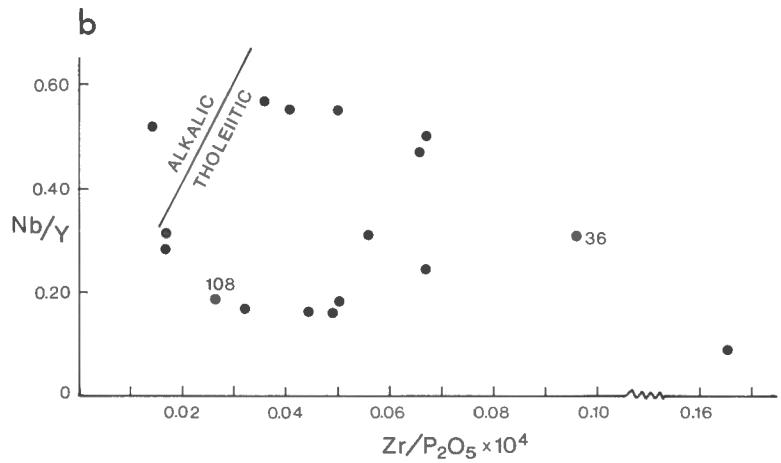

Figure 51. Discrimination between alkalic and tholeiitic compositions in metabasalts.
a) Alkali-silica diagram of Irvine and Baragar (1971). Weight per cent.
b) "Immobile" trace element diagram of Floyd and Winchester (1975).

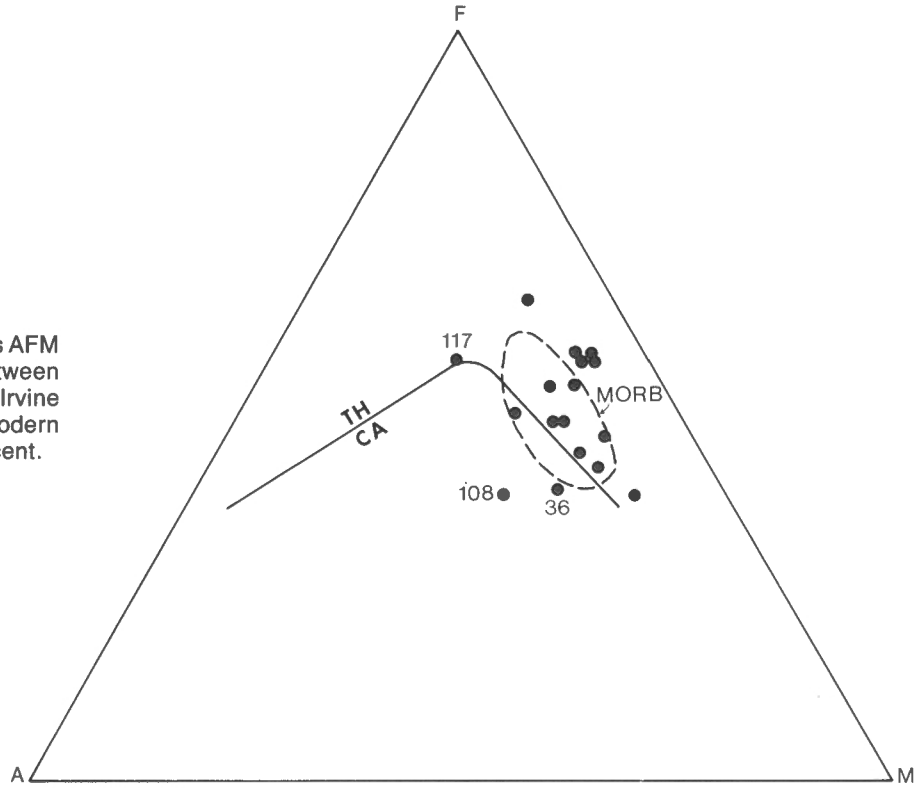

Figure 52. Metabasalts in the igneous AFM diagram, showing the dividing line between tholeiitic and calc-alkaline fields (after Irvine and Baragar, 1971) and the field of modern mid-ocean ridge basalts. Weight per cent.

volcanics but also basic and evolved rocks in these suites. The Ellesmere-Coburg rocks plot mainly in the basic portion of the diagram (Fig. 53). Most fall in the "arc lavas" field and "mid-ocean ridge basalt (MORB)" field, which partly overlaps both the "arc" and "within-plate" fields. Four samples, including the marble-hosted sample 108, are "evolved" rocks according to this diagram. Because several of the other discriminant diagrams are based on more or less primitive basalts, the four "evolved" samples are identified if they plot anomalously in them. In the Zr/Y - Zr plot (Fig. 54), the "basic" Ellesmere-Coburg rocks fall in or near the fields of modern MOR and island arc basalts. In terms of Ti vs. Cr (Pearce, 1975), the rocks are comparable more to ocean floor than island arc tholeiites of modern times (Fig 55); interestingly, a plot of TiO_2 against FeO_t/MgO (Fig. 56) gives the same indication. In the Ti-Zr-Y (Pearce, 1975) and TiO_2-MnO-P_2O_5 (Mullen, 1983) triangles (Fig. 57 and 58), the "basic" rocks show affinity with those of modern island arcs or ocean floors, not with orogenic calc-alkali or within-plate basalts.

Relatively high nickel content distinguishes the Ellesmere-Coburg pyribolites from modern island arc tholeiites but there is partial overlap with MORB (Fig. 59). The bulk of the pyribolites feature the high Ni that is characteristic of Archean tholeiites and possibly an example of a secular change in mantle source-region chemistry since Precambrian time (Gill, 1979).

Few elemental abundance ranges are by themselves diagnostic of particular tectonic settings of igneous rocks but in their relatively high contents of K_2O, Ba and Sr the pyribolites fall outside the ranges for ocean floor basalts given by Miyashiro (1975, Table 4). Rb in the "basic" (non-evolved) rocks is below the lower limit given by Miyashiro (1975) for calc-alkali rocks of continental margins.

Similarity of the Ellesmere-Coburg pyribolites to present-day oceanic (particularly abyssal), rather than orogenic or continental basalts, is also brought out by major/minor element discriminant diagrams (Fig. 56). The rocks plot in the tholeiitic, as distinct from the calc-alkali, field and show the characteristic iron enrichment trend of this group (Miyashiro, 1975).

Assuming uniformitarianism and a volcanism-related origin, we can suggest that the magmas from which the Ellesmere-Coburg metamafites were ultimately derived formed in an environment with oceanic affinity: abyssal oceanic or island arc underlain by oceanic crust. The latter environment is more in keeping with the nature of the rocks associated with the pyribolites.

Ultramafite (um)

With one exception, metamorphosed ultramafic rock has been found only as small pods, lenses and sheets in supracrustal sequences. The exception is a body (not sampled) several hundred metres wide bordered by orthopyroxene-bearing granitic rock at the edge of the Cory Glacier, southeast Ellesmere Island (Map 1573A).

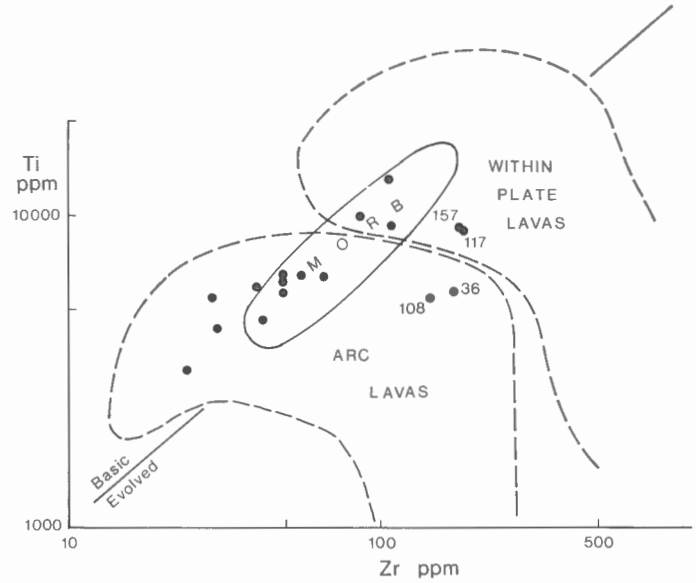

Figure 53. Ti-Zr covariation in metabasalts compared to modern volcanic rocks (after Pearce, 1982).

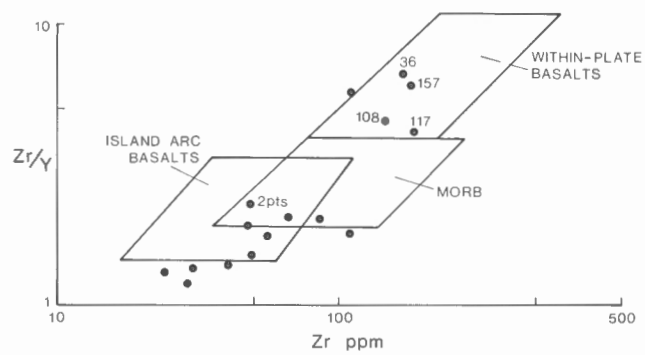

Figure 54. Metabasalts in the Zr/Y vs. Zr discriminant diagram of Pearce and Norry (1979).

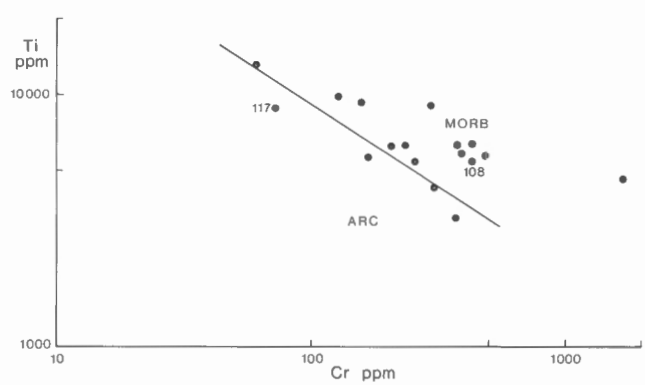

Figure 55. Metabasalts in the Ti-Cr diagram of Pearce (1975), which discriminates ocean floor and island arc basalts.

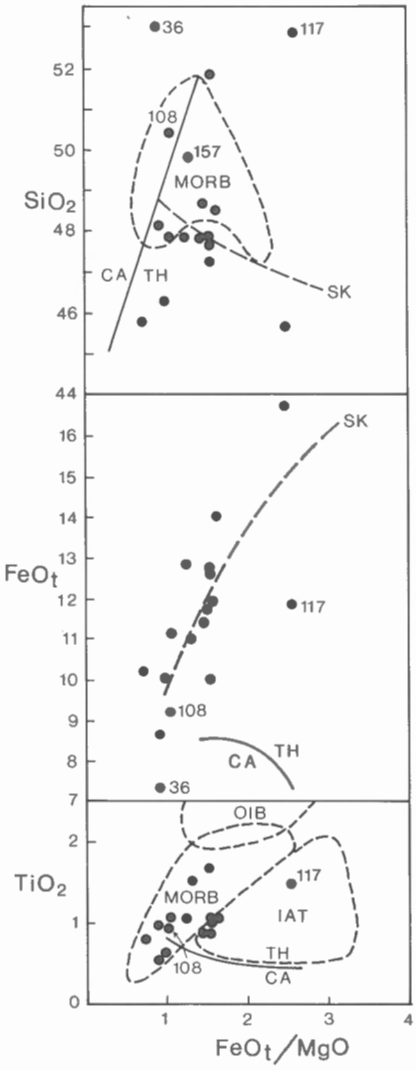

Figure 56. Major and minor element variation diagrams for metabasalts. CA = calc-alkaline, TH = tholeiitic, SK = Skaergaard trend, OIB = oceanic island basalts, IAT = island arc tholeiites. Data sources given in Mengel (1983a, Fig. 8). Weight per cent.

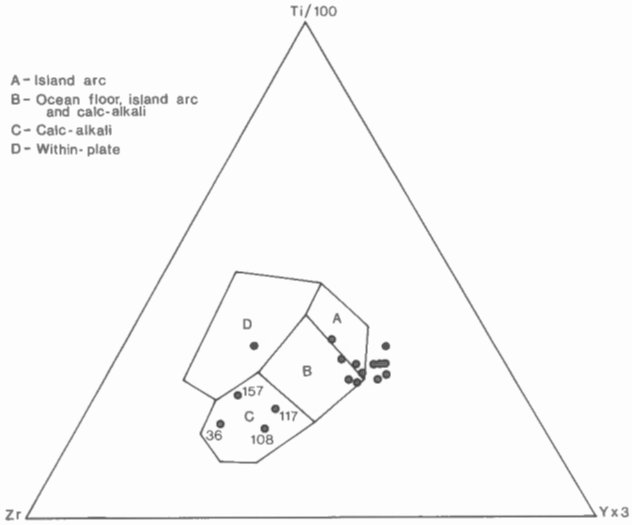

Figure 57. Ti-Zr-Y plot of metabasalts, showing the fields of modern basalts (after Pearce, 1975). Parts per million.

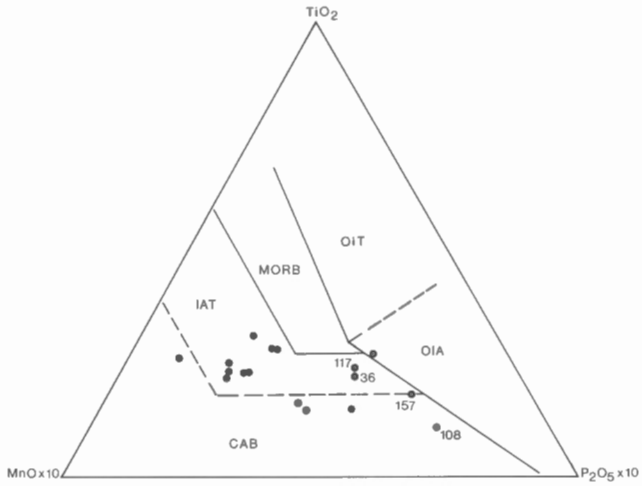

Figure 58. Metabasalts in the discriminant diagram of Mullen (1983). OIT = oceanic island tholeiites, OIA = oceanic island alkalic basalts. Weight per cent.

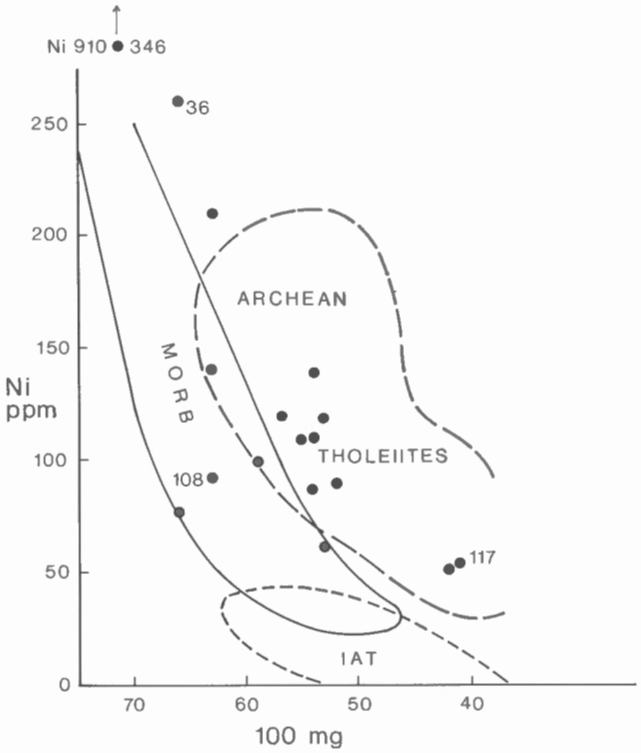

Figure 59. Nickel contents of metabasalts compared to those of Archean and modern tholeiites (after Gill, 1979).

The rocks of the smaller occurrences show well developed millimetre-scale layering; whether the layering is primary magmatic or secondary, induced by deformation and/or metamorphic differentiation, is moot. The rocks are dark green to black and consist of different proportions of olivine, pyroxene and, especially, amphibole in a granoblastic-polygonal texture. Olivine, although invariably altered, is preserved in several specimens and is accompanied by weakly pleochroic orthopyroxene and amphibole, which is colourless anthophyllite or a neutral to pale brown variety of unknown composition. Accessory minerals include green spinel and Fe-Ti oxide.

Olivine-free varieties of ultramafic rock include clinopyroxenite and hornblendite. Clinopyroxenite that forms a lens in metasediments (mainly quartzite and marble) on southern Coburg Island (Map 1574A) is made up of neutral clinopyroxene, subordinate pale yellow amphibole and minor red-brown biotite. Ultramafic amphibolites contain olive-green amphibole paler than that in typical pyribolite and, in addition, subordinate brown biotite or pyroxene.

The ultramafic rocks are most likely of igneous origin and possibly related to the pyribolites.

Orthopyroxene tonalite-granodiorite-granite

Massive to crudely gneissic granitoid rocks with granulite facies mineralogy and of plutonic aspect occur throughout the map area in bodies ranging from intercalations in gneisses to plutons many kilometres across. Clearly intrusive features, such as crosscutting relationships and inclusions of country rock, are comparatively rare and chilled margins absent. None of these rock types can be considered post-tectonic, as gneissic examples of each were found. Mineral assemblages are generally similar, if not identical, to those of the true gneisses. As in the gneisses, compositions range from quartz norite to granite.

Thus distinction between massive plutonic rocks and granitoid gneisses was often subjective during much of the present work. High grade metamorphism and intense deformation caused extensive recrystallization to granoblastic textures, which, combined with a scarcity of dark platy minerals, impart a massive appearance to the quartzofeldspathic rocks. Krupička (1973) referred to the difficulty of recognizing foliation in the quartzofeldspathic rocks of the Truelove Inlet area, northern Devon Island, unless close examination of the outcrop is made. This was a general problem encountered during the reconnaissance mapping, when many of the observations were made from the air or during brief ground stops.

This section, then, deals only with those rocks for which field relations and other indicators provide a reasonably sound basis for postulating an intrusive origin.

Many of the massive rocks are retrograded to a greater or lesser degree, manifested principally by partial to complete replacement of orthopyroxene and incipient microclinization (development of grid twinning in untwinned alkali feldspar). Severe retrogression is marked by reddening of the rock on fresh, as well as weathered, surfaces and is commonly accompanied by abundant veining by leucocratic granite and pegmatite. In the main, the most retrograded rocks are the most granitic ones.

Any one of the massive rock types may locally show abundant veining by granite and pegmatite, in which case it was mapped as a subunit, such as otv or ogv.

Orthopyroxene tonalite (ot, otv)

Generally massive granitoid rocks poor in, or entirely free of, K-feldspar occur widely in Ellesmere and Coburg islands. Most of them are tonalites but more mafic, less quartzose varieties, such as quartz norite, are found locally. Pink granitic to pegmatitic veins are abundant in some outcrops.

Orthopyroxene tonalite, grey to black with a greenish tinge, weathering grey or brown, forms major bodies in the Prince of Wales Mountains, near Beitstad Fiord (Map 1572A) and in northeastern Coburg Island. The rock typically is medium grained and fresh. Striated faces of plagioclase crystals are prominent on freshly broken surfaces and some samples resemble anorthosite. Orthopyroxene tonalite characteristically is a much fresher rock than orthopyroxene granite-granodiorite.

In thin section, orthopyroxene tonalite displays a predominantly equigranular granoblastic texture defined by grains with gently curved boundaries. The characteristic mafic minerals are orthopyroxene, brown biotite, olive hornblende and clinopyroxene and the latter two, particularly clinopyroxene, distinguish the massive tonalites from the majority of the tonalite gneisses. Orthopyroxene is weakly to moderately pleochroic and commonly altered along cracks. Biotite is deep brown, rarely with a red tinge, and has formed relatively late in some rocks (Fig. 60). Hornblende has X = pale greenish brown, Y = brownish green, Z = olive and is generally associated with (possibly replacing) orthopyroxene. Pale green clinopyroxene, commonly present in only trace amount, appears to have completed its crystallization later than orthopyroxene, which it tends to overgrow. Plagioclase crystals are clouded by dust-like inclusions except for clear, narrow margins. Blocky or, less commonly, hair antiperthite is irregularly developed; in the typical orthopyroxene tonalite, a separate K-feldspar is absent. Anorthite content of plagioclase generally falls in the range 29 to 31 % but may attain 38 %; zoning is minor. Apatite is an abundant accessory mineral.

An example of a more mafic variety of tonalitic rock is well exposed at Cape Isabella, where it intrudes marble (Map 1572A). (This rock body is incorrectly shown on the map as unit ogr.) It is of monzonoritic composition, brown-weathering, and rich in orthopyroxene, clinopyroxene, hornblende and biotite. Much of the mafic mineral component tends to be aggregated in hornblende-rich clots, 1-2 cm across.

Mineral chemistry

Minerals from one hornblende+biotite-bearing and two biotite-bearing orthopyroxene tonalites have been analyzed (Appendix, Table 5).

The mafic minerals have compositions comparable with those in compositionally similar orthopyroxene tonalite gneisses. Orthopyroxenes are hypersthene (Fig. 61); only the distinctly pleochroic variety in biotite-orthopyroxene tonalite FS-77-283 has significant alumina, 2.82 %. Biotites have Fe/Fe+Mg 0.3 to 0.4 and TiO_2 4.6 to 5.5 %. The olive hornblende in FS-77-266 is ferrian magnesiohornblende (Rock and Leake, 1984), very similar to that in mafic two-pyroxene tonalite gneiss (Appendix, Table 7). Plagioclase ranges from andesine (An_{38}) to calcic oligoclase (An_{27}) with minor and irregular zoning.

Orthopyroxene granite (og, ogv)

Generally massive, well jointed, K-feldspar-porphyroblastic, orthopyroxene-bearing granitic rock (Fig. 62) underlies most of the coastal region from Heim Peninsula to north of Fram Fiord in southern Ellesmere Island (Map 1573A); it is also found in significant amount around Rosse Bay (Map 1572A) and in smaller bodies elsewhere. Judged from both field studies and thin section examination, plagioclase-rich granite appears to predominate in this unit (Fig. 63). Granodioritic rocks, however, form a significant part of map units og and ogv and even orthopyroxene tonalite is present locally. Whether these various rock types have wholly independent origins or are related by some process of "granitization" (Roots, 1963b; Krupička, 1973) can only be resolved by more detailed work.

Typical rock of map units og and ogv, when examined in thin section, is rarely fresh but the freshest specimens have the greasy green colour characteristic of granulite facies granitoid rocks. Weathering colours are brown to red or pink. Megacrysts of alkali feldspar, 1 to 3 cm long, are common, set in a medium grained granular matrix of feldspar, biotite, orthopyroxene and bluish quartz. Although generally structureless, the orthopyroxene granite in many places shows weak mineral foliation and the feldspar megacrysts may be aligned. More rarely, for example in shear zones, gneissic structure is well developed.

Although uncommon, fragments of gneisses and metasediments are found as inclusions in orthopyroxene granite. They generally show evidence of reaction with the host rock, perhaps even partial assimilation, and may be deformed (Fig. 64).

Intimately associated with the green granites are rocks that are pink or red (rarely white) on both fresh and weathered surfaces. From the air, these pink rocks may be indistinguishable from weathered green granites and indeed may prove in thin section to be identical. Typically, however, the pink variety shows a greater degree of alteration of the mafic minerals and fully retrograded granites are invariably red or pink on both fresh and weathered surfaces. Orthopyroxene is partly to largely replaced by biotite and green hornblende, and primary biotite is partly chloritized. The green and pink granites are juxtaposed in mainly two ways: alternating irregular layers 1 m or so wide or diffusely bordered patches of green rock in pink. Local sharp contacts between the two varieties and intrusive-like features suggest intrusion of pink granite into green but none of this evidence contradicts an in situ transformation of one rock into the other as a consequence of, for example, the influx of water. Retrograde "decharnockitization" phenomena of this kind have been described from the Archean of south India (Allen et al., 1985).

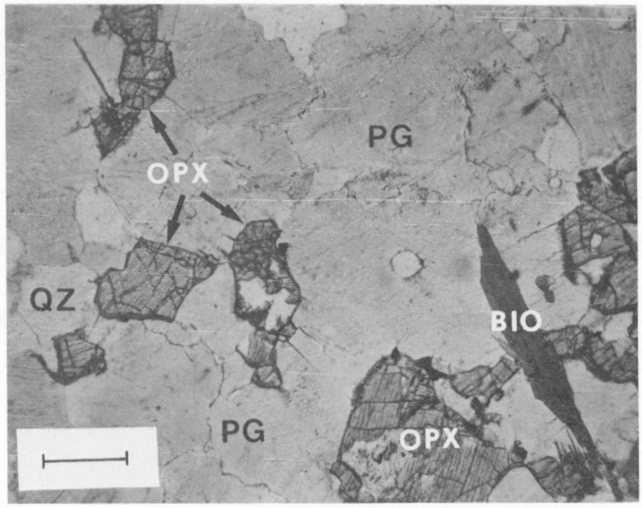

Figure 60. Clouded plagioclase and brown, Ti-rich late biotite in meta-intrusive orthopyroxene tonalite (unit ot; FSM-77-203-1). Plane light. Bar scale 0.5 mm.

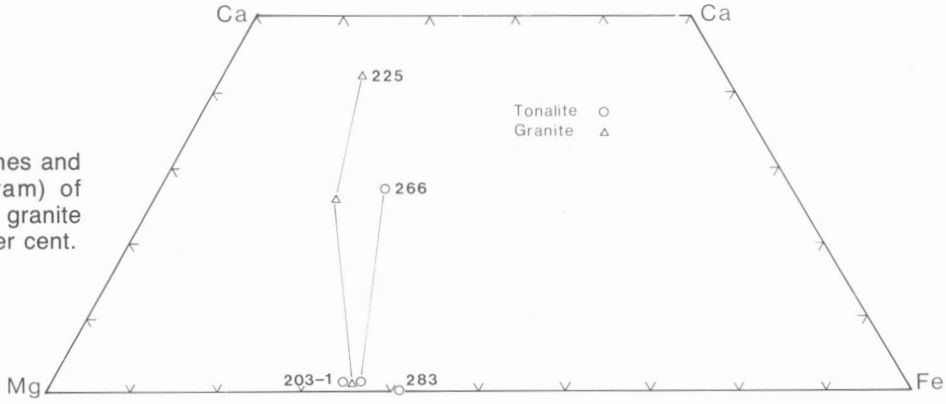

Figure 61. Composition of pyroxenes and amphibole (central part of diagram) of massive, meta-igneous tonalites and granite in terms of Ca, Mg and Fe. Atom per cent.

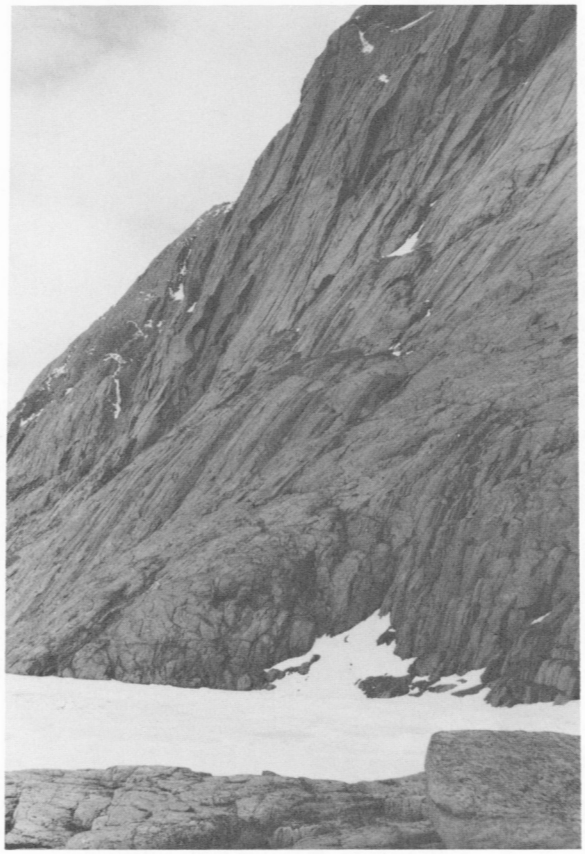

Figure 62. Well jointed, massive orthopyroxene granite (unit og), west shore of Starnes Fiord, southern Ellesmere Island.

Some of the more leucocratic granite veins and sheets in orthopyroxene-bearing granitoid rock lack any diagnostic sign of retrogression. Where they show a diffuse border against orthopyroxene-bearing rock, these granites could possibly be interpreted as relics of a pre-granulite facies stage, i.e. the reverse of a "decharnockitization" process. More likely, though, is that these granites represent relatively low-temperature, hydrous melts emplaced in the waning stages of, or subsequent to, granulite facies metamorphism.

The texture of the orthopyroxene granite and related rocks is invariably modified by cataclasis. They are inequigranular granoblastic rocks in which grain boundaries are embayed or sutured (commonly lobate). Margins of the larger quartz and feldspar grains may be mortared and these minerals are moderately to severely strained. In the fresher rocks, orthopyroxene is distinctly pleochroic (pale pink and green), embayed and partly replaced by brown biotite, green hornblende or fine grained yellow-green sheet silicates. Biotite is dark brown and may be slightly chloritized. Alkali feldspar is coarse to fine hair perthite forming both subhedral porphyroblasts and anhedral groundmass crystals. Shadow perthite (Smith, 1974, p. 417) occurs in some rocks and, in strongly strained ones, diffuse grid twinning is patchily developed, suggestive of incipient microcline. Plagioclase is well twinned and ranges in composition from An_{25} to An_{31}; blocky antiperthite is irregularly developed.

Except for increased plagioclase content at the expense of K-feldspar, granodioritic and tonalitic rocks in map units

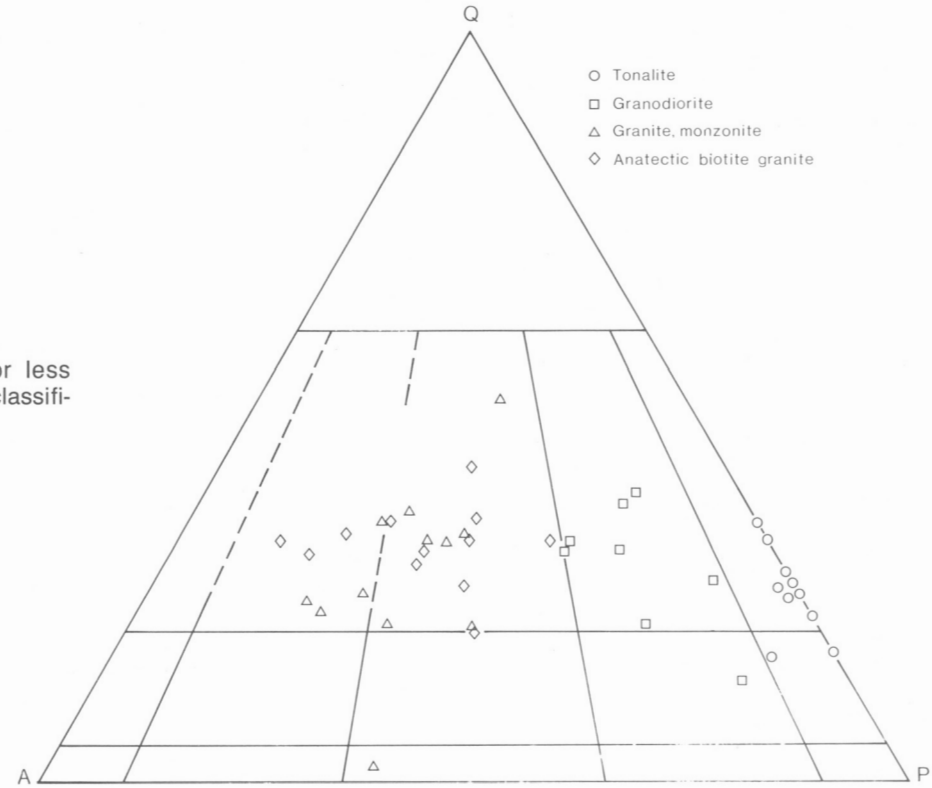

Figure 63. Meta-igneous, more or less massive granitoid rocks in the IUGS classification. Volume per cent.

og and ogv are petrographically similar to the granites. Unlike the massive orthopyroxene tonalites of units ot and otv, however, they contain neither hornblende nor clouded plagioclase.

A less common variety of orthopyroxene granite contains two pyroxenes, hornblende and mesoperthite as virtually the only feldspar. One occurrence of this type is along the Braskerud Glacier (Map 1572A), where massive granite is overlain by layered metasediments; the nature of the contact is unknown. The granite (FSM-77-225) consists of dense mesoperthite clouded by dusty inclusions, quartz, orthopyroxene, pale green clinopyroxene and olive hornblende. Grain size is irregular from fine to medium, probably the result of partial recrystallization due to deformation. Quartz is strained and a little twinned plagioclase forms the outer zones of some mesoperthite grains. Some of the clinopyroxene appears to have overgrown orthopyroxene and is fresh. Pale green actinolite borders crystal margins and cleavage cracks of orthopyroxene grains. Hornblende is associated with the pyroxenes but does not appear to replace them. A very little orange-brown biotite is present as a late growth on the other mafic silicates and Fe-Ti oxide.

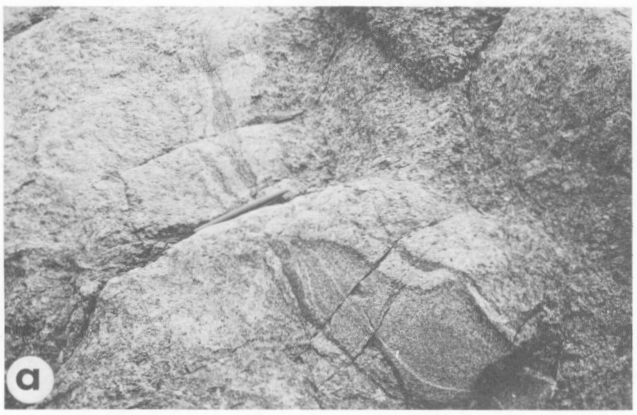

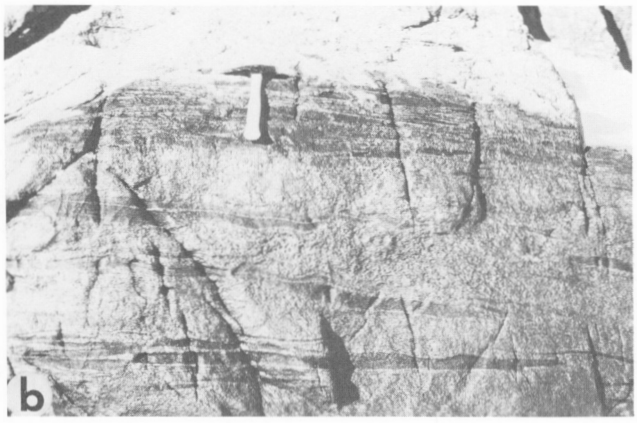

Figure 64. Mafic xenoliths in generally massive, orthopyroxene-bearing granitoid rock.
a) Near Lee Point, east of Grise Fiord settlement, southern Ellesmere Island (pen for scale in middle of photograph).
b) Lindstrom Peninsula, southern Ellesmere Island.

Mineral chemistry

The only mineral chemical data available from the orthopyroxene granite unit were obtained from the hornblende-two pyroxene-mesoperthite granite (FSM-77-225) described above (Appendix, Table 5). Low-alumina hypersthene $Ca_1Fe_{35}Mg_{64}$ is accompanied by augite $Ca_{42}Fe_{16}Mg_{42}$ and olive hornblende (Fig. 61). The latter is more sodic (Na_2O 2.2 %) than most of the hornblendes analyzed from the Ellesmere-Devon terrane and is classified (Rock and Leake, 1984) as ferrian edenitic hornblende (Appendix, Table 7). Broad-beam bulk analysis of the mesoperthite indicates a significant anorthite component of 11 to 13 %.

Retrograded orthopyroxene granite (ogr, ogs, ogp, ogq)

Red or pink granites are ubiquitous throughout the Ellesmere-Devon shield terrane. On Ellesmere Island in particular retrograded orthopyroxene granite forms major bodies or even underlies whole regions, commonly grading into fresher granite.

Although separable into several types, these rocks have a number of features in common. They are pink or red on both weathered and fresh surfaces. Orthopyroxene has been replaced by sheet silicates or amphibole, alkali feldspar is abundant and commonly coarsely megacrystic or porphyroblastic, and the granite as a whole tends to be massive and coarse grained. Granitic and pegmatitic veins and sheets are more abundant than in fresher granites.

In many areas these rocks grade into fresh orthopyroxene granite and because of their superficial similarity, distinction between the two types is frequently difficult in reconnaissance mapping.

Largely structureless, porphyroblastic granites (ogp, ogq) underlie much of the crystalline terrane in Sverdrup Pass and the upper reaches of Beitstad Glacier in the northern part of the map area (Map 1572A). These rocks commonly weather dark reddish, contrasting with the buff Paleozoic sediments that overlie them. They are characterized by abundant K-feldspar porphyroblasts (phenocrysts?) up to 4 cm long, which are generally randomly oriented but locally, as at the head of Flagler Bay, are well aligned imparting a shallow-dipping gneissosity to the rock. The porphyroblasts range from a euhedral to a subhedral, flattened form; no strongly deformed augen were found. The well-aligned porphyroblasts commonly exhibit euhedral form suggestive of growth during the movement that gave rise to their alignment. Thin sections show bands of coarse K-feldspar and quartz alternating with bands of finer grained feldspar, quartz and mafic minerals; all quartz is severely strained and mosaic patterns are common. It thus seems most probable that the alignment of the feldspar porphyroblasts is a consequence of deformation and is not a primary intrusive feature.

The K-feldspar in these rocks typically is microcline with well developed grid twinning and patchy hair perthite. In plane polarized light some of the K-feldspar crystals are identical to the densely hair-perthitic feldspar so widespread in other rocks of the map area; only under crossed nicols is the feldspar recognizable as microcline. Many of the larger porphyroblasts contain small euhedral crystals of plagioclase and droplets of quartz. Whereas the K-feldspar is largely fresh, plagioclase (An_{24-25}) is moderately to strongly altered and myrmekitic. All orthopyroxene has been replaced by fine grained actinolite or a chlorite-biotite mixture. Biotite is dark brown in the less altered (less retrograded) rocks, and greenish brown and partly chloritized in more altered rocks.

Christie (1967) has described the contact between the granites and gneisses on Knud Peninsula as a zone of mingling of the two rock types with abundant veins of pegmatite containing garnet and biotite. According to Christie, the granite in places crosscuts the gneisses but elsewhere grades into them; inclusions of gneiss occur in granite.

A distinctive and unusual variety of granite, thought to have once contained orthopyroxene, outcrops west of Cory Glacier (Map 1573A). Red- to rusty brown-weathering, this pink, coarse grained granite contains K-feldspar crystals up to 5 cm long and is miarolitic. Outcrops are rounded, well jointed and deeply weathered, locally forming tors surrounded by aprons of grus (Fig. 65a). Blake (1978) has discussed the implications of this weathering for the glacial history of the region and provided further illustrations. Despite the coarse grain size, a rough, steeply dipping foliation can locally be discerned (Fig. 65b).

The granite is composed largely of perthitic microcline with excellent grid twinning, occurring both as megacrysts and as smaller grains in the groundmass; sodic plagioclase, strongly sericitized and overgrown by K-feldspar; moderately to slightly strained quartz; brown biotite with Z almost black and slightly chloritized; and accessory fluorite, unevenly distributed in aggregates of small grains up to 0.5 mm in diameter.

Neither orthopyroxene nor pseudomorphs thereof have been found in this granite. The type of perthite in the K-feldspar and the dusky red colour of the granite, however, are very characteristic of retrograded orthopyroxene granite found in many places in the Ellesmere-Devon terrane. Furthermore, although contacts were not examined, the fluorite-bearing granite appears to pass westward into more usual retrograded orthopyroxene granite containing orthopyroxene pseudomorphs and biotite with a Z colour of lower absorption. In laboratory experiments on granitic melts (Clemens and Wall, 1981), biotite is formed in preference to orthopyroxene when fluorine fugacity is high.

Some bodies of retrograded orthopyroxene granite (ogs) are rich in relics of greenish, fresh, orthopyroxene-bearing quartzofeldspathic rocks and may also contain garnet and/or green spinel. Noteworthy occurrences are on Beitstad Fiord and Pim Island (Map 1572A), but this granite is also found in many places elsewhere. The xenoliths typically take the form of sheets, layers and lenses, in roughly parallel alignment, and exhibit sharp boundaries against the enclosing granite. It is in this latter respect and in the presence of aluminous minerals that unit ogs differs from the association of fresh and retrograded orthopyroxene granites described above.

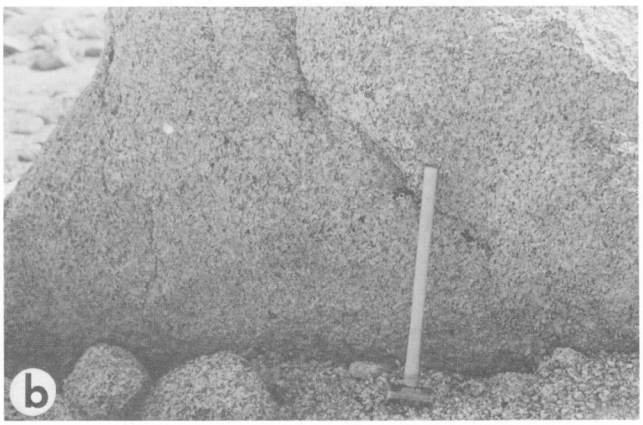

Figure 65. Fluorite-bearing, coarse grained granite (probably a variety of retrograded orthopyroxene granite) west of Cory Glacier, southeast Ellesmere Island.
a) Well jointed tor surrounded by an apron of grus.
b) Rough foliation defined by biotite.

A particularly fine exposure of unit ogs occurs in a small nunatak (not shown on the map) about 24 km northwest of the head of Trinity Glacier (Map 1572A, southern half). A vertical cliff face (Fig. 66) shows the result of disruptive intrusion of pink granite into greenish, gneissic, orthopyroxene-bearing tonalite. Veins of granite and pegmatite cut both granite and tonalite. All orthopyroxene in the granite is pseudomorphed by biotite+chlorite and some of the K-feldspar has the faint grid twinning of incipient microcline. The orthopyroxene of the tonalite is virtually unaltered. Garnet is erratically distributed in both the granite and the tonalite. The granite is distinctly gneissic and exhibits a medium grained granitic texture and highly strained quartz suggestive of deformation during or after intrusion.

Over a distance of less than 1 km, granite and xenoliths become banded gneiss composed of alternating layers of

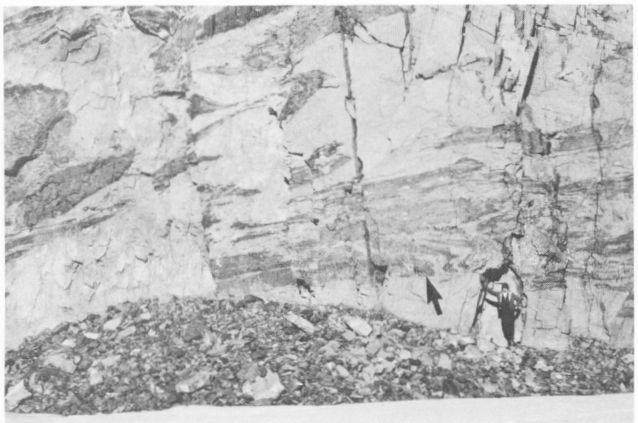

Figure 66. Garnetiferous, gneissic, retrograded orthopyroxene granite (unit ogs) with layers and lenses of gneissic orthopyroxene tonalite, about 24 km NW of the head of Trinity Glacier, Ellesmere Island. This granite (FS-77-331) and tonalite (FS-77-332, from the lens arrowed) were isotopically dated (*see* Fig. 76).

tonalite and granite, providing an outstanding illustration of how even relatively late granitic intrusion was followed by major deformation.

Rock chemistry

Chemical analyses of 5 tonalites, 2 granodiorites, and 9 granites, all more or less massive and orthopyroxene bearing, are listed in Appendix, Table V.

One of the tonalites, FSM-77-28, is a brown-weathering variety containing minor K-feldspar, from unit ogv on the upper reaches of Starnes Fiord (Map 1573A); it plots as a granodiorite in the modified O'Connor diagram (Fig 67). The remaining tonalites are all of the dark grey weathering variety (units ot, otv), devoid of discrete K- feldspar, and plot as tonalites in Figure 67. All four of these tonalites have weight per cent SiO_2 63 to 65, Al_2O_3 16, and CaO 4 to 5 and Na_2O/K_2O 3 to 4. They are metaluminous, molecular $Al_2O_3/(CaO+Na_2O+K_2O)$ being slightly less than, or equal to, unity and all but one are diopside normative. Rb is low and K/Rb correspondingly high, ranging from nearly 500 to 1000 (*see* Fig. 71). Rb/Sr and K/Ba ratios are low, similar to those of lower (depleted) crustal rocks. All in all, the massive tonalites are chemically broadly similar to the orthopyroxene tonalite gneisses and plot in the same fields on the various chemical diagrams.

The two granodiorites show some chemical affinity to the K-rich tonalite FSM-77-28, despite mineralogical differences. Although to some extent occupying an intermediate position between the K-poor tonalites and the K-rich granites, these three rocks appear to be chemically more akin to the former.

Turning to the orthopyroxene granites, three main types can be distinguished chemically.

One of these types is the partly retrograded, K-feldspar-porphyroblastic granite (units og, ogv) that is particularly abundant on the northern shore of Jones Sound (Map 1573A) and around Rosse Bay (Map 1572A). Five examples of this granite have been analyzed (FSM-77-215-2, 265, 13; FS-77-58, 302) and their average composition is also listed in the table. Corundum-normative and rich in SiO_2 (average 74 wt. %), K_2O (5 %) and Rb (190 ppm), they plot well apart from the tonalitic and granodioritic rocks in chemical variation diagrams (Figs. 67-74). K/Rb is less, generally much less, than 500, and Rb is enriched relative to K but one sample plots in the field of anomalous K/Rb ratios in Figure 72. Average K/Rb (221) and K/Ba (55) are comparable to upper crustal values given by Taylor and McLennan (1985, Table 2.6.2).

Compared with Zakrutkin's (1972) average of 140 "orthocharnockites" (Appendix, Table V), the average Ellesmere Island orthopyroxene granite is distinctly more siliceous and potassic and less mafic. The same differences are also found in a comparison with the majority of analogous rocks of the type charnockite suite of Madras, India. However, some K-rich acid varieties do occur among the Madras rocks and an example chemically and mineralogically similar to the Ellesmere rocks is included in Appendix, Table V.

The strongly retrograded granite (units ogp and ogq), rich in microcline and with orthopyroxene represented only by biotite pseudomorphs, outcropping in Sverdrup Pass and on Knud Peninsula (Map 1572A), is probably similar chemically to the orthopyroxene granites just described, but no analytical data are available. A second major orthopyroxene granite type is the retrograded, aluminous mineral-bearing variety, commonly with mafic xenoliths (ogs), represented by two analyses (FSM-77-318, FS-77-151). Both rocks, one with green spinel, the other with garnet, have high SiO_2 (73 wt. %), K_2O (5.52 and 5.86 %) and Rb (200 ppm). Their K/Rb and K/Ba ratios are of upper crustal type.

The third type of granite, the hornblende-two pyroxene-mesoperthite variety, is represented by one sample only (FSM-77-225). Compared with the other granites, it has relatively low SiO_2, K_2O and Rb and high MgO and Na_2O and is the only granite to show normative diopside. Its K/Rb is anomalously high (690). Rb/Sr and K/Ba are low, comparable to the ratios for the tonalites. In general, its chemical affinity lies more with the tonalites and granodiorites than with the granites.

Sample FSM-77-83-2 is a grey, mesoperthite-bearing orthopyroxene granite from 12 km north of Cape Tennyson and Glacier Strait (Map 1573A). Judged by its quartz content (50 vol. %) and chemistry, it may be a silica-enriched rock chemically related to the two pyroxene-mesoperthite granite.

Origin

No clear evidence of an intrusive origin for the massive orthopyroxene tonalites (units ot and otv) has been found in the field. However, the monzonorite at Cape Isabella is

probably related to the tonalite suite and it is definitely intrusive. Per Schei, geologist to the Fram expedition, found large rafts of gneiss, veined by norite and granite, enclosed in hornblende-bearing "bronzite quartz diorite" south of Alexandra Fiord (Bugge, 1910, p. 13). If the host rock belongs to the orthopyroxene tonalite suite of this study, an intrusive origin for the suite receives further support. Certainly the texture and chemistry of the tonalite suite suggest this conclusion. Whether the granulite facies mineralogy resulted from crystallization of a melt under granulite facies conditions or from a subsequent metamorphic overprint is uncertain (*see* below).

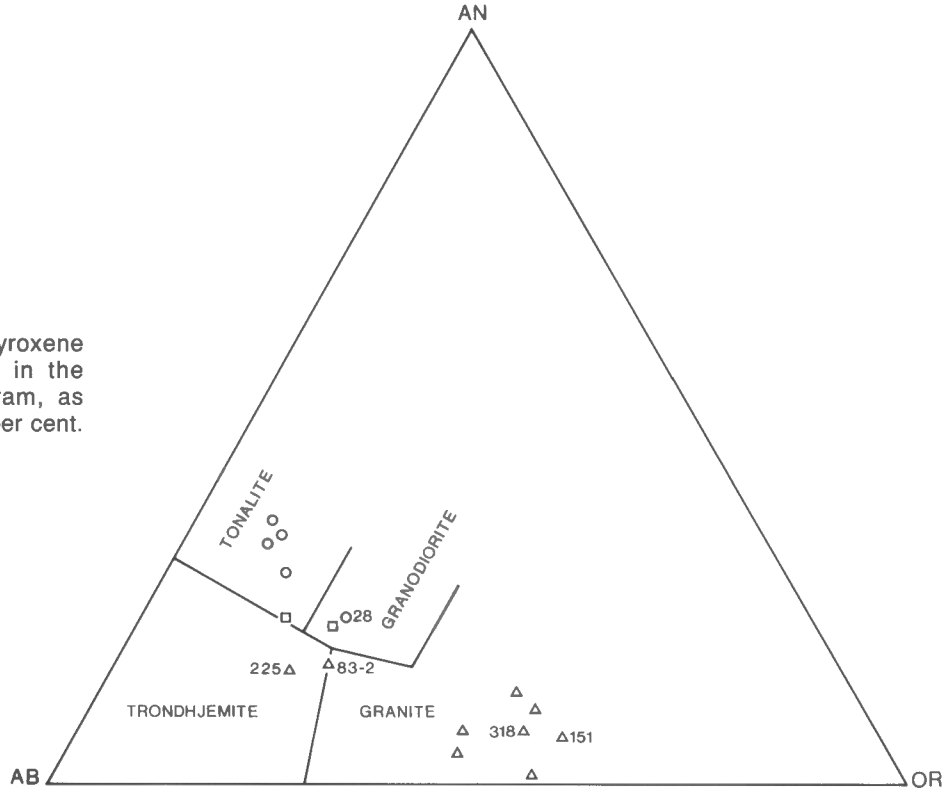

Figure 67. Rocks of the orthopyroxene tonalite-granodiorite-granite suite in the normative O'Connor (1965) diagram, as modified by Barker (1979). Weight per cent. Symbols as in Figure 63.

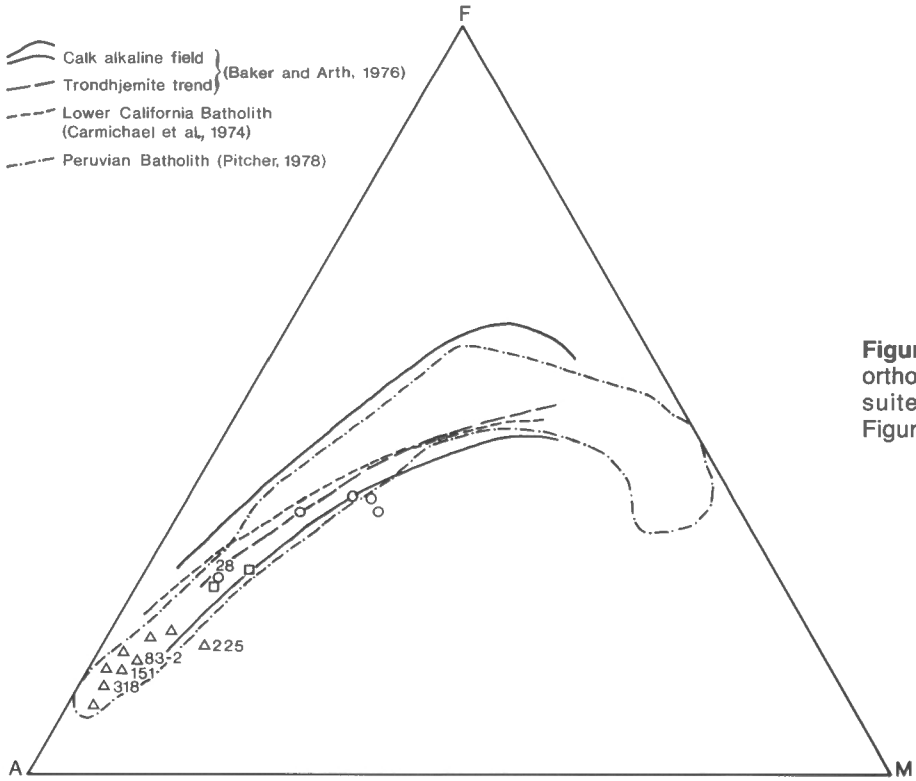

Figure 68. Igneous AFM plot of rocks of the orthopyroxene tonalite-granodiorite-granite suite. Weight per cent. Symbols as in Figure 63.

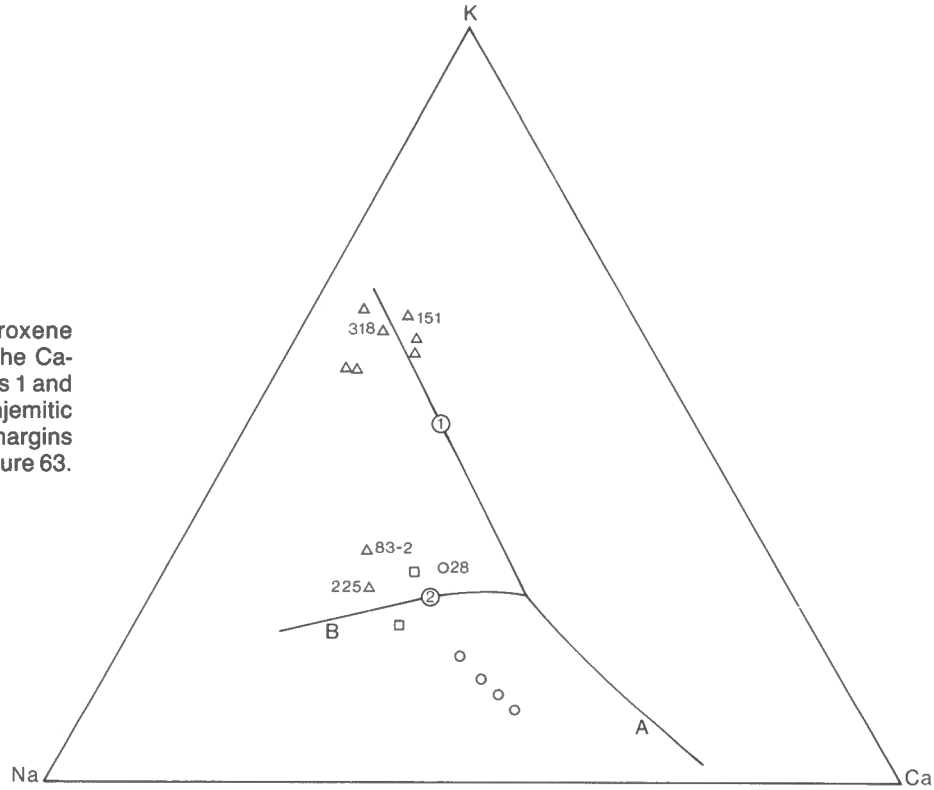

Figure 69. Rocks of the orthopyroxene tonalite-granodiorite-granite suite in the Ca-Na-K diagram. Weight per cent. Curves 1 and 2 are calc-alkaline granitic and trondhjemitic trends, respectively, of continental margins (Barker et al., 1981). Symbols as in Figure 63.

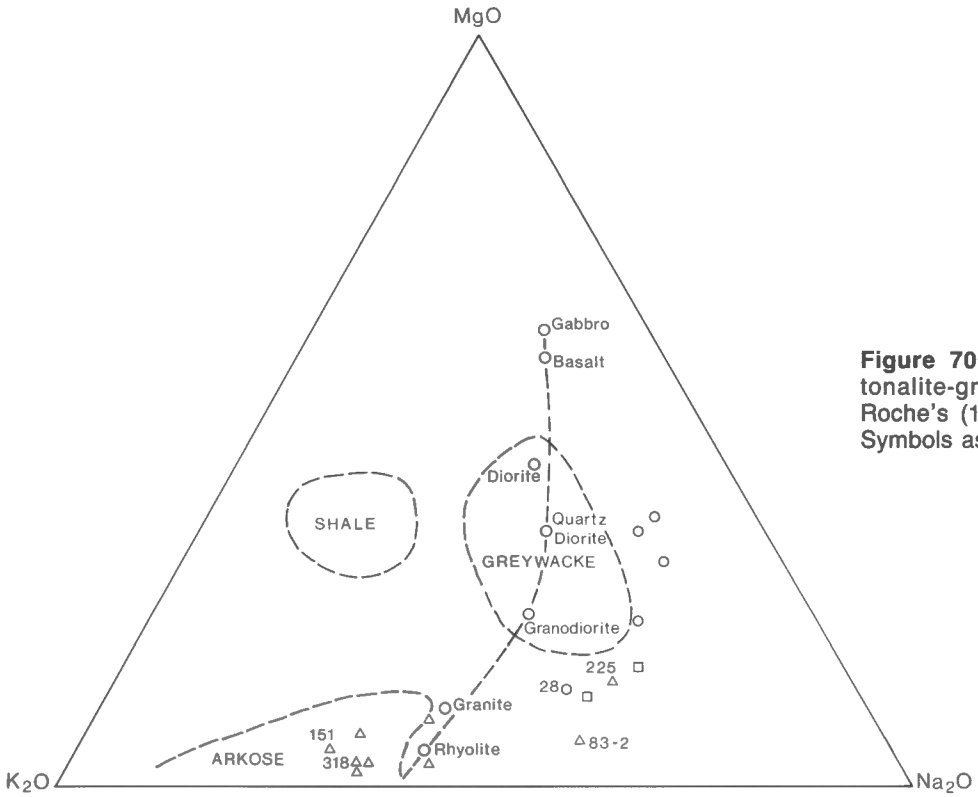

Figure 70. Rocks of the orthopyroxene tonalite-granodiorite-granite suite in La Roche's (1965) diagram. Weight per cent. Symbols as in Figure 63.

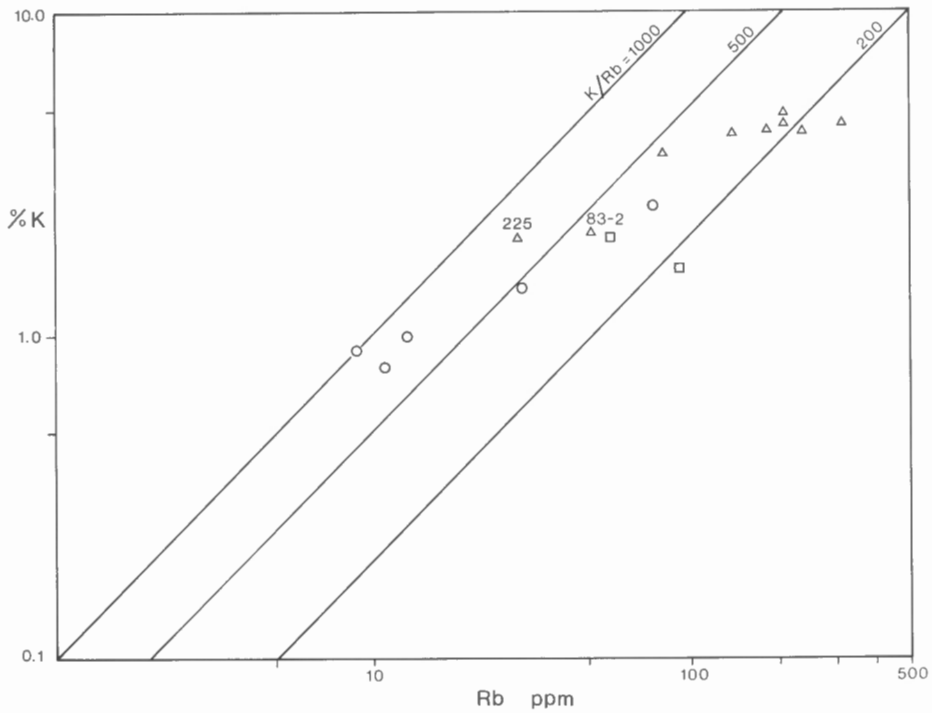

Figure 71. K vs. Rb in the orthopyroxene tonalite-granodiorite-granite suite. Symbols as in Figure 63.

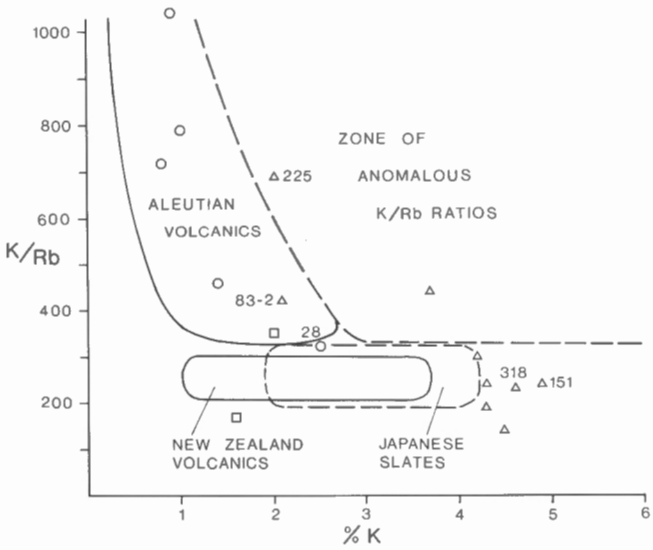

Figure 72. Rocks of the orthopyroxene tonalite-granodiorite-granite suite in Gray's (1977) diagram. Symbols as in Figure 63.

The massive tonalites are likely to have been derived from a mafic source such as basalt or mafic lower crustal rocks: generally, K, Rb and Ba/Sr are low and K/Rb is high (Hanson, 1978). One possible origin is by fractional crystallization of basalt, followed by granulite facies metamorphism under dry conditions (leading to the crystallization of orthopyroxene). There is, however, no sign of an appropriate basaltic source in the surrounding rocks. Simple partial melting of mafic crustal rocks, such as amphibolite, is not a likely mechanism of producing tonalite melt, as its liquidus temperature is extremely high, approaching 1000° C even with excess H_2O (Wyllie, 1977). Temperatures of this magnitude may have been reached locally in the Ellesmere terrane (*see* below) but were very probably exceptional. More likely is a hybrid origin, whereby basaltic magma from the mantle intrudes, partially melts and assimilates crustal rocks, producing a melt of intermediate composition. A variant of this hypothesis is that the tonalite is the recrystallized residue of a mushy magma, which originally consisted of mafic crystals in an acidic liquid that separated and crystallized as granite elsewhere (Wyllie, 1977).

The presence of hornblende and the high Na/K and metaluminous composition of the massive tonalites call to mind the M(mantle)- or I(igneous)-type granites (sensu lato) of oceanic volcanic arcs and continental margins, respectively (Pitcher, 1982). Both granite types are considered to have been derived from mafic igneous material: M-type granite (like the basalts with which it is characteristically associated) directly from the mantle, I-type from mantle-derived rock underplating continental crust (Pitcher, 1982). Considering the abundance of continental rocks in which the massive tonalites find themselves and the evidence for thick crust, I-type granites would appear to be the better analogue of the Ellesmere-Devon rocks. A thick crust would provide both a variety of source rocks and the possibility of sufficient heat buildup to produce a variety of partial melts and

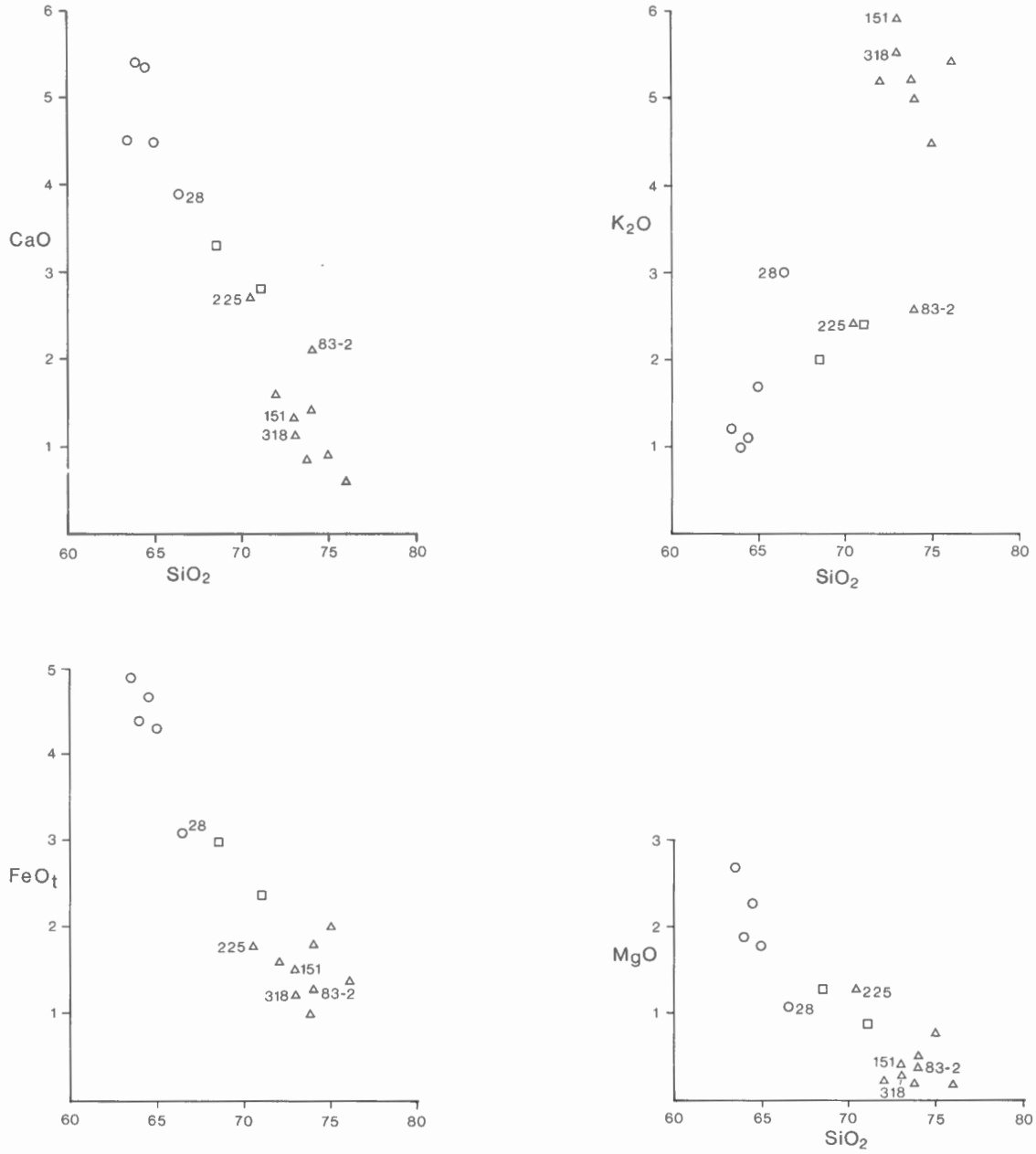

Figure 73. Harker plots of the orthopyroxene tonalite-granodiorite-granite suite. Weight per cent. Symbols as in Figure 63.

mixtures of restite and melt, from which plutonic rocks could crystallize. White and Chappell's (1977) proposal that I-type granitoid rocks crystallized from granitoid melt with admixed residual mafic crystals is consistent with the phase relationships of granitoid rocks (Wyllie, 1977).

In the Paleozoic Lachlan fold belt of southeast Australia, the hinterland region of thickest crust (possibly representing a former continental plate margin) is crowded with intrusions of peraluminous (S-type) granites, formed by anatexis of sialic material, interspersed with greatly subordinate I-type intrusions derived from an igneous source (White and Chappell, 1983). The relative abundances of intrusive rock types are entirely analogous to those in the Ellesmere-Devon terrane, where tonalite intrusions are greatly outnumbered by those of orthopyroxene granite (see below) and S-type granite (*see* the section "Anatectic biotite granite"). The "dryness" of the Ellesmere-Devon granitoid rocks as compared to the Australian rocks, which are free of orthopyroxene, reflects a deeper, water-poor environment of crystallization.

Field evidence clearly shows the massive orthopyroxene granites and related rocks to be of intrusive origin. More than 70 years ago, Bugge (1910) drew attention to the similarity between the orthopyroxene-bearing granitoid

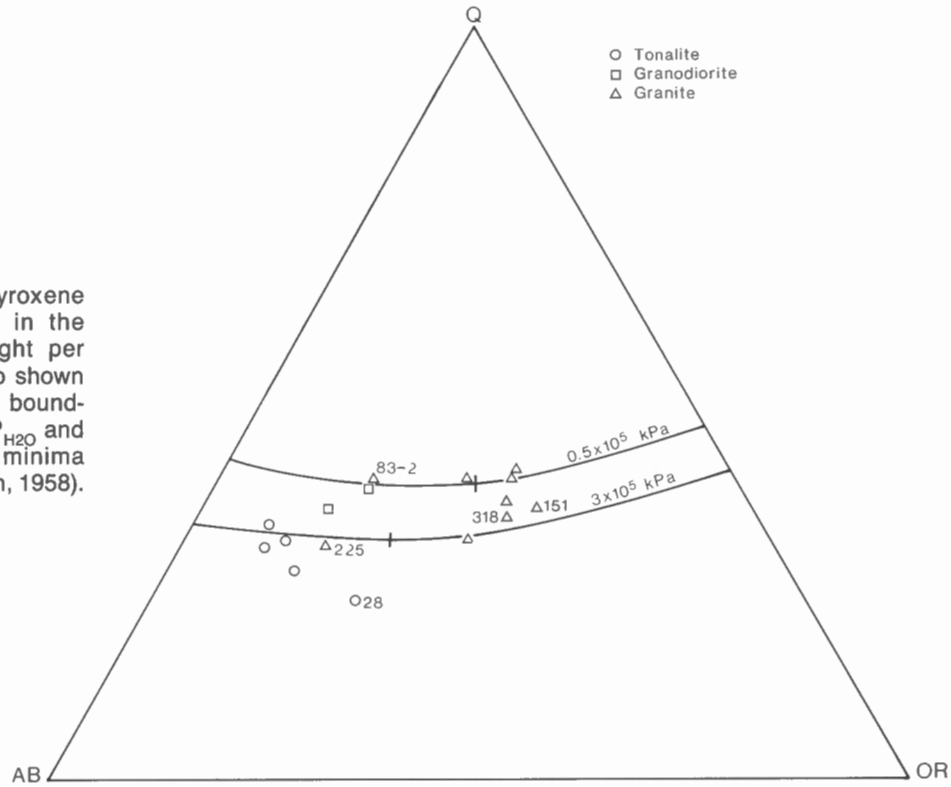

Figure 74. Rocks of the orthopyroxene tonalite-granodiorite-granite suite in the normative Q-Ab-Or diagram. Weight per cent. Symbols as in Figure 63. Also shown are projected quartz-feldspar field boundaries at 0.5 x 10^5 and 3 x 10^5 kPa P_{H_2O} and positions of quaternary isobaric minima (vertical bars) (after Tuttle and Bowen, 1958).

rocks of Ellesmere Island and those of the "charnockite series" of India, Africa, Norway and the Adirondack region of New York state. It is clear from Bugge's discussion that he regarded the Ellesmere rocks as plutonic intrusions ("Eruptivgesteine"). Hence any comparison to charnockites should be limited to those varieties of igneous aspect (i.e. not charnockite gneisses or metasedimentary charnockites).

The question whether charnockite in the sense of an "igneous-looking" orthopyroxene granite can be of primary igneous origin or owes its granulite facies mineralogy to metamorphism is still controversial. The fact that, in the Ellesmere-Devon terrane, older gneisses and younger intrusive rocks are all in the granulite facies makes it difficult to choose between these alternatives.

Although Fe-bearing orthopyroxene appears to be more stable at lower than at higher pressure in granitic systems (Clemens and Wall, 1981), it does form at 8 × 10^5 kPa in water-poor granitic melts in the laboratory (Naney, 1983). In their experiments on siliceous rocks (69-75 wt. % SiO_2), Clemens and Wall (1981) found that orthopyroxene has a wide stability field but tends to react to biotite with falling temperature. Melting of a rhyodacite produced, at 800°C and 5 × 10^5 kPa, a granitic melt with weight per cent SiO_2 72, Na_2O 2, K_2O 4 and H_2O 4 coexisting with orthopyroxene, biotite, plagioclase, quartz and ilmenite as crystalline phases (Clemens and Wall, 1981, Table 2). Clemens and Wall proposed that peraluminous charnockites could form from high-temperature anatexis of peraluminous rocks in the presence of C-O-H fluids.

With few exceptions, orthopyroxene granites from Ellesmere Island have high K_2O, Ba, Rb, Rb/Sr and Ba/Sr and low K/Rb — features indicating a felsic parent (Hanson, 1978). All the granites are corundum-normative and distinctly peraluminous. The position of the granites on the Q-Or side of the minima in the Q-Ab-Or diagram (Fig. 74) is consistent with their being dry melts, as granitic minimum melts become increasingly potassic with decreasing P_{H_2O} (Winkler, 1979, Table 18-2). Fluids attending crystallization may well have been reducing; graphite is common in the cordierite gneisses and carbonate rocks — a possible source of carbon — are abundant in Ellesmere Island.

Thus the properties of the orthopyroxene granites and their possible crystallization conditions are consistent with Clemens and Wall's (1981) model for the development of peraluminous charnockites.

The strongly retrograded, microcline-rich orthopyroxene granites (units ogp, ogq) at the northern margin of the map area locally show relatively well crystallized, albeit fine grained, greenish brown biotite as pseudomorphs of orthopyroxene. Rather than being the result of retrogression during exhumation (the unconformity between Precambrian and Paleozoic is widely exposed in this region), the greenish brown biotite may be the low-temperature replacement of orthopyroxene. Experimental results led Clemens and Wall (1981) to suggest that the common absence of orthopyroxene from granitic rocks is due to its complete reaction with the magma to form biotite at temperatures below 780°C.

A third type of granitic rock that may have crystallized from a partial melt is that of unit ogs, which contains abundant relics of orthopyroxene-bearing quartzofeldspathic rocks and is locally garnetiferous (Fig. 66). The two samples analyzed (FS-77-151, FSM-77-318) are chemically affiliated with the orthopyroxene granites. These rocks may well be analogues of the peraluminous biotite granites, described below under unit ag and interpreted to have originated by anatexis of metapelites. The granites of unit ogs, besides being characterized by orthopyroxene (or pseudomorphs thereof), are more calcic and less peraluminous than those of unit ag, differences that may reflect a different source rock.

The hornblende-two pyroxene-mesoperthite granite is interpreted to be an intrusive rock because of its massive, homogeneous appearance. With only a minute amount of sodic plagioclase fringing a few of the mesoperthite grains, the granite is of the hypersolvus variety and as such must have solidified above the temperature of the feldspar solvus at very low water pressure (Tuttle and Bowen, 1958). The temperature of the feldspar solvus crest increases steeply with increasing anorthite content; increasing total pressure raises the solvus crest; and increasing water pressure lowers the solidus (Morse, 1969). Morse (1969) determined the temperature of the solvus crest for a mesoperthite $Or_{29.6}Ab_{62.2}An_{8.2}$ to be 920°C at a P_{H_2O} ($=P_{tot}$) of 0.5×10^5 kPa, at which pressure the feldspar solidus is just slightly higher than the solvus crest. The higher An content (11-13 %) of the Ellesmere Island mesoperthite (Appendix, Table 5) implies that the original homogeneous feldspar must have crystallized at temperatures even higher than 920°C and at very low P_{H_2O}. Interestingly, an average temperature of 912°C is yielded by the two geothermometers of Kretz (1982) for the orthopyroxene and clinopyroxene in the granite. Temperatures given by the two-pyroxene geothermometers of Powell (1978) and Bertrand and Mercier (1985/86) are 840 and 865°C, respectively.

While temperature estimates obtained from coexisting pyroxenes should be treated with circumspection (*see* the section "Pyribolite and amphibolite"), the feldspar of the mesoperthite granite does provide evidence of very high temperatures being locally attained in the map area, as well as another example of low water pressure.

Such extreme temperatures are generally associated with igneous rather than metamorphic processes. Rollinson (1982) deduced a temperature in excess of 1000°C from the composition of mesoperthite in intrusive granite sheets of the Scourian granulite terrane of Scotland. He interpreted this temperature as being that of granite crystallization prior to granulite facies metamorphism. Applying the latest two-feldspar geothermometric calibrations to Rollinson's analytical data on the plagioclase and orthoclase lamellae of the mesoperthite, Mora and Valley (1985) obtained 825±35°C and suggested this was the temperature of the granulite facies metamorphism.

However, on the strength of the common occurrence of calcic mesoperthite (with up to 18 % An) as the only feldspar in orthogneisses, Sheraton et al. (1980) believed that temperatures of at least 950°C were reached during granulite facies metamorphism in parts of the Napier Complex of East Antarctica.

In the case of the Ellesmere Island mesoperthite granite, the high temperature is thought to reflect intrusive conditions but since intrusion and metamorphism are probably related, the existence of local extreme "hot spots" in the thermal regime as a whole may be inferred.

The abundant evidence of a thick, lithologically diverse crust, high temperatures and widespread anatexis in the Ellesmere-Devon terrane makes derivation from melts an attractive hypothesis for the origin of the massive orthopyroxene-bearing granitoid rocks.

Nonetheless, it has to be admitted that the orthopyroxene of the granitoids may be of metamorphic, rather than igneous, origin, the result of a granulite facies overprint. Newton and Hansen (1983) contended that magmatic charnockites are uncommon and that the great majority of orthopyroxene-bearing intermediate to felsic rocks of high grade terranes are the products of granulite facies metamorphism in the presence of CO_2-rich, H_2O-poor fluids. They postulated dehydration of "wet" crustal rocks by high-temperature CO_2 vapour derived from a mantle diapir or from buried carbonate sediments, resulting in a largely isochemical transformation to granulite facies assemblages. Driven ahead of this CO_2 front would be H_2O-rich fluids that would promote migmatization and K-metasomatism in the lower grade rocks, some of which would subsequently be themselves converted to granulite facies.

Newton and Hansen's (1983) model is in part based on impressive field evidence, mainly from the southern Indian Shield, and its possible relevance to the Ellesmere-Devon terrane is immediately obvious. Migmatites and granitic veining are almost ubiquitous, carbonate sediments are abundant, even possible examples of the granite-to-charnockite transformation are present (*see* the section on orthopyroxene granite above). The K-rich nature of most of the orthopyroxene granites could be due to metasomatism. According to Weaver (1980), the charnockite from Madras, India, listed in Appendix, Table 5 because of its similarity to the Ellesmere Island orthopyroxene granites, acquired its high K content by metasomatism prior to granulite facies metamorphism. The enrichment of Rb relative to K seen in the Ellesmere Island orthopyroxene granites (Fig. 71) may be due to retrogression (Allen et al., 1985) rather than to magmatic differentiation.

In the absence of any information on the composition of fluids during granulite facies metamorphism, and without clear evidence of prograde amphibolite facies rocks, it is difficult to assess the validity of the carbonic metamorphic overprint model of Newton and Hansen (1983) in the Ellesmere-Devon terrane.

Three points can, however, be made. The first concerns Newton and Hansen's reservations as to the likelihood of orthopyroxene-crystallizing felsic magmas being the precursor of charnockites. Newton and Hansen (1983, p.

169) pointed out that charnockites typically form at $8 \pm 2 \times 10^5$ kPa but that experimental work to date suggested that orthopyroxene in granitoid melts has a large stability field only at low pressure. The evidence from Ellesmere Island suggests that large-scale crustal melting occurred at no more than moderate pressures. If the supposition is correct that the fluorite-bearing granite near the Cory Glacier would have crystallized orthopyroxene, had not its crystallization been suppressed by fluorine (Clemens and Wall, 1981), then quite low pressure is indicated, as the granite is miarolitic.

The second point is that magmatism and granulite facies metamorphism may well be part and parcel of one and the same thermal event. Thus crustal melt formation under high grade, water-poor conditions would produce a granulite facies rock, in which case the concept of a metamorphic overprint has little meaning.

Thirdly, migmatization and K-metasomatism (if any) in the Ellesmere-Devon terrane were, in the main, relatively late processes and were not overprinted by granulite facies metamorphism. Of course, this is not to say that there was no earlier migmatization or metasomatism. In fact, the interlayered orthopyroxene tonalite and biotite granite gneisses in southern Devon Island, which gave late Archean and early Proterozoic U-Pb ages, may well represent older migmatite.

Age

U-Pb analyses have been made on zircons from rocks of units ogv and ogs.

The sample of unit ogv is a partly retrograded orthopyroxene granite (FS-77-50) from the eastern shore of Grise Fiord, 8 km NW of Grise Fiord settlement (Map 1573A). The rock carries abundant K-feldspar porphyroblasts up to 3 cm long set in a perthite- and quartz-rich matrix that also includes plagioclase (An_{30}), brown biotite and a little orthopyroxene partly replaced by yellowish sheet silicates. Much of the matrix appears to be recrystallized and many of the prophyroblasts are bordered by finely mortared quartz and feldspar.

The zircon grains are commonly fragments of elongate prisms with stubby terminations. A central small metamict core is mantled by numerous euhedral, fine zones that clearly grew longitudinally more than laterally; length/width ratios of complete prisms are at least 2:1 and up to 4:1. Some grains have a thin, unzoned rim that appears to be a poorly defined overgrowth. Cracks are ubiquitous but the abundance of inclusions differs greatly from grain to grain. The morphology of the zircon crystals suggests that grains inherited from pre-existing rock served as nuclei for new growth from a melt, followed by further growth and corrosion possibly during metamorphism.

Six zircon fractions, two of which were abraded, were analyzed. All are rich in uranium and the richest (1316 to 1534 ppm U) are highly discordant. Abrasion of the zircons has not resulted in a reduction in age discordance and the data points show some scatter about the discordia line, suggesting a disturbed U-Pb system. No doubt the high U content has led to considerable radiation damage in the crystals, viz. the heavy cracking. Nevertheless, the six fractions analyzed form a reasonably linear array, which has an upper intercept on concordia at 1972 +41/−36 Ma (Fig. 75). The lower intercept age is 424 Ma, which is unlikely to have any geological significance. The age of 1972 +41/−36 Ma is taken to be that of granite crystallization and agrees with the result from another variety of retrograded orthopyroxene granite, described below.

The other rocks dated are orthopyroxene granite of unit ogs and an orthopyroxene tonalite lens included in it. The outcrop is described in the section on retrograded orthopyroxene granite and depicted in Figure 66. Both rocks are gneissic and cataclastic and both are veined by granite and pegmatite.

The tonalite (FS-77-332) contains pleochroic orthopyroxene, brown biotite, clear plagioclase (An_{31-34}), quartz and sporadic garnet. Zircon crystals have blunted ends, a length/width ratio of 2:1, and numerous euhedral growth zones; inclusions are rare. Some grains show narrow overgrowths without visible internal structure. Four size fractions (one of them abraded) were analyzed.

Zircons of the granite (FS-77-331), the petrography of which was described earlier, are composed of clearly defined cores and overgrowths. Cores are euhedral, well zoned prisms locally with partly metamict centres. Overgrowths appear to be unzoned, are heavily cracked and pitted, and form rounded mantles to the prismatic cores. Core/overgrowth ratios range from 4:1 to 3:2, exceptionally to 1:1. The crystal morphologies suggest that the cores grew in a melt, the overgrowths during metamorphism. Seven fractions (five sizes, two of which were abraded) were analyzed.

The mineralogy of the tonalite — presence of garnet and distinctly pleochroic orthopyroxene and absence of hornblende and clouded plagioclase — suggests that the rock belongs to the older tonalite gneisses rather than the massive, intrusive tonalites. It was therefore anticipated that the zircons of the tonalite and granite would differ in age: older tonalite, younger granite.

The concordia ages obtained, however, are identical within error limits: 1960 +5/−4 Ma for the tonalite, 1951 +12/−11 Ma for the granite. If all points for the two rocks are plotted together on a concordia diagram (Fig. 76) they define a line with an upper intercept at 1952 +8/−7 Ma and a lower one at 519 Ma. The latter has no apparent geological meaning. The agreement in age is explained if the tonalite in actual fact belongs, not to the older gneisses, but to the massive metaigneous suite and thus formed from a melt at about the same time as the granite. Alternatively, the agreement may be accounted for by invoking the pervasive effect of a major thermal event at about 1.96 Ga, in which granitic melts were produced and which erased any record of an earlier event in the U-Pb system of the tonalite zircons. Lastly, there remains the possibility that the agree-

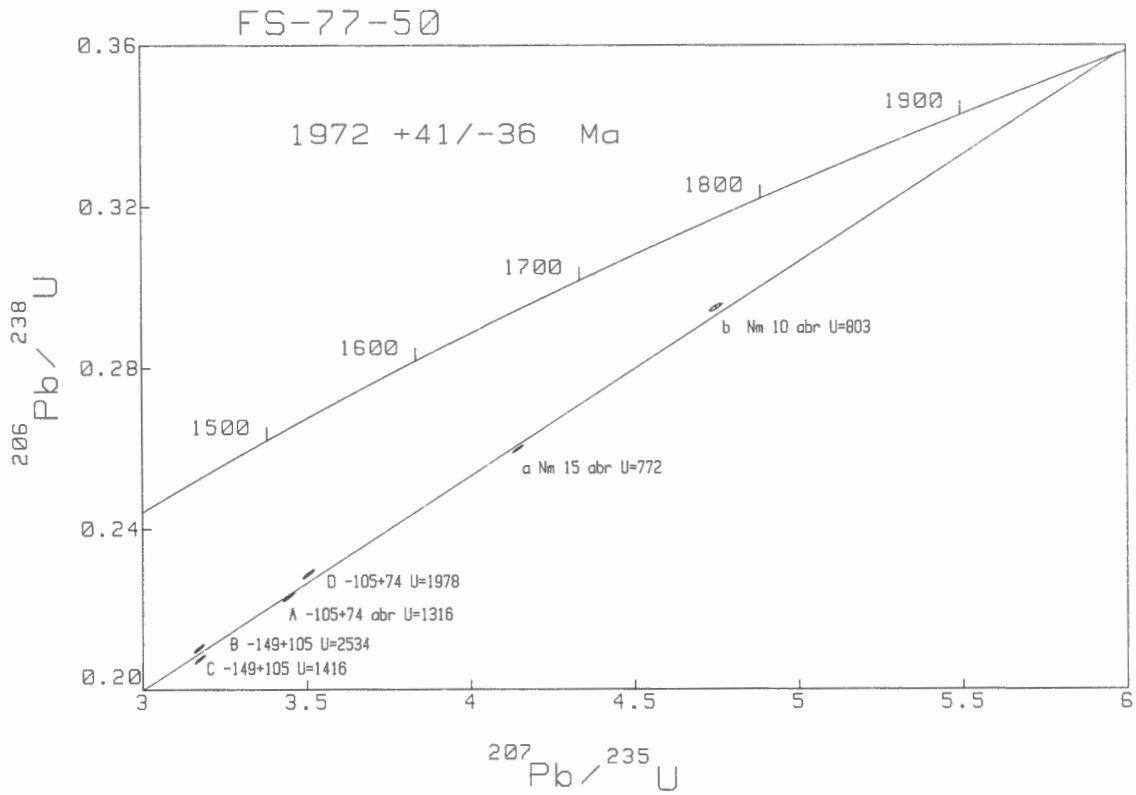

Figure 75. Concordia diagram showing results of U-Pb analyses of zircon from orthopyroxene granite, east shore of Grise Fiord, southern Ellesmere Island. U contents in ppm. Nm = non-magnetic, abr = abraded.

ment in age is purely fortuitous, due to a net effect of contributions from components of different ages — one of magmatism, the other of metamorphism.

Yet the likelihood is strong that magmatism and granulite facies metamorphism were closely related and together constituted a high grade thermal event. The equivalence in time of magmatism and granulite metamorphism in the Lapland granulite complex was suggested by results from several different isotopic systems on different rocks and supported by field evidence (Bernard-Griffiths et al., 1984). The morphologies of the zircons analyzed by Bernard-Griffths and his co-workers resemble those described above and the P-T conditions of the granulite metamorphism in Lapland (Raith, 1984) were very similar to those in the Ellesmere-Devon terrane. In the case of Ellesmere Island, the concurrence of ages at ca. 1.96 Ga from three different rocks with several zircon populations provides a basis for postulating a major thermal event in the latter part of Aphebian time.

Whole-rock Rb-Sr ages of around 1800 Ma have been obtained on granulite facies metaigneous granitoid rocks of the Etah complex at Sunrise Pynt, northwest Greenland (across Smith Sound from Cape Isabella) (P.R. Dawes, pers. comm., 1985). The rocks intrude metasediments and together form, according to Frisch and Dawes (1982), an extension of the crystalline terrane of Ellesmere Island. The difference between the ages from Ellesmere and Greenland may simply reflect use of different isotopic systems for dating.

The orthopyroxene granites of Ellesmere Island appear to be distinctly older than comparable rocks of eastern Baffin Island. Pidgeon and Howie (1975) reported a U-Pb age of 1870 ± 20 Ma on zircon from partly retrograded orthopyroxene granite ("charnockite") from Cumberland Sound, eastern Baffin Island. Pidgeon and Howie interpreted the age to be that of the magmatic activity which preceded granulite facies metamorphism but made no comment on the possible length of the time gap between magmatism and metamorphism.

Anatectic biotite granite (ag, agl)

One of the mineralogically most distinctive granites in the map area is a pink to red variety containing one or more of the minerals, garnet, cordierite, sillimanite and green spinel. This very felsic, medium grained granite occurs throughout the Ellesmere Island crystalline terrane, and larger bodies are especially abundant on Makinson Inlet (Map 1573A) and Baird Inlet and east and west of Jokel Fiord (Map 1572A); it is much less extensively developed on Coburg and Devon islands. From a distance, the granite is indistinguishable from other red-weathering granitic

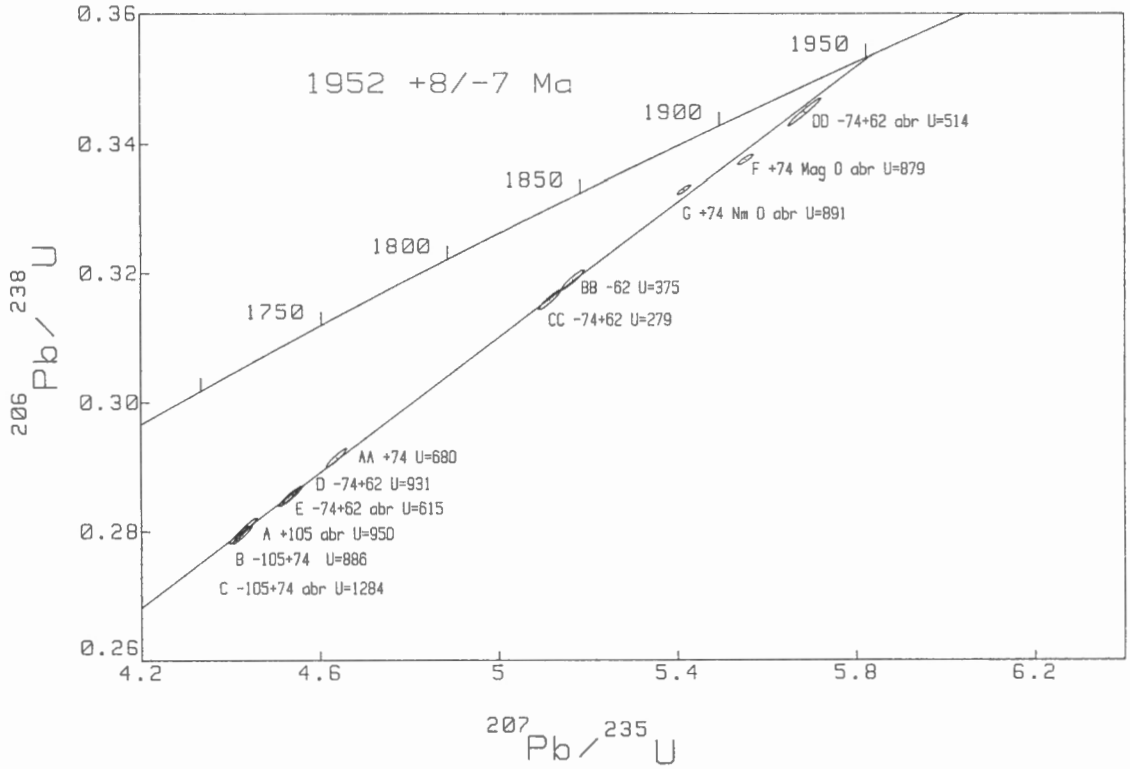

Figure 76. Concordia diagram showing results of U-Pb analyses of zircon from garnetiferous orthopyroxene granite (unit ogs; FS-77-331) and an included lens of gneissic orthopyroxene tonalite (FS-77-332), shown in Figure 66. Zircon fractions from FS-77-332 are labelled by double letters (AA-DD). U contents in ppm. Nm = non-magnetic, abr = abraded.

rocks such as orthopyroxene granite, especially retrograded varieties. Thus the extent of units ag and agl shown on the maps may well be underestimated.

The aluminous mineral-bearing granite occurs in close spatial association with aluminous metasediments. It forms minor layers and stringers in cordierite gneisses to thick sheets containing only minor schlieren of cordierite gneiss. The granite also forms plutons several kilometres long and relatively free of inclusions but such bodies are never far from abundant metasediments. Granite has also invaded orthopyroxene tonalite gneiss, as on the north shore of Makinson Inlet (Frisch, 1983, Fig. 4). In this occurrence, the largely concordant, but clearly intrusive, sheets and veins of felsic garnet-cordierite granite stand in marked contrast to the dark, orthopyroxene-bearing, K-feldspar-free tonalite gneiss. Elsewhere along the same shore identical granite forms the leucosome of migmatitic cordierite gneiss. Nearby, in the cliffs of Bowman Island, granite abounding in subparallel mafic schlieren is beautifully exposed (Fig. 77a). A more regular, lit-par-lit relationship between cordierite gneiss and garnetiferous granite is depicted in Figure 77b, which shows an outcrop on Bache Peninsula (Map 1572A).

With a colour index less than 10, the granite consists mainly of feldspar and quartz; other minerals, typically biotite and two of the abovementioned aluminous minerals, commonly make up only a few per cent of the rock's volume. Due to the paucity of mafic minerals, the granite appears at first sight to be massive but not uncommonly, on closer inspection, turns out to be gneissic, conforming with the gneisses which it has intruded (see Frisch, 1983, Fig. 4).

Alkali feldspar predominates over plagioclase in these rocks (Fig. 63); indeed, in some rocks, discrete plagioclase is absent. The alkali feldspar is partly sericitized and invariably strongly perthitic with, in many specimens, the plagioclase component very coarsely exsolved. Mesoperthite and bluish (in plane light), dense hair perthite (as in many cordierite gneisses) are also common. Poorly developed microcline grid twinning is visible in the K-feldspar of some rocks. Plagioclase is strongly sericitized in most samples and its composition is generally difficult to determine; measurements made fall in the range An_{23-26} with no pronounced zoning. Biotite is chestnut brown and lacks the reddish tint so characteristic of the cordierite gneisses. Biotite flakes are ragged and commonly show chloritization or blackened rims (probably due to oxidation).

The aluminous minerals, garnet, cordierite, sillimanite and green spinel, are erratically distributed but generally at least two of them are present in any one thin section. Garnet crystals, 1 to 4 mm in diameter, are embayed but show only minor alteration (to fine grained biotite or chlorite) along cracks and crystal margins; replacement of garnet by cordierite is rare. A few garnets contain swirls of sillimanite needles, entirely similar to those in the cordierite gneisses.

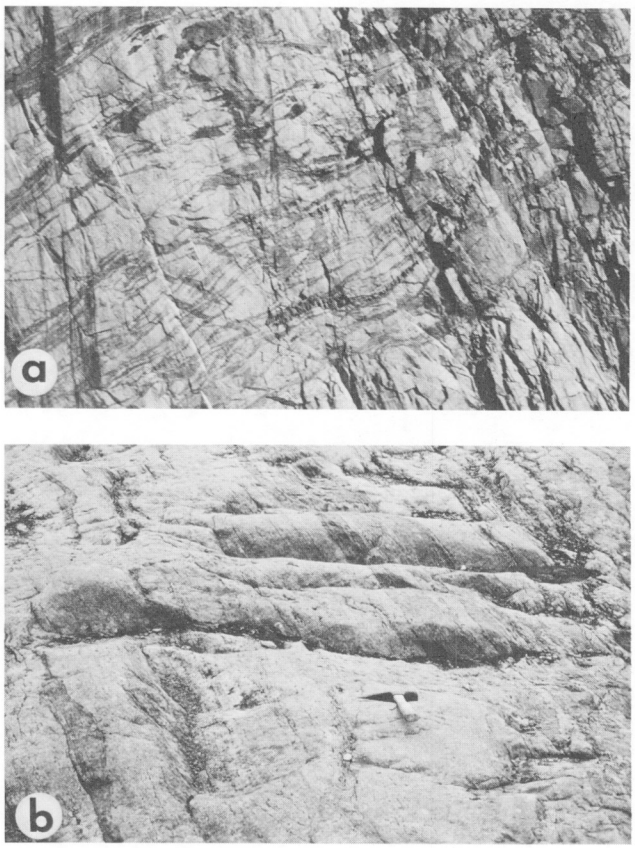

Figure 77. Mafic schlieren and lenses (biotite-rich and locally with orthopyroxene, cordierite and/or garnet) in anatectic biotite granite (units ag, agl). a) Bowman Island, Makinson Inlet. Height of cliff about 60 m. b) Bache Peninsula.

Cordierite crystals are subhedral, 0.7 to 3 mm across, and strongly pinitized. Sillimanite occurs as small prisms aggregated in swirly mats, with which minor green spinel is commonly associated. A notable feature of these granites is that, individually, the aluminous minerals appear much as they do in the cordierite gneisses. The major difference is that, typically, the aluminous minerals form a much smaller component of the granites compared to the gneisses. Also, sillimanite inclusions in garnet are much less common in the granites.

None of the aluminous minerals shows clear evidence of having crystallized from a melt. Garnet and cordierite have the best developed crystal habit but both form crystals that are far from euhedral. Yet neither of the minerals commonly contains inclusions of sillimanite or spinel, as they would if they were derived from a rock such as cordierite gneiss. Furthermore, all the aluminous minerals appear to be stable in the granite. The alteration they show, such as sericitization of feldspar, is merely the manifestation of the late-stage, exhumation-related process that affected the entire Ellesmere-Devon terrane. Thus the aluminous minerals are interpreted to have been in equilibrium with the granitic melt, even if they did not crystallize directly from it.

At the snout of Eastern Glacier, northern Devon Island, a garnetiferous, white granite is enclosed in pyroxene gneisses. Only one brief stop was made during a helicopter traverse to examine this extremely leucocratic rock. At this point the rock is pegmatitic, perthite-rich and contains rounded crystals of pink garnet. It is shown on Map 1574A as a separate unit (pm) and may be a variety of the anatectic granite. It could, however, be a leucogranitic phase of garnet-cordierite migmatite.

Rock chemistry

Eleven samples of red granite free of macroscopic mafic schlieren have been analyzed (Appendix, Table VI). The modal composition listed for each sample was obtained from a single standard-size thin section and, because of the erratic distribution of the aluminous minerals in these rocks, may not be entirely representative of the sample analyzed.

Most of the rocks are strongly potassic with a high K_2O/Na_2O ratio. All are peraluminous, molecular $Al_2O_3/(CaO+Na_2O+K_2O)$ exceeding unity, and normative corundum is generally greater than 2 %. In Debon and Le Fort's (1983) classification of common granitoid rocks, these granites are moderately to highly aluminous, quartz-poor to -rich, leucocratic, and mainly potassic (although ranging to sodic); they plot in sectors I and II of the "characteristic minerals" diagram with an indeterminate slope; and they show a trend of increasing silica with decreasing dark mineral content (Fig. 78). According to Debon and Le Fort (1983), these are characteristics of granites formed by anatexis of continental crust but do not indicate any particular type of aluminous granite association.

Average K/Rb (238) is slightly lower, and Rb/Sr (1.04) and K/Ba (69) are significantly higher, than Taylor and McLennan's (1985, Table 2.15) estimates for the upper continental crust and, of course, are very different from bulk crustal ratios.

Origin

The common occurrence in the field of relatively mafic, aluminous rock of metasedimentary aspect as inclusions in the peraluminous granite, and complete gradation from migmatite to nearly homogeneous, leucocratic granite indicates a genetic relationship between mafic and felsic rock. The nature of the granite further suggests that it crystallized from a melt formed by anatexis of sialic material, the mafic relics being restite or residuum of this process.

Peraluminous character with molecular $Al_2O_3/(CaO+Na_2O+K_2O)$ generally exceeding 1.1, high K/Na, presence of garnet and cordierite and of abundant metasedimentary xenoliths, and absence of hornblende are all earmarks of S(sedimentary source)-type granite (Pitcher, 1982). Laboratory experiments convincingly support the inference from field studies that such granitic melts can be produced by partial fusion at high pressure and temperature of aluminous metasediments (White and Chappell, 1977; Cle-

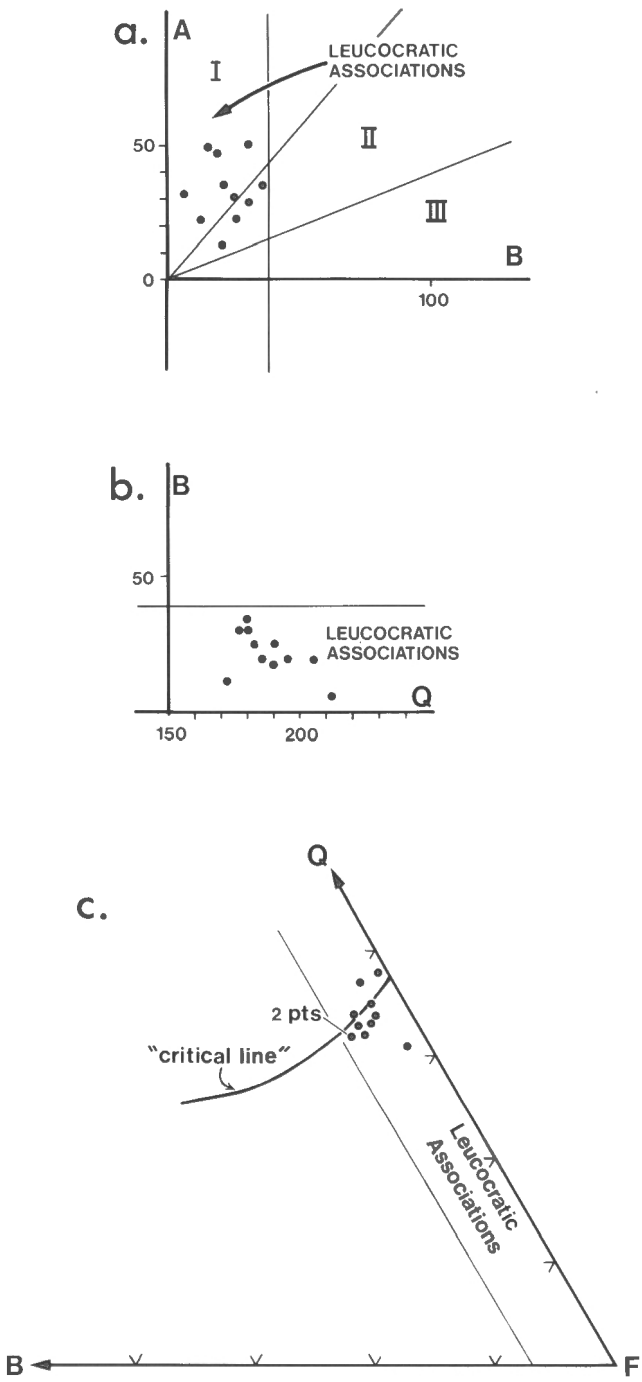

Figure 78. Anatectic biotite granites in Debon and Le Fort's (1983) classification. Numerical values in gram-atoms x 10^3 of each element in 100 g of rock.
a) Peraluminous domain of the "characteristic minerals" diagram. A = Al − (K+Na+2Ca), B = Fe + Mg + Ti. Sector I corresponds to granites with muscovite alone or muscovite>biotite (by volume), II to biotite>muscovite, III to biotite alone.
b) Q = Si/3 − (K+Na+2Ca/3), F = 555 − (Q+B). The rocks show a silico-sodic trend.
c) The rocks are normal in quartz and straddle the "critical line" separating quartz-rich and quartz-poor aluminous granites.

mens and Wall, 1981). At 700-750°C and 5-8 × 10^5 kPa a high grade aluminous pelite partially fuses by breakdown of biotite, producing a melt with high K/Na, high normative quartz and orthoclase, low normative anorthite and relatively high normative corundum. Due to high aluminium content, the melt may crystallize cordierite and garnet, even after its separation from its source material (restite-rich in garnet, cordierite and biotite). Cordierite precipitates mostly at low pressure (less than 3 × 10^5 kPa), garnet at higher pressure (4-5 × 10^5 kPa) and when Fe/(Fe+Mg) of the melt is high (Clemens and Wall, 1981). These results have obvious application to the lithologies and field relations in the Ellesmere-Devon terrane and leave little doubt as to the anatectic origin of the peraluminous red granite.

As can be seen from Figure 85, aluminous metasediment would be necessarily partially molten at approximately the conditions of cordierite formation (4-5 × 10^5 kPa, 600-700°C). The chemical composition of the average peraluminous granite from the map area is very close to that of White and Chappell's (1977) example of a mininum melt plus a small amount of metasedimentary restite (Appendix, Table VI).

The granite is also virtually identical to the garnet + cordierite (+sillimanite)-bearing Kakola granite forming substantial bodies (the largest are more than 20 km long) in the Archean granulite facies terrane of the Turku area, southwest Finland (Hietanen, 1947) (Appendix, Table VI). The Kakola granite is closely associated with garnet-cordierite-sillimanite gneiss and Hietanen (1947) ascribed its origin to "granitization", implying introduction of granitic material from without but clearly recognizing that anatexis was also involved.

Similar rocks of Aphebian age have also been described from the Canadian Shield in northeastern Alberta, between Lake Athabasca and Slave River, by Langenberg and Nielsen (1982). Termed the Slave Granitoids, they are white to pink, medium- to coarse-grained leucogranites containing, in addition to biotite, minor garnet, sillimanite, cordierite, green hercynite spinel, and, locally, orthopyroxene. The occurrence of sillimanite interstitial to perthite illustrated in Langenberg and Nielsen's (1982) Figure 16 is identical to that found in the Ellesmere Island granites. Moderate pressure granulite facies aluminous metasediments (closely resembling the Ellesmere-Devon cordierite gneisses) are associated with the Slave Granitoids as country rocks and as inclusions. Langenberg and Nielsen (1982) interpreted the granites as having formed by anatexis, an interpretation supported by high initial $^{87}Sr/^{86}Sr$ ratio of 0.710.

A question remains as to the extent of partial melting and the distance from the source that the melt has moved. Most of the peraluminous red granite in the map area is closely associated with restite material of high grade pelitic composition. However, some large bodies of granite are relatively free of megascopic bodies (e.g. schlieren) of restite and in places garnet+cordierite-bearing granite has intruded rock unlikely to have been source material, for example, orthopyroxene tonalite gneiss (Frisch, 1983, Fig. 4). Do these occurrences indicate a high degree of melting and extensive separation of melt from source?

Fusion of pelitic rock under high grade conditions is largely "dehydration melting", as H_2O released from the hydrate (e.g. biotite) is dissolved in the melt without formation of a fluid (vapour phase) (Thompson, 1982). Clemens (1984) estimated that, at a pressure of 5×10^5 kPa, a high grade pelite (35 % quartz, 20 % plagioclase, 5 % K-feldspar, 25 % biotite, 10 % sillimanite, 5 % garnet) would yield 16 volume per cent melt by fluid-absent (dehydration) melting. Clemens believed this melt would contain only 5.8 weight per cent H_2O and, because of its low viscosity, small volumes of melt would be able to rise considerable distances, perhaps to about 5 km depth (from a depth of nearly 20 km). Thompson (1982) and Grant (1985), on the other hand, argued that granitic melt will only rarely be able to segregate from restite and move any significant distance.

In the Ellesmere-Devon terrane, certainly, the bulk of the peraluminous granite appears to have remained at or near the site of its generation. Even granite intrusive into pyroxene-bearing quartzofeldspathic gneiss is never far from outcrops of cordierite gneiss, so need not have travelled any great distance. None of the analyzed granites deviates much in chemical composition from that of a minimum melt, suggesting that the degree of partial melting was considerable but not extraordinary.

Considering that the anatectic event, particularly if it is related to regional metamorphism, must have affected all the cordierite gneisses in the map area, it is paradoxical that the cordierite gneisses analyzed show little chemical evidence of being the residua of partial melting. The most likely explanation would seem to be that the chemical criteria used are insufficiently sensitive to record the effects of anatexis.

Alternatively, the larger bodies of peraluminous granite, rather than being merely the result of anatectic melting in overthickened crust, may have required input of heat from an external source, such as a magmatic intrusion, for their formation. (Candidates for such a heat source would be the orthopyroxene-bearing granitoid intrusions described in a preceding section). In that case, the cordierite gneisses would be variably affected depending on their proximity to the intrusive body, with some rocks suffering little modification of their composition.

Given the significant degree of melting implied by the larger, relatively restite-poor bodies of granite, it seems reasonable to compare these bodies with S-type intrusions of modern orogenic belts. S-type granite plutons are characteristic of tectonically-thickened continental crust in encratonic or collisional fold belts (Pitcher, 1982). The closest modern analogues to the Ellesmere-Coburg peraluminous granites would appear to be the S-type granitoid rocks of the Lachlan fold belt in southeast Australia. These are granites and granodiorites containing pyrogenic aluminous minerals, most commonly garnet and cordierite, and aluminous metasedimentary restite material, emplaced in continental crust 40-52 km thick (White and Chappell, 1977, 1983). They contrast with the Ellesmere-Coburg granites in that they are mostly high-level bodies emplaced in low grade sediments and many, like the two-mica (muscovite-biotite) leucogranites typical of fold belts worldwide, contain muscovite. Nevertheless, although their level of emplacement is very different and their mineralogy not identical, the otherwise close lithological and chemical similarity between the Australian and Ellesmere-Coburg peraluminous granites reflects their common origin: partial melting of aluminous metasediments under granulite facies conditions (Clemens and Wall, 1981). Whether the melts were the result of an anomalously high geothermal gradient due to intrusion of mafic magma (Clemens and Wall, 1981) or to tectonic thickening of the crust (Pitcher, 1982) remains open to debate.

Age

An anatexite from the north shore of Makinson Inlet, 23 km west of Boger Point (Map 1573A), was selected for dating. The rock is gneissic, coarse grained and inhomogeneous, garnet+cordierite+biotite-rich segregations alternating with felsic layers. The major mineral constituents are oligoclase, perthite, quartz, red-brown biotite, embayed garnet (2-4 mm in diameter), and partly pinitized cordierite (1-2 mm); green spinel occurs as inclusions in garnet and cordierite. There is virtually no evidence of garnet breaking down to cordierite.

Although much of the rock is thought to have crystallized from a melt, parts of it may be relict aluminous metasediment.

Zircons from the anatexite are composed of two distinct generations. A finely zoned, euhedral prismatic core is mantled by an unzoned, rounded overgrowth; cracks commonly radiate from the edges of the prismatic core. Typically, the core/overgrowth ratio is 1:2. The core zircon appears to have grown in a melt, whereas the unzoned shell may have formed in the solid state during high grade metamorphism. It is also possible, but less likely, that the zircon grains are entirely detrital and acquired their roundness from abrasion during weathering.

Four zircon fractions (three sizes, two of which were abraded) were analyzed. The ages obtained are considerably discordant and the data points form a tight cluster in the U-Pb concordia diagram (Fig. 79). Regression of the data gives upper and lower intercept ages of 1912 +21/−11 and 14 Ma, respectively. The lower intercept age is probably meaningless geologically. The upper intercept age is difficult to interpret because of the two stages of growth — possibly at widely separated times — evident in the zircon crystals and the small spread of data points along discordia. The age may be no more than a mixing age. If so, however, it would probably be weighted in favour of the age of the overgrowth, which forms the bulk of the zircon crystals. Furthermore, the age, within error limits, is of the same order as the ages determined on orthopyroxene granites and included orthopyroxene tonalite of units ogv and ogs. Consequently, the age obtained is provisionally accepted as additional evidence of a major thermal event, which included both magmatism and metamorphism, between 1.9 and 2.0 Ga.

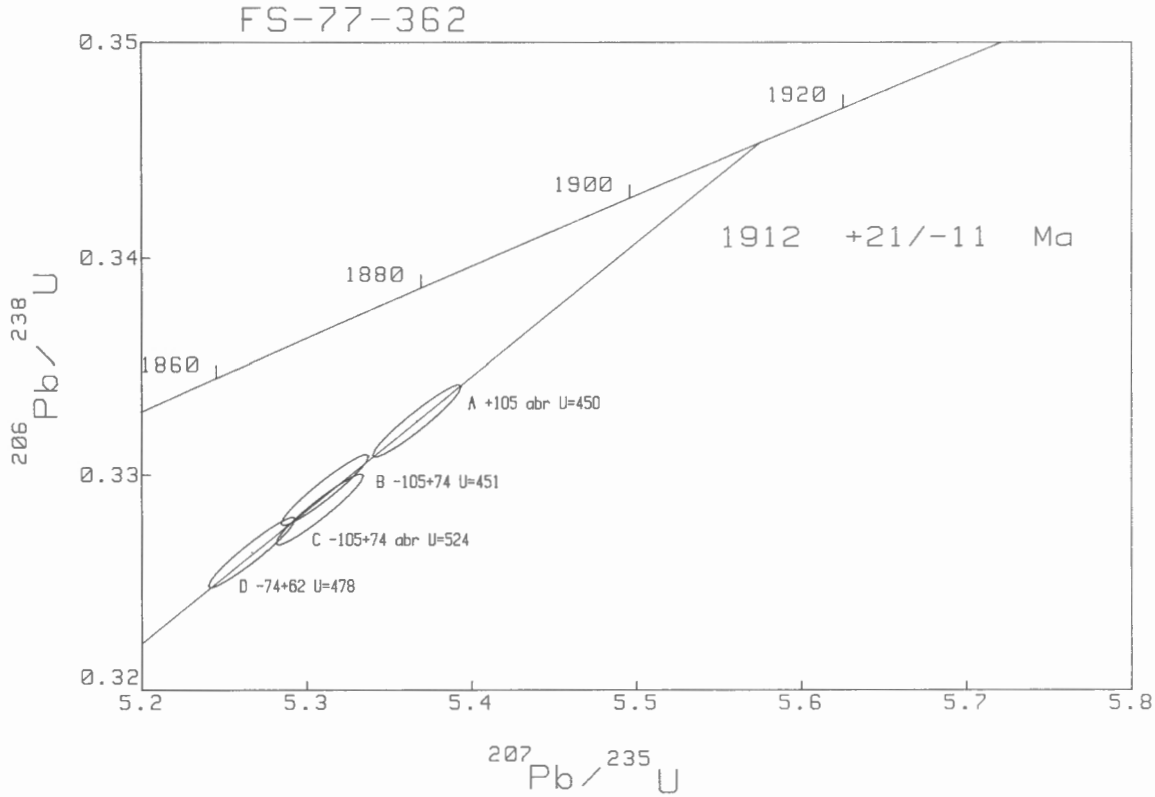

Figure 79. Concordia diagram showing results of U-Pb analyses of zircon from a garnet + cordierite-bearing anatexite of unit agl, Makinson Inlet. U contents in ppm. abr = abraded.

Amphibolite facies acid to intermediate rocks

Rocks with diagnostic amphibolite facies mineralogy occur only locally in the map area and are of limited areal extent. They are found mainly along the western margin of the Precambrian Shield near the contact with Paleozoic rocks of the Arctic Platform and in scattered localities, commonly high-strain zones, throughout the map area. Amphibolite facies rocks are invariably associated with partly retrograded granulite facies rocks.

The hornblende-bearing granitic rocks (hg, hgn) near the ice edge west of the Prince of Wales Mountains (Map 1572A) are typical examples of amphibolite facies rocks. Although partly retrograded granulite facies rocks are also present, the area underlain by amphibolite facies lithologies is exceptionally large. The amphibolite facies gneisses (hgn) are grey or pink and comprise biotite gneiss and thin amphibolite layers and lenses. The feldspars are oligoclase, without antiperthite, and fresh perthitic microcline. Mafic minerals include biotite with an olive Z colour, blue-green hornblende and minor muscovite, epidote and sphene. Analyses of biotite and hornblende with similar optical properties (Appendix, Table 6) in an amphibolite facies granite gneiss (FS-77-344) from near the head of Cadogan Glacier (Map 1572A) show the chemical features of low Ti in both minerals and high Si, low octahedral Al and K in hornblende (Appendix, Table 7) as compared to these minerals in the granulite facies.

Pink, coarse grained to pegmatitic hornblende-biotite granite (hg) contains microcline megacrysts and thin amphibolite sheets, in which the hornblende is blue green and sphene is a common accessory mineral. Quartz veins cut the granite and amphibolite.

Amphibolite facies rocks in the map area generally are characterized by green-tinted biotite, green to blue-green amphibole, plagioclase free of antiperthite, abundant microcline with well developed grid twinning and, commonly, sphene, epidote and muscovite in accessory amounts. By themselves, these rocks show no sign of ever having been at a higher grade. However, their association with clearly retrograded granulite facies rocks and obvious textural and mineralogical gradations between the two facies rarely leave any doubt as to their having been downgraded.

An example of a rock transitional between the amphibolite and granulite facies and closely associated with amphibolite facies gneiss is biotite-cummingtonite tonalite gneiss FS-77-147 (Appendix, Table 6). The gneiss occurs intercalated between pink hornblende-biotite gneiss and amphibolite in a large exposure of unit hgn west of the Prince of Wales Mountains. It is made up of antiperthite-free plagioclase (An_{43}), strained quartz, chestnut-brown biotite, and fine grained aggregates of cummingtonite laths that are clearly pseudomorphing an earlier mineral (Fig. 80); that mineral was almost certainly orthopyroxene. The cummingtonite aggregates are rimmed by a narrow fringe

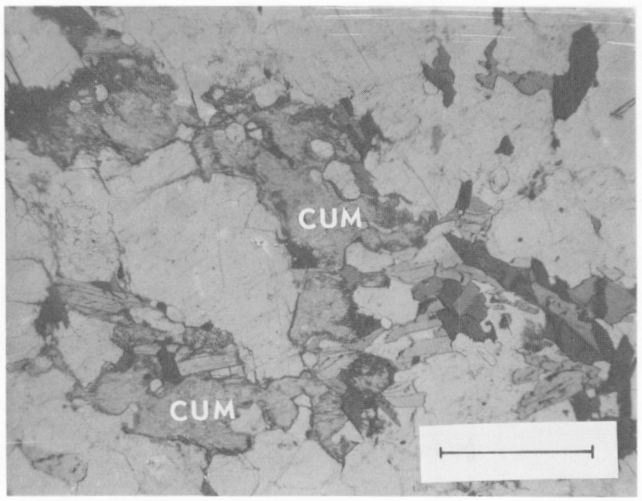

Figure 80. Complete replacement of (ortho?)pyroxene by cummingtonite in amphibolite facies retrograde pyroxene tonalite gneiss (FS-77-147; unit hgn), west of Prince of Wales Mountains, Ellesmere Island. Plane light. Bar scale 1.0 mm.

of pale green amphibole, probably actinolite. Although the cummingtonite is indisputably an amphibolite facies mineral, the biotite displays the deep brown Z colour and high Ti content (4.18% TiO_2) of granulite facies biotite. The equigranular granoblastic texture with equilibrium triple junctions between grains has also been retained from the granulite facies.

There are very few metamorphic rocks in the map area that show no sign of past or present granulite facies mineralogy. Mineralogical and textural gradations consistently indicate retrograde processes. Furthermore, amphibolite facies or strongly retrograded granulite facies rocks are generally related spatially to high structural levels or zones of intense deformation in the basement. The common occurrence of retrograde rocks at or near the Phanerozoic erosion surface suggests that exhumation was an important factor in retrogression. Undoubtedly even more effective in promoting retrogression was the mechanical reworking attending deformation, as Krupička (1973) has documented in the Truelove Inlet area of northern Devon Island.

Metamorphosed acid and intermediate dykes

Retrograded granulite facies dykes of orthopyroxene granite (unit ogd) occur in the southern coastal region of Buchanan Bay, near the northern margin of the map area (Map 1572A). They form a minor, northwesterly trending swarm cutting northerly trending cordierite gneiss and orthopyroxene-bearing granitoid rock. The strong discordancy and a weathering colour slightly darker than that of the country rocks make the dykes look from the air like normal diabase dykes. Up close, they are less easily discerned, particularly where they intrude orthopyroxene granite, which they resemble. Contacts are sharp (Fig. 81) but there

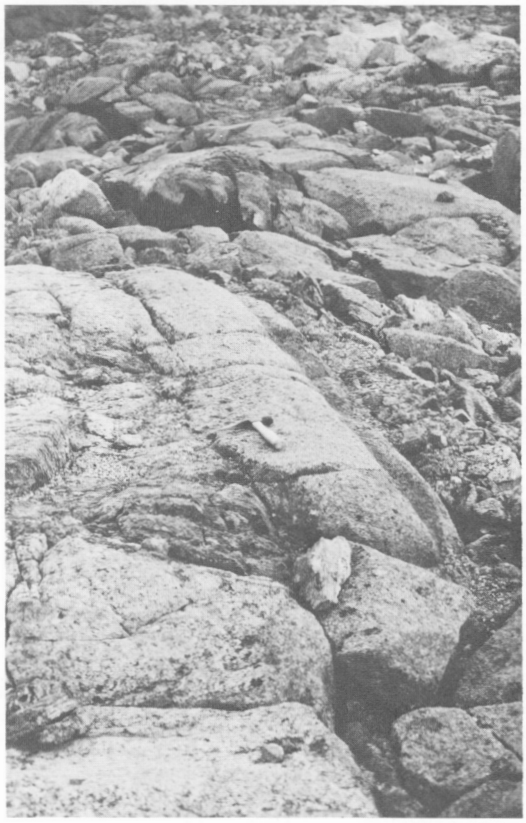

Figure 81. Contact of dark, retrograde orthopyroxene granite dyke (unit ogd) and cordierite gneiss, which has a foliation strongly discordant to the dyke. South shore of Buchanan Bay, Ellesmere Island.

is no change in grain size across the dykes and no thermal effects in the country rocks were observed. The dykes are vertical, locally sinuous and 4 to 8 m thick; one dyke can be traced for 6 km.

The dykes consist of biotite-hornblende granite with pseudomorphs after orthopyroxene. A sample (FS-77-278) from near the margin of an 8 m thick dyke is modally almost a granodiorite (Appendix, Table VII). Its texture is largely granitic and inequigranular with Carlsbad-twinned K-feldspar crystals (4 to 10 mm long) set in a medium grained aggregate of feldspar and mafic minerals. The mafic minerals, which tend to be aggregated in clots, comprise olive hornblende (partly altered to brown biotite), nut-brown biotite and pseudomorphs of intergrown greenish biotite and hornblende after orthopyroxene. Plagioclase is well twinned and normally zoned, An_{25-30}, and irregularly antiperthitic. K-feldspar is perthitic, the larger crystals showing local development of flame perthite, the remainder containing very fine hair perthite. Myrmekite is common and apatite and zircon are major accessory minerals.

A dyke cutting orthopyroxene-bearing granitoid rocks at the northern end of Pim Island (Map 1572A) is also regarded as belonging to the retrograded granulite facies. The dyke was first recognized by Schei and is pictured in

Bugge (1910, opposite p. 10) and in Frisch and Dawes (1982, Fig. 7). The dyke is dark green, schistose and 0.3 m thick, cutting with marked discordance across both greenish orthopyroxene tonalite-granite and pink granite (retrograded orthopyroxene granite?) sheets and veins. As Schei (Bugge, 1910) noted, however, thin veins of pink granite cut the dyke, for the most part concordantly (Frisch and Dawes, 1982, Fig. 7), and portions of the dyke are gneissic. Some of these veins can be followed into the country rock.

The dyke is a fine grained, equigranular rock (grain size 0.2 mm) made up of plagioclase (An_{38}), quartz, chestnut biotite, olive hornblende, aggregates of green chlorite and carbonate that appear to be pseudomorphs after pyroxene, Fe-Ti oxide and apatite. The mafic minerals, especially biotite, define an excellent schistosity. Bugge (1910) noted the presence of minor microcline and orthoclase but no K-feldspar could be identified with certainty by the present author.

Rock chemistry and origin

The sample of retrograded orthopyroxene granite described above was analyzed chemically (Appendix, Table VII). It is less siliceous and more iron-rich than any of the other orthopyroxene granites analyzed and in potassium content is exceeded only by the granites of unit ogs; it is unusually rich in Zr (863 ppm). In general, however, the dyke rock is broadly similar to the majority of orthopyroxene granites in the map area and could well be genetically related. The lack of significant deformation of the dykes indicates their emplacement after the main tectonism but presumably, in view of the high grade mineralogy, at high temperature.

On the basis of its mineral and chemical composition and association with granitic rocks, the dark dyke in northwestern Pim Island was termed kersantite by Schei and Bugge (Bugge, 1910). Bugge did, however, recognize its schistose structure and commented on its metamorphic appearance. When compared with true kersantites (Rock, 1984) (Appendix, Table VII), the dyke has a very high quartz content and is considerably more siliceous and less magnesian. It has high levels of barium and strontium, 4420 and 2268 ppm, respectively, which characterize some lamprophyres but are not unique to kersantites (Rock, 1984).

Taking into account the metamorphic, yet discordant, and chemically evolved nature of the dyke, it appears probable that the dyke represents an intrusion of intermediate composition emplaced late in the tectonic history of the region, during the waning stages of metamorphism. Whether that metamorphism was of granulite grade or lower is uncertain. The occurrence, not far to the northwest, of retrograded orthopyroxene granite and pyribolite dykes suggests that "Schei's dyke" is a retrograded granulite facies rock, probably originally crystallized from magma of intermediate composition.

Structural geology

The structural history of the Ellesmere-Devon crystalline terrane has been long and involved and remains far from adequately known. Considerably more detailed mapping and geochronological work are needed to enlarge our present knowledge, which is limited to the broad essentials.

The map area is divided into two major tectonic blocks, one comprising Ellesmere and Coburg islands, the other, Devon Island. Generally, structures trend northerly in the Precambrian Shield of Ellesmere and Coburg islands and westerly on Devon Island. The numerous deviations from these trends do not invalidate this fundamental contrast in structural grain of the two blocks.

Foliations, which commonly parallel lithological boundaries, in the main dip steeply to moderately but there are areas, such as southern Devon Island and the head of Beitstad Fiord (Map 1572A), where the bulk of the rocks tend to be flat lying. The shallow dipping foliations are not associated with any particular rock type nor are they related to any recognized structure such as a thrust fault or nappe. As has been stressed in earlier sections of this report, foliation characterizes all the metamorphic rocks of the map area, although it may be weakly developed in some rocks of intrusive aspect.

Three periods of folding can be readily recognized in the crystalline rocks. Folds of the first two periods are isoclinal; their axes trend northerly on Ellesmere and Coburg islands and easterly on Devon Island. The earliest folds commonly are difficult to recognize on the ground because of their extreme tightness. Second-period folds, marked by repetition of strata, are generally overturned and locally recumbent. A third major folding event produced broad, open folds with axial planes striking mainly northwesterly (Fig. 82).

Figure 82. Late open fold in supracrustal gneisses, northern margin of Eastern Glacier, Devon Island. Jones Sound and Ellesmere Island in distance.

The earlier folding resulted in intense flattening, which has been accentuated in ductile shear zones (Fig. 83). The latter are particularly common in Devon Island, where they run in a westerly direction and probably gave rise to lineaments such as the straight coastlines prominent in the northeast. Although ductile deformation pervades the entire map area, the degree of deformation in Devon Island is generally distinctly higher than on Ellesmere and Coburg islands.

Late faulting in the crystalline terrane is evidenced by shear zones up to several tens of metres thick, cutting across older structures. An outstanding example occurs along one of the east striking faults south of Truelove Inlet, northern Devon Island. There, a mylonite zone 30 m wide in orthopyroxene tonalite gneiss contains metre-thick pseudotachylyte veins. Shearing appears to have been especially common on Devon Island and the southeastern part of the Shield on Ellesmere Island.

Numerous displaced blocks of Paleozoic strata attest to major faulting in post-lower Paleozoic time (Fig. 84). Throws of several hundreds of metres along normal faults are common. Many of the faults coincide with, or parallel, lineaments in the crystalline terrane and basement structure was probably the main factor in localizing post-Paleozoic faulting. According to Kerr (1980), the waterways between Ellesmere and Greenland and around Devon Island were formed in the Cretaceous-Tertiary Eurekan Orogeny by rifting controlled by structural trends in the Precambrian Shield.

Figure 83. Extreme flattening in ductilely sheared orthopyroxene tonalite gneiss, east of Dundas Harbour, southern Devon Island.

Review of metamorphic conditions

Geothermobarometric data gleaned from diverse mineral assemblages in the Ellesmere-Devon terrane and discussed in preceding sections of this report are brought together in Figure 85. Superimposed on these data are relevant stability curves of certain minerals and melting reactions as well as the fields of metamorphic facies series. It should be remembered that temperature and pressure uncertainties in the data reviewed below are estimated to be 50 to 60°C and 1 to 1.5 $\times$ 10^5 kPa.

The distribution of the data points in the P-T diagram is, of course, critically dependent on temperature values for the various pressure-dependent reactions. As emphasized earlier, determination of temperature is especially difficult for reactions in the pyroxene-bearing quartzofeldspathic gneisses. The temperature estimate of 750°C selected for core compositions was not an entirely arbitrary choice and may even be conservative. Peak temperatures of metamorphism may have exceeded 750-800°C (and probably did locally) but probably not by very much; they were almost certainly higher than 700°C.

The data points in Figure 85 fall into two groupings: one with temperature over 700°C and pressure largely between 5 and 7 $\times$ 10^5 kPa, the other with T and P ranges of 500-700°C and 3-5 $\times$ 10^5 kPa. The latter set is clearly defined by mineral reactions initiated by decompression and a P-T curve drawn through the data points has a shallow slope within the field of the andalusite-sillimanite facies series.

The problem posed by the "high P,T" data set is how closely the data points approach the conditions of the metamorphic climax. The highest pressure recorded by any of

Figure 84. Downfaulted lower Paleozoic strata resting on and against Precambrian gneisses, east shore of Starnes Fiord, southern Ellesmere Island.

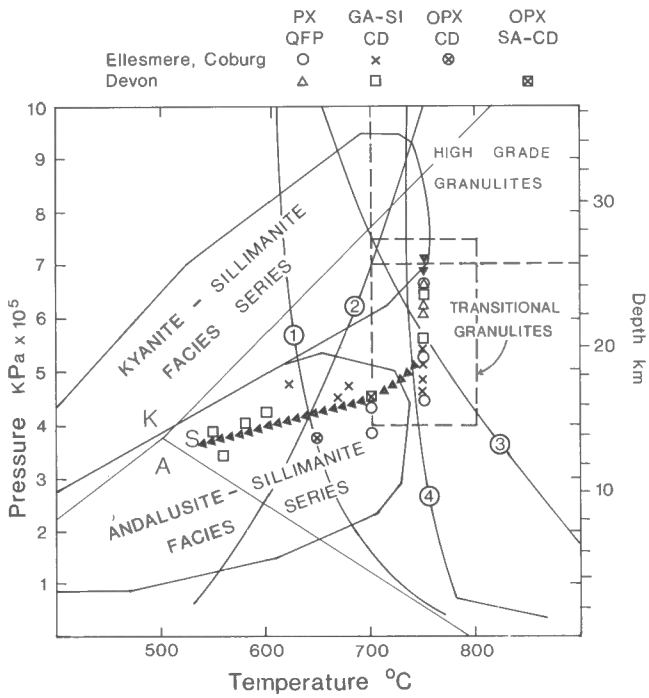

Figure 85. Summary diagram of pressure and temperature data, both calculated and estimated from various geothermobarometric calibrations, in the Ellesmere-Devon terrane; see text for further details. The suggested P-T evolutionary path is very approximate.

Aluminosilicate stability fields after Holdaway (1971); curves 1 and 2 approximately mark the beginning of wet and "dry" (vapour-absent) melting, respectively, in pelites (Thompson and England, 1984); curve 3 approximates the beginning of wet melting in amphibolites (Thompson and England, 1984); curve 4 is for the reaction of biotite with K-feldspar, quartz and $CO_2 + H_2O$ vapour to form orthopyroxene and liquid (Wendlandt, 1981); facies series fields after Thompson and England (1984); fields of high grade and transitional granulites after Newton (1985).

the most reliable geobarometers barely exceeds 7×10^5 kPa and pressures indicated by unzoned garnet + pyroxene + plagioclase range down to values as low as 4.2×10^5 kPa, which are typical of the decompression conditions indicated by other assemblages. How extensively have these assemblages re-equilibrated to lower grade conditions? The lower pressures may well have obtained at temperatures of 700°C and below and may properly belong to the retrograde data set.

The "high P,T", values are characteristic of Newton's (1985) "transitional granulites" (Fig. 85), which are those granulite facies rocks that either are spatially related to a prograde amphibolite facies zone or are undepleted in LIL elements. In the case of the Ellesmere-Devon terrane, amphibolite facies rocks are interpreted to be retrograded granulite facies. Although the P,T conditions indicated by the retrograde data set might be regarded as corresponding to those of the amphibolite facies, the "retrograde" rocks are intimately associated with rocks of unquestionable granulite facies mineralogy and the entire rock package should be regarded as a granulite terrane recording the evolution of pressure, temperature and time during its metamorphic history.

Whereas a pressure-temperature path can fairly readily be drawn through the retrograde data set, its upper part is difficult to define due to uncertainties in the temperatures of the "high P,T" data set and the lack of any truly high grade granulite assemblages well constrained by both pressure and temperature. A suggested path for the rocks of the Ellesmere-Devon terrane is shown in Figure 85. A path with a steep upper part, originating in or near the kyanite-sillimanite facies series field, and a shallower lower part, lying in the sillimanite field of the andalusite-sillimanite facies series, is expected in the case of a rock mass transported to considerable depth as a result of crustal thickening, due, for example, to continental collision, and subsequently uplifted with attendant anatexis and plutonism (Thompson and England, 1984). The highest pressures recorded in the Ellesmere-Devon terrane correspond to a 25 km depth of burial. As these rocks are presently underlain by continental crust of presumably normal thickness, the crust beneath the map area may have been as much as 50-60 km thick at some time in the past. In inferring overthickened crust, it is assumed that neither magmatic underplating nor underthrusting of the crust has occurred on a large scale during later orogeny. Magmatic accretion to the crust should result in a significant temperature rise subsequent to the granulite metamorphism. If the presently exposed granulite facies rocks had been uplifted by low-angle thrusting, belts or slivers of high grade rocks separated from lower grade ones by low-angle faults and shear zones would be expected. No evidence of such relations nor underplating has been found in the Ellesmere-Devon terrane.

Thompson and England's (1984) analysis predicts that deeply buried rocks would experience essentially isothermic decompression of several hundreds of megapascals early in their exhumation. If the range of pressures at constant temperature (750°C) in Figure 85 is real, a steep initial path is also indicated but by no means established on the strength of the present data.

Clearly evident from Figure 85 is the inevitability of crustal melting during the metamorphic evolution of rocks as deeply buried and highly heated as those of the Ellesmere-Devon terrane. Any reasonable P-T path must lie in the melting range of common crustal rocks (Fig. 85) and this, coupled with the probability that high temperatures were maintained over a long period, suggests that additional heat from mantle-derived sources was probably not required to generate the bulk of the intrusive rocks. Thompson and England (1984) emphasized the close connection between deep burial, anatectic melting and andalusite-sillimanite facies series.

The lack of precise geochronological data means we have very little knowledge of the time factor in the P-T evolution. Uplift must have been rapid in order for the evidence of decompression reactions, such as garnet breaking down to cordierite, to have been preserved so well

and so extensively, and for pressures as low as 3-4 × 10^5 kPa to have obtained at temperatures as high as 650-700°C. Rapid uplift, (e.g. 2 mm or more per year (2 mm/a = 2 km/Ma) has been documented or proposed on geological, petrological and geochronological evidence in a number of granulite terranes, Archean to Tertiary in age, with mineral assemblages and reaction textures closely similar to those of the map area. Four examples are the Archean Limpopo Belt, southern Africa (Harris and Holland, 1984), the Hercynian metamorphic complex of southern Calabria, Italy (Schenk, 1984), the Gruf Complex of the Italian Central Alps (Hercynian rocks uplifted in the Tertiary; Droop and Bucher-Nurminen, 1984) and Tertiary granulite facies rocks of the Coast Range, British Columbia (Hollister, 1982).

Origin and tectonic development of the Ellesmere-Devon crystalline terrane

The Precambrian Shield of Ellesmere, Devon and Coburg islands is characterized by interleaved belts of rocks of (late Archean?) supracrustal and infracrustal aspect, intruded by deep-level granitoid rocks. The belts run northerly in Ellesmere and Coburg islands, easterly in Devon Island, but are of broadly similar lithology. The entire terrane was metamorphosed in the medium to low pressure granulite facies, probably in late Aphebian time.

The metasedimentary rocks are of shelf-slope type derived from continental crust and include marble, quartzite, and abundant pelitic-psammitic sediment (shale and subordinate sandstone) represented by garnet-sillimanite-cordierite gneiss. Although the metasedimentary suite comprises shallow to relatively deep water deposits, no abyssal sediments are recognized. Metabasalts, common but not voluminous in the supracrustal sequences, are of oceanic affinity (island arc or mid-ocean ridge) according to their chemistry.

Pyroxene-bearing granitoid gneisses are of infracrustal type and uncertain origin. Tonalites of K-poor dacite composition predominate and gneisses and metabasalts (if related) form a bimodal suite. The gneisses can be interpreted as a calc-alkaline suite, in part probably intrusive, in part possibly volcanic (e.g. tuffs) and thus supracrustal. No basement-cover relationship has been identified and no evidence has been found that any of the granitoid gneisses are older than the metasediments. There is no lithological, structural or geochronological evidence known to the writer in support of the view of Petro-Canada geologists (Gibbins, 1985) that the granitoid gneisses exposed in much of eastern Devon Island and in Ellesmere Island are the oldest rocks in the map area. Although the oldest isotopic ages obtained so far are from Devon Island gneisses, similar rocks from Ellesmere Island have not been dated nor have any supracrustal rocks.

The metasedimentary/metaigneous assemblage suggests a continental margin setting, wherein oceanic as well as continental crust would be involved. Geologists of Petro-Canada rather daringly subdivided the supracrustal rocks of Ellesmere Island into various facies — platform, miogeosynclinal, eugeosynclinal and molasse — now exposed in north-trending belts in the eastern half of the Shield terrane (Gibbins, 1985). While the writer believes such a synthesis to be premature, he agrees with the underlying rationale of a marine basin along a continental edge.

Intrusions ranging from tonalite to granite are considered to have been emplaced contemporaneously with granulite facies metamorphism in the late Aphebian. The bulk of them originated by crustal anatexis resulting from crustal thickening.

The Ellesmere-Devon terrane displays all the main characteristics of Archean- Proterozoic high grade "mobile belts", as defined by, for example, Windley (1984) and Kröner (1986). Such belts commonly border older cratonic blocks of amphibolite grade. "Transitional" granulite terranes (Newton, 1985), in particular, have typically developed from the amphibolite facies by prograde metamorphism, with both facies preserved side-by-side. Amphibolite facies rocks in the Ellesmere-Devon terrane are retrograde but rocks bordering its extension in northwestern Greenland (Frisch and Dawes, 1982) are in apparently prograde amphibolite facies. The contact between granulite and amphibolite facies rocks in Greenland appears to lie between the Inglefield Bredning waterway at 77° 30′N and the area of Thule Air Base, which lies on approximately the 76° 40′N line of latitude (*see* Fig. 1).

At the head of Inglefield Bredning, gneisses and supracrustal rocks are in granulite facies and record peak pressures of 7.5 × 10^5 kPa and temperatures of about 700°C (Nutman, 1984; Garde et al., 1984). To the north, the Precambrian crystalline rocks are in granulite facies, with lithologies and mutual relations similar to those in Ellesmere Island (Frisch and Dawes, 1982). To the south, around Thule Air Base, and beyond, in Melville Bay, the crystalline terrane is entirely in the amphibolite facies (Dawes, 1976).

South of Devon Island, the nearest Precambrian Shield is on Bylot Island and mostly in the granulite facies but most of the shield on neighbouring Baffin Island is of amphibolite grade (Jackson and Morgan, 1978).

As to how the Ellesmere-Devon terrane came to be a high grade gneiss belt bordering the lower grade North American craton can only be speculated on. Anomalous crustal thicknesses are generally accounted for by some form of overthrusting, related to processes such as continental collision (Thompson and England, 1984) or stacking by thrusting of previously thinned or mechanically weakened continental crust (Kröner, 1985). Tectonics of this type would explain the interleaving of belts of diverse lithology in the Ellesmere-Devon terrane, as well as the high grade of metamorphism and extensive crustal melting. However, large-scale thrust tectonics should be evidenced by large recumbent folds and generally flat to shallow dips and these are not immediately obvious as the major structures in the Ellesmere-Devon terrane. But lack of such evidence may only be a reflection of our limited knowledge of the structural geology.

The tectonic picture is in any event complicated by the segmented nature of the Ellesmere-Devon terrane. Devon Island has a structural grain at right angles to that of Ellesmere and Coburg islands and, because of important lithological dissimilarities, cannot be regarded as simply an east-west belt resulting from bending of a north-south belt. If the interleaving of lithologies resulted from thrusting, the direction of thrusting differed radically across the Ellesmere-Devon terrane.

Further work is necessary to assess the real significance of the abundant evidence of east-west stretching and ductile shear in Devon Island. Perhaps the island is actually a major shear zone between the Ellesmere-Coburg and the Bylot-Baffin blocks.

UNMETAMORPHOSED ROCKS

Before the rocks of the sedimentary cover are described, some comment should be made on the nature of the Precambrian basement surface which they unconformably overlie. In general, the crystalline rocks are reddened and moderately to little weathered, but no regolith is developed below the unconformity. As mentioned in a previous section, retrogression is commonly evident in the metamorphic mineral assemblages but there are places, such as at the mouth of Powell Inlet, southern Devon Island, where very fresh, hard orthopyroxene-bearing gneiss directly underlies conglomerate of the Neohelikian Strathcona Sound Formation. Less than 20 km to the north, however, on the eastern shore of Powell Inlet, lies the only occurrence of deeply weathered basement in the map area known to the author. Little altered metasedimentary gneisses rapidly grade upward into a 35 m thick section of deeply weathered material, some of which resembles fault gouge and which is cut by numerous shear planes. The section is overlain by lower Paleozoic rocks. The weathering zone was not studied in detail and its age remains uncertain.

Neohelikian rocks

Thule Group (NT, NT1, NTu, NTb)

At several places on the east coast of Ellesmere Island, the basement is overlain unconformably by gently dipping, unmetamorphosed sedimentary and igneous rocks of the Neohelikian Thule Group. These rocks have been described by Frisch and Christie (1982), Dawes et al. (1982) and Jackson (1986) and only a brief summary is given here.

The Thule Group outcrops mainly in the Cape Combermere-Clarence Head area south of Smith Bay (Map 1573A), north and south of Cadogan Inlet and on Bache Peninsula (Map 1572A). The thickest section, 1060 m thick, occurs on Goding Bay (Map 1572A) but it, like the other sections of the Thule Group on Ellesmere Island, is capped by an erosion surface. On the accompanying geological maps, the Thule Group has been divided into three units.

Strata forming the lower part of the succession comprise quartzose sandstone and conglomerate, stromatolitic dolomite, and varicoloured shale and siltstone of shallow marine to continental origin. Interbedded with the sediments are tholeiitic basalt lava and sills and volcanic breccia, of continental origin.

The upper part of the succession consists almost entirely of sedimentary rocks, chiefly red and green shale, siltstone and sandstone, and orthoquartzite. Basalt sills and lava and minor calcareous rocks are subordinate components of the upper sequence.

A third unit of the Thule Group occurs on the southern shore of Bache Peninsula, between crystalline basement and Cambrian strata, and on Map 1572A is termed the Bache Peninsula sequence. The distribution of this sequence shown on the map is essentially that of the lower part (Camperdown and Bache Peninsula members) of the Rensselaer Bay Formation as mapped by Christie (1967) and tentatively considered by him to be Cambrian. More recent work, the results of which became available after completion of the manuscript map, has redefined the Rensselaer Bay Formation (Peel et al., 1982). The newly defined Rensselaer Bay Formation on Bache Peninsula comprises only the Camperdown Member, which consists of red and green shales, varicoloured sandstone, and minor carbonate rocks and is intruded by Proterozoic basalt sills (Peel et al., 1982). The Rensselaer Bay Formation is correlated with the Thule Group (Dawes et al., 1982). It thins westward on Bache Peninsula, pinching out near the small bay immediately east of Koldewey Point (Christie, 1967). The thinning of the Rensselaer Bay is thought to be an erosional bevelling at the Precambrian-Cambrian unconformity (Peel et al., 1982). The overlying conglomeratic arkose of the Bache Peninsula Member and quartzose sandstone of the Sverdrup Member (Christie, 1967), are assigned by Peel et al. (1982) to the Lower Cambrian Dallas Bugt Formation.

A corrected representation of the geology along the southern shore of eastern Bache Peninsula is shown in Figure 86. The lithology of the Bache Peninsula sequence, given in the legend to Map 1572A, should be amended to read "sandstone, shale, dolomite; basalt sills".

The age of the lower Thule Group is derived mainly from whole-rock K-Ar determinations on basalt from the lavas and sills. The ages obtained cluster around 1100 to 1200 Ma (Dawes et al., 1982).

Strathcona Sound Formation (Nss)

Unmetamorphosed sedimentary rocks assigned to the Strathcona Sound Formation of the Nunatsiaq Group, Bylot Supergroup, outcrop on the southern coast of Devon Island between Burnett Inlet and Croker Bay (Jackson and Iannelli, 1981, p. 295). They unconformably overlie crystalline basement and are themselves overlain by structurally conformable lower Paleozoic strata.

The Strathcona Sound rocks include dolomite conglomerate, green and red shale and siltstone, and variegated quartzose sandstone, all typically thin bedded. The formation is interpreted to have formed in an alluvial plain-tidal zone environment (Jackson and Iannelli, 1981).

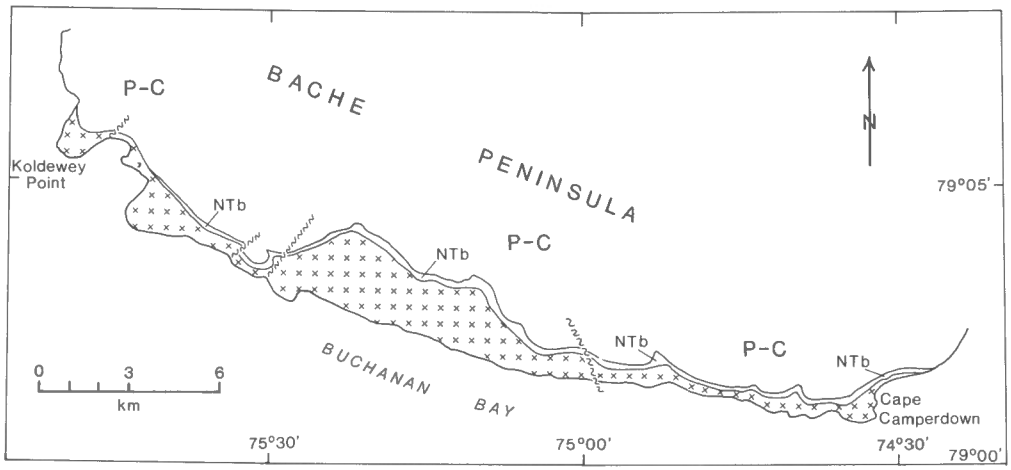

Figure 86. Sketch map of the geology along the southern shore of eastern Bache Peninsula, shown incorrectly on Map 1572A. Crystalline rocks (crosses) are overlain unconformably by the redefined Proterozoic Rensselaer Bay Formation (NTb), comprising sandstone, shale, dolomite and basalt sills, which is correlated with the Thule Group. P-C = Paleozoic strata.

The Strathcona Sound Formation is one of the youngest units of the Bylot Supergroup, which constitutes the filling of the Neohelikian Borden Basin. The outcrops on southern Devon Island are the northernmost exposures of the Borden Basin, a rift zone extending some 300 km through northwestern Baffin Island and coeval with the Thule Basin (Jackson and Iannelli, 1981).

Thus the presence of 1.1-1.2 Ga, unmetamorphosed, at most gently folded sediments of the Thule and Borden basins sets an upper limit to the age of metamorphism and major folding in the map area.

Diabase dykes (Hd, Hda)

Unmetamorphosed diabase dykes cut all Precambrian rocks and were eroded prior to deposition of Paleozoic strata. Although common in Ellesmere Island, they do not appear to favour any particular orientation. Local clusters of preferentially oriented dykes are: northerly dykes south of Smith Bay (Map 1573A); northeasterly dykes on the south coast and in the northern part of the map area; and easterly dykes on the south coast west of Starnes Fiord.

The majority of diabase dykes on Coburg Island trend northerly. A few easterly striking dykes occur in the southern part of the island.

Dykes on Devon Island are preferentially oriented in an easterly direction and form swarms in several areas. Northwest-trending dykes occur in the Cunningham Mountains and elsewhere near the southern coast. These dykes are probably northern extensions of dykes on Bylot Island (Jackson and Davidson, 1975).

The diabase dykes are black to brown weathering, 1-30 m thick, and vertical.

Chill zones and fine grained dykes are porphyritic to glomeroporphyritic, phenocryst phases being plagioclase, clinopyroxene and/or olivine in crystals typically 1 mm long. More coarsely crystallized dykes have subophitic textures and are composed of plagioclase, clinopyroxene, olivine, Fe-Ti oxide, and, less commonly, orthopyroxene. Minor biotite may fringe oxide grains and sulphide is a common accessory. In the more altered dykes, pyroxene has been partly to completely replaced by green hornblende and plagioclase is saussuritized. Olivine is generally at least partly altered and commonly totally replaced by carbonate.

A northeast-trending dyke (unit Hda; FSM-77-11-4) on the western shore of Starnes Fiord (Map 1573A) is unusual in being of apparent alkali basalt affinity, the only such dyke found in the map area. The dyke rock is intergranular gabbro, composed of heavily altered plagioclase laths 2 mm long, euhedral, zoned, pinkish clinopyroxene (2 mm), euhedral, zoned brown hornblende (0.5-1 mm), and subordinate, completely altered olivine(?); Fe-Ti oxide and euhedral apatite (in needles up to 1 mm long) are major accessory minerals. Interstices between many of the plagioclase laths are in part filled by fine grained green biotite, presumably a replacement of iron-rich glass. Both the clinopyroxene and hornblende (kaersutite?) are probably titaniferous and as such characteristic of mafic alkalic rocks.

Chemistry and origin

Eight dykes of basaltic composition from Ellesmere Island have been analyzed (Appendix, Table VIII).

All but one are clearly tholeiitic, having both quartz and hypersthene in the norm. The tholeiitic dykes generally have SiO_2 about 48%, Na_2O between 2 and 2.8% and K_2O between 0.5 and 1.2%, typical values in tholeiitic basalt,

and all seven dykes cluster in the tholeiite field of the alkali-silica diagram (Fig. 87a). Mean TiO_2 at 4 to 5 %, however, is unusually high for basalt in general (Basaltic Volcanism Study Project, 1981). Mean TiO_2, derived from 99 analyses, of Hadrynian diabase dykes of the northern Canadian Shield is 2 % (W.F. Fahrig, pers. comm., 1986). The AFM diagram (Fig. 87b) shows pronounced enrichment of iron, indicating that the dykes crystallized from relatively differentiated basalt magma.

Chemical analysis supports the inference that the Starnes Fiord dyke is alkalic. Weight per cent silica is only 42 and the rock plots as an alkali basalt in the alkali-silica diagram (Fig. 87a) and is classified as such in Irvine and Baragar's (1971) scheme. The small amount of normative hypersthene is attributable to alteration. The analyzed samples has, however, nearly 20 weight per cent normative Fe-Ti oxides and may have been enriched in cumulus crystals and thus not representative of the magma.

Age

Whole-rock K-Ar age determinations have been made on samples of the chilled margins of three diabase dykes from Ellesmere Island and six dykes from Devon Island. The three ages from Ellesmere have been published by Stevens et al. (1982, p. 27).

Results from two dykes in southern Devon Island must be discarded, as the ages obtained are too young: 204 and 97 Ma. Both dykes are overlain by lower Paleozoic deposits. Results on relatively coarsely crystallized rock from the interior of the dykes are 1870 Ma for the "older" dyke and 837 Ma for the "younger". The reason for the anomalously young ages is unknown.

All other ages obtained are at least latest Precambrian, if the age of the Precambrian-Paleozoic boundary recommended by Harland et al. (1982), 590 Ma, is accepted. The oldest date obtained is 1336 ± 15 Ma, from a northerly trending dyke north of the head of Powell Inlet, Devon Island (south coast). Dyke intrusion of this age has not been established in this part of the Canadian Arctic but Christie (1962b) stated that, near Cape Combermere, Ellesmere Island (Map 1573A), Thule Group strata "appear to overlie unconformably some diabase dykes"; this relationship could not be confirmed in the present study. An unmetamorphosed diabase dyke eroded prior to deposition of the Thule Group in the Thule district of western North Greenland has been described and dated at 1563 ± 60 Ma (whole-rock K-Ar) by Dawes et al. (1973). Thus there is both field and radiometric evidence for post-metamorphism, pre-Thule Group dyke intrusion in this area of the High Arctic but further data are required before its significance can be assessed.

The remaining ages from Ellesmere and Devon islands fall in the range 600 to 800 Ma and more closely resemble those of dykes from neighbouring areas of the northern Canadian Shield. Dykes forming large swarms in northern Baffin Island represent at least two major episodes of igneous activity, at 950 Ma (Borden dykes, mostly northwest-trending) and at 750 Ma (Franklin dykes, mostly north-northwest- or north-trending) (Christie and Fahrig, 1983).

A northeast-trending dyke cutting the Thule Group at Goding Bay (Map 1572A) and a west-northwest-trending dyke east of Sverdrup Inlet, northern Devon Island, give ages of 791 ± 60 and 789 ± 10 Ma, respectively. The Goding Bay dyke has very fresh plagioclase but all its pyroxene has been deuterically replaced by green amphibole. Both dykes may have intruded in the Borden episode but subsequently lost argon.

A dyke near, and parallel to, the Goding Bay dyke is petrographically very similar to a north-trending dyke (FS-77-115 in Appendix, Table VIII) cutting basement south of Clarence Head, Ellesmere Island (Map 1573A). (The location of the latter dyke is incorrectly reported in Stevens et al. (1982, p. 27; GSC 81-95) and should read 7.5 km south of Clarence Head, 76° 44′N, 77° 8′W). Both dykes are rich in clinopyroxene and Fe-Ti oxide and yield identical ages, 576 ± 33 and 580 ± 36 Ma. These two dykes may be Franklin intrusions that have suffered significant argon loss.

Two dykes outcropping in northern Devon Island yield ages strongly suggestive of the Franklin event. One, southeast of the head of Truelove Inlet, has phenocrysts of clinopyroxene and altered olivine, trends east, and gives an

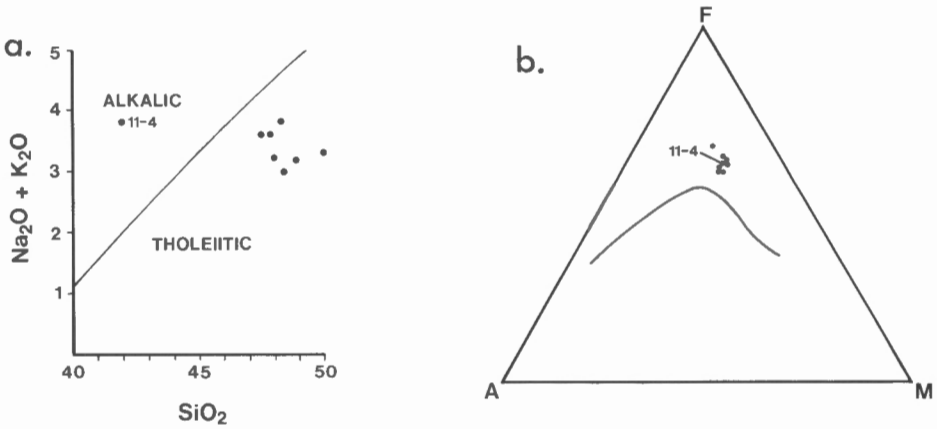

Figure 87. Helikian(?)-Hadrynian diabase dykes. FSM-77-11-4 is the dyke of apparent alkalic affinity from Starnes Fiord.
a) Alkali-silica diagram (after Irvine and Baragar, 1971). Weight per cent.
b) Igneous AFM diagram; dividing line between tholeiitic and calc-alkaline basalts from Irvine and Baragar (1971). Weight per cent.

age of 726 ± 9 Ma. The other, south of Cape Newman Smith, is clinopyroxene- and plagioclase-phyric, strikes west-northwest and yields an age of 625 ± 8 Ma. According to Christie and Fahrig (1983), unaltered, chilled diabase dyke rock generally gives whole-rock K-Ar ages 10-15% less than the age of intrusion, so these dykes may well have been emplaced during the Franklin episode.

Given the diversity and uncertainty of the ages obtained, it is not possible to assign with certainty any of the dykes dated to a particular intrusive episode. We can, however, reasonably conclude that the majority of the diabase dykes intruded during the Hadrynian era.

Phanerozoic rocks (P-C)

Phanerozoic rocks overlying the crystalline basement were examined only cursorily. The bulk of them are Cambrian to Ordovician shelf carbonates of the Arctic Platform (Packard and Mayr, 1982; Thorsteinsson and Mayr, 1987). Judged by the number of outcrops of Paleozoic rocks far to the east of the present margin of the Arctic Platform in Ellesmere Island, the Paleozoic seas must once have covered most, if not all, of the Precambrian Shield.

On eastern Bache Peninsula (Map 1572A), the crystalline basement is overlain by the Neohelikian Rensselaer Bay Formation (*see* above). In the vicinity of Koldewey Point, where the Rensselaer Bay pinches out, the basement is overlain by purple-brown conglomeratic arkose of the Lower Cambrian Dallas Bugt Formation (Peel et al., 1982). The arkose gives way westward to white or buff quartzose sandstone and conglomeratic sandstone (Dallas Bugt Formation), which is seen to rest on the basement in Sverdrup Pass (Peel et al., 1982, Fig. 9), along the western margin of the shield north of Makinson Inlet, and on the south coast of Ellesmere Island west of Starnes Fiord.

At Makinson Inlet and Fram Fiord (Map 1573A), the basal Phanerozoic rocks are varicoloured, chiefly reddish, locally conglomeratic, arkoses, which were assigned to a "pre-Cass Fjord sequence" by Packard and Mayr (1982) and later to the Cambrian Cape Wood Formation by Mayr and Okulitch (1984). It is likely that these rocks are, in fact, also referable to the Dallas Bugt Formation.

The Phanerozoic rocks of Devon Island are described by Thorsteinsson and Mayr (1987). Reddish arkose has not been seen at the base of the Paleozoic succession on the crystalline basement of Devon Island. The oldest Paleozoic formations are the Lower Cambrian Rabbit Point, a thin unit of pale quartzose sandstone, and the unconformably overlying Middle Cambrian Bear Point, which consists principally of limy rocks and dolomite. In some places, the entire Rabbit Point Formation has been eroded and Bear Point rocks rest directly on basement.

Much of western Philpots Island, at the east end of Devon Island, is covered by a thin veneer of dolomitic rubble, probably derived from a Cambrian formation such as the Cass Fjord, lying on poorly exposed crystalline basement (Frisch, 1981).

In Ellesmere Island, Phanerozoic strata at the edge of the Precambrian Shield include, besides the predominant lower Paleozoic rocks, Tertiary sediments. These outcrop north and south of the head of Makinson Inlet and comprise chiefly sandstone, siltstone and coal of the Paleocene Eureka Sound Formation and conglomerate, sandstone and siltstone of the Miocene Beaufort Formation (Riediger et al., 1984). Tertiary rocks have not been found resting directly on Precambrian basement.

ECONOMIC GEOLOGY

Metallic mineral showings in the form of rusty zones, gossans and even massive sulphide lenses are found throughout the Ellesmere-Devon terrane and are particularly common in metasediments on Ellesmere Island. Reports of occurrences such as those in the area of Alexandra Fiord (Map 1572A) by Geological Survey of Canada geologists (Christie, 1962a; Frisch, 1983) prompted prospecting by Petro-Canada Ltd. in 1982 and 1983. Much of the following is taken from a summary of the results of this work by Gibbins (1985).

Petro-Canada's 1982 work turned up 181 mineral occurrences in the Precambrian Shield of Ellesmere Island between Bache Peninsula and Makinson Inlet. Locations of the more important occurrences are plotted in Figure 4-6 of Gibbins (1985). A further 18 occurrences were found in Ellesmere and Devon islands in 1983. The great majority of all these are Cu-Fe sulphide bodies, which are interpreted to be sulphide facies iron-formation. The bodies consist of pods, lenses and layers of semi-massive to massive, coarsely crystalline pyrrhotite (30 to 90%), subordinate pyrite and a little chalcopyrite, lying within metasedimentary gneisses. The largest massive pyrrhotite layer found by Petro-Canada geologists occurs a few kilometres east of the Alexandra Fiord RCMP post and can be traced in outcrop for about 5 km as a discontinuous line of sulphide pods and lenses up to 2 m thick and 15 m long.

Gossans are developed over graphitic metasedimentary gneisses containing disseminated (5 to 20%) pyrrhotite. Such showings are common and may be extensive. At the tip of Thorvald Peninsula, Alexandra Fiord, gossans are up to 8 m wide and 100 m long and contain, in addition to the predominant pyrrhotite, chalcopyrite and subordinate sphalerite.

Some sulphide-rich bodies occur in quartzofeldspathic gneisses but the predominant host is pelitic to semi-pelitic gneiss, commonly rich in biotite, garnet, cordierite and graphite.

Wilson (1974) has pointed out that stratabound sulphides of copper and zinc are common in granulite terranes and has emphasized the beneficial effect of high grade metamorphism in concentrating and recrystallizing originally finely disseminated sulphides. The outstanding example of sulphide mineralization in a high grade metamorphic terrane is the Broken Hill district of southeastern Australia, where lead- zinc-silver ore bodies occur in bimodal felsic-mafic volcanics and pelitic turbidites metamorphosed in the low

pressure, high temperature granulite facies (Willis et al., 1983). The host rock to ore bodies at Broken Hill studied by Plimer (1977) is sillimanite-garnet-biotite gneiss. The considerable similarity with the Broken Hill district in lithology and grade of metamorphism suggests major potential for base metal resources in the Precambrian Shield of Ellesmere Island. However, extensive assay and follow-up work by Petro-Canada on the more promising showings (e.g. one containing 13 % Cu, 0.5 % Ni, 0.225 % Co, 8.23 g/tonne Au, and 8.57 g/tonne Ag at Sands Glacier, at the mouth of Jokel Fiord (Map 1572A)) failed to identify any deposit of commercial significance.

Many fracture and weathering surfaces of gneisses rich in granitic veins and segregations are stained by malachite, which is commonly an alteration of sparsely disseminated chalcopyrite. Copper stain has also been found in the lower part of the Thule Group, where it is probably related to the basalts.

Separate, small showings of arsenopyrite, scheelite and barite were found associated with calcareous rocks by Petro-Canada geologists. Molybdenite in granite veins cutting metasedimentary gneiss at the southern margin of Ekblaw Glacier (Map 1572A) was found during the 1977 work. None of these occurrences is considered to be of economic value.

In general, metallic mineral showings appear to be most abundant in metasedimentary rocks in the northern part of the map area. Compared to Ellesmere Island, Devon seems barren. However, the existence of interstitial, primary scapolite in quartzofeldspathic gneisses in Devon Island indicates that sulphur-bearing fluids (or vapours) circulated during high grade metamorphism.

The harsh climate and extreme remoteness of the map area severely limit prospects for mineral exploration and development. Any future work undertaken clearly should focus on the stratabound copper sulphide mineralization in the metasediments. Another exploration target might be gemstones such as garnet, cordierite, corundum (sapphire and ruby), spinel and sapphirine, all minerals that crystallize particularly readily in granulite grade metamorphism of aluminous metasediments (Wilson, 1974). A third target might be the S-type anatectic biotite granites. Epizonal and mesozonal S-type granites are well known hosts to tin and tungsten deposits (Pitcher, 1982). The Ellesmere Island granites, however, may be of too deep-seated an origin for typical vein- and greisen-type mineralization to have developed.

REFERENCES

(includes references cited in Appendix)

Abbey, S.
1979: "Rock analysis" methods at the Geological Survey of Canada; Geostandards Newsletter, v. 3, p. 97-101.

Ackermand, D., Herd, R.K., and Windley, B.F.
1982: Chemographic relationships in sapphirine-bearing rocks of the Limpopo belt, southern Africa; Revista Brasileira de Geociencias, v. 12, p. 292-300.

Allen, P., Condie, K.C., and Narayana, B.L.
1985: The geochemistry of prograde and retrograde charnockite-gneiss reactions in southern India; Geochimica et Cosmochimica Acta, v. 49, p. 323-336.

Aranovich, L.Ya. and Podlesskii, K.K.
1983: The cordierite-garnet-sillimanite-quartz equilibrium: experiments and applications; *in* Kinetics and Equilibrium in Mineral Reactions, ed. S.K. Saxena; Springer-Verlag, New York, p. 173-198.

Armbruster, T. and Bloss, F.D.
1982: Orientation and effects of channel H_2O and CO_2 in cordierite; American Mineralogist, v. 67, p. 284-291.

Barbey, P. and Cuney, M.
1982: K, Rb, Sr, Ba, U and Th geochemistry of the Lapland granulites (Fennoscandia). LILE fractionation controlling factors; Contributions to Mineralogy and Petrology, v. 81, p. 304-316.

Barbey, P., Capdevila, R., and Hameurt, J.
1982: Major and transition trace element abundances in the khondalite suite of the granulite belt of Lapland (Fennoscandia): evidence for an early Proterozoic flysch belt; Precambrian Research, v. 16, p. 273-290.

Barbey, P., Convert, J., Moreau, B., Capdevila, R., and Hameurt, J.
1984: Petrogenesis and evolution of an early Proterozoic collisional orogenic belt: the granulite belt of Lapland and the Belomorides (Fennoscandia); Geological Society of Finland, Bulletin, v. 56, p. 161-188.

Barker, F.
1979: Trondhjemite: definition, environment and hypotheses of origin; *in* Trondhjemites, Dacites, and Related Rocks, ed. F. Barker; Elsevier, Amsterdam, p. 1-12.

Barker, F. and Arth, J.G.
1976: Generation of trondhjemitic-tonalitic liquids and Archean bimodal trondhjemite-basalt suites; Geology, v. 4, p. 596-600.

Barker, F., Arth, J.G., and Hudson, T.
1981: Tonalites in crustal evolution; Royal Society of London, Philosophical Transactions, Series A, v. 301, p. 293-303.

Barnicoat, A.C.
1983: Metamorphism of the Scourian Complex, NW Scotland; Journal of Metamorphic Geology, v. 1, p. 163-182.

Basaltic Volcanism Study Project
1981: Basaltic Volcanism on the Terrestrial Planets; Pergamon Press, New York, 1286 p.

Berg, J.H.
1977: Regional geobarometry in the contact aureoles of the anorthositic Nain complex, Labrador; Journal of Petrology, v. 18, p. 399-430.

Bernard-Griffiths, J., Peucat, J.J., Postaire, B., Vidal, Ph., Convert, J., and Moreau, B.
1984: Isotopic data (U-Pb, Rb-Sr, Pb-Pb and Sm-Nd) on mafic granulites from Finnish Lapland; Precambrian Research, v. 23, p. 325-348.

Berthelsen, A.
1960: Structural studies in the pre-Cambrian of western Greenland. Part II: Geology of Tovqussap nunâ; Meddelelser om Grønland, Bd. 123, Nr. 1, 223 p.

Bertrand, P. and Mercier, J.C.C.
1985/ The mutual solubility of coexisting ortho- and clinopyroxene:
1986: toward an absolute geothermometer for the natural system?; Earth and Planetary Science Letters, v. 76, p. 109-122.

Bhatia, M.R.
1983: Plate tectonics and geochemical composition of sandstones; Journal of Geology, v. 91, p. 611-627.

Binns, R.A.
1969: Ferromagnesian minerals in high-grade metamorphic rocks; Geological Society of Australia, Special Publication, no. 2, p. 323-332.

Blackburn, W.H.
1974: Origin of the cordierite-bearing gneisses of the Gananoque-Westport area, Ontario; Annales de la Société Géologique de Belgique, v. 97, p. 297-309.

Blake, W., Jr.
1978: Rock weathering forms above Cory Glacier, Ellesmere Island, District of Franklin; *in* Current Research, Part B, Geological Survey of Canada, Paper 78-1B, p. 207-211.

Bohlen, S.R., Wall, V.J., and Boettcher, A.L.
1983: Geobarometry in granulites; *in* Kinetics and Equilibrium in Mineral Reactions, ed. S.K. Saxena; Springer-Verlag, New York, p. 141-171.

Bostock, H.S.
1970: Physiographic subdivisions of Canada; *in* Geology and Economic Minerals of Canada, ed. R.J.W. Douglas; Geological Survey of Canada, Economic Geology Report No. 1, p. 10-30.

Bourne, J.H.
1974: The petrogenesis of the humite group minerals in regionally metamorphosed marbles of the Grenville Supergroup; unpublished Ph.D. thesis, Queen's University at Kingston, Kingston, Ontario, 159 p.

Brown, M. and Earle, M.M
1983: Cordierite-bearing schists and gneisses from Timor, eastern Indonesia: P-T conditions of metamorphism and tectonic implications; Journal of Metamorphic Geology, v. 1, p. 183-203.

Bugge, C.
1910: Petrographische Resultate der 2ten Fram-Expedition; Report of the Second Norwegian Arctic Expedition in "Fram" 1898-1902, no. 22, Videnskabs-Selskabet, Kristiania, 38 p.

Burri, C., Parker, R.L., and Wenk, E.
1967: Die Optische Orientierung der Plagioklase; Birkhäuser Verlag, Basel, 334 p.

Cameron, E.M. and Garrels, R.M.
1980: Geochemical compositions of some Precambrian shales from the Canadian Shield; Chemical Geology, v. 28, p. 181-197.

Carmichael, I.S.E., Turner, F.J., and Verhoogen, J.
1974: Igneous Petrology; McGraw-Hill, New York, 739 p.

Chadwick, B. and Coe, K.
1983: Descriptive text to 1: 100 000 sheet Buksefjorden 63 V. 1 Nord; Grønlands Geologiske Undersøgelse, 70 p.

Christie, K.W. and Fahrig, W.F.
1983: Paleomagnetism of the Borden dykes of Baffin Island and its bearing on the Grenville Loop; Canadian Journal of Earth Sciences, v. 20, p. 275-289.

Christie, R.L.
1962a: Geology, Alexandra Fiord, Ellesmere Island, District of Franklin (map with marginal notes); Geological Survey of Canada, Map 9-1962.
1962b: Geology, southeast Ellesmere Island, District of Franklin (map with marginal notes); Geological Survey of Canada, Map 12-1962.
1967: Bache Peninsula, Ellesmere Island, Arctic Archipelago; Geological Survey of Canada, Memoir 347, 63 p.
1978: A structural reconnaissance of eastern Devon Island: Geological Survey of Canada, Open File 537.

Clemens, J.D.
1984: Water contents of silicic to intermediate magmas; Lithos, v. 17, p. 273-287.

Clemens, J.D. and Wall, V.J.
1981: Origin and crystallization of some peraluminous (S-type) granitic magmas; Canadian mineralogist, v. 19, p. 111-131.

Clough, P.W.L. and Field, D.
1980: Chemical variation in metabasites from a Proterozoic amphibolite-granulite transition zone, south Norway; Contributions to Mineralogy and Petrology, v. 73, p. 277-286.

Collerson, K.D.
1974: Descriptive microstructural terminology for high-grade metamorphic tectonites; Geological Magazine, v. 111, p. 313-318.

Condie, K.C.
1967: Geochemistry of early Precambrian greywackes from Wyoming; Geochimica et Cosmochimica Acta, v. 31, p. 2135-2149.

Coolen, J.J.M.M.M.
1980: Chemical petrology of the Furua Granulite Complex, southern Tanzania; GUA Papers of Geology, Series 1, no. 13-1980, 258 p.

Courtin, G.M. and Labine, C.L.
1977: Microclimatological studies on Truelove Lowland; *in* Truelove Lowland, Devon Island: a High Arctic Ecosystem, ed. L.C. Bliss; University of Alberta Press, Edmonton, p. 73-106.

Dawes, P.R.
1976: Precambrian to Tertiary of nothern Greenland; *in* Geology of Greenland, ed. A. Escher and W.S. Watt; Grønlands Geologiske Undersøgelse, Copenhagen, p. 248-303.

Dawes, P.R. and Christie, R.L.
1982: History of exploration and geology in the Nares Strait region: *in* Nares Strait and the Drift of Greenland: a Conflict in Plate Tectonics, ed. P.R. Dawes and J.W. Kerr; Meddelelser om Grønland, Geoscience 8, p. 19-36

Dawes, P.R., Frisch, T., and Christie, R.L.
1982: The Proterozoic Thule Basin of Greeland and Ellesmere Island: importance to the Nares Strait debate; *in* Nares Strait and the Drift of Greeland: a Conflict in Plate Tectonics, ed. P.R. Dawes and J.W. Kerr; Meddelelser om Grønland, Geoscience 8, p. 89-104.

Dawes, P.R., Rex, D.C., and Jepsen, H.F.
1973: K/Ar whole rock ages of dolerites from the Thule district, western North Greenland; Grønlands Geologiske Undersøgelse, Rapport 55, p. 61-66.

Debon, F. and Le Fort, P.
1983: A chemical-mineralogical classification of common plutonic rocks and associations; Royal Society of Edinburgh, Transactions: Earth Sciences, v. 73, p. 135-149.

Deer, W.A., Howie, R.A., and Zussman, J.
1978: Rock-Forming Minerals, volume 2A, 2nd edition: Single-Chain Silicates; Longman, London, 668 p.

Dostal, J.
1975: The origin of garnet-cordierite-sillimanite bearing rocks from Chandos Township, Ontario; Contributions to Mineralogy and Petrology, v. 49, p. 163-175.

Droop, G.T.R. and Bucher-Nurminen, K.
1984: Reaction textures and metamorphic evolution of sapphirine-bearing granulites from the Gruf Complex, Italian Central Alps; Journal of Petrology, v. 25, p. 766-803.

Ellis, D.J. and Green, D.H.
1979: An experimental study of the effect of Ca upon garnet-clinopyroxene Fe-Mg exchange equilibria; Contributions to Mineralogy and Petrology, v. 71, p. 13-22.

Ellis, D.J., Sheraton, J.W., England, R.N., and Dallwitz, W.B.
1980: Osumilite-sapphirine-quartz granulites from Enderby Land Antarctica - mineral assemblages and reactions; Contributions to Mineralogy and Petrology; v. 72, p. 123-143.

Eskola, P.
1952: On the granulites of Lapland; American Journal of Science, Bowen Volume, p. 133-171.

Ewart, A.
1979: A review of the mineralogy and chemistry of Tertiary-Recent dacitic, latitic, rhyolitic, and related salic volcanic rocks; *in* Trondhjemites, Dacites, and Related rocks, ed. F. Barker; Elsevier, New York, p. 13-121.

Floyd, P.A. and Winchester, J.A.
1975: Magma type and tectonic setting discrimination using immobile elements; Earth and Planetary Science Letters, v. 27, p. 211-218.

Frisch, T.
1981: Further reconnaissance mapping of the Precambrian Shield on Devon Island, District of Franklin; *in* Current Research, Part A, Geological Survey of Canada, Paper 81-1A, p. 31-32.
1983: Reconnaissance geology of the Precambrian Shield of Ellesmere, Devon and Coburg islands, Arctic Archipelago: a preliminary account; Geological Survey of Canada, Paper 82-10, 11 p.

Frisch, T. and Christie, R.L.
1982: Stratigraphy of the Proterozoic Thule Group, southeastern Ellesmere Island, Arctic Archipelago; Geological Survey of Canada, Paper 81-19, 13 p.

Frisch, T. and Dawes, P.R.
1982: The Precambrian Shield of northernmost Baffin Bay: correlation across Nares Strait; *in* Nares Strait and the Drift of Greenland: a Conflict in Plate Tectonics, ed. P.R. Dawes and J.W. Kerr; Meddelelser om Grønland, Geoscience 8, p. 79-88.

Ganguly, J. and Saxena, S.K.
1984: Mixing properties of aluminosilicate garnet: constraints from natural and experimental data, and applications to geothermobarometry; American Mineralogist, v. 69, p. 88-97.

Garde, A.A., Glassley, W.E., and Nutman, A.P.
1984: Two-stage corona growth during Precambrian granulite facies metamorphism of Smithson Bjerge, north-west Greenland; Journal of Metamorphic Geology, v. 2, p. 237-247.

Gebauer, D. and Grünenfelder, M.
1979: U-Th-Pb dating of minerals; *in* Lectures in Isotope Geology, ed. E. Jäger and J.C. Hunziker; Springer-Verlag, Berlin, p. 105-131.

Gibbins, W.A.
1985: Arctic Islands Region; *in* Mineral Industry Report 1982-83, Northwest Territories, ed. J.A. Brophy; Department of Indian Affairs and Northern Development, Ottawa, p. 95-155.

Gill, R.C.O.
1979: Comparative petrogenesis of Archaean and modern low-K tholeiites. A critical review of some geochemical aspects; *in* Origin and Distribution of the Elements, ed. L.H. Ahrens; Pergamon Press, Oxford, p. 431-447.

Gill, R.C.O. and Bridgwater, D.
1979: Early Archaean basic magmatism in West Greenland: the geochemistry of the Ameralik dykes; Journal of Petrology, v. 20, p. 695-726.

Glikson, A.Y.
1979: Early Precambrian tonalite-trondhjemite sialic nuclei; Earth Science-Reviews, v. 15, p. 1-73.

Grant, J.A.
1985: Phase equilibria in partial melting of pelitic rocks; *in* Migmatites, ed. J.R. Ashworth; Blackie and Son, Glasgow, p. 86-144.

Gray, C.M.
1977: The geochemistry of central Australian granulites in relation to the chemical and isotopic effects of granulite facies metamorphism; Contributions to Mineralogy and Petrology, v. 65, p. 79-89.

Guidotti, C.V.
1984: Micas in metamorphic rocks; *in* Micas, ed. S.W. Bailey; Mineralogical Society of America, Reviews in Mineralogy, v. 13, p. 357-467.

Hanson, G.N.
1978: The application of trace elements to the petrogenesis of igneous rocks of granitic composition; Earth and Planetary Science Letters, v. 38, p. 26-43.

Hapuarachchi, D.J.A.C.
1968: Cordierite and wollastonite-bearing rocks of south-western Ceylon; Geological Magazine, v. 105, p. 317-412.

Harland, W.B., Cox, A.V., Llewellyn, P.G., Pickton, C.A.G., Smith, A.G., and Walters, R.
1982: A geologic time scale; Cambridge University Press, Cambridge, 131 p.

Harley, S.L.
1984a: The solubility of alumina in orthopyroxene coexisting with garnet in $FeO-MgO-Al_2O_3-SiO_2$ and $CaO-FeO-MgO-Al_2O_3-SiO_2$; Journal of Petrology, v. 25, p. 665-696.
1984b: An experimental study of the partitioning of Fe and Mg between garnet and orthopyroxene; Contributions to Mineralogy and Petrology, v. 86, p. 359-373.

Harley, S.L. and Green, D.H.
1982: Garnet-orthopyroxene barometry of granulites and peridotites; Nature, v. 300, p. 697-701.

Harris, N.B.W.
1976: The significance of garnet and cordierite from the Sioux Lookout region of the English River gneiss belt, northern Ontario; Contributions to Mineralogy and Petrology, v. 55, p. 91-104.

Harris, N.B.W. and Holland, T.J.B.
1984: The significance of cordierite-hypersthene assemblages from the Beitbridge region of the Central Limpopo Belt; evidence for rapid decompression in the Archean?; American Mineralogist, v. 69, p. 1036-1049.

Hay, P.W.
1965: The stability and occurrence of cordierite in selected gneisses from the Canadian Shield; unpublished Ph.D. thesis, Stanford University, 118 p.

Hensen, B.J. and Green, D.H.
1973: Experimental study of the stability of cordierite and garnet in pelitic compositions at high pressures and temperatures. III. Synthesis of experimental data and geological applications; Contributions to Mineralogy and Petrology, v. 38, p. 151-166.

Hermans, G.A.E.M., Hakstege, A.L., Hansen, J.B.H., and Poorter, R.P.E.
1976: Sapphirine occurrence near Vikesa in Rogaland, southwestern Norway; Norsk Geologisk Tidsskrift, v. 56, p. 397-412.

Hietanen, A.
1947: Archean geology of the Turku district in southwestern Finland; Geological Society of America, Bulletin, v. 58, p. 1019-1084.

Higgins, J.B., Ribbe, P.H., and Herd, R.K.
1979: Sapphirine I. Crystal chemical contributions; Contributions to Mineralogy and Petrology, v. 68, p. 349-356.

Hirst, D.M. and Kaye, M.J.
1971: Factors controlling the mineralogy and chemistry of an Upper Visean sedimentary sequence from Rookhope, County Durham; Chemical Geology, v. 8, p. 37-59.

Holdaway, M.J.
1971: Stability of andalusite and the aluminum silicate phase diagram; American Journal of Science, v. 271, p. 97-131.

Hollister, L.S.
1982: Metamorphic evidence for rapid (2 mm/yr) uplift of a portion of the Central Gneiss Complex, Coast Mountains, B.C.; Canadian Mineralogist, v. 20, p. 319-332.

Hutcheon, I., Froese, E., and Gordon, T.M.
1974: The assemblage quartz-sillimanite-garnet-cordierite as an indicator of metamorphic conditions in the Daly Bay Complex, N.W.T.; Contributions to Mineralogy and Petrology, v. 44, p. 29-34.

Indares, A. and Martignole, J.
1985: Biotite-garnet geothermometry in granulite-facies rocks: evaluation of equilibrium criteria; Canadian Mineralogist, v. 23, p. 187-193.

Irvine, T.N. and Baragar, W.R.A.
1971: A guide to the chemical classification of the common volcanic rocks; Canadian Journal of Earth Sciences, v. 8, p. 523-548.

Jackson, G.D.
1986: Notes on the Proterozoic Thule Group, northern Baffin Bay; *in* Current Research, Part A, Geological Survey of Canada, Paper 86-1A, p. 541-552.

Jackson, G.D. and Davidson, A.
1975: Geology of the Bylot Island map-area; Geological Survey of Canada, Paper 74-29, 12 p.

Jackson, G.D. and Iannelli, T.R.
1981: Rift-related cyclic sedimentation in the Neohelikian Borden Basin, northern Baffin Island; *in* Proterozoic Basins of Canada, ed. F.H.A. Campbell; Geological Survey of Canada, Paper 81-10, p. 269-302.

Jackson, G.D. and Morgan, W.C.
1978: Precambrian metamorphism on Baffin and Bylot islands; *in* Metamorphism in the Canadian Shield, ed. J.A. Fraser and W.W. Heywood; Geological Survey of Canada, Paper 78-10, p. 249-267.

Jahn, B.M. and Zhang, Z.Q.
1984: Archean granulite gneisses from eastern Hebei Province, China: rare earth geochemistry and tectonic implications; Contributions to Mineralogy and Petrology, v. 85, p. 224-243.

Jan, M.Q. and Howie, R.A.
1982: Hornblendic amphiboles from basic and intermediate rocks of Swat-Kohistan, northwest Pakistan; American Mineralogist, v. 68, p. 1155-1178.

Kalsbeek, F. and Leake, B.E.
1970: The chemistry and origin of some basement amphibolites between Ivigtut and Frederikshab, South-West Greenland; Grønlands Geologiske Undersøgelse, Bulletin 90, 36 p.

Kerr, J.Wm.
1980: Structural framework of Lancaster Aulacogen, Arctic Canada; Geological Survey of Canada, Bulletin 319, 24 p.

Kretz, R.
1982: Transfer and exchange equilibria in a portion of the pyroxene quadrilateral as deduced from natural and experimental data; Geochimica et Cosmochimica Acta, v. 46, p. 411-421.

Kröner, A.
1985: Evolution of the Archean continental crust; Annual Review of Earth and Planetary Sciences, v. 13, p. 49-74.
1986: Composition, structure and evolution of the early Precambrian lower continental crust: constraints from geological observations and age relationships; *in* Reflection Seismology: the Continental Crust, ed. M. Barazangi and L. Brown; American Geophysical Union, Geodynamics Series, v. 14, p. 107-119.

Krupička, J.
1973: Granulite facies rocks on northeastern Devon Island, Arctic Archipelago; Geological Survey of Canada, Paper 73-8, 41 p.

Lambert, R.St.J. and Holland, J.G.
1976: Amitsoq gneiss geochemistry: preliminary observations; *in* The Early History of the Earth, ed. B.F. Windley; J. Wiley and Sons, London, p. 191-210.

Langenberg, C.W. and Nielsen, P.A.
1982: Polyphase metamorphism in the Canadian Shield of northeastern Alberta; Alberta Research Council, Bulletin 42, 80 p.

La Roche, H. de
1965: Sur l'existence de plusieurs facies géochimiques dans les schistes paléozoiques des Pyrénées luchonnaises; Geologische Rundschau, v. 55, p. 274-301.

Larsen, E.S., Jr.
1948: Batholith and associated rocks of Corona, Elsinore, and San Luis Rey quadrangles, Southern California; Geological Society of America, Memoir 29, 182 p.

Larsen, O. and Dawes, P.R.
1974: K/Ar and Rb/Sr age determinations on Precambrian crystalline rocks in the Inglefield Land-Inglefield Bredning region, Thule district, western North Greenland; Grønlands Geologiske Undersøgelse, Rapport 66, p. 5-8.

Leake, B.E.
1964: The chemical distinction between ortho- and para-amphibolites; Journal of Petrology, v. 5, p. 238-254.

Lee, S.M. and Holdaway, M.J.
1977: Significance of Fe-Mg cordierite stability relations on temperature, pressure, and water pressure in cordierite granulites; American Geophysical Union, Geophysical Monograph 20, 79-94.

Leelanandam, C.
1970: Chemical mineralogy of hornblendes and biotites from the charnockitic rocks of Kondapalli, India; Journal of Petrology, v. 11, p. 475-505.

Le Maitre, R.W.
1976: The chemical variability of some common igneous rocks; Journal of Petrology, v. 17, p. 589-637.

Leonardos, O.H., Jr. and Fyfe, W.S.
1974: Ultrametamorphism and melting of a continental margin: the Rio de Janeiro region, Brazil; Contributions to Mineralogy and Petrology, v. 46, p. 201-214.

Lindsley, D.H.
1983: Pyroxene thermometry; American Mineralogist, v. 68, p. 477-493.

Lonker, S.W.
1980: Conditions of metamorphism in high-grade pelitic gneisses from the Frontenac Axis, Ontario, Canada; Canadian Journal of Earth Sciences, v. 17, p. 1666-1684.
1981: The P-T-X relations of the cordierite-garnet-sillimanite-quartz equilibrium; American Journal of Science, v. 281, p. 1056-1090.

Low, A.P.
1906: Report on the Dominion Government Expedition to Hudson Bay and the Arctic Islands on board the D.G.S. Neptune 1903-1904; Government Printing Bureau, Ottawa, 355 p.

Maccarrone, E., Paglionico, A., Piccarreta, G., and Rottura, A.
1983: Granulite-amphibolite facies metasediments from the Serre (Calabria, Southern Italy): their protoliths and the processes controlling their chemistry; Lithos, v. 16, p. 95-111.

Martignole, J. and Sisi, J.C.
1981: Cordierite-garnet-H_2O equilibrium: a geological thermometer, barometer and water fugacity indicator; Contributions to Mineralogy and Petrology, v. 77, p. 38-46.

Mayr, U. and Okulitch, A.V.
1984: Geological maps (1:125 000 scale) of North Kent Island and southern Ellesmere Island, N.W.T.; Geological Survey of Canada, Open File 1036.

McCarthy, T.S.
1976: Chemical interrelationships in a low-pressure granulite terrain in Namaqualand, South Africa, and their bearing on granite genesis and the composition of the lower crust; Geochimica et Cosmochimica Acta, v. 40, p. 1057-1068.

McGregor, V.R.
1979: Archean gray gneisses and the origin of the continental crust: evidence from the Godthåb region, West Greenland; *in* Trondhjemites, Dacites, and Related Rocks, ed. F. Barker; Elsevier, Amsterdam, p. 169-204.

Mehnert, K.R.
1968: Migmatites and the Origin of Granitic Rocks; Elsevier, Amsterdam, 393 p.

Mengel, F.C.
1983a: Petrography and geochemistry of amphibolites from the Nordre Strømfjord area in the central part of the Nagssugtoqidian of West Greenland; Grønlands Geologiske Undersøgelse, Rapport 113, 20 p.
1983b: Chemistry of coexisting mafic minerals in granulite facies amphibolites from West Greenland: clues to conditions of metamorphism; Neues Jahrbuch für Mineralogie Abhandlungen, v. 147, p. 315-340.

Miyashiro, A.
1973: Metamorphism and Metamorphic Belts; Halsted Press, New York, 492 p.
1975: Classification, characteristics, and origin of ophiolites; Journal of Geology, v. 83, p. 249-281.

Moore, J.M.
1983: Geochemical and genetic aspects of cordierite gneisses from south/central Namaqualand; Annual Report of the Precambrian Research Unit, University of Cape Town, 18-20, p. 116-131.

Mora, C.I. and Valley, J.W.
1985: Ternary feldspar thermometry in granulites from the Oaxacan Complex, Mexico; Contributions to Mineralogy and Petrology, v. 89, p. 215-225.

Morse, S.A.
1969: Feldspars; Carnegie Institution of Washington, Year Book 67, p. 120-126.

Mukherjee, A. and Rege, S.M.
1972: Stability of wollastonite in the granulite facies: some evidences from the Eastern Ghats, India; Neues Jahrbuch für Mineralogie Abhandlungen, v. 118, p. 23-42.

Mullen, E.D.
1983: $MnO/TiO_2/P_2O_5$: a minor element discriminant for basaltic rocks of oceanic environments and its implications for petrogenesis; Earth and Planetary Science Letters, v. 62, p. 53-62.

Müller, H.
1977: Ueber Pflanzen und Klima auf Coburg Island, N.W.T., Kanada; Geographica Helvetica, v. 32, p. 213-218.

Munasinghe, T. and Dissanayake, C.B.
1980: Are charnockites metamorphosed Archean volcanic rocks? - A case study from Sri Lanka; Precambrian Research, v. 12, p. 459-470.

Naney, M.T.
1983: Phase equilibria of rock-forming ferromagnesian silicates in granitic systems; American Journal of Science, v. 283, p. 993-1033.

Newton, R.C.
1978: Experimental and thermodynamic evidence for the operation of high pressures in Archean metamorphism; *in* Archaean Geochemistry, ed. B.F. Windley and S.M. Naqvi; Elsevier, Amsterdan, p. 221-240.

Newton, R.C.
1983: Geobarometry of high-grade metamorphic rocks; American Journal of Science, v. 283-A, p. 1-28.
1985: Temperature, pressure and metamorphic fluid regimes in the amphibolite facies to granulite facies transition zones; *in* The Deep Proterozoic Crust in the North Atlantic Provinces, ed. A.C. Tobi and J.L.R. Touret; D. Reidel, Dordrecht, p. 75-104.

Newton, R.C. and Hansen, E.C.
1983: The origin of Proterozoic and late Archean charnockites - evidence from field relations and experimental petrology; Geological Society of America, Memoir 161, p. 167-178.

Newton, R.C. and Haselton, H.T.
1981: Thermodynamics of the garnet-plagioclase-Al_2SiO_5-quartz geobarometer; *in* Thermodynamics of Minerals and Melts, ed. R.C. Newton, A. Navrotsky and B.J. Wood; Springer-Verlag, New York, p. 131-147.

Newton, R.C. and Perkins, D., III
1982: Thermodynamic calibration of geobarometers based on the assemblages garnet-plagioclase-orthopyroxene (clinopyroxene)-quartz; American Mineralogist, v. 67, p. 203-222.

Newton, R.C. and Wood, B.J.
1979: Thermodynamics of water in cordierite and some petrologic consequences of cordierite as a hydrous phase; Contributions to Mineralogy and Petrology, v. 68, p. 391-405.

Nutman, A.P.
1984: Precambrian gneisses and intrusive anorthosite of Smithson Bjerge, Thule district, North-West Greenland; Grønlands Geologiske Undersøgelse, Rapport 119, 31 p.

O'Connor, J.T.
1965: A classification for quartz-rich igneous rocks based on feldspar ratios; United States Geological Survey, Professional Paper 525-B, p. 79-84.

O'Hara, M.J. and Yarwood, G.
1978: High pressure-temperature point on an Archaean geotherm, implied magma genesis by crustal anatexis, and consequences for garnet-pyroxene thermometry and barometry; Royal Society of London, Philosophical Transactions, Series A, v. 288, p. 441-456.

Packard, J. and Mayr, U.
1982: Cambrian to Ordovician stratigraphy of southern Ellesmere Island, District of Franklin; *in* Current Research, Part A; Geological Survey of Canada, Paper 82-1A, p. 67-74.

Pearce, J.A.
1975: Basalt geochemistry used to investigate past tectonic environments on Cyprus; Tectonophysics, v. 25, . 41-67.
1982: Trace element characteristics of lavas from destructive plate boundaries; *in* Andesites: Orogenic Andesites and Related Rocks; J. Wiley and Sons, Chichester, p. 525-548.

Pearce, J.A. and Norry, M.J.
1979: Petrogenetic implications of Ti, Zr, Y, and Nb variations in volcanic rocks; Contributions to Mineralogy and Petrology, v. 69, p. 33-47.

Peel, J.S., Dawes, P.R., Collinson, J.D., and Christie, R.L.
1982: Proterozoic-basal Cambrian stratigraphy across Nares Strait: correlation between Inglefield Land and Bache Peninsula; *in* Nares Strait and the Drift of Greenland: a Conflict in Plate Tectonics, ed. P.R. Dawes and J.W. Kerr; Meddelelser om Grønland, Geoscience 8, p. 105-115.

Perchuk, L.L. and Lavrent'eva, I.V.
1983: Experimental investigation of exchange equilibria in the system cordierite-garnet-biotite; *in* Kinetics and Equilibrium in Mineral Reactions, ed. S.K. Saxena; Springer-Verlag, New York, p. p. 199-239.

Perkins, D., III and Chipera, S.J.
1985: Garnet-orthopyroxene-plagioclase-quartz barometry: refinement and application to the English River subprovince and the Minnesota River valley; Contributions of Mineralogy and Petrology, v. 89, p. 69-80.

Pidgeon, R.T. and Howie, R.A.
1975: U-Pb age of zircon from a charnockitic granulite from Pangnirtung on the east coast of Baffin Island; Canadian Journal of Earth Sciences, v. 12, p. 1046-1047.

Pitcher, W.S.
1978: The anatomy of a batholith; Geological Society of London, Journal, v. 135, p. 157-182.
1982: Granite type and tectonic environment; *in* Mountain Building Processes, ed. K.J. Hsü; Academic Press, London, p. 19-40.

Plimer, I.R.
1977: The mineralogy of the high grade metamorphic rocks enclosing the Broken Hill orebodies, Australia; Neues Jahrbuch für Mineralogie Abhandlungen, v. 131, p. 115-139.

Powell, R.
1978: The thermodynamics of pyroxene geotherms; Royal Society of London, Philosophical Transactions, Series A, v. 288, p. 457-469.

Raith, M.
1984: High grade metamorphism in the granulite complex of Finnish Lapland; Geological Society of London, Newsletter, v. 13, no. 5, p. 16-17.

Raith, M., Raase, P., Ackermand, D., and Lal, R.K.
1983: Regional geothermobarometry in the granulite facies terrane of South India; Royal Society of Edinburgh, Transactions: Earth Sciences, v. 73, p. 221-244.

Riediger, C.L., Bustin, R.M., and Rouse, G.E.
1984: New evidence for the chronology of the Eurekan Orogeny from south-central Ellesmere Island; Canadian Journal of Earth Sciences, v. 21, p. 1286-1295.

Robinson, D. and Leake, B.E.
1975: Sedimentary and igneous trends of AFM diagrams; Geological Magazine, v. 112, p. 305-307.

Robinson, P.
1980: The composition space of terrestrial pyroxenes - internal and external limits; *in* Pyroxenes, ed. C.T. Prewitt; Mineralogical Society of America, Reviews in Mineralogy, v. 7, p. 419-494.

Rock, N.M.S.
1984: Nature and origin of calc-alkaline lamprophyres: minettes, vogesites, kersantites and spessartites; Royal Society of Edinburgh, Transactions: Earth Sciences, v. 74, p. 193-227.

Rock, N.M.S. and Leake, B.E.
1984: The International Mineralogical Association amphibole nomenclature scheme: computerization and its consequences; Mineralogical Magazine, v. 48, p. 211-227.

Rollinson, H.R.
1982: Evidence from feldspar compositions of high temperature in granite sheets in the Scourian complex, N.W. Scotland; Mineralogical Magazine, v. 46, p. 73-76.

Roots, E.F.
1963a: Crystalline rocks west of South Cape; Geological Survey of Canada, Memoir 320, p. 275-283.
1963b: Cape Sparbo area; Geological Survey of Canada, Memoir 320, p. 189-194.

Rudnick, R.L., McLennan, S.M., and Taylor, S.R.
1985: Large ion lithophile elements in rocks from high-pressure granulite facies terrains; Geochimica et Cosmochimica Acta, v. 49, p. 1645-1655.

Sauter, P.C.C.
1983: Metamorphism of siliceous dolomites in the high-grade Precambrian of Rogaland, SW Norway; Geologica Ultraiectina, no. 32, 143 p.

Schenk, V.
1984: Petrology of felsic granulites, metapelites, metabasics, ultramafics, and metacarbonates from southern Calabria (Italy): prograde metamorphism, uplift and cooling of a former lower crust; Journal of Petrology, v. 25, p. 255-298.

Schreyer, W. and Abraham, K.
1978: Symplectitic cordierite-orthopyroxene-garnet assemblages as products of contact metamorphism of pre-existing basement granulites in the Vredefort Structure, South Africa, and their relations to pseudotachylite; Contributions of Mineralogy and Petrology, v. 68, p. 53-62.

Seifert, F.
1974: Stability of sapphirine: a study of the aluminous part of the system $MgO-Al_2O_3-SiO_2-H_2O$; Journal of Geology, v. 82, p. 173-204.

Sen, S.K. and Bhattacharya, A.
1984: An orthopyroxene-garnet thermometer and its application to the Madras charnockites; Contributions to Mineralogy and Petrology, v. 88, p. 64-71.

Shaw, D.M.
1968: A review of K-Rb fractionation trends by covariance analysis; Geochimica et Cosmochimica Acta; v. 32, p. 573-601.
1972: The origin of the Apsley gneiss, Ontario; Canadian Journal of Earth Sciences, v. 9, p. 18-35.

Sheraton, J.W. and Black, L.P.
1983: Geochemistry of Precambrian gneisses: relevance for the evolution of the East Antarctic Shield; Lithos, v. 16, p. 273-296.

Sheraton, J.W., Offe, L.A., Tingey, R.J., and Ellis, D.J.
1980: Enderby Land, Antarctica - an unusual Precambrian high-grade metamorphic terrain; Geological Society of Australia, Journal, v. 27, p. 1-18.

Sighinolfi, G.P. , Gorgoni, C., Silva Filho, M.A., and Tanner Oliveira, M.A.
1979: Petrochemistry of an upper Precambrian metasedimentary belt in southern Bahia - the significance of cordierite; Revista Brasileira de Geociencias, v. 9, p. 267-275.

Sills, J.D. and Tarney, J.
1984: Petrogenesis and tectonic significance of amphibolites interlayered with metasedimentary gneisses in the Ivrea Zone, Southern Alps, northwest Italy; Tectonophysics, v. 107, p. 187-206.

Smith, J.V.
1974: Feldspar Minerals, volume 2: Chemical and Textural Properties; Springer-Verlag, New York, 690 p.

Speer, J.A.
1980: Zircon; *in* Orthosilicates, 2nd ed., ed. P.H. Ribbe; Mineralogical Society of America, Reviews in Mineralogy, v. 5, p. 67-112.

Stephenson, N.C.N.
1984: Two-pyroxene thermometry of Precambrian granulites from Cape Riche, Albany-Fraser Province, Western Australia; Journal of Metamorphic Geology, v. 2, p. 297-314.

Stevens, R.D., Delabio, R.N., and Lachance, G.R.
1982: Age determinations and geological studies, K-Ar isotopic ages, Report 16; Geological Survey of Canada, Paper 82-2, 56 p.

Stockwell, C.H.
1982: Proposals for time classification and correlation of Precambrian rocks and events in Canada and adjacent areas of the Canadian Shield; Part I: A time classification of Precambrian rocks and events; Geological Survey of Canada, Paper 80-19, 135 p.

Streckeisen, A.
1976: To each plutonic rock its proper name; Earth-Science Reviews, v. 12, p. 1-33.

Tarney, J.
1976: Geochemistry of Archaean high-grade gneisses, with implications as to the origin and evolution of the Precambrian crust; *in* The Early History of the Earth, ed. B.F. Windley; J. Wiley and Sons, London, p. 405-417.

Taylor, A.
1955: Geographical discovery and exploration in the Queen Elizabeth Islands; Geographical Branch, Canada, Memoir 3, 172 p.

Taylor, S.R. and McLennan, S.M.
1985: The Continental Crust: Its Composition and Evolution; Blackwell Scientific Publications, Oxford, 312 p.

Thompson, A.B.
1976: Mineral reactions in pelitic rocks: II. Calculation of some P-T-X (Fe-Mg) phase relations; American Journal of Science, v. 276, p. 425-454.
1982: Dehydration melting of pelitic rocks and the generation of H_2O-undersaturated granitic liquids; American Journal of Science, v. 282, p. 1567-1595.
1984: Fe-Mg continuous crystalline solutions in garnet and cordierite and their use in geothermometry-barometry; *in* Thermométrie et Barométrie Géologiques, v. 1, ed. M. Lagache; Société Française de Minéralogie et de Cristallographie, p. 153-175.

Thompson, A.B. and England, P.C.
1984: Pressure-temperature-time paths of regional metamorphism. II. Their inference and interpretation using mineral assemblages in metamorphic rocks; Journal of Petrology, v. 25, p. 929-955.

Thorsteinsson, R. and Mayr, U.
1987: The sedimentary rocks of Devon Island, Canadian Arctic Archipelago; Geological Survey of Canada, Memoir 411, 182 p.

Turner, F.J.
1981: Metamorphic Petrology: Mineralogical, Field and Tectonic Aspects, 2nd ed.; McGraw-Hill, New York, 524 p.

Turnock, A.C. and Eugster, H.P.
1962: Fe-Al oxides: phase relationships below 1000°C; Journal of Petrology, v. 3, p. 533-565.

Tuttle, O.F. and Bowen, N.L.
1958: Origin of granite in the light of experimental studies in the system $NaAlSi_3O_8$-$KAlSi_3O_8$-SiO_2-H_2O; Geological Society of America, Memoir 74, 153 p.

Van Reenen, D.D.
1983: Cordierite + garnet + hypersthene + biotite-bearing assemblages as a function of changing metamorphic conditions in the Southern Marginal Zone of the Limpopo Metamorphic Complex; *in* The Limpopo Belt, ed. W.J. van Biljon and J.H. Legg; Geological Society of South Africa, Special Publication 8, p. 143-167.

Vielzeuf, D.
1983: The spinel and quartz associations in high grade xenoliths from Tallante (S.E. Spain) and their potential use in geothermometry and barometry; Contributions to Mineralogy and Petrology, v. 82, p. 301-311.

Weaver, B.L.
1980: Rare-earth element geochemistry of Madras granulites; Contributions to Mineralogy and Petrology, v. 71, p. 271-279.

Weaver, B.L. and Tarney, J.
1983: Elemental depletion in Archaean granulite-facies rocks; *in* Migmatites, Melting and Metamorphism, ed. M.P. Atherton and C.D. Gribble; Shiva Publishing, Nantwich, p. 250-263.

Weaver, B.L., Tarney, J., Windley, B.F., Sugavanam, E.B., and Venkata Rao, V.
1978: Madras granulites; geochemistry and P-T conditions of crystallization; *in* Archaean Geochemistry, ed. B.F. Windley and S.M. Naqvi; Elsevier, Amsterdam, p. 177-204.

Wells, P.R.A.
1979: Chemical and thermal evolution of Archaean sialic crust, southern West Greenland; Journal of Petrology, v. 20, p. 187-226.

Wendlandt, R.F.
1981: Influence of CO_2 on melting of model granulite facies assemblages: a model for the genesis of charnockites; American Mineralogist, v. 66, p. 1164-1174.

White, A.J.R. and Chappell, B.W.
1977: Ultrametamorphism and granitoid genesis; Tectonophysics, v. 43, p. 7-22.
1983: Granitoid types and their distribution in the Lachlan Fold Belt, southeastern Australia; Geological Society of America, Memoir 159, p. 21-34.

Willis, I.L., Brown, R.E., Stroud, W.J., and Stevens, B.P.J.
1983: The Early Proterozoic Willyama Supergroup: stratigraphic subdivision and interpretation of high to low-grade metamorphic rocks in the Broken Hill Block, New South Wales; Geological Society of Australia, Journal, v. 30, p. 195-224.

Wilson, A.F.
1974: The mineral potential of granulite terranes and other highly metamorphosed segments of the earth's crust; *in* Géologie des Domaines Cristallins, ed. J. Bellière and J.C. Duchesne; Société Géologique de Belgique, p. 301-321.

Windley, B.F.
1984: The Evolving Continents, 2nd ed.; J. Wiley and Sons, Chichester, 399 p.

Winkler, H.G.F.
1979: Petrogenesis of Metamorphic Rocks, 5th ed.; Springer-Verlag, New York, 348 p.

Woodford, P.J. and Wilson, A.F.
1976: Chemistry of coexisting pyroxenes, hornblendes and plagioclases in mafic granulites, Strangways Range, central Australia; Neues Jahrbuch für Mineralogie Abhandlungen, v. 128, p. 1-40.

Wyllie, P.J.
1977: Crustal anatexis: an experimental review; Tectonophysics, v. 43, p. 41-71.

Yund, R.A., Ackermand, D., and Seifert, F.
1980: Microstructures in the alkali feldspars from the granulite complex of Finnish Lapland; Neues Jahrbuch für Mineralogie Monatshefte, Jg. 1980, p. 109-117.

Zakrutkin, V.V.
1972: Chemistry of charnockitic granites and their genesis; International Geology Review, v. 14, p. 481-487.

APPENDIX

MINERAL AND ROCK ANALYSES

Tables 1 to 7 - Mineral analyses
Tables I to VIII - Rock analyses

Mineral analyses

In the tables, C and R refer to core and rim, respectively.

For strongly zoned or inhomogeneous minerals, maximum and minimum values measured, rounded off the nearest 0.1 per cent, are given. Wherever possible, however, extreme values were excluded from computation of the analysis tabulated.

All Fe is given as FeO, except where a value for Fe_2O_3 is shown, in which case divalent and trivalent Fe have been calculated from stoichiometry.

Anorthite content of plagioclase marked by an asterisk was determined optically.

Rock analyses

Trace element abundances, except S (weight per cent element), are given in parts per million.

Key to mineral abbreviations

Modal minerals

Accs	Zircon; apatite, Fe-Ti oxide, sulphide (except where these are shown separately)
Act	Actinolite
Ap	Apatite
Bio	Biotite (incl. phlogopite)
Cd	Cordierite
Chu	Clinohumite
Cpx	Clinopyroxene
Cum	Cummingtonite
Ga	Garnet
Hbl	Hornblende
Kf	K-feldspar (incl. perthite)
Ol	Olivine
Opx	Orthopyroxene
Ox	Fe-Ti oxide, sulphide
Pg	Plagioclase
Qz	Quartz
Sa	Sapphirine
Sca	Scapolite
Si	Sillimanite
Sp	Spinel
Wo	Wollastonite
Zo	Zoisite

Normative minerals

Q	Quartz
OR	Orthoclase
AB	Albite
AN	Anorthite
NE	Nepheline
C	Corundum
OL	Olivine
DI	Diopside
HY	Hypersthene
MT	Magnetite
HM	Hematite
CM	Chromite
IL	Ilmenite
AP	Apatite
PR	Pyrite
CC	Calcite

Abbreviations for modal minerals are capitalized in the tables of mineral analyses and in lower case in the tables of rock analyses. tr = trace

Table 1A. Analyses and structural formulae of minerals of orthopyroxene-free cordierite gneiss

FS-77-191

	GA C	GA R	CD	BIO	BIO		SP	PG
SiO_2	36.17	35.67	47.68	38.56	38.17		0.43	
TiO_2	0.10	0.07	0.07	2.31	2.44	(2.1-3.1)	0.08	
Al_2O_3	21.53	21.34	32.94	15.40	15.80		57.87	
Cr_2O_3	0.11	0.16		0.11	0.13		2.14	
Fe_2O_3							1.08	
FeO	34.00	37.10	7.80	12.08	13.92	(11.5-16.0)	34.60	
MnO	0.41	0.58	0.06					
MgO	5.94	3.47	9.13	17.40	15.29	(14.1-17.9)	4.47	
CaO	0.87	0.99						
Na_2O								
K_2O				9.85	9.57			
	99.13	99.38	97.68	95.71	95.32		100.67	
Fe	74.41	83.29	32.36	26.04	33.81		81.72	An*25
Mg	23.17	13.86	67.62	71.96	66.19		18.28	
Ca	2.42	2.85	0.02					
Fe/Fe + Mn + Mg	0.76	0.85	0.32	0.26	0.34		0.82	
Notes				included in GA	discrete			
O	24		18	22			32	
Si	5.816	5.819	4.936	5.645	5.649		0.096	
Ti	0.012	0.009	0.005	0.254	0.272		0.013	
Al	4.080	4.103	4.019	2.657	2.757		15.301	
Cr	0.013	0.021		0.013	0.015		0.380	
Fe^3							0.182	
Fe^2	4.574	5.062	0.675	1.479	1.723		6.491	
Mn	0.056	0.081	0.005					
Mg	1.424	0.843	1.409	3.797	3.374		1.495	
Ca	0.149	0.173						
Na								
K				1.839	1.806			
	16.125	16.110	11.049	15.685	15.596		23.958	

FSM-77-247-3

	GA C	GA R	CD
SiO_2	36.84	36.49	48.29
TiO_2	0.10	0.08	0.11
Al_2O_3	21.53	21.25	32.95
Cr_2O_3	0.04	0.09	
FeO	32.18	35.01	8.33
MnO	0.88	1.14	0.10
MgO	7.31	5.34	8.80
CaO	0.74	0.88	0.01
Na_2O			0.02
K_2O	99.62	100.08	99.81
Fe	69.73	77.11	34.67
Mg	28.23	20.97	65.27
Ca	2.04	1.92	0.06
Fe/Fe + Mn + Mg	0.70	0.77	0.35
O	24		18
Si	5.844	5.850	4.962
Ti	0.012	0.010	0.008
Al	4.025	4.015	3.990
Cr	0.005	0.011	
Fe	4.259	4.694	0.716
Mn	0.118	0.154	0.008
Mg	1.729	1.277	1.348
Ca	0.125	0.117	0.001
Na			0.004
K	16.127	16.128	11.037

FS-80-55

	GA C	GA R	CD	BIO	BIO		SP	PG
SiO_2	37.45	36.77	48.13	36.87			0.59	
TiO_2	0.08	0.07	0.08	4.37	(3.9-5.2)		0.06	
Al_2O_3	21.95	21.50	33.13	16.51			59.32	
Cr_2O_3	0.12	0.09		0.04			0.49	
FeO	32.40	35.04	7.41	15.11	(11.7-18.5)		33.73	
MnO	0.87	0.97	0.09				0.05	
MgO	6.88	4.83	9.47	13.77	(10.8-16.3)		4.22	
CaO	1.34	1.41	0.03					
Na_2O								
K_2O				10.15				
	101.09	100.68	98.34	96.82			98.46	
Fe	69.85	77.07	30.45	38.11			81.77	An*29-31
Mg	26.44	18.95	69.37	61.89			18.23	
Ca	3.71	3.98	0.18					
Fe/Fe + Mn + Mg	0.71	0.78	0.30	0.38			0.82	
Note							Zn-bearing	
O	24		18	22			32	
Si	5.856	5.859	4.939	5.437			0.134	
Ti	0.009	0.009	0.006	0.485			0.010	
Al	4.048	4.038	4.007	2.870			15.838	
Cr	0.014	0.012		0.005			0.089	
Fe	4.236	4.670	0.636	1.883			6.390	
Mn	0.115	0.131	0.008				0.010	
Mg	1.604	1.148	1.449	3.026			1.425	
Ca	0.225	0.241	0.004					
Na								
K				1.909				
	16.105	16.108	11.051	15.595			23.895	

FS-77-216

	GA C	GA R	CD	BIO	BIO		SP	PG	BIO	SI
SiO_2	37.63	36.75	48.69	37.40	37.44		0.73		36.82	36.37
TiO_2	0.19	0.10	0.08	2.79	1.85	(1.7-2.9)	0.07		0.56	0.07
Al_2O_3	21.64	21.47	33.23	15.52	15.83		56.47		18.37	61.10
Cr_2O_3	0.13	0.13		0.02			0.11		0.10	
Fe_2O_3							4.17			
FeO	35.74	36.52	6.61	17.74	15.22	(15.1-18.1)	35.23		15.92	1.63
MnO	0.65	0.86	0.06				0.08		0.04	0.04
MgO	5.18	3.69	10.11	13.30	14.88	(12.9-15.0)	3.90		14.94	0.37
CaO	1.02	1.24	0.02							0.02
Na_2O			0.04							0.44
K_2O			0.05	9.44	9.78				9.64	0.13
	102.18	100.76	98.89	96.21	94.98		100.76		96.39	100.17
Fe	77.21	81.71	26.78	42.80	36.47		84.87		37.41	
Mg	19.96	14.73	73.09	57.20	63.53		15.13		62.59	
Ca	2.83	3.56	0.13							
Fe/Fe + Mn + Mg	0.78	0.83	0.27	0.43	0.36		0.85			
Notes	1 analysis			high Fe	low Fe			An^*_{28}	pale green alteration of CD	mantles SP
O	24		18	22			32		22	
Si	5.894	5.885	4.952	5.591	5.612		0.185		5.442	
Ti	0.022	0.012	0.006	0.314	0.208		0.012		0.062	
Al	3.996	4.053	3.983	2.736	2.796		15.043		3.200	
Cr_3	0.016	0.016		0.003			0.020		0.012	
Fe_2							0.709			
Fe	4.682	4.891	0.582	2.218	1.908		6.659		1.968	
Mn	0.086	0.117	0.005				0.015		0.005	
Mg	1.210	0.882	1.533	2.985	3.324		1.314		3.292	
Ca	0.172	0.213	0.003							
Na			0.007							
K			0.006	1.801	1.867				1.818	
	16.078	16.069	11.057	15.627	15.715		23.927		15.799	

FSM-77-218-1

	GA C	GA R	CD	BIO	BIO		SP	PG
SiO_2	37.85	37.36	48.56	36.91	36.90		0.47	
TiO_2	0.13	0.07	0.06	5.85	5.66	(3.9-5.8)	0.07	
Al_2O_3	21.50	21.31	32.72	13.50	13.75		58.81	
Cr_2O_3	0.06	0.15		0.24	0.09		0.59	
Fe_2O_3							1.92	
FeO	30.58	33.08	6.36	13.76	9.20	(8.9-13.8)	31.20	
MnO	0.26	0.34	0.04	0.01			0.02	
MgO	8.78	6.76	10.36	14.44	17.54	(13.8-18.5)	6.54	
CaO	0.78	0.91	0.02					
Na_2O								
K_2O				9.96	9.86			
	99.94	99.98	98.12	94.67	93.00		99.82	
Fe	64.75	71.44	25.58	34.84	22.75		73.84	An*25
Mg	33.13	26.04	74.33	65.16	77.25		26.15	
Ca	2.12	2.52	0.09				0.01	
Fe/Fe + Mn + Mg	0.66	0.73	0.26	0.35	0.23	(0.22-0.37)	0.74	
Note:	1 analysis							
O	24		18	22			32	
Si	5.911	5.911	4.970	5.556	5.528		0.105	
Ti	0.016	0.009	0.005	0.662	0.638		0.012	
Al	3.957	3.974	3.947	2.395	2.427		15.431	
Cr	0.007	0.019		0.029	0.010		0.104	
Fe3							0.322	
Fe2	3.994	4.377	0.544	1.732	1.153		5.809	
Mn	0.034	0.045	0.003	0.001			0.004	
Mg	2.044	1.595	1.581	3.239	3.917		2.170	
Ca	0.131	0.154	0.002					
Na								
K				1.912	1.884			
	16.094	16.084	11.052	15.526	15.557		23.957	

FSM-77-273-4

	GA C	GA R	BIO	BIO		SP	PG
SiO_2	38.68	36.97	38.86			0.43	
TiO_2	0.16	0.05	5.08	(4.1-5.9)		0.07	
Al_2O_3	22.43	21.62	14.50			58.72	
Cr_2O_3	0.07	0.18	0.15			0.28	
Fe_2O_3						2.50	
FeO	26.48	33.18	13.43	(12.2-14.4)		32.12	
MnO	0.40	0.77	0.01			0.10	
MgO	10.56	6.55	14.66	(13.4-16.3)		6.01	
CaO	0.85	1.02					
Na_2O							
K_2O			9.87				
	101.63	100.34	94.56			100.23	
Fe	58.86	71.90	33.96			76.24	An*28-30
Mg	38.90	25.28	66.04			23.76	
Ca	2.24	2.82					
Fe/Fe + Mn + Mg	0.60	0.73	0.34			0.76	
O	24		22			32	
Si	5.870	5.849	5.533			0.096	
Ti	0.018	0.007	0.573			0.012	
Al	4.012	4.032	2.566			15.397	
Cr	0.009	0.023	0.018			0.049	
Fe^3						0.419	
Fe^2	3.615	4.389	1.686			5.976	
Mn	0.052	0.104	0.001			0.019	
Mg	2.389	1.543	3.279			1.993	
Ca	0.138	0.172					
Na							
K			1.890				
	16.103	16.119	15.546			23.961	

Remarks Andesine (An_{32}) mantles around Si in KF; all cordierite altered.

FS-82-D-14

	GA C	GA R	CD	BIO		PG
SiO_2	37.20	37.25	49.04	37.49		
TiO_2	0.02	0.10	0.08	3.59	(2.8-3.8)	
Al_2O_3	21.76	21.49	33.32	15.55		
Cr_2O_3	0.11	0.10		0.23		
FeO	33.74	35.77	6.71	16.41	(10.3-17.0)	
MnO	0.47	0.51	0.5	0.01		
MgO	6.96	5.25	9.58	13.01	(12.4-17.4)	
CaO	0.91	0.97	0.01			
Na_2O			0.13			
K_2O				10.02		
	101.17	101.44	99.37	96.31		
Fe	71.30	77.14	28.19	41.44		An*25
Mg	26.22	20.19	71.78	58.56		
Ca	2.48	2.67	0.03			
Fe/Fe + Mn + Mg	0.72	0.78	0.28	0.41		
Note	1 analysis					
O	24		18	22		
Si	5.835	5.882	4.962	5.586		
Ti	0.002	0.012	0.006	0.402		
Al	4.023	4.001	3.989	2.731		
Cr	0.014	0.012		0.027		
Fe	4.428	4.724	0.570	2.045		
Mn	0.063	0.068	0.005	0.001		
Mg	1.627	1.237	1.451	2.889		
Ca	0.154	0.164	0.001			
Na			0.025			
K				1.905		
	16.144	16.100	11.029	15.586		

FS-77-268

	GA	BIO	BIO	SP	PG
SiO_2	38.06	36.26	37.14	0.84	
TiO_2	0.09	4.70	3.03	0.08	
Al_2O_3	21.74	16.32	16.58	56.56	
Cr_2O_3	0.09	0.15	0.07	0.77	
Fe_2O_3				3.27	
FeO	32.52	19.44	15.82	34.61	
MnO	0.60	0.01		0.10	
MgO	7.18	11.24	14.16	4.21	
CaO	0.69				
Na_2O					
K_2O		9.87	9.70		
	100.97	97.99	96.50	100.44	
Fe	70.38	49.24	38.53	83.33	An*23-24
Mg	27.71	50.76	61.47	16.67	
Ca	1.91				
Fe/Fe + Mn + Mg	0.71	0.49	0.39	0.83	
Notes		high Fe	low Fe		
O	24	22		32	
Si	5.934	5.392	5.492	0.190	
Ti	0.011	0.525	0.337	0.014	
Al	3.994	2.861	2.891	15.054	
Cr	0.011	0.018	0.008	0.137	
Fe3				0.556	
Fe2	4.240	2.417	1.956	6.536	
Mn	0.079	0.002		0.019	
Mg	1.669	2.492	3.121	1.417	
Ca	0.115				
Na					
K		1.873	1.831		
	16.053	15.580	15.636	23.923	

Table 1A (cont.)

FS-78-33

	GA C	GA R	CD	BIO		PG
SiO_2	36.63	36.48	48.68	35.91		
TiO_2	0.02	0.06	0.06	4.09	(3.2-4.9)	
Al_2O_3	21.51	21.48	33.39	18.77		
Cr_2O_3	0.02	0.08		0.08		
FeO	33.60	35.31	7.16	17.12	(14.9-18.0)	
MnO	0.69	0.88	0.07	0.01		
MgO	8.15	4.85	9.70	11.80	(11.4-12.6)	
CaO	1.37	1.16	0.01			
Na_2O						
K_2O				9.79		
	99.99	100.32	99.07	95.57		
Fe	72.56	77.70	29.29	44.88		An°30-31
Mg	23.66	19.03	70.66	55.12		
Ca	3.78	3.27	0.05			
Fe/Fe + Mn + Mg	0.74	0.80	0.29	0.45		
O	24		18	22		
Si	5.835	5.841	4.951	5.416		
Ti	0.002	0.010	0.005	0.464		
Al	4.040	4.054	4.002	2.981		
Cr	0.002	0.010		0.010		
Fe	4.447	4.728	0.609	2.159		
Mn	0.092	0.119	0.006	0.001		
Mg	1.459	1.158	1.470	2.652		
Ca	0.233	0.199	0.001			
Na						
K				1.884		
	16.140	16.119	11.044	15.567		

FSM-77-307

	GA R	CD	BIO		SP	PG
SiO_2	36.97	47.52	36.76		0.40	
TiO_2	0.08	0.06	4.52	(3.9-5.7)	0.11	
Al_2O_3	21.32	32.61	14.48		57.45	
Cr_2O_3	0.19		0.27		0.57	
Fe_2O_3					1.84	
FeO	35.22	7.72	15.31	(13.6-17.3)	33.20	
MnO	0.44	0.04	0.01		0.03	
MgO	5.51	9.29	13.77	(12.4-14.9)	4.85	
CaO	0.89	0.01				
Na_2O						
K_2O			10.02			
	100.62	97.25	95.14		98.45	
Fe	78.25	31.78	38.42		80.13	An°27
Mg	21.27	68.15	61.58		19.87	
Ca	2.48	0.07				
Fe/Fe + Mn + Mg	0.77	0.32	0.38		0.80	
O	24	18	22		32	
Si	5.877	4.940	5.540		0.091	
Ti	0.010	0.005	0.512		0.019	
Al	3.995	3.996	2.572		15.443	
Cr	0.024		0.032		0.103	
Fe^3					0.316	
Fe^2	4.682	0.671	1.930		6.332	
Mn	0.059	0.004	0.001		0.006	
Mg	1.306	1.440	3.094		1.849	
Ca	0.152	0.001				
Na						
K			1.927			
	16.105	11.057	15.608		23.959	

FS-80-83

	GA C	GA R	GD	BIO	SP
SiO_2	37.13	35.93	47.12	35.97	0.34
TiO_2	0.09	0.06	0.08	3.99	0.08
Al_2O_3	21.80	21.07	32.25	15.38	57.60
Cr_2O_3	0.08	0.14		0.23	0.60
Fe_2O_3					1.55
FeO	32.21	35.94	8.68	20.87	38.57
MnO	0.60	0.90	0.10	0.01	0.02
MgO	7.49	4.06	8.44	9.46	2.93
CaO	0.84	1.10	0.02		
Na_2O			0.01		
K_2O				10.11	
	100.24	99.20	96.70	96.00	99.69
Fe	69.07	80.59	35.56	55.31	87.90
Mg	28.62	16.24	63.34	44.69	12.10
Ca	2.31	3.17	0.10		
Fe/Fe + Mn + Mg	0.70	0.82	0.36	0.55	0.88
O					
Si	5.841	5.850	4.950	5.519	0.078
Ti	0.011	0.007	0.006	0.461	0.014
Al	4.043	4.043	3.994	2.778	15.511
Cr	0.010	0.018		0.028	0.108
Fe^3					0.266
Fe^2	4.238	4.893	0.763	2.677	6.987
Mn	0.080	0.124	0.009	0.001	0.004
Mg	1.756	0.986	1.322	2.163	0.998
Ca	0.142	0.192	0.002		
Na			0.002		
K				1.979	
	16.121	16.113	11.048	15.606	23.966

Table 1B. Analyses and structural formulae of minerals of orthopyroxene-cordierite gneiss

FSM-77-101-4

	GA C	GA R	CD	BIO					OPX	SP		PG
SiO_2	39.28	38.34	49.21	38.86	39.24	38.80	38.67		49.56	0.90	0.36	
TiO_2	0.12	0.06	0.08	4.03	4.10	4.73	4.09	(3.4-5.4)	0.20	0.09	0.08	
Al_2O_3	22.68	22.26	33.40	15.25	14.29	14.72	14.86		6.94	59.80	59.30	
Cr_2O_3	0.15	0.14		0.12	0.13	0.13	0.08		0.12	1.26	1.39	
Fe_2O_3										1.38	2.52	
FeO	22.76	26.48	3.38	9.12	6.84	9.52	11.24	(9.5-11.5)	21.08	27.41	28.81	
MnO	0.85	1.59	0.11	0.01			0.01		0.34	0.09	0.10	
MgO	12.88	9.68	11.44	19.40	20.49	18.56	18.06	(17.8-18.8)	21.88	9.22	8.37	
CaO	1.02	1.20	0.02	0.01		0.01			0.07			
Na_2O			0.08									
K_2O				9.65	9.85	10.22	9.86					
	99.76	99.75	97.72	96.45	94.94	96.69	96.87		100.19	100.15	100.93	
Fe	48.41	58.53	14.18	20.87	15.78	22.34	25.87		35.02	63.55	67.58	An°27
Mg	48.80	38.10	85.67	79.11	84.22	77.63	74.11		64.83	36.44	32.42	
Ca	2.79	3.37	0.15	0.02		0.03	0.01		0.15			
Fe/Fe + Mn + Mg	0.49	0.58	0.14	0.21	0.16	0.22	0.26		0.35	0.83	0.67	
Notes				Included in GA		discrete				discrete	assocd. w/OPX	
O	24		18		22				6		32	
Si	5.926	5.917	4.986	5.565	5.856	5.577	5.579		1.831	0.195	0.078	
Ti	0.013	0.007	0.006	0.434	0.445	0.511	0.444		0.006	0.015	0.013	
Al	4.033	4.050	3.989	2.574	2.428	2.494	2.527		0.302	15.296	15.233	
Cr	0.018	0.017		0.014	0.014	0.015	0.009		0.004	0.216	0.240	
Fe^3										0.225	0.413	
Fe^2	2.874	3.418	0.286	1.093	0.825	1.145	1.358		0.851	4.975	5.251	
Mn	0.109	0.208	0.009	0.001			0.002		0.011	0.017	0.018	
Mg	2.897	2.227	1.728	4.142	4.404	3.978	3.884		1.205	2.983	2.719	
Ca	0.166	0.198	0.002	0.001		0.002			0.003			
Na			0.016									
K				1.783	1.811	1.874	1.816					
	16.036	16.042	11.022	15.587	15.583	15.598	15.617		4.013	23.922	23.965	
Remarks	OPX - distinctly pleochroic; BIO - orangey brown.											

FS-80-84

	OPX	BIO	CD	SP	SA	PG
SiO_2	50.59	38.99	49.00	0.36	13.45	60.33
TiO_2	0.14	3.91	0.07	0.04		
Al_2O_3	4.02	14.02	33.47	61.61	60.34	24.47
Cr_2O_3	0.08	0.03		0.08		
Fe_2O_3				2.56		
FeO	18.54	9.07	3.46	23.61	9.15	0.17
MnO	0.26	0.02	0.06	0.09	0.05	
MgO	25.73	19.53	12.18	11.64	16.47	
CaO	0.05		0.02			5.90
Na_2O			0.01			7.82
K_2O		10.20				0.22
	99.41	95.77	98.26	100.09	99.46	98.91
Fe	26.76	20.67	13.70	55.61	23.75	An 29.0
Mg	71.15	79.33	86.22	44.39	76.25	Ab 69.7
Ca	0.09		0.08			Or 1.3
Fe/Fe + Mn + Mg	0.29	0.21	0.14	0.56	0.24	
O	6	22	18	32	20	
Si	1.865	5.647	4.944	0.077	1.622	
Ti	0.004	0.426	0.005	0.006		
Al	0.175	2.393	3.980	15.494	8.578	
Cr	0.002	0.004		0.013		
Fe_2				0.427		
Fe	0.572	1.099	0.291	4.213	0.922	
Mn	0.008	0.002	0.005	0.016	0.005	
Mg	1.414	4.216	1.832	3.702	2.982	
Ca	0.002		0.002			
Na			0.003			
K		1.885				
	4.042	15.672	11.062	23.948	14.089	
Remarks	OPX - slightly pleochroic; BIO - orangey brown; SA - blue to blue with violet tinge.					

FSM-77-212

	GA C	GA R	CD	BIO	OPX	SP		PG
SiO_2	38.08	37.16	49.26	38.83	47.74	0.38	0.28	61.15
TiO_2	0.13	0.08	0.06	3.50	0.21	0.07	0.05	
Al_2O_3	22.35	21.60	33.05	14.17	7.53	59.98	61.78	24.51
Cr_2O_3	0.05	0.06		0.02	0.09	0.60	0.53	
Fe_2O_3						1.06	0.23	
FeO	29.88	31.38	5.32	11.05	24.79	30.83	27.88	0.05
MnO	0.61	1.10	0.07	0.03	0.21	0.16	0.06	
MgO	8.92	7.10	10.62	17.72	19.74	6.89	9.06	
CaO	0.83	1.07			0.04			5.75
Na_2O			0.01					8.05
K_2O				10.70				0.27
	100.85	99.53	98.39	96.02	100.35	99.97	99.87	99.78
Fe	63.81	69.08	21.94	25.91	41.30	72.13	63.49	An 27.9
Mg	33.93	27.90	78.01	74.09	58.62	27.87	36.51	Ab 70.5
Ca	2.26	3.02	0.05		0.08			Or 1.6
Fe/Fe + Mn + Mg	0.64	0.69	0.22	0.26	0.41	0.72	0.63	
Notes						mantled by CD	OPX	
O	24		18	22	6	32		
Si	5.873	5.883	4.999	5.676	1.795	0.064	0.061	
Ti	0.015	0.010	0.005	0.385	0.006	0.012	0.008	
Al	4.064	4.031	3.953	2.442	0.334	15.601	15.785	
Cr	0.005	0.008		0.002	0.003	0.105	0.091	
Fe^3						0.176	0.038	
Fe^2	3.854	4.152	0.451	1.350	0.780	5.690	5.054	
Mn	0.080	0.148	0.006	0.003	0.007	0.030	0.011	
Mg	2.049	1.676	1.806	3.862	1.106	2.267	2.928	
Ca	0.136	0.182			0.002			
Na								
K				1.995				
	16.076	16.090	11.020	15.715	4.033	23.965	23.976	
Remarks	OPX - strongly pleochroic; BIO - chestnut.							

Table 2A. Analyses and structural formulae of minerals of garnet-free orthopyroxene-bearing quartzofeldspathic gneiss

FS-77-69

	OPX	BIO	PG	
SiO_2	47.55	37.23	59.51	
TiO_2	0.15	5.66		
Al_2O_3	5.79	13.58	26.12	
Cr_2O_3	0.10	0.04		
FeO	25.89	13.22	0.19	
MnO	0.53	0.04		
MgO	19.56	15.85		
CaO	0.08		7.84	
Na_2O			6.80	
K_2O		9.87	0.38	
	99.64	95.49	100.65	
Fe	42.55	31.88	An 37.4	(37-39)
Mg	57.29	68.12	Ab 60.3	(54-61)
Ca	0.16		Or 2.2	(1.4-2.7)
Fe/Fe + Mn + Mg	0.42	0.32		
O	6	22		
Si	1.817	5.532		
Ti	0.004	0.632		
Al	0.261	2.379		
Cr	0.003	0.005		
Fe	0.827	1.643		
Mn	0.017	0.005		
Mg	1.114	3.511		
Ca	0.003			
Na				
K		1.871		
	4.046	15.578		

Remarks OPX – strongly pleochroic; BIO - slightly reddish brown.

FS-77-182

	OPX	BIO	PG	
SiO_2	50.49	37.78	59.60	
TiO_2	0.18	5.10		
Al_2O_3	3.95	14.39	25.52	
Cr_2O_3	0.06	0.08		
FeO	19.22	11.61	0.11	
MnO	0.08			
MgO	25.81	17.37		
CaO	0.08		7.18	
Na_2O			6.76	
K_2O		10.14	0.73	
	99.89	96.47	99.90	
Fe	29.43	27.37	An 35.4	(33-38)
Mg	70.42	72.73	Ab 60.3	
Ca	0.15		Or 4.3	(3.2-5.6)
Fe/Fe + Mn + Mg	0.29	0.27		
O	6	22		
Si	1.858	5.510		
Ti	0.005	0.559		
Al	0.171	2.474		
Cr	0.002	0.009		
Fe	0.592	1.416		
Mn	0.003			
Mg	1.416	3.777		
Ca	0.003			
Na				
K		1.887		
	4.050	15.632		

Remarks OPX – distinctly pleochroic; BIO - pale chestnut.

FS-77-207

	OPX	CPX	HBL	BIO	PG
SiO_2	52.13	52.09	45.25	37.68	61.33
TiO_2	0.11	0.18	1.81	5.50	
Al_2O_3	0.85	1.63	8.85	12.90	24.90
Cr_2O_3	0.05	0.10	0.20	0.06	
FeO	22.40	9.62	12.13	12.00	0.19
MnO	0.65	0.26	0.13	0.01	
MgO	23.83	14.58	15.14	16.97	
CaO	0.58	21.10	11.69		6.22
Na_2O		0.30	1.22		7.11
K_2O			1.16	9.80	1.19
	100.70	99.86	97.38	94.92	100.94
Fe	34.08	15.36	22.43	28.41	An 30.3
Mg	54.60	41.48	49.89	71.59	Ab 62.8
Ca	1.32	43.16	27.68		Or 6.9
Fe/Fe + Mn + Mg	0.34	0.27	0.31	0.28	
O	6	6	23	22	
Si	1.937	1.949	6.671	5.597	
Ti	0.003	0.005	0.201	0.615	
Al	0.037	0.072	1.502	2.259	
Cr	0.001	0.003	0.023	0.007	
Fe	0.896	0.301	1.496	1.491	
Mn	0.021	0.008	0.016	0.001	
Mg	1.319	0.813	3.328	3.757	
Ca	0.027	0.846	1.846		
Na		0.022	0.349		
K			0.218	1.857	
	4.041	4.019	15.650	15.584	

Remarks OPX - slightly pleochroic; CPX - very pale green; HBL - olive; BIO - chestnut.

FS-77-332

	OPX	BIO	PG	
SiO_2	47.70	37.58	60.66	
TiO_2	0.19	5.08		
Al_2O_3	6.46	14.65	25.19	
Cr_2O_3	0.08	0.04		
FeO	25.40	12.46	0.07	
MnO	0.48			
MgO	20.17	16.22		
CaO	0.05		6.86	
Na_2O			7.31	
K_2O		10.09	0.47	
	100.53	96.12	100.36	
Fe	41.35	30.12	An 32.5	(31~34)
Mg	58.55	69.88	Ab 64.7	
Ca	0.10		Or 2.8	
Fe/Fe + Mn + Mg	0.41	0.30		
O	6	22		
Si	1.800	5.520		
Ti	0.005	0.561		
Al	0.287	2.536		
Cr	0.002	0.004		
Fe	0.802	1.531		
Mn	0.015	0.001		
Mg	1.135	3.551		
Ca	0.002			
Na				
K		1.891		
	4.048	15.595		

Remarks OPX – strongly pleochroic; BIO - pale yellow to orange brown.

FSM-77-104

	OPX	CPX		BIO	PG	
SiO_2	52.03	52.57	52.07	38.81	61.59	
TiO_2	0.14	0.10	0.27	5.46		
Al_2O_3	0.81	1.24	2.04	12.87	25.05	
Cr_2O_3	0.08	0.16	0.15	0.07		
FeO	22.02	8.61	9.90	11.36	0.16	
MnO	0.44	0.16	0.21	0.02		
MgO	24.04	15.12	14.28	17.60		
CaO	0.61	21.67	21.31		6.17	
Na_2O		0.07	0.27		8.01	
K_2O				9.92	0.29	
	100.17	99.70	100.50	95.91	101.27	
Fe	33.54	13.60	15.79	26.59	An 29.4	(27-31)
Mg	65.27	42.55	40.62	73.41	Ab 69.0	(67-71)
Ca	1.19	43.85	43.59		Or 1.6	(1.3-2.4)
Fe/Fe + Mn + Mg	0.34	0.24	0.28	0.27		
Notes		low Fe	high Fe			
O	6	6		22		
Si	1.938	1.961	1.938	5.849		
Ti	0.004	0.003	0.008	0.801		
Al	0.036	0.054	0.090	2.219		
Cr	0.002	0.005	0.004	0.008		
Fe	0.686	0.269	0.308	1.391		
Mn	0.014	0.005	0.007	0.002		
Mg	1.335	0.841	0.792	3.840		
Ca	0.024	0.866	0.850			
Na		0.005	0.019			
K				1.852		
	4.039	4.009	4.016	15.562		

Remarks OPX – pleochroic; CPX - neutral to very pale green; BIO - brown.

FS-78-10

	OPX	CPX	HBL	BIO	PG
SiO_2	50.24	51.58	42.27	36.08	59.45
TiO_2	0.07	0.08	1.58	4.99	
Al_2O_3	0.98	1.72	10.40	13.81	26.50
Cr_2O_3	0.04	0.10	0.06	0.04	
FeO	29.75	11.87	18.58	19.76	0.14
MnO	1.01	0.36	0.19	0.10	
MgO	17.96	12.92	10.46	11.61	
CaO	0.54	21.38	11.33		7.88
Na_2O		0.12	1.24		7.01
K_2O			1.46	9.61	0.30
	100.59	100.13	97.57	96.00	101.28
Fe	47.63	19.06	35.92	48.84	An 37.7
Mg	51.27	36.98	36.02	51.16	Ab 60.6
Ca	1.10	43.96	28.06		Or 1.7
Fe/Fe + Mn + Mg	0.47	0.34	0.50	0.49	
O	6	6	23	22	
Si	1.939	1.947	6.442	5.506	
Ti	0.002	0.002	0.182	0.572	
Al	0.044	0.077	1.867	2.484	
Cr	0.001	0.003	0.007	0.005	
Fe	0.960	0.375	2.369	2.522	
Mn	0.033	0.011	0.024	0.013	
Mg	1.034	0.727	2.376	2.641	
Ca	0.022	0.865	1.850		
Na		0.009	0.365		
K			0.284	1.870	
	4.035	4.018	15.766	15.613	

Remarks OPX - pleochroic; CPX - pale green; HBL - olive; BIO - deep chestnut.

FSM-77-311

	OPX	BIO		PG	KF
SiO_2	49.08	38.33	38.33	63.88	63.07
TiO_2	0.16	4.32	5.48 (4.2-5.9)		
Al_2O_3	5.04	13.42	13.68	24.13	21.26
Cr_2O_3	0.08		0.03		
FeO	21.53	8.90	10.72 (8.8-10.9)	0.12	0.03
MnO	0.85	0.05	0.05		
MgO	22.88	19.20	17.49 (17.1-19.4)		
CaO	0.04			4.98	2.93
Na_2O				8.56	4.57
K_2O		10.09	10.17	0.35	7.92
	99.66	94.31	95.95	102.02	99.78
Fe	34.52	20.64	25.58	An 23.8	14.2 (13-15)
Mg	65.40	79.36	74.42	Ab 74.2	40.1 (37-46)
Ca	0.08			Or 2.0	45.7 (39-49)
Fe/Fe + Mn + Mg	0.34	0.21	0.26		
Notes		low Fe	high Fe		
O	6	22			
Si	1.837	5.643	5.596		
Ti	0.005	0.479	0.601		
Al	0.222	2.328	2.355		
Cr	0.002	0.001	0.003		
Fe	0.674	1.096	1.309		
Mn	0.027	0.006	0.007		
Mg	1.277	4.213	3.806		
Ca	0.002				
Na					
K		1.896	1.895		
	4.046	15.662	15.572		

Remarks OPX - strongly pleochroic; BIO - orangey brown.

FSM-77-35

	OPX	BIO	PG	KF	
SiO_2	48.27	36.97	60.63		
TiO_2	0.20	4.38			
Al_2O_3	2.37	12.88	25.58		
Cr_2O_3	0.14	0.10			
FeO	34.74	19.05	0.09		
MnO	0.66	0.04			
MgO	14.48	12.69			
CaO	0.21		6.96		
Na_2O			7.41		
K_2O		9.87	0.35		
	101.07	95.78	101.02		
Fe	57.13	45.73	An 33.5	2-3	1
Mg	42.43	54.27	Ab 64.5	12-18	10
Ca	0.44		Or 2.0	79-86	89
Fe/Fe + Mn + Mg	0.57	0.46			
Notes					exsolved from PG
O	6	22			
Si	1.898	5.530			
Ti	0.006	0.502			
Al	0.110	2.311			
Cr	0.004	0.013			
Fe	1.142	2.427			
Mn	0.022	0.005			
Mg	0.848	2.880			
Ca	0.009				
Na					
K		1.878			
	4.039	15.646			

Remarks OPX - strongly pleochroic; BIO - deep chestnut.

FS-82-D-19A

	OPX	BIO	PG
SiO_2	49.73	35.69	56.69
TiO_2	0.16	6.46	
Al_2O_3	2.71	14.60	28.43
Cr_2O_3	0.10	0.10	
FeO	29.19	16.79	0.16
MnO	0.40	0.05	
MgO	18.57	12.73	
CaO	0.14		10.07
Na_2O			5.65
K_2O		9.47	0.25
	101.00	95.89	101.25
Fe	46.72	42.54	An 48.9
Mg	53.00	57.46	Ab 49.7
Ca	0.28		Or 1.4
Fe/Fe + Mn + Mg	0.47	0.42	
O	6	22	
Si	1.898	5.373	
Ti	0.005	0.732	
Al	0.122	2.591	
Cr	0.003	0.011	
Fe	0.932	2.114	
Mn	0.013	0.006	
Mg	1.057	2.856	
Ca	0.006		
Na			
K		1.819	
	4.036	15.502	

Remarks OPX - slightly pleochroic; BIO - orangey brown

FS-78-14

	OPX	CPX	BIO	PG	
SiO_2	49.91	51.41	35.91	57.87	
TiO_2	0.13	0.14	5.89		
Al_2O_3	1.32	2.02	13.54	27.33	
Cr_2O_3	0.05	0.09	0.03		
FeO	29.01	12.22	19.25	0.11	
MnO	0.65	0.23	0.02		
MgO	17.38	12.87	12.01		
CaO	1.99	21.37		9.04	
Na_2O		0.39		6.16	
K_2O			9.56	0.28	
	100.44	100.74	96.21	100.79	
Fe	46.39	19.54	47.36	An 44.1	(42-45)
Mg	49.54	36.69	52.64	Ab 54.3	
Ca	4.07	43.77		Or 1.6	
Fe/Fe + Mn + Mg	0.48	0.35	0.47		
O	6	6	22		
Si	1.929	1.933	5.457		
Ti	0.004	0.004	0.673		
Al	0.060	0.089	2.425		
Cr	0.002	0.003	0.004		
Fe	0.938	0.384	2.447		
Mn	0.021	0.007	0.003		
Mg	1.001	0.721	2.720		
Ca	0.082	0.861			
Na		0.028			
K			1.853		
	4.037	4.030	15.582		

Remarks OPX - distinctly pleochroic; CPX - pale green; BIO - deep chestnut

FS-78-25

	OPX	HBL	BIO	PG
SiO_2	48.31	41.05	37.24	60.91
TiO_2	0.15	1.85	4.71	
Al_2O_3	1.04	10.27	11.88	25.33
Cr_2O_3	0.10	0.10	0.05	
FeO	37.58	20.43	18.99	0.27
MnO	1.18	0.28	0.05	
MgO	12.17	9.20	13.03	
CaO	0.81	10.99		6.63
Na_2O		1.73		7.48
K_2O		1.87	9.89	0.41
	101.14	97.55	95.84	101.03
Fe	62.58	40.13	44.96	An 32.1
Mg	36.13	32.21	55.02	Ab 65.5
Ca	1.29	27.66	0.02	Or 2.4
Fe/Fe + Mn + Mg	0.62	0.55	0.45	
O	6	23	22	
Si	1.932	6.357	5.678	
Ti	0.005	0.192	0.540	
Al	0.049	1.875	2.135	
Cr	0.003	0.012	0.006	
Fe	1.257	2.646	2.421	
Mn	0.040	0.034	0.007	
Mg	0.726	2.123	2.963	
Ca	0.026	1.823		
Na		0.519		
K		0.370	1.924	
	4.038	15.951	15.674	

Remarks OPX - slightly pleochroic; HBL - olive with brown tinge; BIO - very slightly reddish brown.

Table 2B. Analyses and structural formulae of minerals of garnetiferous orthopyroxene-bearing quartzofeldspathic gneiss

FS-77-68

	GA	BIO		OPX	SP		PG	KF
SiO_2	37.40	38.06	37.87	38.00	47.46	0.31	0.27	60.80	64.61
TiO_2	0.07	4.73	4.91	5.05	0.20	0.08	0.19		
Al_2O_3	22.38	14.57	14.25	14.13	6.96	60.04	62.58	24.43	19.24
Cr_2O_3	0.08	0.11	0.07	0.08	0.06	1.62	1.60		
FeO	30.44	11.49	13.31	9.48	25.50	29.39	28.05	0.09	0.10
MnO	0.46			0.01	0.15	0.03	0.02		
MgO	8.54	19.46	16.41	17.57	20.44	6.38	8.48		
CaO	0.81				0.03			5.30	0.84
Na_2O				0.02			8.20	2.32	
K_2O		9.91	9.84	9.82				0.30	12.57
	100.18	96.32	96.66	96.17	100.82	97.85	101.19	99.12	99.59
Fe	65.16	21.46	31.27	26.83	41.15	72.10	64.99	An 25.9	4.2
Mg	32.61	78.54	68.73	73.17	58.79	27.90	35.01	Ab 72.4	21.0
Ca	2.23				0.06			Or 1.7	74.8
Fe/Fe + Mn + Mg	0.66	0.22	0.31	0.27	0.41	0.72	0.65		
Notes			discrete low Fe	discrete high Fe	included in GA		included in OX		
O	24		22		6	32			
Si	5.828	5.494	5.545	5.546	1.784	0.069	0.058		
Ti	0.008	0.513	0.540	0.554	0.006	0.013	0.031		
Al	4.111	2.479	2.459	2.430	0.309	15.844	15.790		
Cr	0.010	0.013	0.008	0.009	0.002	0.287	0.271		
Fe	3.967	1.145	1.629	1.402	0.802	5.503	5.022		
Mn	0.061			0.001	0.006	0.004			
Mg	1.984	4.189	3.581	3.822	1.146	2.129	2.706		
Ca	0.135				0.001				
Na									
K		1.826	1.839	1.829					
	16.104	15.659	15.601	15.598	4.055	23.851	23.882		

Remarks OPX - strongly pleochroic; BIO - slightly reddish brown.

FS-D-82-7D

	GA	BIO	OPX	PG
SiO_2	37.91	36.74	51.70	49.04
TiO_2	0.09	6.72	0.12	
Al_2O_3	22.00	14.48	2.40	32.43
Cr_2O_3	0.13	0.15	0.11	
FeO	27.93	13.30	23.24	0.07
MnO	0.67	0.02	0.18	
MgO	6.63	14.52	22.45	
CaO	3.23		0.17	15.21
Na_2O				2.61
K_2O		10.18		0.14
	100.59	96.11	100.37	99.50
Fe	58.88	33.94	36.61	An 5.7
Mg	32.41	66.06	63.04	Ab 23.5
Ca	8.71		0.35	Or 0.8
Fe/Fe + Mn + Mg	0.63	0.34	0.37	
O	24	22	6	
Si	5.860	5.438	1.924	
Ti	0.011	0.748	0.003	
Al	4.009	2.527	0.105	
Cr	0.016	0.018	0.003	
Fe	3.611	1.646	0.724	
Mn	0.088	0.002	0.006	
Mg	1.988	3.203	1.246	
Ca	0.534		0.007	
Na				
K		1.921		
	16.117	15.503	4.018	

Remarks OPX - slightly pleochroic; BIO - reddish brown.

FS-78-20

	GA	OPX	CPX	HBL	PG
SiO_2	36.73	48.46	50.35	40.92	59.92
TiO_2	0.07	0.09	0.15	1.77	
Al_2O_3	20.85	1.11	1.91	11.19	26.21
Cr_2O_3	0.07	0.05	0.11	0.07	
FeO	30.84	36.33	16.78	21.20	0.14
MnO	1.15	0.43	0.19	0.09	
MgO	3.09	13.43	10.16	8.31	
CaO	7.16	0.56	20.78	11.21	7.48
Na_2O			0.12	1.49	8.94
K_2O				1.89	0.35
	99.76	100.46	100.55	98.14	101.04
Fe	57.76	59.57	27.27	42.07	An 36.8
Mg	12.08	39.25	29.45	29.41	Ab 61.4
Ca	20.16	1.18	43.28	28.51	Or 2.0
Fe/Fe + Mn + Mg	0.82	0.60	0.48	0.59	
O	24	6	6	23	
Si	5.908	1.933	1.935	6.306	
Ti	0.009	0.003	0.004	0.206	
Al	3.915	0.052	0.086	2.033	
Cr	0.008	0.001	0.003	0.008	
Fe	4.149	1.212	0.539	2.732	
Mn	0.157	0.015	0.006	0.011	
Mg	0.740	0.798	0.582	1.910	
Ca	1.234	0.024	0.856	1.852	
Na			0.009	0.445	
K				0.372	
	16.120	4.038	4.020	15.875	

Remarks GA - pink; OPX - slightly pleochroic; CPX - pale green; HBL - olive.

FSM-77-114-1

	GA C	GA R	BIO			OPX	PG	
SiO_2	37.11	37.25	37.30	36.50		49.28	56.28	
TiO_2	0.08	0.08	4.23	4.76	(4.2-4.9)	0.14		
Al_2O_3	21.37	21.49	15.61	14.97		4.06	27.61	
Cr_2O_3	0.11	0.09	0.09	0.12		0.14		
FeO	29.88	31.17	12.77	16.41	(12.8-16.6)	26.92	0.10	
MnO	1.25	1.31				0.40		
MgO	7.58	7.15	15.83	13.73	(13.3-16.0)	18.84		
CaO	2.09	1.56				0.11	9.59	
Na_2O							5.82	
K_2O			10.34	10.20			0.24	
	99.47	100.10	96.17	96.69		99.89	99.84	
Fe	64.86	67.89	31.15	40.14		44.40	An 47.0	(49-46)
Mg	29.33	27.75	68.85	59.86		55.37	Ab 51.6	
Ca	5.81	4.36				0.23	Or 1.4	
Fe/Fe + Mn + Mg	0.67	0.69	0.31	0.40		0.44		
Notes			low Fe	high Fe			zoned: (core-rim)	
O	24		22			6		
Si	5.866	5.873	5.467	5.445		1.881		
Ti	0.009	0.009	0.467	0.534		0.004		
Al	3.981	3.994	2.706	2.633		0.183		
Cr	0.013	0.012	0.011	0.014		0.004		
Fe	3.951	4.110	1.571	2.048		0.859		
Mn	0.167	0.175				0.013		
Mg	1.786	1.680	3.473	3.053		1.072		
Ca	0.354	0.264				0.004		
Na								
K			1.940	1.941				
	16.127	16.117	15.657	15.668		4.020		

Remarks OPX - distinctly pleochroic; BIO - chestnut.

FSM-77-63-9

	GA C	GA R	BIO		OPX	SP	PG		
SiO_2	37.10	37.49	38.48	37.80	49.16	0.32	57.93	56.41	59.61
TiO_2	0.13	0.10	3.91	4.77	0.22	0.05			
Al_2O_3	21.67	21.78	14.71	13.75	4.94	61.21	26.18	27.49	25.18
Cr_2O_3	0.14	0.13	0.12	0.19	0.17	0.70			
Fe_2O_3						0.27			
FeO	28.35	29.75	8.16	13.31	26.09	26.41	0.14	0.12	
MnO	0.73	0.75	0.02	0.01	0.24	0.03			
MgO	9.14	8.77	20.20	16.18	19.22	9.75			
CaO	1.63	1.29			0.10		7.86	9.40	6.64
Na_2O							6.73	5.79	6.20
K_2O			10.51	10.33			0.39	0.33	2.70
	98.88	100.07	96.09	96.34	100.14	98.74	99.23	99.52	100.33
Fe	60.68	63.24	18.48	31.57	43.14	60.53	An 38.4	46.4	(35-51) 31.5
Mg	34.86	33.23	81.52	68.43	56.64	39.46	Ab 9.4	51.7	53.3
Ca	4.46	3.52			0.22		Or 2.2	1.9	15.2
Fe/Fe + Mn + Mg	0.62	0.64	0.18	0.32	0.43	0.60			
Notes	SI inclusions	included in GA				included in GA	low Ca	high Ca	K-rich
O	24		22		6	32			
Si	5.837	5.850	5.544	5.575	1.862	0.070			
Ti	0.016	0.017	0.424	0.529	0.006	0.008			
Al	4.019	4.007	2.500	2.391	0.221	15.736			
Cr	0.016	0.017	0.014	0.022	0.005	0.121			
Fe^3						0.044			
Fe^2	3.730	3.883	0.984	1.641	0.827	4.817			
Mn	0.097	0.100	0.002	0.001	0.008	0.006			
Mg	2.143	2.040	4.340	3.558	1.085	3.170			
Ca	0.274	0.216			0.004				
Na									
K			1.933	1.943					
	16.132	16.125	15.741	15.660	4.018	23.972			

Remarks OPX - strongly pleochroic; BIO - orangey brown.

FSM-77-220

	GA			BIO		OPX
SiO_2	37.27	37.54	38.42	38.42	38.41	47.23
TiO_2	0.09	0.06	0.15	3.97	3.23	0.24
Al_2O_3	21.56	21.86	21.46	14.32	14.14	7.28
Cr_2O_3	0.07	0.05	0.06	0.03	0.03	0.05
FeO	29.88	31.99	32.97	8.09	12.00	26.67
MnO	2.22	2.74	2.47	0.05	0.01	0.63
MgO	8.25	6.98	5.86	19.77	17.80	18.28
CaO	0.61	0.50	0.43			0.01
Na_2O						
K_2O				10.51	10.46	
	99.95	101.72	99.82	95.16	96.09	100.39
Fe	65.86	70.98	75.00	18.66	27.45	45.00
Mg	32.42	27.60	23.76	81.34	72.55	54.99
Ca	1.72	1.42	1.24			0.01
Fe/Fe + Mn + Mg	0.64	0.68	0.72	0.19	0.27	0.45
Notes		late GA rimming AP	late GA rimming OX	included in GA		discrete
O	24			22		6
Si	5.857	5.854	5.829	5.593	5.635	1.795
Ti	0.011	0.007	0.017	0.434	0.356	0.007
Al	3.994	4.018	4.049	2.456	2.445	0.326
Cr	0.008	0.007	0.008	0.003	0.004	0.002
Fe	3.928	4.172	4.415	0.985	1.473	0.848
Mn	0.295	0.363	0.335	0.006	0.001	0.020
Mg	1.934	1.622	1.398	4.291	3.891	1.036
Ca	0.102	0.084	0.073			
Na						
K				1.951	1.957	
	16.129	16.127	16.124	15.719	15.762	4.034

Remarks OPX - strongly pleochroic; BIO - chestnut; oligoclase (An_{20}) rims on GA against KF

FS-77-294

	GA C	GA R	BIO		OPX	KF
SiO_2	36.05	36.00	38.74		47.00	65.29
TiO_2	0.13	0.09	3.78	(3.1-4.4)	0.24	
Al_2O_3	21.30	21.15	13.49		3.58	19.59
Cr_2O_3	0.06	0.08	0.01		0.08	
FeO	34.97	36.76	16.60	(15.9-19.8)	34.66	0.07
MnO	1.87	2.08	0.01		0.58	
MgO	4.64	3.63	13.95	(12.5-14.8)	13.09	
CaO	1.25	1.08			0.06	0.94
Na_2O						3.81
K_2O			9.85			10.91
	100.27	100.87	96.43		99.29	100.61
Fe	77.96	82.40	40.03		59.68	An 4.5
Mg	18.48	14.50	59.94		40.18	Ab 33.1
Ca	3.58	3.10	0.03		0.14	Or 62.4
Fe/Fe + Mn + Mg	0.77	0.81	0.40		0.60	
O	24		22		6	
Si	5.802	5.810	5.758		1.882	
Ti	0.016	0.011	0.423		0.007	
Al	4.041	4.024	2.363		0.169	
Cr	0.008	0.010	0.001		0.003	
Fe	4.705	4.962	2.064		1.161	
Mn	0.255	0.284	0.001		0.020	
Mg	1.114	0.873	3.090		0.781	
Ca	0.216	0.187			0.003	
Na						
K			1.868			
	16.158	16.161	15.568		4.026	

Remarks OPX - strongly pleochroic; BIO - chestnut.

FS-77-289

	GA	BIO	OPX	SP	PG
SiO_2	37.54	37.60	47.70	0.41	65.72
TiO_2	0.10	4.32	0.24	0.08	
Al_2O_3	21.87	14.51	8.33	56.18	22.09
Cr_2O_3	0.09	0.04	0.09	0.38	
Fe_2O_3				4.15	
FeO	30.46	12.84	23.45	28.82	0.05
MnO	1.04		0.22	0.07	
MgO	8.23	16.37	19.94	8.09	
CaO	0.89				4.21
Na_2O					8.32
K_2O		10.39			0.40
	100.04	96.27	99.97	100.18	100.79
Fe	66.21	30.55	39.75	69.31	An 21.3
Mg	31.86	69.45	60.25	30.69	Ab 76.3
Ca	1.92				Or 2.4
Fe/Fe + Mn + Mg	0.66	0.31	0.40	0.69	
O	24	22	6	32	
Si	5.874	5.560	1.787	0.090	
Ti	0.012	0.478	0.007	0.013	
Al	4.033	2.515	0.368	15.117	
Cr	0.011	0.005	0.003	0.066	
Fe^3				0.688	
Fe^2	3.989	1.579	0.735	5.313	
Mn	0.138		0.007	0.013	
Mg	1.920	3.589	1.114	2.658	
Ca	0.116				
Na					
K		1.950			
	16.093	15.676	4.021	23.958	

Remarks OPX - strongly pleochroic: pink to pale bluish; BIO - chestnut; trace sillimanite in KF; PG mantles SP in OPX.

Table 3. Analyses and structural formulae of minerals of marble and calc-silicate rock

FS-77-20B

	CPX		HBL			BIO	
SiO_2	54.13	54.27	47.38	(44.9-49.7)	56.50	40.65	37.95
TiO_2	0.03	0.01	0.33	(0.1-0.5)	0.03	4.04	6.45
Al_2O_3	1.26	1.92	9.47	(7.4-12.0)	1.36	13.69	13.95
Cr_2O_3	0.06	0.11	0.07		0.02	0.14	0.06
FeO	1.07	2.28	1.92		1.21	1.54	1.28
MnO	0.03	0.05	0.02		0.04	0.05	0.12
MgO	18.49*	17.51	21.68		24.44	26.58	25.58
CaO	25.19	25.27	13.01		13.32		
Na_2O	0.17	0.14	3.16		1.03		
K_2O			0.76		0.12	8.39	6.82
	100.43	100.66	97.80		98.07	95.08	92.33
Fe	1.60	3.46	3.36		1.95	3.14	2.72
Mg	49.72	47.39	67.52		70.45	96.86	97.28
Ca	48.68	49.15	29.12		27.60		
Fe/Fe + Mn + Mg	0.03	0.07	0.05		0.03	0.03	0.03
Notes	low Fe	high Fe		discrete	overgrowth on CPX	1 grain	1 grain
O		6		23		22	
Si	1.954	1.965	6.865		7.721	5.858	5.416
Ti	0.001		0.035		0.003	0.423	0.692
Al	0.054	0.043	1.570		0.219	2.246	2.346
Cr	0.002	0.003	0.008		0.002	0.015	0.009
Fe	0.032	0.069	0.226		0.138	0.179	0.153
Mn	0.001	0.001	0.002		0.005	0.006	0.015
Mg	0.995	0.945	4.546		4.979	5.515	5.463
Ca	0.974	0.980	1.961		1.950		
Na	0.012	0.010	0.862		0.273		
K			0.136		0.021	1.490	1.242
	4.025	4.016	16.011		15.311	15.533	15.335

Remarks CPX, HBL, BIO - colourless.

FSD-77-148-1

	CPX	SCA	WO
SiO_2	52.43	44.88	50.82
TiO_2	0.05		
Al_2O_3	1.47	27.30	0.44
Cr_2O_3	0.15	0.06	0.20
FeO	8.08	0.12*	0.24
MnO	0.06		0.04
MgO	13.84	0.43	0.39
CaO	24.80	19.61	46.52
Na_2O	0.19	3.29	0.04
K_2O		0.43	
	100.87	96.12	98.69

*Total iron as Fe_2O_3

Fe	12.58	0.56	0.36
Mg	38.40	2.76	0.11
Ca	49.02	96.68	99.53
Fe/Fe + Mn + Mg	0.25	0.17	0.75
O	6		18
Si	1.946	6.991	5.969
Ti	0.001		
Al	0.064	5.009	0.056
Cr	0.004		0.014
Fe	0.251	0.019	0.021
Mn	0.002		
Mg	0.766	0.093	0.007
Ca	0.978	3.262	5.856
Na	0.014	0.991	0.014
K		0.075	
	4.026	16.440	11.937

Remarks SCA analysis recalculated on basis of (Si + Al) atoms = 12

FSM-77-62

	CPX	
SiO_2	54.26	53.38
TiO_2		
Al_2O_3	0.83	0.85
Cr_2O_3	0.12	0.12
FeO	3.35	6.22
MnO	0.05	0.11
MgO	17.05	15.04
CaO	24.83	24.64
Na_2O	0.30	0.13
K_2O		
	100.79	100.49
Fe	5.10	9.63
Mg	48.36	41.50
Ca	48.53	48.87
Fe/Fe + Mn + Mg	0.10	0.19
Notes	low Fe	high Fe
O	6	
Si	1.970	1.969
Ti		
Al	0.035	0.037
Cr	0.004	0.004
Fe	0.102	0.192
Mn	0.002	0.003
Mg	0.923	0.827
Ca	0.966	0.974
Na	0.021	0.009
K		
	4.023	4.015

Remarks SCA inclusions

FS-77-223

	CPX	CHU	SP
SiO_2	55.11	38.54	0.17
TiO_2		0.17	0.05
Al_2O_3	0.27	0.06	68.94
Cr_2O_3	0.06		0.15
Fe_2O_3			1.54
FeO	0.51	2.41	3.47
MnO	0.02	0.09	0.06
MgO	19.61	55.19	25.76
CaO	25.16	0.12	
Na_2O			
K_2O			
	100.74	96.58	100.14
Fe	0.75	2.39	9.55
Mg	51.53	97.47	90.23
Ca	47.52	0.14	0.22
Fe/Fe + Mn + Mg	0.01	0.02	0.10
O	6	17	22
Si	1.975	4.046	0.033
Ti		0.013	0.007
Al	0.011	0.07	15.705
Cr	0.002		0.029
Fe^3			0.224
Fe^2	0.015	0.212	0.561
Mn		0.008	0.010
Mg	1.048	8.637	7.422
Ca	0.966	0.013	
Na			
K			
	4.018	12.937	23.985

Remarks CHU-weakly pleochroic (very pale yellow); SP - very pale green

FSM-77-198

	CPX	HBL	BIO	ZO		PG	
SiO_2	54.16	54.76	41.69	38.94		51.25	50.35
TiO_2		0.04	0.42	0.01			
Al_2O_3	1.59	3.97	14.19	32.86		30.91	31.74
Cr_2O_3	0.10	0.09	0.05	0.09			
FeO	1.39	2.22	2.12	0.46*			0.03
MnO	0.13	0.15	0.11				
MgO	18.24	22.39	26.15	0.38			
CaO	24.95	13.15		24.53		13.44	14.26
Na_2O		0.60				3.65	3.19
K_2O		0.23	10.42			0.11	0.09
	100.56	97.60	95.15	97.27		99.36	99.66
	* Total Fe as Fe_2O_3						
Fe	2.11	3.76	4.35	1.25	An	66.7	70.8 (66-76)
Mg	49.35	67.87	95.65	2.11	Ab	32.7	28.7
Ca	48.54	28.57		96.64	Or	0.6	0.5
Fe/Fe + Mn + Mg	0.04	0.05	0.04	0.37			
O	6	23	22	32			
Si	1.952	7.547	5.855	2.978			
Ti		0.004	0.044				
Al	0.067	0.645	2.349	2.962			
Cr	0.003	0.010	0.006	0.005			
Fe	0.042	0.256	0.249	0.028			
Mn	0.004	0.018	0.014				
Mg	0.980	4.600	5.475	0.044			
Ca	0.964	1.942		2.010			
Na		0.160					
K		0.040	1.866				
	4.012	15.222	15.858	8.025			

Remarks HBL - colourless; BIO - colourless to very pale brown.

FSM-77-107-1

	OL	CHU		SP	
				C	R
SiO_2	40.25	37.41	37.28	0.17	0.19
TiO_2	0.04	0.51	0.46	0.13	0.08
Al_2O_3				64.59	65.60
Cr_2O_3				0.22	0.21
Fe_2O_3				4.37	1.72
FeO	14.85	9.02	10.01	12.16	12.26
MnO	0.38	0.27	0.27	0.28	0.19
MgO	45.80	50.43	50.10	19.81	19.54
CaO	0.02	0.01	0.05		
Na_2O					
K_2O					
	101.34	97.65	98.17	101.73	99.79
Fe	15.39	9.12	10.07	31.31	28.39
Mg	84.59	90.87	89.86	68.69	71.61
Ca	0.02	0.01	0.07		
Fe/Fe + Mn + Mg	0.15	0.09	0.10	0.31	0.28
Notes		low Fe	high Fe		
O	4	17		32	
Si	0.996	4.011	3.996	0.034	0.038
Ti	0.001	0.041	0.037	0.020	0.012
Al				15.239	15.539
Cr				0.035	0.034
Fe^3				0.658	0.262
Fe^2	0.307	0.809	0.897	2.036	2.074
Mn	0.008	0.025	0.025	0.047	0.033
Mg	1.690	8.061	8.006	5.911	5.891
Ca		0.001	0.006		
Na					
K					
	3.003	12.948	12.967	23.980	23.982

Remarks CHU - pleochroic (colourless to yellow); SP has green cores and brownish green rims

FSM-77-190-2

	OL	CHU	SP
SiO_2	42.88	38.47	0.13
TiO_2	0.06	0.47	0.14
Al_2O_3			69.31
Cr_2O_3			0.09
Fe_2O_3			0.89
FeO	2.68	1.83	2.33
MnO	0.14	0.12	0.09
MgO	54.95	55.06	26.37
CaO	0.03	0.06	
Na_2O			
K_2O			
	100.74	96.01	99.35
Fe	2.66	1.83	6.25
Mg	97.30	98.09	93.75
Ca	0.04	0.08	
Fe/Fe + Mn + Mg	0.03	0.02	0.06
Note		overgrows OL	
O	4	17	32
Si	1.008	4.051	0.025
Ti	0.001	0.037	0.020
Al			15.800
Cr			0.014
Fe^3			0.130
Fe^2	0.053	0.161	0.377
Mn	0.003	0.011	0.015
Mg	1.926	8.644	7.803
Ca	0.001	0.007	
Na			
K			
	2.992	12.911	23.983

Remarks CHU - pleochroic (colourless to yellow); SP - pale brown.

FS-77-41

	CPX	GA
SiO_2	53.82	39.22
TiO_2	0.02	
Al_2O_3	1.31	22.47
Cr_2O_3	0.07	0.08
FeO	4.04	0.60
MnO	0.01	0.03
MgO	16.19	0.35
CaO	24.49	36.90
Na_2O	0.22	
K_2O		
	100.17	99.65
Fe	6.29	1.24
Mg	44.90	1.29
Ca	48.81	97.47
Fe/Fe + Mn + Mg	0.12	0.48
O	6	24
Si	1.968	5.926
Ti		
Al	0.056	4.001
Cr	0.002	0.010
Fe	0.124	0.076
Mn		0.004
Mg	0.883	0.079
Ca	0.960	5.974
Na	0.016	
K		
	4.010	16.070

Table 4. Analyses and structural formulae of minerals of pyribolite

FS-77-157

	OPX	CPX	HBL	BIO		PG	
SiO_2	50.90	51.66	42.48	37.37		56.75	
TiO_2	0.21	0.26	2.97	5.05			
Al_2O_3	0.96	1.82	10.74	13.33		28.06	
Cr_2O_3	0.12	0.13	0.20	0.33			
FeO	26.72	10.97	14.30	15.55		0.12	
MnO	0.40	0.17	0.09				
MgO	20.24	13.78	12.47	14.81			
CaO	0.83	21.17	11.39			9.92	
Na_2O		0.09	1.79	0.06		5.64	
K_2O			1.37	9.66		0.25	
	100.38	100.05	97.90	96.16		100.74	
Fe	41.84	17.51	27.98	37.07	An	48.5	52-59
Mg	56.49	39.20	43.47	62.92	Ab	50.0	40-47
Ca	1.67	43.29	28.55	0.01	Or	1.5	1.1-1.7
Fe/Fe + Mn + Mg	0.42	0.31	0.39	0.37			
Notes							in HBL-rich layer
O	6	6	23	22			
Si	1.937	1.941	6.341	5.570			
Ti	0.006	0.007	0.333	0.566			
Al	0.043	0.081	1.890	2.342			
Cr	0.004	0.004	0.024	0.039			
Fe	0.850	0.345	1.785	1.938			
Mn	0.013	0.005	0.011	0.001			
Mg	1.148	0.772	2.774	3.290			
Ca	0.034	0.852	1.822				
Na		0.006	0.518	0.017			
K			0.261	1.838			
	4.035	4.013	15.759	15.601			

Remarks OPX-weakly pleochroic; HBL - very pale brown to chestnut; BIO-reddish brown.

FSM-77-113-2

	OPX	CPX	BIO	PG		ACT
SiO_2	50.81	51.60	36.59	50.09		53.17
TiO_2	0.16	0.15	5.40			0.23
Al_2O_3	0.81	1.61	13.11	32.49		3.35
Cr_2O_3	0.04	0.12	0.18	0.14		0.11
FeO	29.30	12.36	17.49			14.66
MnO	0.52	0.24	0.01			0.17
MgO	18.69	13.33	13.14			15.05
CaO	0.87	20.89		15.03		11.96
Na_2O		0.39		2.84		
K_2O			9.55	0.16		0.28
	101.20	100.69	95.47	100.75		98.98
Fe	45.98	19.65	42.75	An 73.8	(73-78)	
Mg	52.27	37.78	57.25	Ab 25.2		
Ca	1.75	42.57		Or 1.0		
Fe/Fe + Mn + Mg	0.46	0.34	0.43			
O	6	6	22			
Si	1.941	1.940	5.551			
Ti	0.005	0.004	0.616			
Al	0.037	0.071	2.344			
Cr	0.001	0.004	0.021			
Fe	0.936	0.389	2.219			
Mn	0.017	0.008	0.002			
Mg	1.064	0.747	2.972			
Ca	0.036	0.842				
Na		0.028				
K			1.848			
	4.037	4.033	15.573			

Remarks OPX-weakly pleochroic; CPX-neutral; BIO-orangey brown; ACT-very pale green, in x-cutting late vein.

FS-82-D-24B

	OPX	CPX	HBL	BIO	PG	
SiO_2	50.50	51.47	42.37	36.89	49.70	
TiO_2	0.11	0.16	1.82	5.94		
Al_2O_3	1.62	2.54	11.28	13.39	32.66	
Cr_2O_3	0.08	0.12	0.14	0.10		
FeO	26.66	10.38	15.19	15.74	0.17	
MnO	0.48	0.18	0.09	0.02		
MgO	20.69	13.82	12.29	14.42		
CaO	0.40	21.24	10.76		15.36	
Na_2O		0.10	1.51		2.64	
K_2O			1.79	9.82	0.13	
	100.54	100.01	97.24	96.12	100.66	
Fe	41.62	16.68	29.85	37.97	An 75.7	(54-79)
Mg	57.58	39.59	43.06	62.03	Ab 23.5	(21-44)
Ca	0.80	43.73	27.08		Or 0.8	(0-1.6)
Fe/Fe + Mn + Mg	0.42	0.29	0.41	0.38		
O	6	6	23	22		
Si	1.917	1.929	6.378	5.509		
Ti	0.003	0.004	0.205	0.667		
Al	0.072	0.112	2.001	2.356		
Cr	0.002	0.004	0.016	0.012		
Fe	0.846	0.325	1.912	1.965		
Mn	0.015	0.006	0.011	0.003		
Mg	1.170	0.772	2.758	3.211		
Ca	0.016	0.853	1.735			
Na		0.008	0.440			
K			0.343	1.833		
	4.041	4.013	15.799	15.556		

Remarks OPX-pleochroic; HBL - olive; BIO - deep chestnut

Table 4 (cont.)

FSM-77-24-1

	OPX	CPX		HBL	PG
SiO_2	49.72	50.95	51.25	42.06	48.58
TiO_2	0.10	0.18	0.46	1.81	
Al_2O_3	0.91	1.86	1.76	10.89	33.49
Cr_2O_3	0.08	0.10	0.14	0.14	
FeO	32.39	13.13	13.00	17.56	0.22
MnO	0.80	0.34	0.29	0.15	
MgO	16.19	12.14	12.27	10.67	
CaO	0.55	21.02	20.81	11.14	16.23
Na_2O		0.27	0.21	2.19	2.27
K_2O				1.03	0.12
	100.74	99.97	100.19	97.64	100.91
Fe	52.28	21.27	21.13	34.53	An 79.2
Mg	46.58	35.07	35.53	37.41	Ab 20.1
Ca	1.14	43.66	43.54	28.06	Or 0.7
Fe/Fe + Mn + Mg	0.52	0.37	0.37	0.48	
Notes			rims HBL		
O	6		6	23	
Si	1.940	1.938	1.941	6.377	
Ti	0.003	0.005	0.013	0.207	
Al	0.042	0.083	0.079	1.946	
Cr	0.003	0.003	0.004	0.016	
Fe	1.057	0.418	0.412	2.227	
Mn	0.027	0.011	0.009	0.020	
Mg	0.942	0.688	0.693	2.412	
Ca	0.023	0.857	0.845	1.809	
Na		0.020	0.015	0.643	
K				200	
	4.037	4.023	4.011	15.857	

Remarks OPX-weakly pleochroic; HBL - very pale brown to brown.

FSM-77-63-4

	OPX	CPX	HBL	BIO	PG
SiO_2	52.01	52.14	41.85	35.57	60.06
TiO_2	0.12	0.12	1.84	4.85	
Al_2O_3	1.10	2.09	10.89	14.28	26.13
Cr_2O_3	0.06	0.13	0.16	0.07	
FeO	24.23	9.80	14.87	15.96	0.09
MnO	0.67	0.29	0.13	0.05	
MgO	22.42	14.39	12.52	14.68	
CaO	0.71	21.16	11.22		7.40
Na_2O		0.15	2.26		7.26
K_2O			1.22	9.57	0.22
	101.32	100.29	96.96	96.02	101.16
Fe	37.22	15.66	26.84	37.90	An 35.6
Mg	61.38	40.98	43.28	62.10	Ab 63.1
Ca	1.40	43.36	27.88		Or 1.3
Fe/Fe + Mn + Mg	0.37	0.27	0.40	0.38	
O	6	6	23	22	
Si	1.935	1.943	6.329	5.468	
Ti	0.003	0.003	0.209	0.545	
Al	0.048	0.092	1.941	2.517	
Cr	0.002	0.004	0.019	0.008	
Fe	0.754	0.305	1.880	1.996	
Mn	0.021	0.009	0.016	0.007	
Mg	1.244	0.799	2.822	3.271	
Ca	0.028	0.846	1.818		
Na		0.011	0.861		
K			0.234	1.826	
	4.035	4.012	15.929	15.638	

Remarks OPX-distinctly pleochroic; CPX-very pale green; HB-olive; BIO-deep chestnut.

FSM-77-173-2

	OPX	CPX	HBL	PG	
SiO_2	50.97	51.78	43.44	55.11	
TiO_2	0.13	0.13	1.41		
Al_2O_3	1.18	2.04	10.03	29.29	
Cr_2O_3	0.09	0.13	0.24		
FeO	25.74	10.64	14.57	0.23	
MnO	0.61	0.25	0.11		
MgO	21.12	13.87	13.49		
CaO	0.68	20.49	10.82	11.43	
Na_2O		0.16	1.83	4.88	
K_2O			1.31	0.33	
	100.52	99.49	97.25	101.27	
Fe	40.06	17.27	27.77	An 55.3	(53-59)
Mg	58.59	40.13	45.82	Ab 42.8	
Ca	1.36	42.60	26.41	Or 1.9	
Fe/Fe + Mn + Mg	0.40	0.30	0.38		
O	6	6	23		
Si	1.928	1.949	6.504		
Ti	0.004	0.004	0.159		
Al	0.053	0.090	1.770		
Cr	0.003	0.004	0.028		
Fe	0.815	0.335	1.825		
Mn	0.019	0.008	0.014		
Mg	1.191	0.778	3.011		
Ca	0.028	0.826	1.736		
Na		0.012	0.533		
K			0.250		
	4.041	4.006	15.830		

Remarks OPX-weakly pleochroic; CPX-very pale green, HBL-pale yellowish to greenish brown.

FSM-77-108

	CPX	BIO	PG	
SiO_2	52.85	36.82	65.59	
TiO_2	0.06	3.59		
Al_2O_3	1.25	13.15	22.27	
Cr_2O_3	0.12	0.09		
FeO	9.88	18.35	0.21	
MnO	0.26	0.07		
MgO	13.52	13.81		
CaO	22.10		2.99	
Na_2O	0.74	0.02	9.59	
K_2O		9.74	0.33	
	100.78	95.64	100.98	
Fe	15.86	42.70	An 14.4	
Mg	38.69	57.30	Ab 83.7	
Ca	45.45		Or 1.9	
Fe/Fe + Mn + Mg	0.29	0.43		
O	6	22		
Si	1.967	5.601		
Ti	0.002	0.411		
Al	0.055	2.358		
Cr	0.003	0.011		
Fe	0.308	2.335		
Mn	0.008	0.010		
Mg	0.750	3.132		
Ca	0.881			
Na	0.054	0.005		
K		1.891		
	4.028	15.754		

Remarks CPX-pale green; BIO - pale brown to brown.

FSM-77-148-2

	OPX	CPX	BIO	PG	
SiO_2	52.54	51.06	38.73	54.37	
TiO_2	0.16	0.26	4.73		
Al_2O_3	1.28	2.81	12.92	29.53	
Cr_2O_3	0.05	0.11	0.06		
FeO	20.51	9.11	9.85	0.28	
MnO	0.45	0.22	0.04		
MgO	25.62	14.57	19.20		
CaO	0.61	21.64		11.61	
Na_2O		0.13		4.57	
K_2O			9.98	0.53	
	101.22	99.91	95.53	100.89	
Fe	30.83	14.51	22.34	An 56.6	
Mg	68.20	41.34	77.66	Ab 40.3	
Ca	1.17	44.15		Or 3.1	
Fe/Fe + Mn + Mg	0.31	0.26	0.22		
O	6	6	22		
Si	1.922	1.909	5.651		
Ti	0.004	0.007	0.519		
Al	0.055	0.124	2.223		
Cr	0.002	0.003	0.010		
Fe	0.627	0.285	1.202		
Mn	0.014	0.007	0.005		
Mg	1.397	0.812	4.176		
Ca	0.024	0.867			
Na		0.009			
K			1.857		
	4.045	4.023	15.643		

Remarks OPX-trace HBL inclusions; BIO-chestnut.

FS-77-257

	OPX	CPX	HBL	PG	
SiO_2	51.27	52.30	44.19	49.35	
TiO_2	0.10	0.06	1.06		
Al_2O_3	1.05	1.57	10.34	33.28	
Cr_2O_3	0.08	0.12	0.15		
FeO	24.84	9.82	14.26	0.23	
MnO	0.64	0.28	0.15		
MgO	21.53	14.69	13.72		
CaO	0.77	21.71	11.17	16.11	
Na_2O		0.12	1.92	2.24	
K_2O			0.70	0.11	
	100.28	100.47	97.66	101.32	
Fe	38.68	15.12	26.89	An 79.4	(78-81)
Mg	59.78	41.16	46.12	Ab 20.0	
Ca	1.54	43.72	26.99	Or 0.6	
Fe/Fe + Mn + Mg	0.39	0.27	0.37		
O	6	6	23		
Si	1.936	1.947	6.548		
Ti	0.003	0.002	0.118		
Al	0.047	0.069	1.807		
Cr	0.002	0.003	0.017		
Fe	0.784	0.299	1.767		
Mn	0.020	0.009	0.019		
Mg	1.212	0.815	3.031		
Ca	0.031	0.866	1.774		
Na		0.009	0.551		
K			0.133		
	4.035	4.019	15.765		

Remarks OPX-weakly pleochroic; CPX - very pale green; HBL-olive

Table 5. Analyses and structural formulae of minerals of orthopyroxene tonalite and granite

FS-77-283

	OPX	BIO	PG		
SiO_2	49.63	36.74	59.71	59.33	
TiO_2	0.17	5.32			
Al_2O_3	2.82	14.32	25.84	25.92	
Cr_2O_3	0.08	0.06			
FeO	26.05	16.17	0.43	0.25	
MnO	0.91	0.05			
MgO	20.57	13.78			
CaO	0.19		7.31	7.55	
Na_2O			7.13	6.67	
K_2O		9.88	0.34	0.27	
	100.42	96.32	100.78	99.99	
Fe	41.38	39.70	An 35.5	37.8	(34-38)
Mg	58.24	60.30	Ab 62.5	60.6	
Ca	0.38		Or 2.0	1.6	
Fe/Fe + Mn + Mg	0.41	0.40			
Notes			low Ca	high Ca	
O	6	22			
Si	1.885	5.488			
Ti	0.005	0.598			
Al	0.126	2.521			
C	0.002	0.007			
Fe	0.827	2.020			
Mn	0.029	0.006			
Mg	1.164	3.068			
Ca	0.008				
Na					
K		1.883			
	4.046	15.591			

Remarks OPX-distinctly pleochroic; BIO - chestnut.

FS-77-266

	OPX	HBL	BIO	PG	
SiO_2	51.33	44.74	37.01	61.64	60.94
TiO_2	0.12	1.71	5.47		
Al_2O_3	0.93	8.36	13.21	24.96	24.22
Cr_2O_3	0.06	0.08	0.04		
FeO	23.14	14.22	14.07	0.18	0.28
MnO	0.71	0.19	0.08		
MgO	22.84	14.19	15.42		
CaO	0.71	11.37		6.28	6.10
Na_2O		1.69		7.65	7.23
K_2O		1.02	9.69	0.45	0.77
	99.84	97.57	94.99	101.16	99.54
Fe	35.74	26.29	33.86	An 30.4	30.3
Mg	62.86	46.78	66.14	Ab 67.0	65.1
Ca	1.40	26.93		Or 2.6	4.6
Fe/Fe + Mn + Mg	0.36	0.36	0.34		
Notes					K-rich
O	6	23	22		
Si	1.939	6.655	5.552		
Ti	0.003	0.191	0.618		
Al	0.041	1.467	2.336		
Cr	0.002	0.009	0.005		
Fe	0.729	1.769	1.765		
Mn	0.023	0.024	0.010		
Mg	1.282	3.148	3.448		
Ca	0.029	1.812			
Na		0.487			
K		0.194	1.855		
	4.042	15.758	15.589		

Remarks OPX-non-pleochroic (neutral); HBL-olive, BIO-chestnut; PG-clouded.

FSM-77-225

	OPX	CPX	HBL	KF		ACT
SiO_2	51.80	52.02	45.90	65.60	65.02	50.80
TiO_2	0.15	0.13	1.34			
Al_2O_3	0.64	1.46	7.10	21.45	21.05	1.83
Cr_2O_3	0.08	0.15	0.09			0.16
FeO	22.71	10.00	11.29	0.21	0.22	7.70
MnO	0.78	0.30	0.17			0.10
MgO	23.08	14.37	16.14			19.65
CaO	0.68	20.39	11.17	2.39	2.42	11.65
Na_2O		0.55	2.17	6.66	7.23	0.42
K_2O			1.03	5.21	4.01	0.27
	99.92	99.37	96.40	101.52	99.95	92.58
Fe	35.08	16.20	20.77	An 11.6	11.9	(11-13)
Mg	63.57	41.49	52.90	Ab 58.3	64.6	(57-66)
Ca	1.35	42.31	26.32	Or 30.1	23.5	(22-32)
Fe/Fe + Mn + Mg	0.35	0.28	0.28			
Notes				mesoperthite		rims OPX
O	6	6	23			
Si	1.944	1.958	6.818			
Ti	0.004	0.004	0.149			
Al	0.028	0.065	1.243			
Cr	0.002	0.004	0.010			
Fe	0.713	0.315	1.403			
Mn	0.025	0.010	0.021			
Mg	1.292	0.808	3.574			
Ca	0.028	0.822	1.778			
Na		0.040	0.624			
K			0.195			
	4.036	4.024	15.815			

Remarks OPX - slightly pleochroic; CPX - pale green; HBL - olive; ACT - pale green

FSM-77-203-1

	OPX	BIO	PG	
SiO_2	51.83	38.46	62.39	
TiO_2	0.16	4.82		
Al_2O_3	1.30	12.68	24.53	
Cr_2O_3	0.07	0.06		
FeO	22.50	11.58	0.26	
MnO	0.48	0.06		
MgO	23.85	17.81		
CaO	0.43		5.86	
Na_2O			7.85	
K_2O		9.94	0.59	
	100.42	95.23	101.48	
Fe	34.34	26.74	An 28.2	(27-30)
Mg	64.83	73.26	Ab 68.4	(67-70)
Ca	0.83		Or 3.4	(2.4-5.2)
Fe/Fe + Mn + Mg	0.34	0.27		
O	6	22		
Si	1.923	5.680		
Ti	0.004	0.513		
Al	0.057	2.207		
Cr	0.002	0.007		
Fe	0.701	1.430		
Mn	0.015	0.007		
Mg	1.323	3.919		
Ca	0.017			
Na				
K		1.871		
	4.042	15.634		

Remarks OPX-pleochroic; BIO-brown, PG-clouded.

Table 6. Analyses and structural formulae of minerals of amphibolite facies gneiss

FS-77-147

	CUM	BIO	PG
SiO_2	53.50	35.62	57.25
TiO_2	0.09	4.18	
Al_2O_3	0.80	14.14	27.50
Cr_2O_3	0.09	0.06	
FeO	29.54	22.18	0.09
MnO	0.42	0.04	
MgO	15.76	10.40	
CaO	0.54		8.93
Na_2O	0.05		6.48
K_2O	0.06	9.37	0.23
	100.85	95.99	100.48
Fe	50.65	54.47	An 42.7
Mg	48.17	45.53	Ab 56.0
Ca	1.18		Or 1.3
Fe/Fe + Mn + Mg	0.51	0.54	
O	23	22	
Si	7.794	5.492	
Ti	0.010	0.485	
Al	0.137	2.570	
Cr	0.010	0.007	
Fe	3.599	2.861	
Mn	0.052	0.006	
Mg	3.423	2.391	
Ca	0.084		
Na	0.014		
K	0.011	1.844	
	15.134	15.658	

Remarks CUM-replacement of OPX; BIO-deep chestnut.

FS-77-344

	BIO	HBL
SiO_2	38.23	47.52
TiO_2	1.56	0.17
Al_2O_3	13.43	5.93
Cr_2O_3	0.04	0.05
FeO	17.85	16.44
MnO	0.19	0.32
MgO	14.29	13.51
CaO		11.49
Na_2O		1.29
K_2O	9.81	0.58
	95.40	97.40
Fe	41.20	29.77
Mg	58.80	43.58
Ca		26.65
Fe/Fe + Mn + Mg	0.41	0.40
O	22	23
Si	5.790	7.097
Ti	0.178	0.020
Al	2.398	1.043
Cr	0.004	0.006
Fe	2.261	2.054
Mn	0.025	0.040
Mg	3.227	3.008
Ca		1.839
Na		0.374
K	1.895	0.129
	15.778	15.510

Remarks BIO-very pale brown to pale olive; HBL-very pale yellowish to slightly bluish green.

Table 7. Hornblende analyses recalculated according to the method of Rock and Leake (1984)

	1	2	3	4	5	6	7	8	9	10	11	12	13	14	15	16	17
SiO_2	45.25	42.27	41.05	40.92	47.38	56.50	54.78	42.48	44.19	42.06	43.44	41.85	42.37	44.74	45.90	53.50	47.52
Al_2O_3	8.65	10.40	10.27	11.19	9.47	1.36	3.97	10.74	10.34	10.89	10.03	10.89	11.28	8.36	7.10	.80	5.93
Fe_2O_3	0.00	0.00	0.00	0.00	0.00	0.00	0.00	0.00	0.00	0.00	0.00	0.00	0.00	0.00	0.00	0.00	0.00
FeO	12.13	18.58	20.43	21.20	1.92	1.21	2.22	14.30	14.26	17.56	14.57	14.87	15.19	14.22	11.29	29.54	16.44
MgO	15.14	10.46	9.20	8.31	21.68	24.44	22.39	12.47	13.72	10.67	13.49	12.52	12.29	14.19	16.14	15.76	13.51
CaO	11.89	11.33	10.99	11.21	13.01	13.32	13.15	11.39	11.17	11.14	10.82	11.22	10.76	11.37	11.17	.54	11.49
Na_2O	1.22	1.24	1.73	1.49	3.16	1.03	.60	1.79	1.92	2.19	1.83	2.26	1.51	1.89	2.17	.05	1.29
K_2O	1.16	1.46	1.87	1.89	.76	.12	.23	1.37	.70	1.03	1.31	1.22	1.79	1.02	1.03	.06	.68
TiO_2	1.81	1.58	1.65	1.77	.33	.03	.04	2.97	1.06	1.81	1.41	1.84	1.82	1.71	1.34	.09	.17
MnO	.13	.19	.26	.09	.02	.04	.15	.09	.15	.15	.11	.13	.09	.19	.17	.42	.32
Cr_2O_3	.20	.06	.10	.07	.07	.02	.09	.20	.15	.14	.24	.16	.14	.08	.09	.09	.05
Total	97.38	97.57	97.55	98.14	97.80	98.07	97.80	97.80	97.66	97.84	97.25	96.96	97.24	97.57	96.40	100.85	97.40
Cations per formula unit																	
O =	23.0	23.0	23.0	23.0	23.0	23.0	23.0	23.0	23.0	23.0	23.0	23.0	23.0	23.0	23.0	23.0	23.0
Si	6.551	6.312	6.241	6.208	6.837	7.698	7.505	6.264	6.396	6.278	6.351	6.224	6.241	6.523	6.704	7.729	6.953
Al	1.477	1.832	1.842	2.002	1.565	.219	.642	1.868	1.765	1.917	1.730	1.910	1.960	1.438	1.223	.136	1.024
Fe^3	.822	.921	.833	.723	.186	.138	.254	.555	1.061	.711	1.076	.754	.975	.912	.762	.384	.931
Fe^2	.646	1.398	1.763	1.966	.039	0.000	0.000	1.207	.664	1.480	.704	1.095	.895	.821	.617	3.183	1.080
Mg	3.269	2.329	2.086	1.880	4.529	4.966	4.576	2.742	2.962	2.375	2.941	2.777	2.700	3.085	3.516	3.395	2.948
Ca	1.813	1.812	1.790	1.822	1.952	1.944	1.931	1.799	1.732	1.781	1.695	1.788	1.698	1.776	1.748	.084	1.801
Na	.342	.359	.510	.438	.858	.272	.159	.512	.539	.634	.519	.652	.431	.478	.614	.014	.366
K	.214	.278	.383	.366	.136	.021	.040	.258	.129	.196	.244	.232	.336	.190	.192	.011	.127
Ti	.197	.177	.189	.202	.035	.003	.004	.329	.115	.203	.155	.206	.202	.188	.147	.010	.019
Mn	.016	.024	.034	.012	.002	.005	.017	.011	.018	.019	.014	.016	.011	.023	.021	.051	.040
Total	15.35	15.44	15.65	15.62	15.94	15.27	15.13	15.54	15.38	15.59	15.43	15.65	15.45	15.43	15.54	15.00	15.29
Check on Oxygen (+CL, F) equivalence of above cations																	
Oxeq =	23.00	23.00	23.00	23.00	23.00	23.00	23.00	23.00	23.00	23.00	23.00	23.00	23.00	23.00	23.00	23.00	23.00
IMA (1978) Classification Parameters																	
CANA	2.000	2.000	2.000	2.000	2.000	1.971	1.992	2.000	2.000	2.000	2.000	2.000	2.000	2.000	2.000	.098	2.000
NAB	.187	.188	.210	.178	.048	.026	.061	.201	.268	.219	.305	.212	.302	.224	.252	.014	.199
NAKA	.370	.449	.663	.626	.946	.267	.138	.569	.400	.611	.458	.671	.456	.444	.554	.011	.294
ALVI	.028	.143	.083	.210	.201	0.000	.146	.132	.162	.195	.081	.134	.201	0.000	0.000	0.000	0.000
MGFE	.835	.625	.542	.489	.991	1.000	1.000	.694	.817	.616	.807	.717	.751	.790	.851	.516	.732

General notes for the above table: Results have not been checked or adjusted for high cation totals. Total Fe determined as FeO has been reallocated wherever possible between Fe^2 and Fe^3. Number of oxygens was pre-set to 23. Sum of cations S2 was brought to 13.0 by redistribution of total Fe between Fe^2 and Fe^3.

IMA (1978) names for the above table:

Garnet-free orthopyroxene tonalite gneiss
1. FS-77-207
   Ferrian Magnesio-hornblende
2. FS-78-10
   Potassian Ferrian Tschermakitic Hornblende
3. FS-78-25
   Potassian Magnesian Hastingsite

Garnet-orthopyroxene tonalite gneiss
4. FS-78-20
   Potassian Magnesian Hastingsite

Marble and calc-silicate rock
5. FS-77-20B
   Edenitic Hornblende
6. FS-77-20B
   Warning: All FeO has been converted to Fe_2O_3 but sum of cations S2 still more than 13.0.
   Tremolite
7. FS-77-198
   Warning: All FeO has been converted to Fe_2O_3 but sum of cations S2 still more than 13.0.
   Tremolite

Pyribolite
8. FS-77-157
   Titanian Potassian Magnesian Hastingsitic Hornblende
9. FSM-77-257
   Ferri-tschermakitic Hornblende
10. FSM-77-24-1
    Magnesian Hastingsitic Hornblende
11. FSM-77-173-2
    Ferri-tschermakitic Hornblende
12. FSM-77-63-4
    Magnesio-hastingsite
13. FS-82-D-24B
    Potassian Ferrian Tschermakite

Orthopyroxene tonalite and granite
14. FS-77-256
    Ferrian Magnesio-hornblende
15. FSM-77-225
    Ferrian Edenitic Hornblende

Amphibolite facies gneiss
16. FS-77-147
    Cummingtonite
17. FS-77-344
    Ferrian Magnesio-hornblende

ROCK ANALYSES

Table I. Chemical analyses of garnet-sillimanite-cordierite gneisses and some comparisons

	FSM-77											FS-77												
	4	72-4	75	119	121-1	211-3	214	245-1	218-1	273-4	307	59	62	143	160	153	268	175	177	202	208	1	2	3
SiO_2	62.4	77.1	72.2	58.8	75.2	59.8	56.9	61.8	57.3	67.5	71.1	74.1	78.2	58.6	76.7	57.1	70.7	57.9	72.1	65.9	64.2	60.8	65.0	64.4
TiO_2	0.85	0.40	0.56	0.93	0.04	1.16	0.81	0.62	0.83	0.62	0.36	0.20	0.41	0.77	0.08	1.00	0.61	0.86	0.53	0.61	0.71	0.76	0.76	0.62
Al_2O_3	17.8	12.0	13.4	14.6	15.0	22.5	21.0	20.0	20.3	17.0	14.9	12.0	9.5	20.7	14.8	20.2	14.4	20.3	13.2	16.3	16.8	17.7	16.2	15.5
Fe_2O_3	1.9	0.2	0.8	1.2	0.1	3.2	0.9	0.3	0.8	0.3	2.7	1.2	0.9	2.2	0.2	1.9	1.6	2.1	0.8	1.2	1.6	8.0	6.3	6.54
FeO	6.3	2.0	4.2	10.5	0.5	9.3	7.8	5.8	7.5	4.6		6.7	3.1	5.3	0.7	7.1	4.2	6.5	3.2	5.4	5.4			
MnO	0.07	0.01	0.07	0.17	0.02	0.24	0.10	0.09	0.07	0.06	0.03	0.20	0.32	0.07	0.06	0.08	0.09	0.09	0.06	0.11	0.06	0.09	0.06	
MgO	3.34	1.22	2.93	6.43	0.24	4.02	3.49	2.28	4.05	1.95	0.70	1.96	1.15	2.60	0.23	4.15	1.56	3.17	1.17	2.48	2.08	3.49	2.51	3.12
CaO	0.97	0.64	0.37	1.33	0.82	0.41	1.22	1.40	0.94	1.14	2.51	0.26	0.31	0.98	1.12	0.64	1.01	1.50	1.89	1.19	0.96	2.17	0.52	2.22
Na_2O	1.4	1.7	0.4	1.0	3.1	0.8	2.0	1.8	1.8	1.6	4.1	1.3	0.8	2.1	3.8	0.9	1.8	1.1	2.1	2.4	2.0	2.6	1.4	3.74
K_2O	2.58	4.19	3.02	2.35	4.17	2.51	4.57	3.83	4.97	4.17	2.77	1.11	4.12	5.32	1.86	3.97	3.10	3.31	2.85	3.43	3.90	2.86	4.83	2.44
H_2O	0.7	0.4	0.6	1.4	0.6	0.8	0.6	0.5	1.1	1.0	0.8	0.7	0.7	0.8	0.4	2.6	0.6	0.8	0.3	0.7	0.5			
CO_2	0.2								0.1		0.1	0.2	0.1	0.1	0.1	0.1		1.0	0.2	0.2	0.1			
P_2O_5	0.06	0.08	0.06	0.09	0.13	0.06	0.09	0.10	0.08	0.09	0.13	0.02	0.06	0.10	0.05	0.07	0.09	0.07	0.08	0.12	0.08			
Total	98.4	99.9	98.6	98.8	99.9	99.8	100.3	98.5	99.8	100.0	100.5	100.0	99.7	99.6	100.1	99.8	99.9	98.7	98.5	100.0	98.4			
S	0.01	0.02	0.02	0.02	0.02	0.03	0.08	0.03	0.15	0.27		0.03		0.01		0.41	0.02	0.01	0.01	0.09	0.01	0.66	0.65	
Ba	460	1040	880	330	405	655	1385	730	1110	735	860	775	1395	1030	645	665	695	670	805	595	850	550	492	
Rb	139	120	105	110	115	113	199	120	176	154	137	36	149	207	26	127	118	147	89	157	128	91	174	88
Sr	105	100	59	33	56	97	231	59	250	195	208	27	109	216	259	120	185	119	247	160	226	199	69	424
Ni	92		17	11		89	83	18	52	37	61	46		43		110		39	12	46	22	127	57	
Zn	170	60	70	240	30	230	140	90	160	140	60	180	70	120	50	170	70	130	60	130	80	323	114	
Zr	207	266	252	195	39	274	182		239	319	209	375	100	84	61	251	303	252	379	194	226			
Cu	8	14	21	14	9	16	96	6	47	34	81	29	31	17	9	190	7	19	18	65	11	66	75	
B		26			28					37	27	37	32	17	26			26	21	17		33	25	
Be	2.2						3.2		2.6		3.5	4.1										3.0	4.4	
Co	28	11	17	11		39	27	12	21	17	30	15	23	21		29	8	24	11	16	15	35	22	
Cr	210	21	73	40		170	130	85	160	77	120	12	45	130		160	63	110	45	110	110	133	105	
La	59	79	38	32	45	52	81	59	91	120	86	50	32	89	59	72	84	110	81	52	35	24	43	
Pb	30	53	29	26	58	46	38	8	22	40	41	22	56	40	40	31	34	35	36	41	33	26	22	
V	170	52	83	110	29	200	210	100	150	100	180	29	77	160	28	240	78	150	62	91	110	130	188	
Y	34	12	36	34	13	81	38	190	42	39	38	138	33	50	14	40	44	63	38	36	40	18	25	
Nb	14	11	13	11	4	27	16		19	18	13	7	11	15	5	15	15	25	10	15	16			
Yb		2.4			3.6							7.2	2.1		3.2			2.7	2.5					
K/Rb	154	290	239	177	301	184	191	265	234	225	168	256	230	213	594	259	218	187	266	181	257	259	230	230
Rb/Sr	1.32	1.20	1.78	3.33	2.05	1.16	0.86	2.07	0.70	0.79	0.66	1.33	1.37	0.96	0.10	1.06	0.64	1.24	0.36	0.98	0.55	0.46	2.52	0.21
K/Ba	46	33	28	59	85	32	27	44	37	47	27	12	24	43	24	50	37	41	29	48	38	43	81	

All rocks prefixed FSM-77 and FS-77 are garnet-sillimanite-cordierite-biotite (-plagioclase-K-feldspar)-quartz gneisses, except FSM-77-121-1 and FS-77-59 and FS-77-160, which lack biotite.
1. Weighted average, recalculated volatile-free to 100%, of 406 Archean shales from the Canadian Shield (Cameron and Garrels, 1980). Total iron as Fe_2O_3.
2. Weighted average, recalculated volatile-free to 100%, of 326 Aphebian shales from the Canadian Shield (Cameron and Garrels, 1980). Total iron as Fe_2O_3.
3. Average of 23 Early Precambrian greywackes, Wyoming (Condie, 1967). Total iron as Fe_2O_3.

Table II. Chemical and modal analyses of orthopyroxene-bearing tonalitic-quartz noritic gneisses and some comparisons

	FELSIC																										
	FSM-77											FS-77			FSM-77			FS-77	MAFIC								
	79	85	87	116-1	126	128	203-1	219	250	309	114-1	318	350	361	131	226	261	205	10	366	104	1	2	3	4
SiO_2	65.0	67.0	65.4	76.4	71.1	67.3	68.1	63.3	62.0	64.8	69.2	69.3	69.3	67.7	66.9	65.2	66.2	69.1	60.8	58.1	63.2	66.4	65.01	69.0	66.7
TiO_2	0.57	0.59	0.64	0.20	0.21	0.37	0.38	0.55	0.50	0.46	0.43	0.42	0.35	0.45	0.52	0.59	0.41	0.47	0.88	0.73	0.84	0.48	0.58		0.47
Al_2O_3	16.3	16.0	16.2	12.8	16.5	13.8	16.5	16.7	17.3	17.3	13.8	16.1	16.3	16.9	14.8	15.3	16.2	15.3	15.8	18.1	15.2	15.8	15.91	14.0	16.0
Fe_2O_3	0.5	1.8	2.2	0.8	0.5	0.7	0.9	2.2	2.5	1.7	1.1	1.4	1.3	1.5	0.9	1.3	1.2	1.9	1.0	0.9	1.7	1.3	2.43	4.5	
FeO	3.5	2.3	2.5	1.3	0.9	5.1	1.8	2.9	3.7	2.7	3.9	1.8	2.1	1.9	3.3	3.0	2.0	2.0	6.0	6.0	3.5	3.0	2.30		3.8
MnO	0.06	0.03	0.03	0.03	0.03	0.08	0.04	0.09	0.10	0.07	0.10	0.04	0.05	0.05	0.06	0.08	0.05	0.06	0.12	0.14	0.08	0.07	0.09		0.06
MgO	1.83	1.85	1.95	0.22	0.57	2.95	1.86	2.86	3.13	2.02	2.58	1.15	1.28	1.22	3.57	2.82	1.77	1.79	5.72	5.02	3.75	2.35	1.78	2.4	1.5
CaO	4.50	3.81	3.90	1.98	4.16	2.78	4.18	4.38	4.87	4.65	3.90	3.54	3.52	3.88	4.23	4.74	4.99	4.83	6.89	6.98	5.80	4.33	4.32	4.4	3.9
Na_2O	4.3	3.9	4.3	4.9	4.7	4.2	5.0	4.3	4.4	4.6	2.1	4.3	3.8	4.8	3.1	4.3	4.3	3.9	2.0	2.4	4.2	4.0	3.79	3.6	4.5
K_2O	1.00	1.43	1.42	1.21	1.01	1.20	1.18	1.71	0.72	1.30	1.11	1.45	1.28	1.58	1.85	1.02	0.98	1.16	0.92	1.08	1.02	1.22	2.17	2.0	1.5
H_2O	0.5	0.7	0.6	0.5	0.4	0.7	0.4	0.3	0.4	0.4	0.5	0.6	0.3	0.4	0.7	0.5	0.3	0.4	0.4	0.5	0.7	0.5	1.19		
CO_2	0.1-	0.2	0.4			0.2		0.1			0.1					0.1	0.1	0.1	0.3	0.1	0.2	0.3	0.1	0.06	
P_2O_5	0.16	0.2	0.7	0.06	0.05	0.04	0.15	0.31	0.17	0.21	0.09	0.17	0.08	0.14	0.34	0.16	0.15	0.19	0.27	0.16	0.20	0.2	0.15		0.14
Total	98.3	99.7	100.2	100.1	100.1	99.2	100.3	99.5	99.8	100.2	99.0	100.3	99.7	100.3	100.4	99.1	98.8	100.6	100.3	100.3	100.1	99.7	99.78		
S	0.02	0.08	0.08	0.04	0.01	0.01	0.02	0.01	0.02	0.05	0.04	0.03	0.02	0.02	0.05	0.02	0.02	0.02	0.06	0.04	0.03				
Ba	630	730	885	530	645	355	510	860	315	480	375	600	380	330	805	370	375	440	735	485	545	550			298
Rb	13	30	36	30	12	19	19	45	7	28	69	70	34	42	76	59	13	34	79	107	12	40			71
Sr	580	650	686	174	542	112	668	871	369	548	100	487	522	589	783	1230	741	551	836	731	462	572			343
Ni	13	13	24					19	33	15	32				64	44	23	23	49	45	76				
Zn	70	110	100	40	60	60	90	110	80	80	80	90		100	90	70	60	70	100	110	80				
Zr	189	213	231	191	89	59	98	97	94	136	188	157	97	141	174		115	122	143	82	127				
Cu	7	21	14	8	8	28	7	6	18	17	38	20	6	66	100	11	19	17	49	9	13				
B			19	24	25	17			19	17	15	29		17	15	23	22	28	20	50	28				
Be												3.9		2.4	2.3				2.2	2.1	2.7				
Co	17	13	20			12		11	20	12	21	10			18	24	14	15	22	31	28				
Cr	30	25	37			15	14	36	48	28	31	12	12	11	140	71	30	48	240	85	170				
La	60	95	120	77	78	63	46	47	92	96	62	92	68	70	93	98	94	80	83	88	95				
Pb	24	28	35	21	32	26	22	27	23	23	29	29	35	35	33	39	22	22	30	36	31				
V	95	96	120	28	42	87	58	82	130	88	100	86	66	76	82	110	82	88	170	220	130				
Y	10	10	8	23	1	9	5	11	13	8	23	6	13	10	16	21	5	12	24	14	11				
Nb	7	5	5	18	3	5	4	7	5	6	12	7	6	9	9		5	7	9	5	5				
Yb				4.4	2.5							2.3													
CIPW Norm																									
Q	22.67	28.83	24.74	38.58	29.93	25.23	22.77	18.44	17.30	19.41	36.91	29.34	32.26	23.74	26.68	21.85	24.65	31.33	19.47	14.38	18.00				
OR	6.04	8.53	8.46	7.18	5.98	7.20	6.98	10.18	4.28	7.69	6.85	8.59	7.61	9.34	10.98	6.11	5.89	6.84	5.44	6.39	6.06				
AB	37.17	33.30	36.68	41.62	39.86	36.07	42.33	36.66	37.44	38.96	18.03	36.49	32.34	40.63	26.29	36.88	37.02	32.92	16.92	20.33	35.73				
AN	21.09	16.96	15.83	8.87	20.36	12.35	19.11	19.22	23.18	21.77	18.39	16.50	17.04	17.35	19.17	19.70	22.39	16.81	30.79	32.36	19.71				
C	0.59	1.89	1.85	0.19	0.23	0.95		0.79		0.36	2.54	1.43	2.47	0.94	1.06			1.45	0.23	1.14					
Di							0.54									1.97	0.53				4.03				
HY	9.88	5.90	6.50	2.08	2.34	15.87	5.83	9.42	11.89	7.84	12.47	4.34	5.44	4.58	13.36	9.75	6.31	5.82	23.37	21.78	11.49				
MT	0.74	2.63	3.22	0.87	0.73	1.03	1.31	3.21	3.65	2.47	1.62	2.04	1.90	2.18	1.31	1.91	1.77	2.75	1.45	1.31	2.48				
CM	0.05	0.03	0.03	0.01	0.03	0.03	0.03	0.03	0.03	0.03	0.04	0.01	0.03	0.03	0.04	0.04	0.01	0.03	0.07	0.03	0.06				
IL	1.11	1.13	1.23	0.38	0.40	0.71	0.72	1.05	0.96	0.87	0.83	0.80	0.68	0.85	0.99	1.14	0.79	0.89	1.29	1.39	1.22				
AP	0.39	0.48	0.41	0.14	0.12	0.10	0.36	0.74	0.40	0.50	0.22	0.40	0.16	0.33	0.81	0.38	0.36	0.45	0.64	0.38	0.48				
PR	0.04	0.15	0.15	0.08	0.02	0.02	0.04	0.02	0.04	0.09	0.08	0.06	0.04	0.04	0.09	0.04	0.04	0.04	0.11	0.07	0.06				
CC	0.23	0.46	0.92			0.46		0.23			0.23				0.23	0.23	0.23	0.68	0.23	0.46	0.69				
K/Rb	639	398	327	335	699	524	516	315	854	385	134	172	312	312	202	144	626	283	97	84	706	253			175
Rb/Sr	0.022	0.046	0.052	0.17	0.022	0.17	0.028	0.052	0.019	0.051	0.69	0.14	0.065	0.071	0.10	0.048	0.018	0.062	0.12	0.15	0.026	0.070			0.21
Ba/Sr	1.09	1.12	1.29	3.04	1.56	3.17	0.76	0.99	0.85	0.88	3.75	1.23	0.59	0.56	1.06	0.30	0.51	0.80	1.16	0.66	1.20	0.96			0.87
K/Ba	13	18	13	19	10	28	19	16	19	22	24	20	30	40	19	23	22	22	10	18	16	18			42
Mode																									
Pg	67.9	63.0	64.3	59.4	65.4	55.0	72.1	68.0	75.8	71.5	52.6	64.7	64.4	65.3	54.6	62.5	68.4	57.3	52.9	59.7	58.4				
Kf	0.3		0.8	0.6	0.5			1.9		0.2			1.3	1.4	3.9										
Qz	21.3	24.8	20.3	36.6	31.6	27.5	22.1	17.4	7.7	16.9	26.2	25.3	27.8	25.9	29.7	27.2	19.4	27.9	17.9	7.9	17.5				
Opx	5.7	6.1	10.3	1.1	2.1	11.8	3.6	10.1	11.4	6.5	7.1	5.0	2.1	3.7	3.8	7.5	6.6	3.8	21.8	18.3	10.3				
Cpx (Ga)										(3.2)					1.4		2.2				8.7				
Hbl																	0.2	0.5			0.2				
Bio	4.1	4.7	1.5	1.4	0.1	5.2	0.8	0.1	2.2	2.2	10.1	3.8	3.1	2.0	10.8	0.8	4.8	9.2	6.4	13.3	2.8				
Ox	0.8	1.3	2.9	0.8	0.2	0.4	1.3	2.0	3.0	2.3	0.8	1.2	1.0	1.5	1.2	2.0	0.2	1.2	0.5	0.3	1.8				
Ap	0.1	0.1		0.1	0.1		0.1	0.5	0.1	0.2				0.1	0.6		0.1	0.1	0.5	0.5	0.1				
Accs			0.1			0.1				0.2			0.3	0.1			0.1				0.2				

1. Average orthopyroxene-bearing tonalitic-quartz noritic gneiss.
2. Average dacite (Le Maitre, 1976)
3. Modern back-arc sand from a continental island arc tectonic setting (Bhatia, 1983, Table 6, analysis 11). Analysis recalculated volatile-free to 100%. Total iron as Fe_2O_3.
4. Average Amitsoq tonalitic gneiss, West Greenland (McGregor, 1979, Table 4). Total iron as FeO.

Table III. Chemical and modal analyses of orthopyroxene-bearing granodioritic and granitic gneisses and some comparisons

	GRANODIORITIC									GRANITIC													
	FSM-77					FS-77		FSM-77		FSM-77				FS-77									
	47	76	172	215-1	315-1	317	296	44	153	65-2	103-1	113-9	141	22	140	301	1	2	3	4	5	6
SiO_2	71.0	64.9	73.2	65.8	66.5	64.9	69.1	63.5	69.7	67.8	71.3	70.0	67.1	69.8	63.1	72.4	67.6	69.7	66.09	71.30	71.66	65.7
TiO_2	0.42	0.50	0.28	0.86	0.54	0.56	0.13	0.78	0.33	0.44	0.47	0.42	0.54	0.41	0.41	0.27	0.46	0.42	0.54	0.31	0.39	0.99
Al_2O_3	14.5	16.3	14.1	15.6	15.7	16.7	16.7	16.2	13.8	15.8	12.8	14.7	15.2	14.8	15.0	14.7	15.5	14.7	15.73	14.32	14.13	14.15
Fe_2O_3	0.8	0.8	1.3	2.0	2.0	1.6	0.5	2.5	1.1	0.7	0.5	1.6	2.1	1.3	1.1	0.8	1.4	1.2	1.38	1.21	1.75	
FeO	2.4	4.4	1.2	2.7	2.1	2.5	0.6	2.5	1.3	2.4	2.7	1.7	2.3	2.6	5.0	1.1	2.2	2.1	2.73	1.64	1.17	5.8
MnO	0.04	0.06	0.04	0.07	0.05	0.06	0.02	0.06	0.04	0.05	0.05	0.07	0.07	0.04	0.11	0.02	0.05	0.05	0.06	0.05	0.05	0.09
MgO	1.35	1.81	0.72	1.95	1.93	1.99	0.38	2.80	1.42	1.45	0.59	1.20	1.92	1.06	5.80	0.84	1.59	1.14	1.74	0.71	1.24	1.1
CaO	2.69	3.97	3.01	3.73	3.85	3.90	3.11	4.81	3.07	2.57	1.79	2.66	3.79	2.85	0.81	2.39	3.56	2.68	3.83	1.84	3.17	3.8
Na_2O	2.5	3.2	4.1	3.4	3.7	3.8	4.5	3.5	4.7	3.4	2.8	3.5	3.2	3.5	2.0	4.4	3.7	3.3	3.75	3.88	3.05	3.5
K_2O	4.71	3.00	1.50	2.38	2.52	2.81	3.06	2.96	2.68	4.20	5.55	3.17	3.57	3.46	5.81	2.87	2.76	3.80	2.73	4.07	3.28	3.4
H_2O	0.4	0.8	0.4	0.5	0.5	0.8	0.3	0.3	0.5	0.5	0.5	0.6	0.8	0.3	0.8	0.8	0.5	0.5	1.04	0.77		
CO_2		0.1		0.1	0.1		0.2	0.1			0.1			0.1	0.1	0.1	0.1		0.06	0.05		
P_2O_5	0.12	0.21	0.09	0.26	0.23	0.14	0.07	0.36	0.13	0.21	0.16	0.14	0.31	0.13	0.09	0.06	0.18	0.18	0.19	0.12	0.06	0.31
Total	100.7	100.1	99.9	99.1	99.7	99.3	98.7	100.4	98.2	99.5	98.5	99.7	100.7	100.4	100.0	100.4	99.6	99.8	99.90	100.07		
S		0.03	0.01	0.02	0.02	0.03	0.01	0.02	0.02	0.01	0.09	0.05	0.02	0.02		0.03						
Ba	1085	540	390	1190	1370	810	910	1720	1375	1135	1015	2240	945	1165	1095	625	1043	1188				750
Rb	187	85	56	106	55	111	47	59	35	202	283	76	187	89	282	75	82	152				86
Sr	216	285	307	481	656	548	476	1016	897	442	129	230	587	358	80	433	542	363				220
Ni	37			21	21	21		33	13				37									
Zn	80	70	80	80	90	90	40	90	60	70	100	100	80	90	80	70						
Zr	181	152	107	249	166	148	154	190	97	159	354	169	153	116	268	113						
Cu	14	12	5	31	5	21	31	8	18	9	10	22	9	7	15	8						
B	24		18			22	28			19		21	17			30						
Be	2.3				3.1	3.8	2.4			3.2			2.9									
Co	14	11	9.2	11	19	10		14	9.4		9.2	7.5	16		7.2							
Cr	38	6.4	6.2	44	38	46		68	43	39	5.7	9.4	53	10	9.3	7.8						
La	110	57	69	82	120	88	98	99	53	74	130	99	85	43	54	93						
Pb	56	28	24	38	29	43	38	35	37	55	54	34	28	19	41	45						
V	71	76	34	82	110	88	39	100	52	65	44	57	80	52	48	45						
Y	29	39	16	18	9	10	2	16	9	20	42	12	16	6	43	4						
Nb	9	15	12	12	4	9	4	7	4	11	27	10	9	8	19	7						
Yb							3.0				2.8					2.7						
CIPW Norm																						
Q	29.40	21.58	36.18	26.32	24.70	21.29	24.91	18.32	27.12	23.66	33.40	30.17	23.97	27.75	15.71	29.91						
OR	27.73	17.85	8.90	14.25	15.00	15.82	18.38	17.41	12.58	25.05	32.43	18.88	21.06	20.43	34.52	16.99						
AB	21.06	27.26	34.84	29.15	31.54	32.57	38.69	29.57	40.70	29.04	17.25	29.85	27.03	29.59	17.02	37.30						
AN	12.52	17.81	14.41	16.39	17.09	18.17	13.93	19.75	10.86	11.49	7.34	12.38	16.54	12.65	3.31	10.72						
C	0.68	1.31	0.48	1.52	0.87	1.06	0.96			1.51	0.88	1.02		0.66	4.24	0.43						
Di								0.76	3.24													
HY	6.81	11.26	2.52	7.26	6.20	7.43	1.44	7.89	3.05	6.83	5.24	4.10	6.36	5.67	22.36	2.47						
MT	0.87	1.17	1.89	2.94	2.92	2.35	0.74	3.62	1.63	1.02	0.74	2.34	3.04	1.88	1.60	1.16						
CM	0.03	0.01	0.01	0.03	0.03	0.03	0.03	0.03	0.03	0.03	0.02	0.03	0.03	0.03	0.01	0.03						
IL	0.79	0.96	0.53	1.25	1.03	1.06	0.25	1.48	0.64	0.84	0.91	0.80	1.02	0.78	0.78	0.51						
AP	0.28	0.50	0.21	0.62	0.55	0.34	0.17	0.90	0.32	0.50	0.39	0.33	0.73	0.31	0.21	0.19						
PR		0.06	0.02	0.04	0.04	0.06	0.02	0.04	0.04	0.02	0.17	0.09	0.04	0.04		0.06						
CC		0.23		0.23	0.23		0.46	0.23			0.23			0.23	0.23	0.23						
K/Rb	209	293	222	188	380	195	540	415	493	173	163	346	158	323	171	318	279	208				328
Rb/Sr	0.86	0.30	0.18	0.22	0.084	0.20	0.099	0.058	0.039	0.46	2.19	0.33	0.32	0.25	3.52	0.17	0.15	0.42				0.39
Ba/Sr	5.02	1.89	1.27	2.47	2.09	1.48	1.91	1.69	1.53	2.57	7.87	9.74	1.61	3.25	13.69	1.44	1.92	3.27				3.41
K/Ba	36	46	32	17	15	27	28	14	12	31	45	12	31	25	44	38	22	26				39
Mode																						
Pg	45.8	52.2	64.0	45.9	57.2	53.4	58.2	52.5	39.2	35.4	28.2	38.3	29.2	43.0	0.3	41.4						
Kf	13.5	13.1	11.7	12.1	9.8	10.1	13.8	6.8	19.2	22.7	30.5	26.1	33.7	23.7	59.3	27.3						
Qz	26.8	21.5	20.5	26.5	22.3	23.4	25.9	19.7	26.4	31.7	29.7	29.9	30.6	22.8	23.8	26.4						
Opx	8.2	11.4	0.6	8.4	5.8	6.7	1.6	6.3	2.8	8.1	8.4	1.7	3.3	6.6	7.4	2.0						
Cpx								3.6	2.6													
Hbl								5.3	6.3													
Bio	5.1	0.6	1.9	3.5	2.2	4.3		3.8	0.3	1.5	3.1	3.3	1.9	1.9	9.2	1.9						
Ox	0.3	0.6	1.3	2.5	2.2	2.0		1.6	1.1	0.5	0.8	0.6	0.8			1.9						
Ap	0.3	0.4	0.1	0.1	0.4	0.1	0.1	0.4		0.1	0.2		0.3	0.3								
Accs		0.2	0.1		0.1		0.5		0.1		0.1	0.1	0.2	1.7								

1, 2. Average orthopyroxene-bearing granodioritic and granitic (excluding FS-77-140) gneiss, respectively.
3, 4. Average granodiorite and granite, respectively (Le Maitre, 1976).
5. Holocene sand, Salton Basin, California, from an active continental margin-type tectonic setting (Bhatia, 1983, Table 7, analysis 22). Analysis recalculated volatile-free to 100%.
6. Average Amitsoq augen gneiss, West Greenland (McGregor, 1979, Table 4). Total iron as FeO.

Table IV. Chemical and modal analyses of pyribolites and amphibolites

	FSM-77					FS-77											
	24-1	63-4	113-2	108	117	21	36	157	257	346	319	259	213	215	276	279	293
SiO_2	47.2	47.8	47.7	50.4	52.8	51.8	53.0	49.7	46.3	45.8	48.1	48.6	45.6	47.8	47.6	48.5	47.8
TiO_2	1.06	1.04	1.65	0.90	1.48	1.53	0.96	1.50	0.72	0.77	0.53	0.91	2.18	1.06	0.92	1.04	0.97
Al_2O_3	14.2	13.3	14.7	11.5	15.0	15.5	14.8	14.8	16.6	11.4	16.9	14.7	13.9	14.6	16.8	12.8	13.9
Cr_2O_3	0.05	0.08		0.06			0.08	0.06	0.06	0.23	0.07	0.05		0.06			
Fe_2O_3	1.5	3.9	1.1	2.7	1.8	1.4	2.0	1.5	2.7	3.3	2.1	3.0	7.7	2.9	2.1	3.7	3.7
FeO	10.5	9.3	11.7	6.8	10.2	8.7	6.8	9.7	7.6	7.2	5.4	9.0	9.8	8.5	9.5	10.7	9.2
MnO	0.26	0.25	0.26	0.18	0.19	0.15	0.14	0.20	0.16	0.19	0.16	0.24	0.33	0.25	0.21	0.17	0.26
MgO	7.64	10.2	8.28	8.68	4.62	6.44	9.41	8.35	9.78	13.9	7.82	7.76	6.84	10.7	7.86	8.61	8.06
CaO	15.5	8.79	11.0	10.2	8.16	8.42	7.80	9.65	13.1	13.0	16.0	14.0	10.5	9.82	12.3	10.8	11.3
Na_2O	0.9	2.6	1.1	3.1	3.1	3.1	2.9	2.8	1.8	2.1	1.8	1.1	1.9	2.7	1.8	1.1	2.1
K_2O	0.39	1.05	0.75	3.11	1.41	0.83	1.37	0.52	0.49	0.82	0.49	0.13	0.58	0.76	0.41	0.80	0.87
H_2O	0.5	1.4	0.8	0.9	0.7	0.5	0.4	0.8	1.2	1.4	0.7	0.3	0.8	0.7	0.8	1.7	1.5
CO_2		0.4	0.1	0.1	0.2	0.2	0.2	0.3	0.1	0.2	0.1	0.2	0.2	0.3	0.2	0.2	0.2
P_2O_5	0.04	0.34	0.17	0.56	0.28	0.27	0.20	0.50	0.06	0.07	0.14	0.09	0.16	0.11	0.10	0.10	0.23
Total	99.7	100.4	99.3	99.2	100.0	98.8	99.9	100.4	100.7	100.4	100.3	100.1	100.3	100.3	100.6	100.2	100.1
S	0.05	0.01	0.02	0.05	0.16	0.06	0.02	0.02	0.07	0.05	0.06	0.01	0.05	0.02	0.01	0.23	0.04
Ba	42	480	380	1700	530	490	560	170	60	48	140	26	69	190	31	63	860
Rb	9	12	46	106	42	11	51	5	11	23	9	7	10	11	7	17	20
Sr	134	440	145	916	270	547	391	1077	127	180	110	132	144	145	159	85	170
Ni	62	98	110	93	56	120	260	120	210	910	77	87	53	140	110	91	140
Zn	120		160	100	150	140	100	140	90	120	80	130	110	150	140	100	110
Zr	66	49	86	145	185	112	172	182	30	47	24	29	107	49	49	56	40
Cu	35	120	12	26	49	40	5	12	100	11	47	26	26	3	8	8	47
B						20			44	70			38	70	19	17	150
Be			2.9	2.9	2.9						2.0				3.2		4.7
Co	46	45	56	31	44	52	44	32	64	98	45	60	57	63	57	48	73
Cr	240	380	130	430	73	160	490	300	310	1700	370	260	61	430	170	210	390
La			54	57	91	76	59	54	64	53	61	61	49	36	68	50	49
Pb	27	23	26	24	25	24	27	17	27	33	30	26	21	17	29	25	23
V	340	310	380	200	280	220	220	200	350	330	260	380	600	350	310	340	640
Y	32	21	42	32	45	20	26	30	22	25	18	24	60	32	32	32	29
Nb	3	11	23	6	21	11	8	17	4	6	5	4	3	5	5	1	9
CIPW Norm																	
Q					2.73	1.40						2.15	1.53			2.43	
OR	2.32	6.26	4.50	18.68	8.38	4.98	8.14	3.08	2.91	4.89	2.91	0.77	3.44	4.51	2.42	4.79	5.21
AB	7.67	22.20	9.44	17.95	26.38	26.85	24.66	23.78	14.57	8.17	13.28	9.33	18.11	22.94	15.22	9.43	18.00
AN	33.78	21.72	33.44	8.42	22.98	26.34	22.89	28.37	35.94	19.45	36.71	34.86	27.75	25.58	36.53	27.98	26.27
NE				4.72					0.40	5.29	1.09						
DI	35.45	14.16	16.61	31.14	12.29	10.68	10.80	13.48	22.85	35.05	33.26	26.85	17.93	16.72	18.47	19.89	22.59
HY	10.04	12.06	28.38		20.33	23.67	27.32	19.59				19.20	16.93	3.03	13.04	26.86	12.29
OL	6.15	14.00	2.11	11.59			0.35	6.61	17.44	19.78	7.92			19.91	8.77		7.20
MT	2.19	5.71	1.62	3.98	2.63	2.06	2.91	2.18	3.93	4.83	3.06	4.36	11.19	4.22	3.04	5.43	5.43
IL	2.03	1.99	3.18	1.74	2.83	2.95	1.83	2.86	1.37	1.48	1.01	1.73	4.15	2.02	1.75	2.00	1.87
AP	0.21	0.81	0.41	1.35	0.67	0.65	0.48	1.19	0.14	0.17	0.33	0.21	0.38	0.26	0.24	0.24	0.55
CM	0.07	0.12	0.04	0.12	0.03	0.04	0.12	0.09	0.09	0.34	0.10	0.07	0.04	0.09	0.06	0.06	0.06
PR		0.02	0.04	0.10	0.30	0.11	0.04	0.09	0.13	0.09	0.11	0.02	0.09	0.04	0.02	0.44	0.08
CC		0.92	0.23	0.23	0.46	0.46	0.46	0.68	0.23	0.46	0.23	0.46	0.46	0.69	0.45	0.46	0.46
Mode																	
Pg	48.8	42.0	47.1	48.4	47.6	49.2	46.5	46.8	38.9	24.4	48.4	48.6	49.2	26.4	45.4	22.6	24.1
Opx	15.4	16.2	28.8		5.2	23.8	26.4	18.8	15.4	17.9	8.3	19.2	18.8	20.3	20.2		
Cpx	20.2	10.8	19.3	30.1	7.1	22.1	21.8	14.3	5.4	8.5	18.6	25.0	9.1	7.7	12.2		
Hbl	13.6	26.3			30.7		0.2	15.1	39.9	48.8	24.2	4.6	16.1	44.9	21.8	72.1*	75.1
Bio		3.8	2.9	20.7	6.3	1.1	4.2	1.8			0.2					4.4	
Ox	2.0	0.9	1.9	0.8	3.1	3.8	0.9	3.2	0.4	0.4	0.3	2.6	6.8	0.7	0.4	0.9	0.8

* 48.7% green hornblende, 23.4% brown hornblende

Table V. Chemical and modal analyses of orthopyroxene tonalites, granodiorites and granites and some comparisons

	TONALITE					GRANODIORITE		GRANITE											
	FSM-77				FS-77	FSM-77		FSM-77				FS-77		FSM-77		FS-77			
	28	115-1	156-1	213	266	68	235	83-2	215-2	265	13	58	302	225	318	151	1	2	3
SiO_2	66.4	64.9	64.4	63.4	64.3	71.1	68.4	73.9	74.2	75.1	72.3	76.3	73.7	70.4	73.0	73.0	74.3	69.82	72.9
TiO_2	0.42	0.91	0.69	0.57	0.54	0.33	0.41	0.17	0.17	0.17	0.22	0.17	0.16	0.26	0.20	0.25	0.18	0.72	0.18
Al_2O_3	16.7	16.3	16.0	16.4	16.0	15.1	16.0	13.9	13.5	12.4	13.8	12.4	14.5	14.6	13.6	14.0	13.3	14.56	13.8
Fe_2O_3	0.9	1.2	1.9	2.0	1.9	1.1	1.5	0.7	1.2	1.1	0.9	0.4	0.8	0.9	0.6	0.6	0.9	1.29	2.39
FeO	2.3	3.2	3.0	3.1	2.7	1.4	1.7	0.7	0.7	1.0	0.8	0.8	0.3	1.0	0.7	1.0	0.7	1.85	
MnO	0.07	0.07	0.09	0.09	0.07	0.03	0.05	0.01	0.02	0.02	0.02	0.01	0.01	0.03	0.01	0.03	0.02		.02
MgO	1.09	1.78	2.33	2.74	2.88	0.87	1.29	0.44	0.54	0.77	0.25	0.20	0.27	1.27	0.29	0.42	0.41	0.90	0.72
CaO	3.93	4.50	5.35	4.53	5.44	2.84	3.28	2.12	1.43	0.88	1.62	0.59	0.85	2.71	1.12	1.27	1.07	2.82	1.15
Na_2O	4.5	4.6	4.4	4.2	4.2	4.1	4.9	4.2	2.6	3.3	2.9	2.9	3.9	5.0	3.1	2.7	3.1	3.02	3.23
K_2O	2.99	1.87	1.13	1.23	0.95	2.38	1.95	2.56	5.02	4.49	5.21	5.39	5.19	2.41	5.52	5.86	5.06	4.00	5.13
H_2O	0.4	0.6	0.5	0.3	0.5	0.4	0.5	0.4	0.6	0.5	0.4	0.6	0.8	0.3	0.4	0.4	0.6		
CO_2	0.1		0.1		0.2	0.1	0.1	0.1	0.1			0.2	0.1	0.1	0.1	0.3	0.1		
P_2O_5	0.14	0.30	0.25	0.26	0.19	0.11	0.15	0.06	0.06	0.05	0.06	0.18	0.12	0.12	0.08	0.11	0.09		0.14
Total	100.0	100.0	100.1	98.8	99.9	99.9	100.2	99.3	100.1	99.8	98.5	100.1	100.7	99.0	98.7	99.9	99.8	98.98	99.66
S		0.04	0.01	0.02	0.02		0.02	0.03	0.01	0.02			0.02	0.02	0.01		0.02		
Ba	810	615	390	555	510	725	535	660	1185	1125	660	405	460	1180	825	715	767		683
Rb	78	30	9	13	11	57	94	50	139	84	180	312	233	29	197	201	190		138
Sr	378	596	583	848	579	423	540	287	279	154	157	67	135	745	235	139	158		96
Ni			40	36	53		10							20					
Zn	90	90	90	100	70	60	70	50	40	70	80	60	30	70	90	70			
Zr	161	262	142	111	160	117	200	88	167	136	172	128	113	89	146	212			
Cu	10	9	10	15	58	5	30	6	9	6	6	12	8	8	89	8			
B				23	29		20			33	18	25	32	28	24	28			
Be							2.5						7.2						
Co	9.8	8.8	21	28	21		14			9.8				12					
Cr	14	13	71	52	78		7.7			5.7	5.1			42		6.0			
La	71	73	69	99	96	43		31	68	84	76	49	65	100	75	130			
Pb	31	25	26	32	19	32	28	32	61	32	60	49	63	37	63	55			
V	74	82	120	130	110	34	62	34	28	30	27	23	32	57	33	27			
Y	10	17	11	14	10	9	9	5	16	7	5	14	4	11	3	26			
Nb	13	23	7	6	7	5	8	4	3	13	11	19	8	4	4	11			
Yb											3.0	3.5	2.9		2.7	4.4			
CIPW Norm																			
Q	17.97	19.18	20.06	20.04	20.86	30.98	23.67	35.14	36.59	35.79	32.26	38.07	29.56	25.27	31.84	32.35			
OR	17.73	9.92	6.70	7.37	5.65	14.14	11.55	15.29	29.79	26.72	31.38	31.99	30.69	14.42	33.17	34.78			
AB	39.05	39.12	37.34	36.05	35.75	34.87	41.56	35.93	22.10	28.12	25.01	24.65	33.02	42.85	26.67	22.94			
AN	16.14	18.98	20.63	21.08	22.13	12.80	14.69	9.60	6.10	4.07	7.79	0.49	2.80	10.41	4.48	3.70			
C				0.55		1.12	0.46	0.75	1.57	0.64	0.60	1.62	1.44		0.93	1.87			
DI	1.55	1.21	3.01		2.00									1.92					
HY	4.87	7.30	7.29	10.18	8.84	3.34	4.47	1.48	1.37	2.57	1.02	1.37	0.67	2.97	1.18	2.02			
MT	1.31	1.75	2.76	2.94	2.77	1.60	2.18	1.03	1.75	1.61	1.33	0.58	0.94*	1.32	0.88	0.87			
CM	0.01	0.01	0.04	0.03	0.03	0.03	0.01	0.03	0.01	0.01	0.03	0.01	0.01	0.01	0.03	0.03			
IL	0.80	1.74	1.31	1.10	1.03	0.63	0.78	0.33	0.32	0.33	0.43	0.32	0.30	0.50	0.39	0.48			
AP	0.33	0.71	0.59	0.62	0.45	0.26	0.36	0.14	0.14	0.12	0.14	0.43	0.28	0.29	0.19	0.26			
PR		0.08	0.02	0.04	0.04		0.04	0.06	0.02	0.04			0.04	0.04	0.02				
CC	0.23		0.23		0.46	0.23	0.23	0.23	0.23			0.46	0.23		0.23	0.69			
*includes 0.49% HM																			
K/Rb	318	462	1042	785	717	347	172	425	300	444	240	143	185	690	233	242	221		309
Rb/Sr	0.21	0.050	0.015	0.015	0.019	0.13	0.17	0.17	0.50	0.54	1.15	4.66	1.72	0.039	0.84	1.44	1.20		1.44
Ba/Sr	2.14	1.03	0.67	0.65	0.88	1.71	1.05	2.30	4.25	7.30	4.20	6.04	3.41	1.58	3.51	5.14	4.85		7.11
K/Ba	31	22	24	18	15	27	30	32	35	33	66	110	94	17	56	68	55		62
Molecular $Al_2O_3/(CaO + Na_2O + K_2O)$	0.93	0.93	0.88	1.01	0.90	1.04	0.99	1.03	1.10	1.04	1.03	1.05	1.07	0.93	1.04	1.07			
Mode																			
Pg	62.1	62.3	62.8	68.0	64.5	39.0	39.5	27.8 M	26.8	20.9	25.5	23.9	24.0	29.2 M	19.4	18.1			
Kf	1.6	0.2				21.2	20.6	20.3	33.1	40.2	33.9	37.2	48.1	29.3	53.2	53.6			
Qz	22.1	24.3	22.9	14.1	21.9	26.6	28.6	50.2	28.6	32.6	28.2	33.9	23.3	29.1	21.6	22.2			
Opx	7.0	7.1	9.7	15.0	3.8	6.8	3.9	0.7	6.0	1.8	8.3	1.8	2.2	2.2	2.8[a]	1.6[a]			
Cpx (Ga)	0.1	tr	0.4											2.3		(1.1)			
Hbl	4.6	3.8	0.6	tr	4.9		0.2							6.1					
Bio	1.6	0.8	2.3	1.6	4.4	5.1	6.4	0.6	3.8	3.8	3.8	2.9	2.2	0.5	2.2	2.3			
Ox	0.8	1.2	1.2	1.2	0.4	1.1	0.7	0.4	1.5	0.7	0.2		0.1	0.9	0.5[b]	0.7			
Ap	0.1	0.3	0.1	tr	0.1		0.1							0.3	0.1	0.2			
Accs						0.2			0.2		0.1	0.3	0.1	0.1	0.2	0.2			

M mesoperthite divided equally between plagioclase and K-feldspar; FSM-77-83-2 contains 7.6% discrete plagioclase
a biotite pseudomorphs
b includes 0.2% green spinel

1. Average of FSM-77-215-2, 265, and 13 and FS-77-58 and 302.
2. Average of 140 "orthocharnockites" (Zakrutkin, 1972, Table 2, col. 4).
3. Acid charnockite, Pallavaram, Madras, India (Weaver et al., 1978, Table 2, specimen MP 22).

Table VI. Chemical and modal analyses of anatectic biotite granites and some comparisons

	FSM-77							FS-77						
	20-1	67-2	181	207-2	295	303-1	317-3	9	167	260	349	1	2	3
SiO_2	73.2	74.1	72.8	71.5	72.8	73.5	71.6	73.7	71.4	77.1	74.3	73.3	73.55	73.98
TiO_2	0.24	0.08	0.23	0.42	0.20	0.14	0.18	0.24	0.24	0.01	0.14	0.19	0.11	0.26
Al_2O_3	13.7	14.3	14.3	13.9	14.0	14.1	14.7	14.5	14.8	13.3	14.3	14.2	14.72	13.51
Fe_2O_3	0.3	0.4	0.5	0.4	0.7	0.5	0.5	0.7	0.4	0.1	0.6	0.5	0.39	0.33
FeO	1.6	0.5	0.7	1.8	1.4	0.6	1.9	0.8	1.7	0.5	0.7	1.1	0.75	1.43
MnO	0.02	0.01	0.01	0.04	0.06	0.01	0.03	0.02	0.03	0.12	0.01	0.03	tr	0.05
MgO	0.38	0.21	0.26	0.73	0.54	0.45	0.82	0.53	0.96	0.11	0.33	0.48	0.20	0.38
CaO	1.77	0.83	0.63	0.97	0.90	0.73	0.64	1.70	1.60	0.54	0.96	1.02	0.83	1.45
Na_2O	2.6	3.3	2.3	2.8	2.5	3.2	2.1	3.9	3.5	3.8	3.0	3.0	2.99	3.05
K_2O	5.10	5.78	6.37	5.61	6.16	5.28	6.87	3.52	4.03	4.08	4.77	5.23	5.78	4.71
H_2O	0.4	0.5	0.7	0.5	0.6	0.6	0.5	0.4	1.0	0.2	0.7	0.6	0.64	0.52
CO_2	0.1				0.1				0.3	0.1	0.1	0.1		0.11
P_2O_5	0.06	0.13	0.16	0.13	0.12	0.26	0.10	0.09	0.07	0.12	0.14	0.12	0.03	0.15
Total	99.5	100.1	99.0	98.8	100.1	99.4	99.9	100.1	100.0	100.1	100.0	99.9	100.20	99.91
S	0.09			0.02	0.02	0.02	0.01	0.02	0.01	0.01	0.03			
Ba	1105	250	260	670	1065	265	930	525	1310	86	405	625		
Rb	180	242	262	260	226	230	172	112	128	52	141	182		
Sr	259	119	65	145	177	69	291	321	351	12	109	174		
Zn	180	60	70	50	50	60	40	100	80	20	60			
Zr	173	54	111	292	203	82	208	102	176	16	89			
Cu	100	15	14	36	9	15	13	26	9	12	8			
B	16	23	24		46	36	25		21	28				
Be		2.2				2.9								
Co				11	11	9.5		7.7						
Cr	5.5			15	7.6	5.2	9.6							
La	83		39	130	140	74	67	69	63					
Pb	39	74	66	55	48	45	60	55	43	27	57			
V	30	18	23	46	35	33	46	48	29	18	19			
Y	6	16	7	18	45	4	26	7	9	9	22			
Nb	8	3	12	19	15	10	4	7	6	3	7			
Yb		3.7	2.5		3.8	2.5	2.5	3.4		4.3	2.2			
CIPW Norm														
Q	33.96	30.96	34.13	30.40	31.94	33.39	29.67	33.24	30.97	38.25	36.71			
OR	30.39	34.27	38.30	33.71	36.58	31.58	40.81	20.86	24.04	24.13	28.36			
AB	22.19	28.02	19.80	24.09	21.26	27.40	17.86	33.09	29.90	32.18	25.54			
AN	7.82	3.28	2.12	4.03	3.06	1.95	2.53	7.87	5.64	1.26	3.24			
C	1.07	1.42	2.91	1.80	2.11	2.45	2.90	1.40	2.66	2.17	3.04			
HY	3.11	0.98	1.15	4.19	3.08	1.57	4.86	1.81	4.86	1.28	1.34			
MT	0.44	0.58	0.74	0.59	1.02	0.73	0.73	1.02	0.59	0.15	0.88			
CM	0.01	0.03	0.01	0.01	0.01	0.01	0.03	0.01	0.01	0.03	0.01			
IL	0.46	0.15	0.44	0.81	0.38	0.27	0.34	0.46	0.46	0.02	0.27			
AP	0.14	0.31	0.39	0.31	0.29	0.62	0.24	0.21	0.17	0.28	0.33			
PR	0.17		0.02	0.04	0.04	0.04	0.02	0.04	0.02	0.02	0.06			
CC	0.23				0.23				0.69	0.23	0.23			
K/Rb	235	198	202	179	226	191	332	261	261	651	281	238		
Rb/Sr	0.69	2.03	4.03	1.79	1.28	3.33	0.59	0.35	0.36	4.33	1.29	1.04		
Ba/Sr	4.27	2.10	4.00	4.62	6.02	3.84	3.20	1.64	3.73	7.17	3.72	3.59		
K/Ba	38	192	203	70	48	165	61	56	26	394	98	69		
Molecular $Al_2O_3/(CaO + Na_2 + K_2O)$	1.05	1.09	1.21	1.11	1.12	1.15	1.22	1.09	1.13	1.11	1.20	1.13		
Mode														
Pg	21	39 M	28	11	14	27.5 M	29	40	34	33 M	30.5 M			
Kf	38	39	40	50	50	27.5	39	23	36	33	30.5			
Qz	31	19	28	29	28	39	30	31	24	32	33			
Bio	8	tr	3	8	4	4	tr	3	2		2			
Cd	2	2				2			2					
Ga				2	4		tr	1	1	tr				
Sl			tr							1	tr			
Sp		tr	tr					tr			2			
Ox			tr	tr	tr		tr	1	tr		1			
Accs			tr	tr										

M mesoperthite divided equally between plagioclase and K-feldspar; FS-77-9 contains 18% discrete plagioclase
1. Average anatectic biotite granite.
2. Kakola granite, Turku, Finland (Hietanen, 1947, Table 6, col. 1).
3. S-type granite containing altered cordierite crystals as a residual source component, New England Batholith, Australia (White and Chappell, 1977, Table I, col. 4).

Table VII. Chemical and modal analyses of retrograde granulite facies metadykes and some comparisons

	FS-77			
	278	312	1	2
SiO_2	68.2	59.1	57.92	51.45
TiO_2	0.93	1.64	2.13	1.16
Al_2O_3	13.8	14.6	16.71	14.77
Fe_2O_3	1.8	5.0	4.08	2.62
FeO	2.7	3.8	4.26	5.06
MnO	0.05	0.09	0.13	0.12
MgO	0.97	2.43	1.70	6.24
CaO	2.24	4.56	3.86	5.99
Na_2O	2.5	2.8	3.68	2.95
K_2O	5.48	3.62	3.50	3.36
H_2O	0.5	1.0	1.19	2.76
CO_2	0.2	0.6		1.74
P_2O_5	0.37	1.05	0.16	0.66
Total	99.7	99.3	99.32	98.88
S	0.01			
Ba	1435	4420		
Rb	198	95		
Sr	229	2268		
Ni		14		
Zn	80	140		
Zr	863	310		
Cu	41	41		
B	20	25		
Be		3.6		
Co		15		
Cr	6.4	25		
La	120	250		
Pb	48	106		
V	53	160		
Y	73	48		
Nb	32	26		
Yb	4.4	2.3		
CIPW Norm				
Q	27.32	19.45		
OR	32.61	21.73		
AB	21.30	24.07		
AN	7.48	12.16		
C	1.04	1.72		
HY	4.44	6.20		
MT	2.63	7.38		
CM	0.03	0.01		
IL	1.78	3.16		
AP	0.88	2.53		
PR	0.02	0.23		
CC	0.46	1.39		
K/Rb	230	316		
Rb/Sr	0.86	0.04		
Ba/Sr	6.27	1.95		
K/Ba	32	7		
Mode				
Pg	38.7	55[b]		
Kf	22.1			
Qz	21.3	13		
Opx	3.4[a]	3[c]		
Hbl	5.4			
Bio	8.2	21		
Ox	0.3	6		
Ap	0.6	2		
Accs				

a green hornblende and biotite pseudomorphs
b includes minor K-feldspar?
c chlorite and carbonate pseudomorphs after clino- or orthopyroxene
1. Schei's "kersantite" dyke (from which sample FS-77-312 was taken) (Bugge, 1910, p. 18).
2. Average kersantite (Rock, 1984, Table 3, col. 3).

Table VIII. Chemical analyses of diabase dykes.

	FS-77							FSM-77
	114A	114B	115	128	129	137	165	11-4
SiO_2	48.25	47.78	48.00	48.40	47.79	48.05	49.9	42.0
TiO_2	4.92	5.01	4.96	5.00	4.71	3.99	4.14	4.99
Al_2O_3	11.75	11.98	11.98	12.71	12.52	13.32	12.0	11.77
Fe_2O_3	4.70	5.63	3.94	4.83	4.05	8.05	2.8	6.1
FeO	9.10	8.80	10.30	9.10	10.80	7.20	12.5	9.3
MnO	0.27	0.26	0.19	0.28	0.22	0.19	0.21	0.28
MgO	5.43	5.86	5.65	5.59	5.53	5.39	4.25	5.88
CaO	8.37	8.42	9.13	8.69	8.74	8.93	8.39	10.9
Na_2O	2.83	2.56	2.59	2.45	2.48	2.61	2.1	2.4
K_2O	1.02	1.07	1.04	0.55	0.82	0.66	1.20	1.38
H_2O	2.20	2.40	2.00	1.60	0.80	1.40	0.5	2.8
CO_2			0.10	0.60	0.30	0.80	0.1	0.4
P_2O_5	0.50	0.50	0.51	0.55	0.52	0.44	0.67	1.00
Total	99.34	100.27	100.39	100.33	99.28	99.03	98.08	99.1
S	0.06		0.06	0.07	0.08	0.03	0.06	0.43
Ba	330	320	270	150	190	180	320	430
Rb	39	47	27	7	12	14	34	38
Sr	450	420	500	540	510	440	572	741
Ni	140	130	120	100	100	110	80	37
Zn							200	180
Zr	390	370	390	360	370	320	586	311
Cu	290	220	250	310	330	230	300	28
B	59	52				54		
Co	62	52	60	52	60	60	49	51
Cr	98	93	81	87	100	46	45	18
La							46	
Pb							41	39
V	480	450	470	560	560	480	380	415
Y							68	36
Nb							45	77
Yb	9	10	10	9	10	9		
Irvine-Baragar Norm (Irvine and Baragar, 1971)								
Q	5.88	6.29	4.33	9.15	5.33	8.92	8.31	
OR	6.21	6.47	6.25	3.28	4.94	3.99	7.22	8.44
AB	24.60	22.11	22.22	21.00	21.26	22.71	18.07	20.99
AN	16.82	18.43	18.28	22.32	20.90	23.29	20.11	17.65
OL								2.53
DI	18.13	16.68	19.22	11.08	14.44	3.14	14.30	22.97
HY	10.40	10.76	12.74	13.63	15.96	19.01	17.92	4.22
MT	7.02	8.34	5.80	7.09	5.96	8.17	4.13	9.14
CM	0.03	0.03	0.03	0.03	0.04	0.03		
IL	9.61	9.72	9.57	9.60	9.08	7.77	8.00	9.80
AP	1.18	1.17	1.21	1.29	1.22	1.04	1.58	2.40
PR	0.13		0.12	0.15	0.17	0.06	0.13	0.91
CC			0.23	1.38	0.69	1.87	0.23	0.94
K/Rb	217	189	320	652	567	391	293	301
Rb/Sr	0.09	0.11	0.05	0.01	0.02	0.03	0.06	0.05

N.B. Trace element determinations, except for Rb, in all samples prefixed FS-77, except 165, were made by optical emission spectroscopy and are expected to be accurate to within ± 15 per cent of value reported. Measurement limits in ppm for elements not reported are: Zn 200, B 50, La 100, Pb 700, Y 40, Yb 4; Nb was not sought. Rb was measured using the "screw rod" technique (Abbey, 1979).